

University of Bath



PHD

Impact of Driver Behaviour Management on the Energy Usage of Conventional, Hybrid and Electric Vehicles

Hari, Deepak

Award date:
2016

Awarding institution:
University of Bath

[Link to publication](#)

General rights

Copyright and moral rights for the publications made accessible in the public portal are retained by the authors and/or other copyright owners and it is a condition of accessing publications that users recognise and abide by the legal requirements associated with these rights.

- Users may download and print one copy of any publication from the public portal for the purpose of private study or research.
- You may not further distribute the material or use it for any profit-making activity or commercial gain
- You may freely distribute the URL identifying the publication in the public portal ?

Take down policy

If you believe that this document breaches copyright please contact us providing details, and we will remove access to the work immediately and investigate your claim.

Download date: 13. Aug. 2019

Impact of Driver Behaviour Management on the Energy Usage of Conventional, Hybrid and Electric Vehicles

Deepak Hari

A thesis submitted for the degree of Doctor of Philosophy

University of Bath

Department of Mechanical Engineering

February 2016

COPYRIGHT

Attention is drawn to the fact that copyright of this thesis rests with the author. A copy of this thesis has been supplied on condition that anyone who consults it is understood to recognise that its copyright rests with the author and that they must not copy it or use material from it except as permitted by law or with the consent of the author.

This thesis may be made available for consultation within the University Library and may be photocopied or lent to other libraries for the purposes of consultation with effect
from **February 2019**

Signed on behalf of the Faculty / School of

This page is intentionally left blank

Acknowledgements

I would like to thank my supervisors Prof. Chris Brace and Dr. Sam Akehurst for their invaluable guidance and mentoring, and also for giving me the opportunity to pursue a postgraduate degree. This work would not have been possible without the contribution from people at Ashwoods Automotive, most notably Lloyd Ash, Mark Roberts, David Buckingham, Dan Regan and John Poxon. I would also like to thank Chris Vagg for his assistance at various stages of the research and also other fellow members of Powertrain and Vehicle Research Centre (PVRC) for their help and support. Robert Gusthart and his team of technicians played a key role in assisting me for the experimental testing activities conducted at the University of Bath.

Thanks to all my friends and family for their unwavering support throughout the process. My parents Bindu Hari and G. Hari have always provided me limitless love and support throughout my studies and I am immensely grateful for this. I would also like to thank my sister Divya Hari and brother in law Ajith Kumar for constantly reminding me of what is important. My baby niece Nishka, who always brings a smile to my face deserves a special mention.

Abstract

Rise in atmospheric CO₂ emissions have sparked a global concern for environment and sustainability in the last few years. Strict regulations have forced automotive manufacturers to adopt newer technologies aimed at reducing tailpipe emissions. However, these technologies take time to be adopted by different manufacturers, and thus their effect can only be seen after a decade or so. A much cheaper and quicker method of reducing CO₂ emissions (and also fuel consumption) from vehicles is to change the driving style of people, by reducing their aggressivity. The challenge is in ensuring that this improved driving behaviour persists over time to sustain the savings in fuel consumption.

A driver advisory tool was developed to reduce aggressive driving behaviour. The device sits inside the vehicle and provides instantaneous audible and visual feedback to drivers on their driving style, on an ongoing basis. The device was tested on 15 vehicles and over 39,000kms worth of data was collected. An average improvement of 7.6% in fuel consumption was seen across the fleet, with drivers being 16.4% less aggressive using the device.

The development and calibration of a low cost axial flux electric motor with a new Variable Air Gap technology is also discussed. Changing the air gap enabled mechanical field weakening that provided 45% increase in the maximum speed of the motor. This technology has the potential to be used in various applications, to work without the need for a gearbox.

The electric motor was fitted in a fully electric vehicle used to test an updated version of the driver advisory tool. For this version of the device, drivers were also given feedback on their braking style. Effective braking enabled a 40% increase in recovering energy that would otherwise be wasted as heat. The device helped drivers achieve an increase of 32% in the distance travelled per kWh of net battery energy. This improvement was identified to be an effect of reduction in aggressive driving and increase in regenerative braking.

Contents

Acknowledgements.....	iii
Abstract	iv
Chapter 1 - Introduction	1
1.1. Introduction	2
1.2. Transport and greenhouse gases.....	3
1.3. Summary	11
Chapter 2 - Literature Review.....	13
2.1. Fuel consumption reduction.....	14
2.2. Hybrid and electric vehicle powertrains	18
2.2.1. Series Hybrid vehicle	21
2.2.2. Parallel Hybrid vehicles	24
2.2.3. Series parallel hybrid vehicle	25
2.3. Permanent magnet axial flux electric motors.....	28
2.4. Driver behaviour	42
2.5. Summary	69
2.6. Research Aims and Objectives	71
2.7. Work division	72
2.8. Research Contributions	75
Chapter 3 - Driver Behaviour analysis.....	77
3.1. Field trials	78
3.1.1. Results from field trials	83
3.2. Preliminary data analysis	91
3.2.1. Prediction of driver behaviour improvement	99
3.3. Parameterised data analysis.....	106
3.3.1. Detailed data analysis	106
3.3.2. Use of other metrics	117
3.4. Summary	124
Chapter 4 - Updated version of driver advisory tool.....	126
4.1. Introduction	127
4.2. Addition of sensitivity function.....	130
4.3. Minimum pedal issue	134
4.4. Cruise control detection	136
4.5. Gear up-shift algorithm	142

4.5.1.	Determination of highest gear ratio	143
4.5.2.	Up-shift light algorithm	149
4.6.	Idling logic	155
4.7.	Change from pedal position to engine load	163
4.8.	Summary	170
Chapter 5 -	Electric motor testing and development	173
5.1.	Axial flux electric motor testing	174
5.1.1.	Test rig setup at University of Bath	175
5.1.2.	Test procedure	177
5.2.	Variable air gap concept	187
5.2.1.	Variable air gap rig tests	189
5.2.2.	Chassis dynamometer testing of mule vehicle	191
5.2.3.	Discussion	197
5.3.	Validation test rig development	202
5.3.1.	Rig hardware	203
5.3.2.	Rig software	205
5.3.3.	Automated test procedure	207
5.3.4.	Benefits of test automation	214
5.4.	Summary	217
Chapter 6 -	Electric vehicle testing.....	219
6.1.	Electric version of the driver advisory tool	220
6.2.	Electric vehicle and driver advisory tool testing	222
6.3.	Simulation of electric vehicle	229
6.3.1.	Results and discussion	231
6.4.	Summary	237
Chapter 7 -	Conclusion	240
7.1.	Driver behaviour and fuel consumption	241
7.2.	Low cost electric powertrain	243
7.3.	Driver behaviour and the range of an electric vehicle.....	244
7.4.	Future work	247
REFERENCES		249
Appendix A – Labview code for automated validation rig		255
Appendix B – Validation rig manual		256

List of figures

Figure 1-1 - Cost vs exhaust CO2 reduction in vehicles.....	6
Figure 1-2 - Price breakdown of a permanent magnet electric motor	7
Figure 1-3 - Price breakdown of a lithium ion battery pack.....	7
Figure 2-1 - A micro-hybrid system	19
Figure 2-2 - A mild hybrid system.....	19
Figure 2-3 - A full hybrid system	20
Figure 2-4 - Series hybrid vehicle configuration.....	21
Figure 2-5 - Parallel hybrid vehicle configuration	25
Figure 2-6 - Series-Parallel hybrid vehicle configuration.....	26
Figure 2-7 - Representation of an Ashwoods retro fit hybrid system	27
Figure 2-8 - Spoke type rotor with ferrite magnets	31
Figure 2-9 - Ferrite magnetic material required to produce similar power to rare earth magnets	31
Figure 2-10 - Forces acting on segmented magnets in the rotor of an electric machine.....	34
Figure 2-11 - Torque speed envelope of a standard permanent magnet synchronous motor	37
Figure 2-12 - (a) Magnetic flux lines for axial flux machine (b) Flux densities of axial flux machine.....	40
Figure 2-13 - Axial flux motor construction.....	40
Figure 2-14 - Structure of model used in Van der Voort's driver behaviour improvement tool.....	52
Figure 2-15 - Representation of the IPS logic used in the initial driver advisory tool algorithm.....	66
Figure 2-16 - Schematic representation of the initial driver advisory tool algorithm	66
Figure 2-17 - Work division for the thesis	73
Figure 3-1 - Instrument panel display of the driver advisory tool.....	82
Figure 3-2 - Engine speed vs torque of a Ford Transit 2.2L Duratorq 110PS.....	87
Figure 3-3 - Probability distribution of engine speed (Baseline vs Interface trials)	91
Figure 3-4 - Cumulative probability of Inertial Power Surrogate (m^2/s^3)	92
Figure 3-5 - Acceleration and deceleration histogram for vans	93
Figure 3-6 - Rate of change of pedal usage for baseline and interface trials	96
Figure 3-7 - Cumulative probability of pedal busyness	96
Figure 3-8 - Quadratic fit showing average engine speed being reduced.....	101
Figure 3-9 - Linear fit showing average values of IPS being reduced	101
Figure 3-10 - Residual plot for fitted model of baseline vs interface engine speed.....	103
Figure 3-11 - Contour plot of the predicted fuel savings with the use of the driver advisory tool	105
Figure 3-12 - Percentage of time Van 1 spent in different sets of acceleration	108
Figure 3-13 - Percentage of time Van 1 spent in different sets of engine speeds	109
Figure 3-14 - Plot showing the relation between Relative Positive Acceleration and Fuel savings	111
Figure 3-15 - Plot showing the relation between Inertial Power Surrogate and Fuel savings	113
Figure 3-16 - Number of Warning 1s, Warning 2s and Violations recorded for interface trials	121

Figure 3-17 - Warnings and violations for Vans 1, 2 and 3 on a daily basis during interface trials	121
Figure 4-1 - Schematic representation of the updated version of the driver advisory tool.....	128
Figure 4-2 - Difference in sensitivity settings for the same vehicle data	132
Figure 4-3 - Minimum pedal position for Euro 5 Ford Transit van	134
Figure 4-4 - Representation of the algorithm used to detect minimum pedal position	135
Figure 4-5 - Acceleration events with zero pedal that are NOT due to cruise control	139
Figure 4-6 - Acceleration events with no pedal usage that are due to cruise control	140
Figure 4-7 - Ratio of vehicle speed to engine speed plot for a van	145
Figure 4-8 - Algorithm to detect ratio of the highest gear of the vehicle	146
Figure 4-9 - Ratio of vehicle speed to engine speed exhibiting all 6 gears of a Ford Transit van	148
Figure 4-10 - Preliminary version of the gear shift logic used in the driver advisory tool	150
Figure 4-11 - Gear shift logic used in the updated version of the driver advisory tool.....	150
Figure 4-12 - Complete gear shift logic used in the updated version of the driver advisory tool.....	153
Figure 4-13 - Longest idling period for a van during field trials	157
Figure 4-14 - Idling warning and penalty logic used in the driver advisory tool	160
Figure 4-15 - Idling warnings and penalties conveyed to drivers.....	161
Figure 4-16 - Relation between pedal position and engine load for a Euro 5 Ford Transit van.....	164
Figure 4-17 - Change in vehicle speed, pedal position and engine load of a van	165
Figure 4-18 - Pedal position and engine load during cold start conditions of a van	165
Figure 4-19 - Algorithm for determining the minimum load of an engine.....	167
Figure 4-20 - Probability density of pedal and engine speed of the best and worst drivers	169
Figure 4-21 - Probability density of Pedal position and Engine Speed for all the vans	170
Figure 5-1 - The electric motor test facility setup at the University of Bath	177
Figure 5-2 - Voltage vs Speed plot for the 72V standard motor	181
Figure 5-3 - No load temperature rise for 72V standard motor.....	183
Figure 5-4 - Torque speed envelope for a 72V standard motor.....	184
Figure 5-5 - Efficiency map of the 72V standard motor	185
Figure 5-6 - Determination of the optimum air gap for the variable air gap control strategy.....	188
Figure 5-7 - Torque speed envelope for 72V electric motor with different air gaps	190
Figure 5-8 - Torque speed envelope for new 72 windings electric motor (simulated to 72V _{DC}).....	191
Figure 5-9 - Toro buggy used as mule vehicle for chassis dynamometer testing.....	192
Figure 5-10 - Motor torque vs speed for different air gaps on Toro mule vehicle.....	196
Figure 5-11 - Ke vs air gap for both 8 windings and 72 windings machine	197
Figure 5-12 - Direction of magnetic flux lines for a single rotor motor.....	199
Figure 5-13 - Direction of magnetic flux lines for a dual rotor	199
Figure 5-14 - Torque and power for the 72 windings dual rotor motor.....	201
Figure 5-15 – Motor validation test rig frame with motors connected	203
Figure 5-16 - Schematic representation of the motor validation test rig	204

Figure 5-17 - Graphical User Interface for the test rig software	206
Figure 5-18 - Flow diagram of the automated test procedure for the motor validation rig	208
Figure 5-19 - Start screen of the validation test rig automated software	209
Figure 5-20 - No load test run screen on the validation test rig software	211
Figure 5-21 - Peak torque test run screen for the validation rig	212
Figure 5-22 - Main test program run screen on the validation rig software	213
Figure 5-23 - Probability density of K_e for motors tested using the validation rig	215
Figure 5-24 - Probability density of max efficiency of different motors on the validation rig	216
Figure 6-1 - Schematic representation of the algorithm of driver advisory tool for electric vehicles ...	221
Figure 6-2 - Representation of the IPS logic used in the driver advisory tool for electric vehicles	223
Figure 6-3 - The Nemo vehicle converted to a fully electric vehicle	224
Figure 6-4 - Cumulative probability of the deceleration values for the driver advisory tool	226
Figure 6-5 - Battery SOC and vehicle speed for one full charge run of the Nemo electric vehicle	228
Figure 6-6 - Electric vehicle system model used for simulation	230
Figure 6-7 - Vehicle range and its relation to average inertial power surrogate of the simulated vans	234
Figure 6-8 - Cumulative probability of the deceleration values of the simulated data	235
Figure 6-9 - Percentage increase in regenerative braking against the percentage increase in simulated electric vehicle range	236
Figure 6-10 - DC voltage, SOC and vehicle range for Driver 7	236
Figure 7-1 - Improvements in different driving characteristics using the driver advisory tool for conventional and electric vehicles	246

List of tables

Table 2-1 - Driving pattern parameters identified by Eva Ericsson to assess driving behaviour	62
Table 3-1 - Specification of the different Ford Transit vans used in the field trials	79
Table 3-2 - Details of companies and their vehicles that were involved in the field trials	81
Table 3-3 - Calculated results from test data collected from the field trial experiment.....	84
Table 3-4 - Percentage change in parameters for each of the 15 vans involved in field trials	86
Table 3-5 - Analysis of different driving pattern parameters for Van 6	115
Table 3-6 - Analysis of different driving pattern parameters for Van 2	119
Table 4-1 - Idling logic warning time selector options	159
Table 5-1 - Motor specifications obtained from testing the standard 72V Ashwoods electric motor...	175
Table 5-2 - Electric motor test plan.....	178
Table 5-3 - Duty cycle operation for the 72V standard motor	186
Table 5-4 - Toro mule vehicle chassis dynamometer testing points	195
Table 6-1 - Specification of the electric vehicle tested	224
Table 6-2 - Simulation results of the benefits of electric version of the driver advisory tool	232

List of acronyms

IMechE – Institution of Mechanical Engineers

EV – Electric vehicle

REEV – Range Extender Electric vehicle

R&D – Research and Development

IC – Internal Combustion

NO_x – Nitrous oxide

DC – Direct Current

AC – Alternating Current

WOT – Wide Open Throttle

NVH – Noise, Vibration and Harshness

ECU – Electronic Control Unit

PM – Permanent Magnet

EMF – Electro-Motive Force

PWM – Pulse Width Modulated

FOC – Field Oriented Control

I_d – Direct Current

I_q – Quadrature Current

CAN – Controller Area Network

NEDC – New European Drive Cycle

S.D. – Standard Deviation

IPS – Inertial Power Surrogate

IPS_{ST} – Short Term Inertial Power Surrogate

IPS_{LT} – Long Term Inertial Power Surrogate

LED – Light Emitting Diode

OBD – On-Board Diagnostics

BSFC – Brake Specific Fuel Consumption

KERS – Kinetic Energy Recovery System

RPA – Relative Positive Acceleration

V/E – Ratio of Vehicle speed to Engine speed

K_t – Motor torque constant

K_e – Motor back EMF constant

IEC – International Electrotechnical Commission

VAG – Variable Air Gap

DAQ – Data Acquisition

GUI – Graphical User Interface

SOC – State Of Charge

Chapter 1 - Introduction

This chapter provides an introduction into the research area involving driver behaviour improvement and electric hybrid vehicle powertrain. It also highlights the need to reduce fuel consumption, which is discussed in relation to carbon dioxide and other greenhouse gas emissions from the transport sector.

1.1. Introduction

Global concern for environmental and sustainability issues have risen in the past few years mainly due to the rise in atmospheric CO₂ levels. Global warming is now a widely accepted fact and the concentration of carbon dioxide in the atmosphere is now over 390 parts per million (ppm). Studies have shown that the CO₂ concentration levels have to be limited to under 450ppm for the planet to be habitable – with an average temperature rise of less than 2°C [1]. The transport sector is responsible for 21% of greenhouse gas emissions in the UK, of which road transport vehicles form a significant (up to 80%) contribution [2]. At the current rate of growth of world population and accelerated industrialisation of developing countries, the global CO₂ emissions are set to increase beyond the 450ppm limit. This has now sparked the attention of policy makers, automotive manufacturers and engineers worldwide, who are focussed on different approaches to combatting greenhouse gas emissions.

The European Union and the UK government have introduced CO₂ reduction targets for a number of sectors, of which power and transport are significant contributors. Different potential avenues are being considered, some more effective, while others displace a problem from one sector to another. In 2008, the UK government introduced a legally binding target that aims to reduce CO₂ emissions by 80% of 1990's levels by 2050. This meant all sectors of the economy have to explore different ways to make this achievable. Similarly the Kyoto protocol was established to reduce CO₂ emissions from all sectors, but to date there is no evidence of the protocol having mitigated greenhouse emissions, but it has clearly raised awareness of the issue. CO₂ levels in the UK have risen by 4.4% from 2011 to 2012, a serious increase, considering

major changes being made to reduce greenhouse gas emissions from different sectors [1].

Another growing concern is the scarcity of oil, which has always been a significant contributor to the economic development of the world. Readily available fossil fuels are beginning to run out; even though estimated reserves would be enough for the next few decades, extracting it would become more challenging and hence expensive [1]. The power generation sector has had significant changes that contributed to its reduction in greenhouse gases in the last two decades. Using cleaner fuels, reduction in use of coal and moving into renewable and nuclear sources have helped reduce CO₂ emissions from this sector. Due to practical and infrastructure limitations, further improvement in this sector will take time. This has led to focus being on reducing greenhouse emissions from the transport sector, which is the single biggest contributor to CO₂ emissions after energy generation.

1.2. Transport and greenhouse gases

Environment officials and policy makers have now introduced stringent regulations for road transport vehicles for their significant share in CO₂ emissions from the transport sector. The UK government set a legally binding fleet maximum of 130g/km CO₂ for manufacturers by 2015 and 100g/km by 2020. But the Institution of Mechanical Engineers (IMechE) believes that for the proposed 80% reduction CO₂ levels by 2050, the target should be 30g/km limit by 2050, to compensate for the increasing mileage and fleet size of manufacturers [1]. Implementation of Euro emissions regulations has considerably reduced the greenhouse gas emissions from

automobiles since 1992. The newest changes to Euro 5 and 6 have introduced stricter emissions standards from new vehicles [3]. Recent years have shown considerable advancement in the development of Internal Combustion (IC) engines, through the use of turbo charging, complex electronic fuel injection, exhaust gas recirculation, fully variable valve timing and lift etc. Some IC engines have 40-45% overall efficiency compared to the 30% efficiency that they had 15 years ago. Some petrol engines already achieve under 100g/km CO₂ and this number can drop even further with effective turbocharging and start-stop technologies. Diesel engine emissions will be more difficult to address once they plateau around the 80g/km mark. The challenge then will be to reduce NO_x and particulate emissions. Widespread usage of turbo and supercharging technologies in the future by manufacturers will increase overall efficiency in vehicles, and when these technologies are coupled with low carbon fuels like biofuels, the CO₂ emissions of vehicles may come down to 70g/km by 2020 [1]. Taylor, Alex [4] believes there could still be 6-15% improvement in fuel consumption from further development of IC engine technology in the coming decade. Hybridisation of vehicle powertrain using electric motors to regenerate and store energy during braking (to be used when pulling away), start-stop technologies (micro hybrid) etc. have the potential of further reducing the fuel savings to about 21-28%.

Since IC engines contribute to 23% of CO₂ emissions in the UK, there has been a heavy focus on powertrain hybridisation and the shift towards electric vehicles. Manufacturers pursue different hybrid powertrain architectures depending on their requirement. Some choose IC engine and electric powertrain hybrid solution, while others prefer pursuing hydrogen power. Some have attempted flywheel energy

storage during braking, while others use Lithium-ion battery packs for the same. Pure electric vehicles (EVs) are gaining popularity mainly due to their zero exhaust emissions capability. The UK government introduced a plug in grant worth 25% of the cost (up to £5000) of an electric or hybrid car that can be plugged in to be charged or 20% of the cost (up to £8000) for a hybrid plug in or electric van [5]. Recent survey conducted by the Department of Transport [6] showed that people were put off from buying electric cars due to a number of reasons, the most prominent of which were recharging time, range of the vehicle and initial cost. Other reasons to why people steered away from pure electric vehicles included the availability of charging points and frequency of recharge required, whilst 23% admitted that nothing encourages them to buy a fully electric vehicle.

The price of electric vehicles is one of the major issues affecting people from moving to electric cars. A huge proportion of the cost of the electric vehicle comes from its primary energy storage capacity, which is a battery pack. The range of electric vehicles is dependent on the vehicle type and also the drive cycle. Choosing the right battery voltage for a particular vehicle depends mainly on the type of application the vehicle is intended to be used for. For example, electric golf karts tend to run at a lower system voltage of 36-48V, for their low power requirement and to reduce costs, while automotive manufacturers tend to have production electric and hybrid vehicle cars at 400-600V, for high power requirements and to reduce the magnitude of DC current flowing through the cables for improved safety. Manufacturers have chosen lithium-ion battery modules, due to their performance, lighter weight and power density when compared to conventional automotive lead acid battery packs. Apart

from clever strategies to save energy when driving the vehicle, preserving battery life is a major part of the control strategy of the vehicle, which prevents manufacturers from fully using its potential. Wider issues like supply of lithium and cobalt will need to be increased, leading to increase in mining and refining, which are both very energy intensive. Recycling of batteries is also to be addressed, due to the chemicals present in them [1].

Figure 1-1 shows the IMechE's prediction of cost of vehicles in comparison to the engine technology the manufacturer adopts. It is evident that moving away from conventional internal combustion powertrain technology adds significantly higher cost. Use of rare earth magnets in electric motors adds significant cost to the powertrain. An essential part of a permanent magnet electric motor is the rotor which has magnetic material attached to it. Neodymium magnets is one of the most widely used rare earth magnet in automotive applications, made up of an alloy of Neodymium, boron and cobalt [7]. These materials are used in low volumes compared to others minerals, but they are quite important in clean energy solutions.

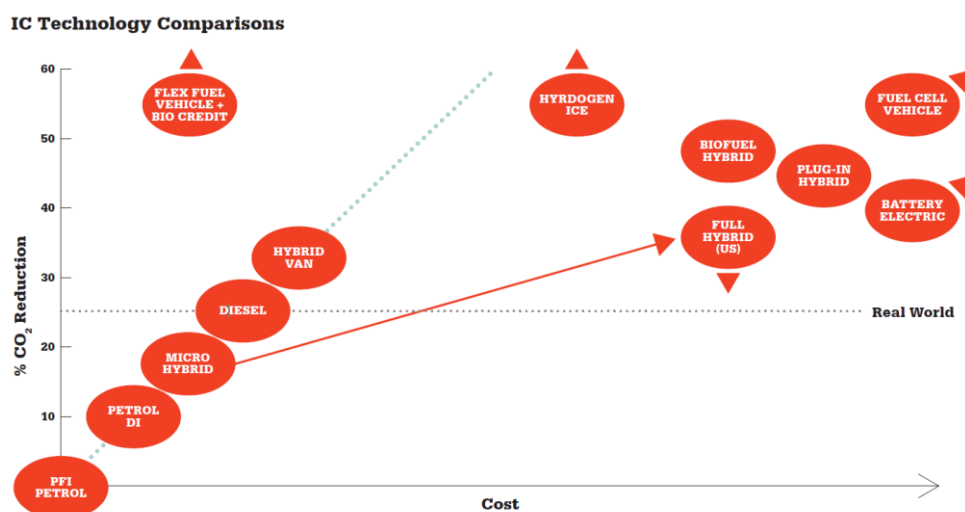


Figure 1-1 - Cost vs exhaust CO₂ reduction in vehicles (Source: IMechE Low Carbon Vehicle report ^[1])

Another reason for high price is the concentration of these materials in one country. China produces 95% of the rare earth elements and 76% of the world's total of rare earth magnet production [7].

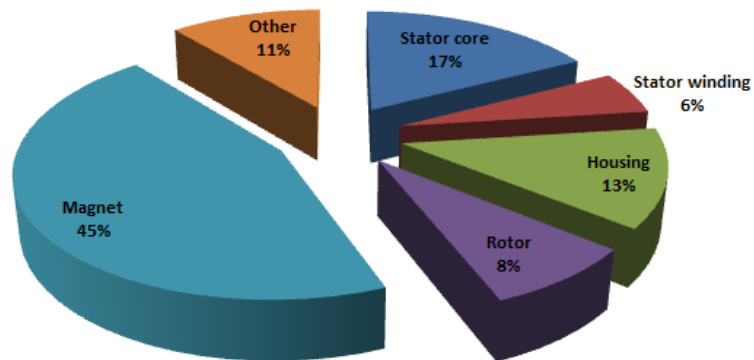


Figure 1-2 - Price breakdown of a permanent magnet electric motor (Source: Electric Motors and Critical Materials Breakout) ^[8]

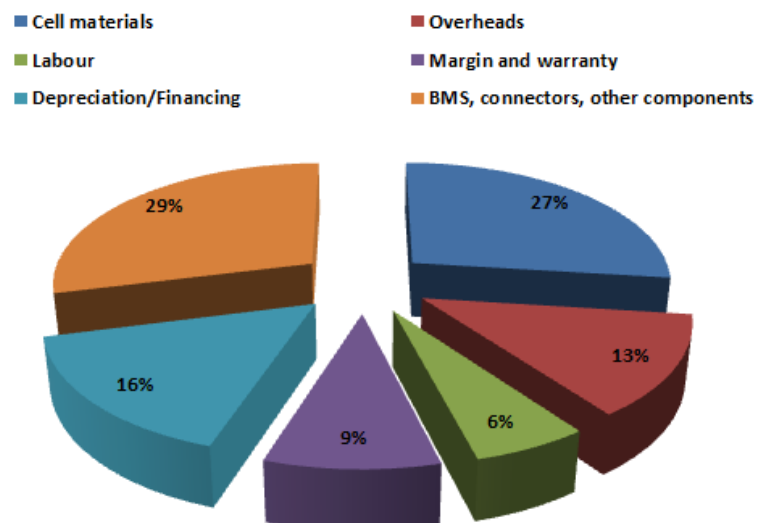


Figure 1-3 - Price breakdown of a lithium ion battery pack ^[9]

Figure 1-2 shows the price breakdown of a permanent magnet electric motor. Instability in the price of rare earth materials causes significant fluctuations in the production cost of electric machines for automotive manufacturers. Neodymium is considered a critical element in the move towards of clean energy and its supply is even more critical in the future move towards electric powered vehicles [8]. The cost of lithium-ion batteries which are widely used in automotive applications is another hurdle manufacturers need to overcome to achieve widespread acceptance of electric vehicles.

Manufacturers are trying to reduce cost in different areas of battery technology to reduce the overall production cost of the vehicle. Figure 1-3 shows the price breakdown of a lithium ion battery with Nickel-Manganese-Cobalt elements as cathode and graphite as anode. Major portion of the battery cost is in the anode, cathode and electrolyte, followed by smaller components, like connectors, fuses, safety disconnects, and battery management systems [9]. Although these components are comparatively cheaper than the cell materials, the number of different parts makes their costs at par with the cell materials. Research and development costs come under overheads with all other indirect costs. Research into new battery technology is mostly secretive. The US and Japan lead the world in terms of investment into battery R&D, followed by South Korea and China with significant government money being channelled to develop new battery technology. The US research spend profile is more transparent and more than half the total fund is spent on improving or developing new cell technologies (cell chemistry). A quarter of the expenditure is spent on research on the pack assembly, which includes battery

management systems and ancillary components, while the rest is spent on development of anodes, cathodes, electrolyte [9] etc.

It is clear that battery powered hybrid and electric vehicles help reduce tailpipe emissions, but their initial and infrastructure costs restrict the manufacturer's ability to adopt the technology. There has been a significant increase in focus on methods to reduce the cost of various components in the electric powertrain. This research looks into the development of low cost permanent magnet machines along with an industrial partner – Ashwoods Automotive Ltd.

Another method of reducing fuel consumption (and hence CO₂ emissions) quickly and effectively is by changing how people drive their cars. Driver behaviour is a very important factor in automotive engineering, as no matter what technology is added to new vehicles, it depends on the drivers to make the optimum choice in parameters like pedal usage, gear selection etc. that affect the performance and fuel consumption of the vehicle. The author's work revolves around improving driver behaviour to save on fuel consumption in internal combustion engine powered vehicles, and to save on battery energy use on electric and hybrid electric vehicles.

Focus on driver behaviour improvement has increased considerably in the last decade, with automotive manufacturers developing 'shift lights' to ask drivers to shift up or down a gear and 'eco-mode' to encourage them to drive economically. These technologies helps owners drive their vehicles more economically, but for drivers who do not drive their own vehicles, there is no motivation or obligation to follow the advice provided to them by these driver assist systems. The author worked on developing a driver behaviour improvement device for commercial fleet of vehicles to

help improve fuel consumption. The initial version was developed and trialled on Ford Transit vehicles, and later a final updated generic version was developed to be fitted on to any type of vehicle. The next step involved the development and testing of a similar system on electric vehicles, to help save on battery capacity and potentially battery life, by smoothening the load on it.

The development and testing of low cost axial flux motors, and optimising their performance and control strategy for traction applications was undertaken as part of the thesis. A new technology where the air gap between the stator windings and rotor magnet is changed was trialled, and a control strategy for this mechanism was developed. The testing and performance assessment of the motors was crucial as this motor formed part of the powertrain of the all-electric vehicle that was used to test the electric version of the driver advisory tool. The device was developed with the intention to assist drivers in reducing harsh accelerations and at the same time brake more effectively, so as to reduce the instantaneous power consumption from the batteries and increase the effectiveness of the regenerative braking capacity, and hence improve the range of the vehicle.

This research was performed when the author of the thesis was working as a Knowledge Transfer Fellow and Research Assistant at the University of Bath. Funding for the research work was received from the Knowledge Transfer Partnership of the UK, and Innovate UK (known as Technology Strategy Board – TSB earlier). The work described in this thesis has been developed in conjunction with the projects mentioned below:

1. Knowledge Transfer Partnership – Next generation hybrid vehicle for reduction in CO₂ emissions
2. Innovate UK – LCSLREEM – Low Cost Scalable Low Rare Earth Electric Machine
3. Innovate UK – CEPS – Complete Electric Propulsion System

1.3. Summary

There is a rise in the number of hybrid and electric vehicles appearing in the market currently. Whether the motivation is to save money on fuel or the status of appearing 'green', electric vehicles are gaining popularity among consumers. Manufacturers are now trying to lower the costs of electric powertrains. At the same time, drivers are being encouraged to drive more economically to save fuel, as this is the quickest and the easiest way to reduce fuel consumption in the short term. The current generation of driver assist and behaviour improvement devices focusses on the safety aspects of the vehicle, like collision warning and lane departure systems. The study into driver behaviour assessment and monitoring is not only useful to improve driving style and reduction of fuel consumption, but also beneficial to developing and improving drive cycles that are more representative of real world driving. This is also particularly important in driverless car development (autonomous vehicles).

This research improves on existing literature regarding driver behaviour and its impact on fuel consumption of the vehicle. Its novelty also extends on existing literature in understanding the links between driver behaviour and its effect on the energy consumption of an electric vehicle. There have been different concepts attempted for improving driver behaviour for fuel consumption. This research

pertains to the development of a driver behaviour improvement device for IC engine powered vehicles that provide instant feedback to the driver and then adapting the same for fully electric vehicles.

Reduction in energy usage can also be achieved through improvement in efficiency of the powertrain system. Implementation of novel motor technologies, optimisation and development of robust strategies and test procedures are an essential part of this process. Generally, improvement in efficiency translates to an increase in cost, however this research has focussed on improving the powertrain efficiency and reduction in cost of the same. The combined effect of driver behaviour improvement with advanced electric powertrain has the potential to substantially improve energy savings from the vehicle.

Hence, this research attempts to fill the gap in literature to identify whether driver behaviour improvement can help increase the range of the electric vehicle by reducing the draw on the battery, and also smoothen the load and hence increase battery life. Electric motors were tested with variable air gap technology concept to try and avoid the use of a gearbox in the vehicle. The system was then tested on a fully electric vehicle which was then used to test the driver behaviour improvement device to understand if battery energy can be saved by using the driver feedback tool.

Chapter 2 - Literature Review

This chapter focusses on the current research done in the field of electric motors and driver behaviour improvement. Different hybrid and electric vehicle architectures are explained along with existing attempts to improve driver behaviour. Research into existing traction motor technology and the development of low cost electric motors by the industrial partner is also discussed. The scope of the research work and the various work packages involved are described here.

2.1. Fuel consumption reduction

Most consumers prefer fuel efficient vehicles as the price of fuel is on a steady rise. This has accelerated the research and implementation of more efficient components into the powertrain of vehicles. Diesel engine efficiencies have increased to 45% in the last decade, which were 30% to start with. The current rate of progress will see them to improve further and plateau around 80-90g/km CO₂ tailpipe emissions, beyond which it will be the nitrous oxides emissions that limit its usage [1].

High boosting of engines is currently being implemented in petrol engines to improve fuel consumption and reduce tailpipe emissions. Turbocharging improves part load efficiencies, which is where most drivers operate their engines at. Ford EcoBoost technology is currently being sold in different vehicles ranging from the Ford Fiesta to Lincoln and Mercury brand cars. Boosting helps downsize the engine and still obtain the same or better performance from the base engine but with lesser consumption of fuel and fewer emissions. The EcoBoost technology helps reduce the engine size by 35% and provide fuel consumption savings of around 12%, and 15% reduction in tailpipe emissions [10]. R&D work conducted at the University of Bath showed that a 55% engine size reduction from a 5 litre V8 to a highly boosted 2.2 litre inline four cylinder engine can provide up to 35% reduction in tailpipe CO₂ emissions [11].

Diesel engines on the other hand have already been efficient, and focus is currently on meeting the particulate and NO_x emissions standards. This is more difficult compared to achieving better combustion efficiencies in petrol engines. There is also significant progress in second generation biofuels (mainly produced from biomass) being used in diesel powertrains recently. These will help further reduce the NO_x

emissions and also reduce the 'well to wheel' emissions from automobiles [12]. As improvements in IC engine efficiency have slowed down, there has been a shift towards manufacturers concentrating on alternative powertrain technologies in conjunction with IC engines, to improve overall vehicle efficiency.

Technologies like hydrogen fuel cell hybrids need more time to be accepted, as hydrogen extraction and storage technologies need to be improved. This again highlights the need to consider 'Well to Wheel' emissions to understand the potential benefits/drawbacks of using fuel cells, as mentioned by Stobart [13]. Utilising existing technologies and improving them is easier and a less expensive option for OEMs. Intelligent control of alternators where it brakes the engine by charging the 12V battery and prevents the vehicle from accelerating while going downhill (when the driver lifts off the accelerator pedal), is one way of reducing parasitic loads from the alternator [14, 15]. It also uses an intelligent battery management system to determine the state of charge of the battery before performing the intelligent switching ON/OFF of the alternator. When accelerating, the alternator does not load the engine, thereby saving fuel. BMW classifies this under their 'Efficient Dynamics' technology range, currently on most of their new generation diesel engines, while Ford use the 'ECONetic' badge for the same technology [16, 17]. Intelligent alternator control strategy involves reducing the alternator load when the vehicle is running slow or idling. Thus the battery is used in conjunction with the alternator to power ancillary equipment. At high speeds and braking or coasting, the alternator powers all the ancillary units and also charges the battery. This technology is believed to save around 4-5% in fuel consumption [18].

As turbocharging converts kinetic energy of the exhaust into rotational energy of a turbine, some manufacturers use another effective method to save on fuel consumption by converting the heat energy in the exhaust to electrical energy to charge the battery, using thermoelectric generators. They work on the principle of Seebeck effect, defined in the 19th century, which is the conversion of temperature difference into electricity. The BMW i8 uses this technology to charge the battery pack when the vehicle is cruising on the motorway, powered by the IC engine [16]. Turbo-compounding technologies are used as benchmark to compare other thermal heat recovery solutions [19]. Studies comparing different vehicles fitted with thermoelectric generators showed that they are most effective on heavy commercial trucks which have a large amount of waste heat energy due to the large size of their engine [19], high number of miles driven in a year and low sensitivity to extra mass added from the new system. A thermoelectric generator system can produce around 0.4kW for city driving cycles and up to 2kW for highway driving cycles [20]. This can save 3% on fuel consumptions, but the cost of implementation of this technology in passenger cars still outweigh the benefits, but is a good option for vehicles that fall into a higher price bracket. The limitations include the extra weight, high cost (in the order of £2500/kW) and increase in pumping loss in the engine (due to kinetic energy reduction in the exhaust with the presence of a thermoelectric generator) [20].

The complexity and low efficiency improvement of the above mentioned systems makes electric battery powered hybrid technologies a preferred option. The cost and complexity of the integration of these systems are higher than modifications of IC engine components, but the improvement in efficiency and drivability of hybrid

powertrains make it a promising technology. The last few years have seen a move into hybrid and electric vehicles, with most mainstream manufacturers having at least one model that showcases their 'green' technology. A number of different routes have been considered to hybridise conventional IC engine architectures. Each manufacturer selects a type of powertrain architecture depending on their requirements and the cost to benefit ratio. Micro-hybrids were introduced in automobiles with the use of 'start-stop' technologies. This is now being adopted by most of the mainstream manufacturers due to the reduction in fuel consumption during idling at traffic lights or when in heavy traffic.

Another significant reduction in fuel consumption is by the use of electric motor/generator to regenerate power and store it during braking of the vehicle. This converts kinetic energy of the vehicle into useful electrical power, rather than waste it as heat in the brakes. If the electric machine is coupled to the crankshaft end of the engine, it can also help in preventing the engine from stalling. Another benefit of using an electric motor in the powertrain is the ability to perform cold cranking to start the engine. The engine needs a significantly high amount of fuel to start when it is cold, while the electric motor can start the engine without any such issues and bring it up to idling speed before fuel is injected. A micro-hybrid with regenerative braking and cold start mode can save up to 12% in fuel consumption, while if it has boost capacities to provide extra power to the wheels, it has the potential to save up to 18% in fuel consumption. Hybrid technologies add complexity and weight, but the proven results of fuel consumption reduction make it a promising option. A series parallel hybrid system that can recharge the battery and at the same time power the

road wheels as in the case of a Toyota Prius can save around 25% in fuel consumption [21]. Around 17% savings in fuel consumption can be observed when a petrol engine vehicle is hybridised using start stop technology and assist during hilly or high power conditions [4]. On the other hand, driver behaviour improvements can save 10-15% in fuel consumption just by driving smoothly and not being aggressive [22]. This will be discussed in detail later in the chapter.

Consumers always prefer vehicles with better fuel economy. Due to limitations of improvement in internal combustion technology, manufacturers tend to adopt hybrid electric vehicle architecture even though they are more complex and add extra weight. There is still room for improvement in this technology in the areas of energy storage and weight reduction. Reduction in cost of these components is another need before they are adopted as mainstream technologies.

2.2. Hybrid and electric vehicle powertrains

Hybrid vehicles are those that have two or more different sources powering the vehicle. In this research, the focus is on hybrid electric vehicles, meaning the IC engine is used in conjunction with an electric motor/generator and a battery pack. A conventional hybrid electric vehicle will consist of an IC engine, electric motor/generator and a motor controller/inverter. There are plenty of ways to configure each of the above mentioned components, ranging from AC or DC motor/generator to asynchronous or permanent magnet machines. However, most units work on the same principle of converting electrical energy from the battery to mechanical energy to assist the engine in delivering power, and converting

mechanical energy to electrical energy during vehicle braking to recharge the batteries. Hybrid electric vehicles are constantly improving since they were first made commercially available. New generation of hybrid cars even have cold start assist (to avoid extremely rich mixture being used that causes high consumption of fuel) and start stop technology, where the electric motor is used to crank the engine when it is switched off when idling [21]. Improvement in efficiency is key for hybrid vehicles, and hence manufacturers choose different configurations depending on the improvements they observe and the cost to benefit ratio of the system.

Hybrid electric vehicles are classified based on the varying degree of hybridisation present in them. A hybrid vehicle with just 'start stop' technology where the alternator/integrated starter motor initiates quick restart of the

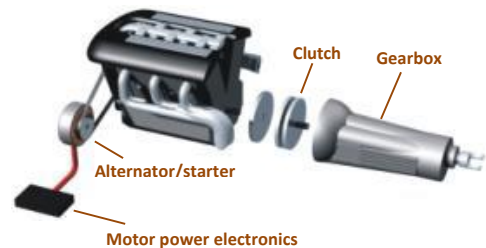


Figure 2-1 - A micro-hybrid system [21]

engine, prevents stalling and also provides good regenerative capability is usually termed as a 'micro hybrid vehicle' (Figure 2-1) [23].

In a 'mild hybrid vehicle', the alternator is usually replaced with an electric machine that assists the engine in delivering power (Figure 2-2). This can be during overtaking manoeuvres or cold cranking of the engine to bring it up to a

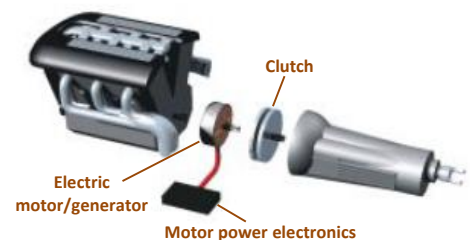


Figure 2-2 - A mild hybrid system [21]

desired speed before injection of fuel. The control strategy used in this type of hybrid vehicle is to assist the engine when it operates in a low efficiency region, to reduce fuel consumption and also to help improve the transient response of the system. It

also provides extra torque in regions where the engine performance is low, for example - low speed high torque conditions. So, the electric motor can assist in pull away to compensate for the low end response of the vehicle. This is notably useful in turbocharged downsized engines where low speed performance is poor.

A simple example of a full hybrid system is shown in Figure 2-3. The difference is the presence of an additional clutch between the engine and the electric machine. When this clutch is engaged, the system works similar to a mild hybrid, where the electric

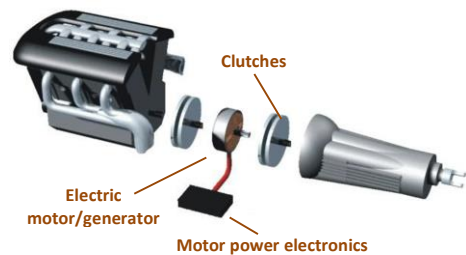


Figure 2-3 - A full hybrid system [21]

machine works to assist the engine when required, say acceleration events or cold start conditions etc. When the clutch is disengaged, the electric motor can provide power to the wheels through the second clutch and gearbox unit, so that the vehicle then works in fully electric mode. It has all the advantages of a mild hybrid system with the incorporation of a pure electric mode for the vehicle. The battery pack for the vehicle is charged during braking and coasting with the help of regenerative braking technologies. The battery recharge capabilities of this type of vehicle are limited by the number of braking and coasting events, hence the battery pack may not have the required state of charge to be beneficial for all electric mode. To compensate for this, manufacturers add the capability for the vehicle battery pack to be charged by an external source, say a wall socket in the house or an electric vehicle charging station. This type of hybrid vehicle is called a 'plug in hybrid vehicle'. Plug in hybrid vehicles usually have a transformer with a rectifier to increase/decrease the

incoming voltage to the required battery voltage before converting it to a DC voltage. If DC fast charging stations are used, a DC/DC converter is used to step up/down the incoming voltage to the battery voltage required for the vehicle. Plug in hybrids are adopted by a number of manufacturers ranging from Toyota, Honda and BMW to Porsche and McLaren. Different configurations of plug in hybrid vehicles are possible, but most of them adhere to series, parallel or series parallel architectures, which are described below.

2.2.1. Series Hybrid vehicle

A series hybrid vehicle is one in which the IC engine is not connected to the road wheels to provide tractive effort, but is connected to an electric generator that charges the battery pack. In this configuration, another electric motor or a set of electric motors are used to provide tractive effort to propel the vehicle. The IC engine is mechanically linked to a generator unit that produces electricity, which is converted using power electronics into DC energy and stored in the battery. For traction purposes, the electrical energy from the battery is transferred to a traction motor via the inverter to produce rotational motion at the wheels.

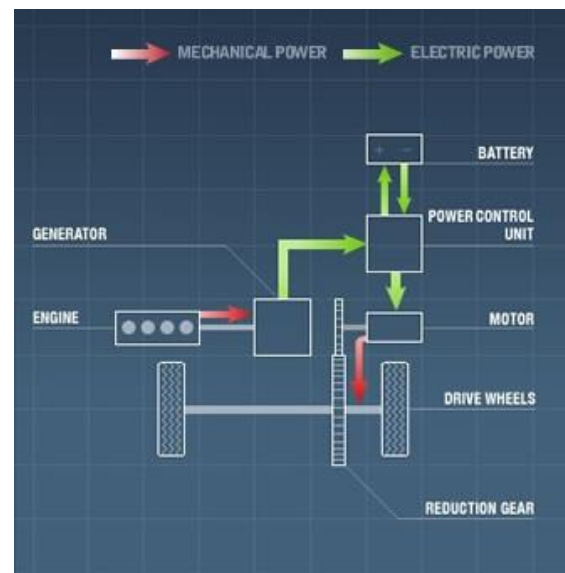


Figure 2-4 - Series hybrid vehicle configuration ^[24]

Series hybrid vehicles tend to have a much bigger electric motor when compared to parallel hybrid vehicles, mainly due to their role as the sole provider of traction to the road wheels. They also use a smaller IC engine, as this is used to spin a generator that generates electrical energy, and not to drive the wheels. Series hybrid vehicles have the advantage of tuning the IC engine to its most optimum point and running at this point indefinitely to charge the batteries. Since their sole purpose is to spin a generator, transient response and other performance factors considered for a normal car engine can be ignored. This provides further reduction in the fuel consumption of the vehicle when compared to IC engine propelled vehicles. Figure 2-4 shows a simple representation of a series hybrid vehicle. It can be seen that the engine is not mechanically connected to the road wheels in this case, but linked to electric generator. Here the engine is 'electrically coupled' to the road wheels [24]. The generator is connected to a power control unit that has a motor controller/inverter to transform the AC voltage generated to DC to be stored in the battery. Another motor controller is used to convert DC battery power to AC power to be fed into the drive motors. Here, the motors connected to the wheels will be rated to a higher power than the generator connected to the engine. The engine in this case can be of a reduced capacity. This type of hybrid vehicle is also called a 'Range Extender Electric Vehicle (REEV)', when the engine operates when the battery state of charge falls below a certain point. Often the IC engine is cranked by the generator unit in motoring mode, which helps reduce the weight of the unit by avoiding the need for a starter motor.

Ribau *et.al* [25] analysed different fuel based range extenders to determine the best possible solution for reduction in fuel consumption. A conventional SI engine with wide open throttle (WOT) operation in a range of different speeds was considered as the baseline engine. The other engines considered were – an over expansion cycle IC engine, Wankel engine and a Microturbine. The over-expansion cycle proved to be the most optimum solution as it had two modes of operation – moderate power and a high power condition, which was optimally chosen with the help of a control strategy. This engine worked on a lean mixture and had a late inlet valve closing cycle, which helped achieve a 6% reduction in energy usage and 9% reduction in total CO₂ emissions from extraction to exhaust [25]. The Wankel engine is known for its high power to weight ratio and lower noise, vibration and harshness (NVH) [26]. It is also lighter than a conventional IC engine of the same power, but due to heat losses, poor combustion chamber sealing and high oil consumption during warm up, this engine consumes more fuel than a reciprocating engine. However, the lightness of the engine and low vibrations due to no reciprocating parts are the reasons for considering Wankel engines for range extenders. It was observed by Govindaswamy *et.al* [27] that the Wankel engine produced the least interior noise when taking structure borne, intake and exhaust borne noises into account. Among reciprocating engines, it was seen that a six cylinder engine working at the optimum efficiency region produced least noise, while among two cylinder engines, the two cylinder horizontally opposed engine produced the least noise.

Aharon *et.al* [28] studied the use of alternative power sources for range extender electric vehicles. A renewable energy range extender (RERE) was considered which

utilised solar energy. As this technology is heavily dependent on solar irradiance and temperature, this would be applicable only for a few hours in a day and also power output from this source would vary in a day. This is not applicable to a range extender engine as constant power should be supplied to the generator to provide energy to the battery. Apart from considering an IC engine as a fuel based range extender (FBRE), fuel cells were considered for this application. But the cost of the system and storage of hydrogen led to the conclusion that the most optimum solution for range extender electric vehicles is a small IC engine. This conclusion was based on exhaust emissions, extraction to exhaust emissions (also known as well to wheel emissions) and also cost of the system [25, 29].

Due to the engine not being part of the driveline for a series hybrid, NVH is not taken lightly in case of these vehicles. As the engine does not drive the wheels, it can be located away from the rest of the drivetrain, but it might be closer to the passengers and not separated by acoustic insulation generally used in vehicles. Some series hybrid vehicles use the engine without the flywheel and depend on the generator rotor inertia to act as a flywheel. Dynamic generator torque control strategies are generally used in these cases, where the generator output torque is controlled based on the engine torque profile to obtain a smooth power into the battery pack. This strategy is used by Mahle, FEV and many other range extender adopters [30, 31].

2.2.2. Parallel Hybrid vehicles

In this configuration of hybrid electric vehicle, the electric motor works in parallel to the IC engine to provide traction to the road wheels. Here, the engine is connected to the drive axle via a gearbox as in the case of a normal IC engine vehicle, but the

electric motor is what drives the wheels as well. This can either be to assist the vehicle in the acceleration phase, or even to drive the vehicle in fully electric mode.

A parallel hybrid vehicle configuration consists of an IC engine and a motor/generator that powers the road wheels. Electric power from the battery is transferred to the electric motor via a power control unit (motor controller/inverter), that converts DC power into AC to drive the electric machine to power the road wheels.

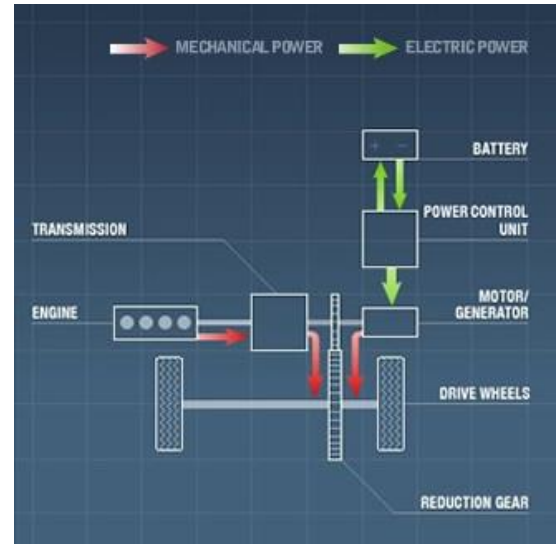


Figure 2-5 - Parallel hybrid vehicle configuration ^[24]

The control strategy is usually embedded in the ECU of the vehicle. This configuration often takes advantage of the high torque that electric motors produce at zero speed. Usually the electric motor is used at low speeds and also to assist the engine during the acceleration phase. In all other conditions, the vehicle runs on the IC engine. When braking, the kinetic energy in the wheels is converted to electrical energy by the generator using regenerative braking, gets stored as useful energy in the battery. One of the advantages of a parallel hybrid system is that it requires only one inverter, due to the presence of only one motor/generator unit.

2.2.3. Series parallel hybrid vehicle

A newer development in hybrid vehicle configuration is the combination of both the above mentioned systems. As shown in Figure 2-6, the IC engine is connected to a power split device that splits the power to the generator and the road wheels. The

engine not only charges the battery here, but also powers the road wheels. A separate electric motor unit is connected to the wheels to assist the engine in delivering power to wheels, or even run the vehicle in fully electric mode. The power split unit is optimised so that the maximum efficiency is achieved from the whole system. Hence, this type of

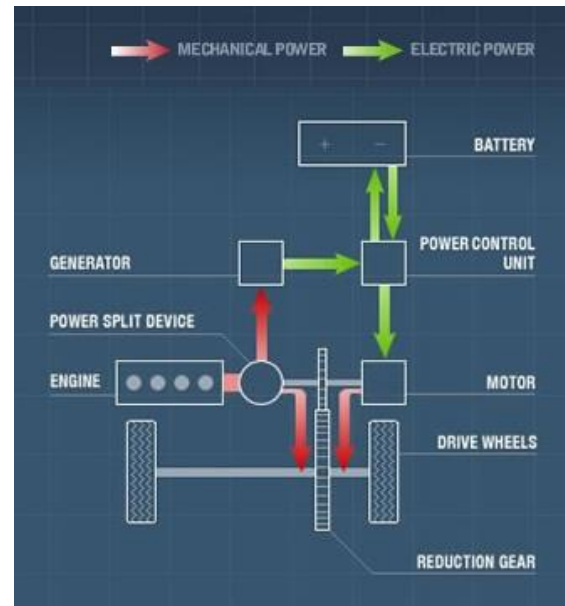


Figure 2-6 - Series-Parallel hybrid vehicle configuration ^[24]

hybrid vehicle is also called a Power Split hybrid vehicle. The electric motor is used for propulsion in low speed high torque conditions, and also during the acceleration phase to assist the IC engine. This type of configuration is more complex and expensive compared to the previous two, but more and more manufacturers are adopting this now as it has most opportunity to tune between best efficiency/fuel consumption and drivability. Toyota Prius, Chevrolet Volt, BMW i8 and many other hybrid vehicle manufacturers use this combination along with the plug in option, so as not to rely on the engine alone for recharging the battery. The efficiency advantage over other configurations has to still be carefully assessed, as there is loss of energy during conversion of energy from one type to another.

Ashwoods hybrid electric vehicle

The industrial partner Ashwoods Automotive develop retrofit hybrid systems for commercial vehicles. It consists of a motor/generator unit and battery pack with a

battery management system. The electric machine is connected to the propeller shaft of the vehicle by the use of pulleys and a drive belt. In relation to the size of the engine, the motor provides an additional 20% power. The architecture used here makes this a parallel hybrid vehicle. Kinetic energy recovered from the road wheels during braking is stored in the battery by the generator, which is then used to assist the engine in delivering power to the road wheels. The pulley reduction ratio is determined based on the final drive ratio of the vehicle and the application it is intended to be used for.

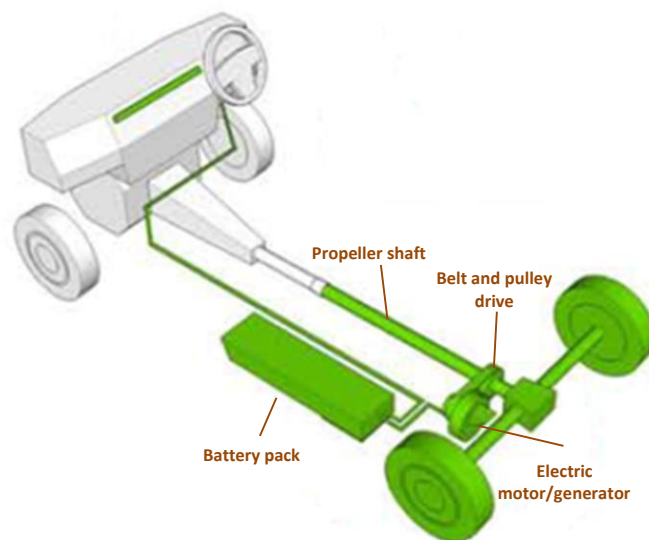


Figure 2-7 - Representation of an Ashwoods retro fit hybrid system

The retro fit hybrid system has a battery management unit, which makes sure all the cells in the battery are well balanced and healthy. The system also has safety features in place where it checks battery temperature and shuts down power delivery in case a fault is detected or if the battery overheats. Fitting the retrofit hybrid system only takes 2 hours. The system relies on the vehicle On-Board Diagnostics (OBD) to obtain key parameters of the vehicle like – vehicle speed, engine speed, engine load etc. to

deliver the optimum response from the motor/generator. It also has a dashboard display unit to show the driver the motor's instantaneous response (whether it is assisting or braking). Since the system does not modify the existing Electronic Control Unit (ECU) or any other component of the vehicle, the customer does not lose the manufacturer's warranty on the vehicle. The author was only involved in the final testing of the Ashwoods hybrid vehicle and hence this does not form an essential part of the thesis.

2.3. Permanent magnet axial flux electric motors

Due to the increase in the number of hybrid and electric vehicles, there has been a rise in the usage of AC electric motors in traction applications [32]. Permanent magnet (PM) machines are more preferred due to their high power density and efficiency when compared to induction machines of the same size [33]. Even though they happen to be more expensive than squirrel cage induction, their higher efficiency, adaptability and power density make them a preferred choice for traction applications by most automotive manufacturers. One of the biggest reasons for their increase in efficiency is the reduction in rotor losses by eliminating field excitation losses, which are present in the case of an induction machine [34]. This increases the power to weight ratio of permanent magnet machines and also its efficiency.

A number of factors need to be considered when choosing the optimum motor for traction applications. The use of permanent magnetic material does add cost to the machine, but these materials significantly reduce some of the losses seen in induction machines. Induction machines have to be designed to the minimum air gap physically

possible for minimum losses between the stator and rotor coils. This causes more stray losses from leakage inductance of both coils, which might interfere with the stator core giving rise to eddy currents. Also, rotor copper loss in these motors contribute to 15-25% of the total losses in the system [35]. Stray losses in the case of PM machines are again lower than those of induction machines of the same size, mainly due to the higher air gap between the stator coils and the rotor magnets. This allows PM machines to have around 30-40% higher power density when compared to a similar sized induction machine [33, 36]. Unlike induction machines which tend to be forced air cooled and thus have vents on their covers, permanent magnet machines tend to be completely covered so as to avoid dust and dirt accumulating on the magnets, which may reduce their performance. Hence, most of the permanent magnet machines for traction applications tend to be liquid cooled. Permanent magnet machines tend to have higher reliability compared to their induction machine counterparts, mainly due to the absence of brushes. The internal design of PM machines allow them to be modular in construction if needed.

Due to smaller and lighter permanent magnets replacing rotor copper coils, a PM machine tends to have better dynamic response compared to an induction machine [37]. This is particularly important in providing optimum drivability and transient response to the vehicle. Due to the absence of field current required through the rotor, PM machines provide increased flexibility of control when compared to induction machines. They also have high torque maintained for a longer speed, which is advantageous in the acceleration phase of the vehicle. They also have better regenerative braking capacity due to advanced motor inverter specifications.

Induction machines are less efficient at higher speeds due to the reduction in motor flux in the constant power region (because of increased back EMF), which requires an increase in stator current to maintain the torque required [35].

Using induction machines do not help reduce the overall cost of the vehicle significantly, since their cost of manufacturing is still relatively high due to the tight tolerances required for small air gap between the stator and the rotor [38]. Axial flux motors offer more opportunities for reduction in cost, even though permanent magnets tend to be of higher cost compared to aluminium or copper used in induction machine rotors. While the stator of an induction machine contributes 38% of the total material cost of the machine and the rotor contributes 23%, in a permanent magnet machine the rotor alone is responsible for 45% of the material cost of the machine [38]. This is due to the expensive permanent magnets in the rotor, which consists of rare earth materials. Thus, it can be said that the magnets contribute to a significant proportion of the total cost of the machine.

Many manufacturers have attempted using ferrites in machines, mainly due to their low price (around 1/10th of a Neodymium magnet for the same power). Ferrites are weaker than rare earth magnets for the same size and hence a larger ferrite rotor has to be used to obtain the same power as a rare earth magnet. Ferrites are ferromagnetic materials composed of iron oxide and metallic elements. Being ferromagnetic, they can be magnetised and de-magnetised by the application of a magnetic field. Hard ferrite materials are more resistant to demagnetisation and find applications in speakers and some electric motors, whilst soft ferrites are prone to demagnetisation and are used to make ferrite cores for cables and transformers.

Ferrites have a residual flux density that is a third of a rare earth magnet [39]. Due to ferrites being weaker than rare earth machines, they provide surprisingly high efficiency at high speed low load regions due to less field weakening currents required.

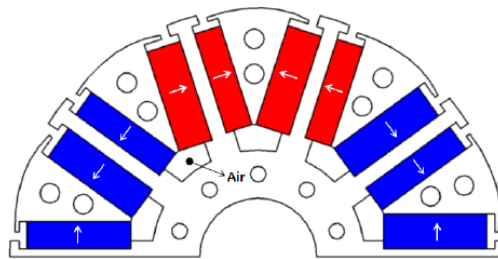


Figure 2-8 - Spoke type rotor with ferrite magnets [40]

Sung Il *et al* [40] attempted to achieve the same power density from a permanent magnet machine on a ferrite magnet machine. A spoke rotor design was chosen that helped reduce the risk of demagnetisation and helped reduce the amount of rare earth magnetic material in the machine that would otherwise have been required. As shown in Figure 2-8, the ferrite magnets are split into pairs on either side of the steel core poles of the stator and the thickness of the ferrites on either side are different.

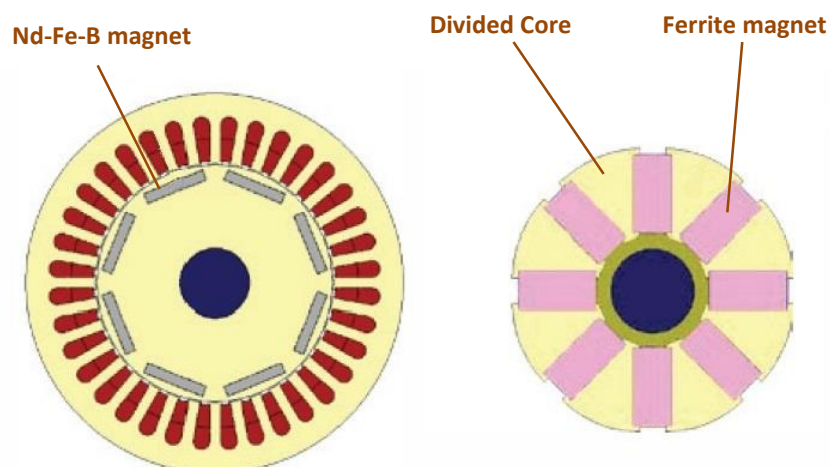


Figure 2-9 - Ferrite magnetic material required to produce similar power to rare earth magnets [39]

Ferrite motors can achieve up to 90% of the rated torque of the rare earth magnet machine, but at a lower maximum torque. Also, it requires a higher current to produce the same torque, and adds more weight [39]. This lower efficiency is due to the weaker flux density in the air gap from the ferrites, compared to rare earth materials. But when taking into account the exclusive supply limitations of rare earth magnetic materials, high cost and high eddy current losses, ferrites prove to be a viable option. Being weaker, more magnet material is required to obtain a similar performance to that of a rare earth magnet. Figure 2-9 shows an indication of the amount of ferrite magnet material required to produce similar effects of that of a rare earth magnet (Neodymium in this case). It needs to be noted that in this case, the researchers wanted to achieve the same power density (per volume, not mass) using ferrites as that of a rare earth magnet motor.

Another advantage is that ferrites are flexible in their method of magnetisation. Ferrites being weaker than rare earth magnets generate lesser back EMF compared to their rare earth counterparts. This allows ferrite machines to achieve more torque at a higher speed. It has the same effect of mechanically field weakening the motor (by increasing the gap between the stator and the rotor). It provides a higher efficiency compared to electrical field weakening, because there is very little 'negative' current required to weaken the field, as it has already been done due to the flux lost in the higher air gap. The drive for lower cost in electric machines provides an opportunity to use low cost ferrite materials, but careful thought is required to make a compromise between weight, cost and performance when using non rare earth materials.

Another method of reducing the price of electric motors is to reduce manufacturing/assembly costs. Assembly and testing costs for an induction machine tend to be around 30% of the total cost, while it is around 21% in the case of a permanent magnet machine [38]. Induction machines require expensive tooling and man hours due to the extremely tight tolerance between the stator and rotor. Permanent magnet machines tend to operate with a slightly higher air gap, hence less expensive machines are required for the assembly processes. Modular construction of the stator and rotor components helps reduce manufacturing and assembly costs in the long run. If the same windings are used in different machines with different concentrations, a set of windings can be made as standard. Studies have shown that standardising windings and rotor magnet configurations allows for lower manufacturing costs [41]. Axial flux motors offer the highest potential to standardise windings and magnets, as they are not as tightly wound as in the case of radial flux machines. Axial flux machines with modular windings tend to be of concentrated winding architecture rather than lap winding. In this case, the copper coils can be pre-wound and slotted onto the stator poles. This is a very simple process compared to tight winding around the stator as in the case of a radial flux machine, where the winding process happens in situ with the stator assembly process. The disadvantage of pre-wound coils being inserted onto the stator poles is the higher air gap between the coil and the stator pole (due to higher tolerances in pre-winding the coils). This causes field to weaken in the air gap due to loss in flux density between the coil and the stator pole. To overcome this issue, manufacturers tend to fill the gap between the stator pole and the coil with materials that have higher magnetic permeability than air.

Using standard size magnets (segmented pieces) can prove to be useful in reducing production costs, but careful analyses need to be done to avoid unwanted cogging which can be caused due to more gaps between each magnet piece. Segmenting magnets allows magnets of different sizes to be used in different combinations for different motor requirements. Segmented magnets can be arranged one next to the other or stacked one on top of the other, depending on their application to achieve the desired flux distribution. The arrangement of segmented magnets can be changed to produce a sinusoidal or a trapezoidal back EMF from the machine [42]. Figure 2-10 shows the forces acting on segmented magnets in an electric motor. Magnets S_1 and S_3 experience repulsive forces from magnet S_2 , while they are subjected to attractive forces by magnets N_1 and N_3 . These forces cause the magnets to detach from their location. This is a problem for segmented rotor machines, even though they have lower eddy current losses in the magnets compared to standard rare earth magnet machines.

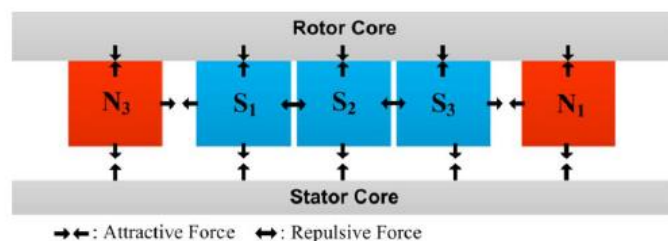


Figure 2-10 - Forces acting on segmented magnets in the rotor of an electric machine [42]

Axial flux motors are gaining more popularity in the field of electric machines, mainly due to their high power density and reduced axial length compared to radial flux machines, which allow for better packaging in certain applications. Radial flux

permanent magnet motors have higher torque per amp and torque density compared to induction machines due to the absence of rotor windings. This increases the efficiency as there is lesser rotor losses, but at the same time increases manufacturing costs as the magnets have to be placed on the surface of the rotor and need to be secure [34]. Manufacturing costs are further increased when segmented magnets are used for reduction in eddy current losses in the motor. Axial flux permanent magnet motors have the advantage of easier construction, lesser core material, higher torque density and hence higher efficiency [34]. Their thin disc like structure provides high torque per volume and high torque per weight. In an axial flux motor, the active torque producing component is the radial length, which is the distance between the inner and the outer stator radii [43]. The axial length is dependent on the flux density in the stator and rotor yoke. An axial flux motor's torque output performance is directly proportional to its length and to the square of the diameter.

Axial flux motors tend to outperform their radial flux counterparts when the number of stator poles are greater than 10 and the length to diameter ratio is less than 0.3 [44]. If the diameter remains the same and the number of poles are increased, the active torque producing component of the motor remains unchanged and facilitates reducing the axial length of the machine [43]. This helps in increasing the torque density of the machine. However, there needs to be a trade-off chosen between the number of poles and the stator diameter. A conventional axial flux motor has a single rotor and stator configuration. In cases of higher power requirement, a double stator with a rotor sandwiched in between can be used. This requires no rotor yoke, while if

a double rotor with sandwiched stator is used, a stator yoke can be avoided. This allows for further reduction in the axial length for a double rotor or stator design [44]. Another advantage of axial flux motors is the ability to stack them in situations where space is restricted. The easily stackable design of these motors makes them customisable to different automotive and off-highway applications. This provides flexibility for manufacturers in choosing a low cost and low weight specification hybrid, or add more units for a high power boosting system if required.

Permanent magnet AC machines run using a Variable Frequency Drive (or controller). The drive usually consists of a DC link from the battery or a voltage supply source, a rectifier bridge converter and an inverter to convert DC voltage to AC and vice versa. The present generation of inverters consists of IGBTs to switch ON and OFF based to generate a Sinusoidal Pulse Width Modulated (SPWM) signal. The control strategy for the PWM signal is loaded onto a microprocessor that determines the opening and closing of the Insulated Gate Bipolar Transistor (IGBT) gates. This controller operates on a feedback mechanism, relying on different parameters like speed, encoder position, current output, incoming voltage level etc. Based on these parameters and the required torque output, the controller creates a PWM voltage signal based on the intersections between a reference sine wave and a saw toothed carrier wave frequency signal. This produces the required voltage and frequency to drive a current through the motor to produce torque.

Figure 2-11 shows the torque speed envelope of a standard permanent magnet synchronous machine. The first region of constant torque is one of the biggest advantages of electric motors over internal combustion engines for traction

applications. Electric motors have maximum torque from zero speed, which helps significantly on pull away from standstill for automotive and other traction applications. Maximum current can be applied until the '*base speed*' or '*knee point*' of the machine, which is the maximum applicable AC voltage at the terminals of the motor. The maximum AC electric current in the windings till this point will remain constant, while the frequency of the AC sinusoidal signal increases with increase in speed. This relation is given by the formula –

$$N = \frac{120 * f}{P} \quad - (1)$$

where, N is the speed in rev/min, f is the electrical frequency and P is the number of magnet poles in the machine [45].

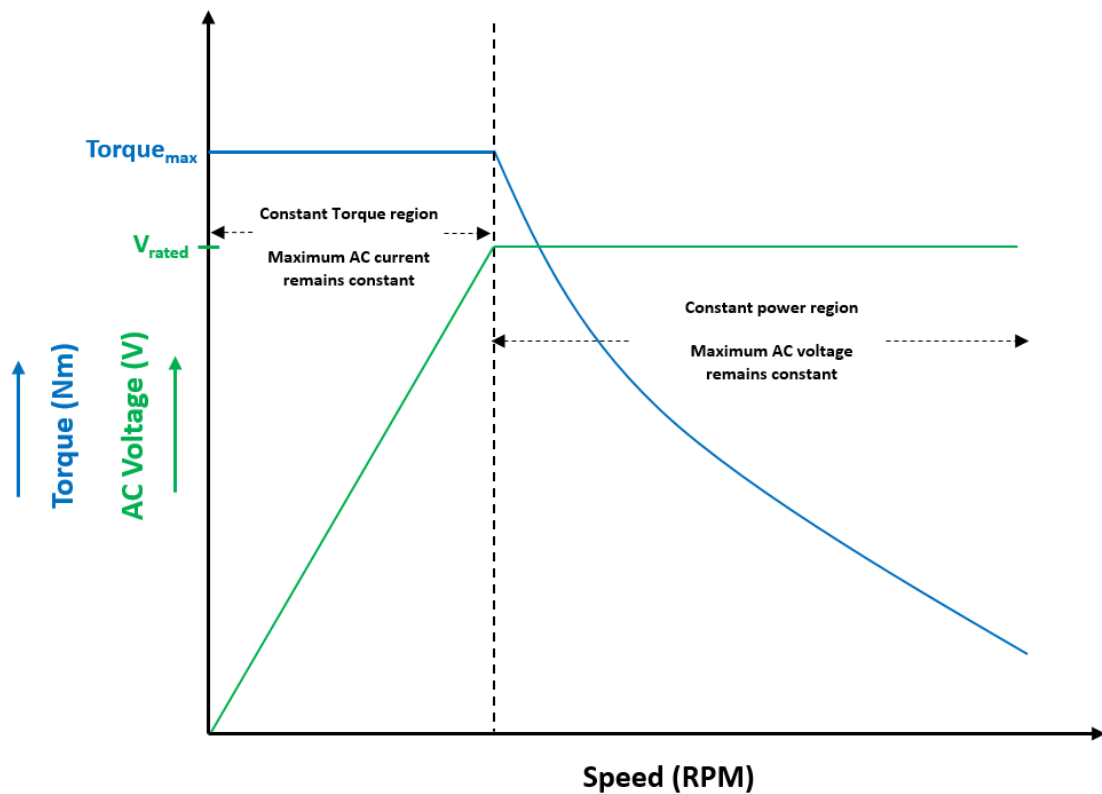


Figure 2-11 - Torque speed envelope of a standard permanent magnet synchronous motor

This formula holds for any synchronous electric machine. At the knee point, the motor controller will not be able to apply any further voltage due to the high back EMF generated by the machine. This means that the machine will no longer be able to sustain a constant torque value beyond this point. Theoretically this is the maximum speed that the electric motor can achieve (which is restricted by the system DC voltage), as the back EMF reaches a critical value opposing the system voltage thus prohibiting the flow of any further current. Present generation of electric motor controllers can go to a higher speed employing a phenomenon known as field weakening.

Field weakening is a common procedure in induction squirrel cage and brushed DC machines where winding currents are reduced to lower the back EMF of the machine so as to attain a higher speed. However, a permanent magnet machine does not have field windings, and the magnets apply a constant magnetic field. The AC current in the coils of a PM machine has two components – I_d and I_q . I_d is the active component of current (called direct current) that produces torque and I_q is the reactive component of current (called quadrature current) that produces the field. To achieve maximum torque, the I_d has to be maximum. Field weakening in permanent magnet machines is achieved by increasing the I_q component of current, which opposes the field induced by the permanent magnets. This method of controlling the active and reactive currents by an inverter is called Field Oriented Control (FOC). Thus, to drive a current through the machine, the system AC voltage must be higher than the opposing EMFs, which include the voltage drop due to the resistance in the coil, the drop due to the inductance of the coil and also the back EMF of the machine.

$$V > \text{Resistance load} + \text{Inductive load} + \text{Rate of change of flux} \quad - (2)$$

where, V is the system AC voltage; Resistive load is $I_d \cdot R_d$, where I_d is the direct current, R_d is the resistance of the coil; Inductive load is $L_d \cdot dI_d/dt$, where L_d is the self-inductance of the coil; Rate of change of flux gives an indication of the back emf.

On application of the opposing magnetising current, the back EMF value remains constant and the voltage and frequency can be increased, which in turn increases the speed of the machine. However, the maximum torque of the machine is lowered due to the reduction in the effective magnetic field in the air gap of the motor. This can be carried out to a point where the I_q reaches its maximum limit and there is no more direct current to produce torque in the machine. This is the system limit of the motor and inverter when the motor is specified to a certain voltage level. A big concern for field or flux weakening of permanent magnet machines is that the opposing field has the potential danger of demagnetising the permanent magnets. However, using materials with higher coercivity like Samarium-Cobalt magnets allows for increasing the field weakening current component without demagnetising the magnets [46].

Figure 2-12 shows the magnetic flux lines for an axial flux machine [47]. The short yoke increases the power density and reduces the stator losses. Due to the modular construction of the machine, it has long end-windings and poor copper fill factor, which reduces its efficiency compared to radial flux machines. However, taking into account the low cost construction of these machines, a small reduction in efficiency (~2-3%) is usually acceptable. The figure also shows the flux densities of a double rotor axial flux machine. It can be seen that under full load, the flux density is around 1.8 tesla [47].

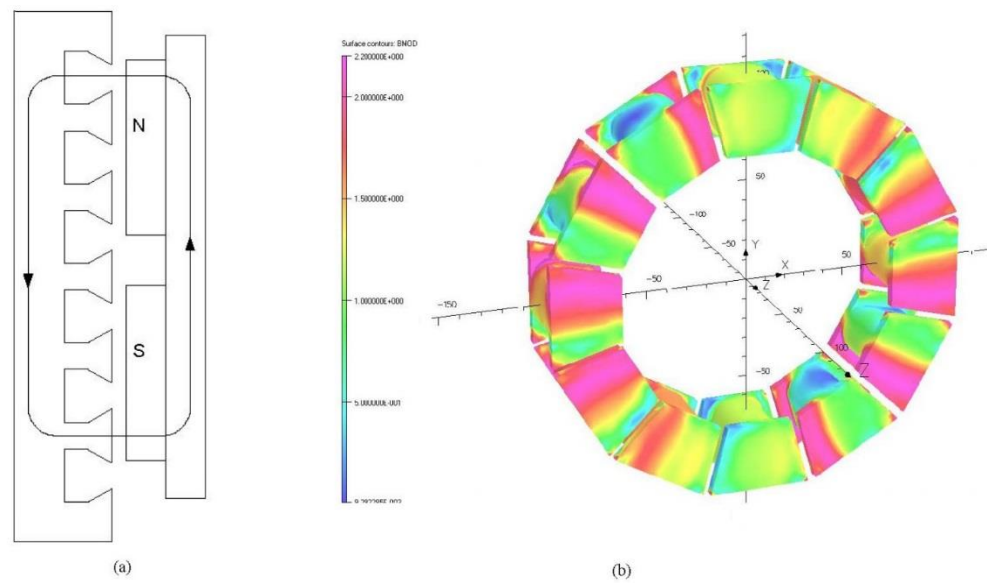


Figure 2-12 - (a) Magnetic flux lines for an axial flux machine (b) Flux densities of an axial flux machine ^[47]

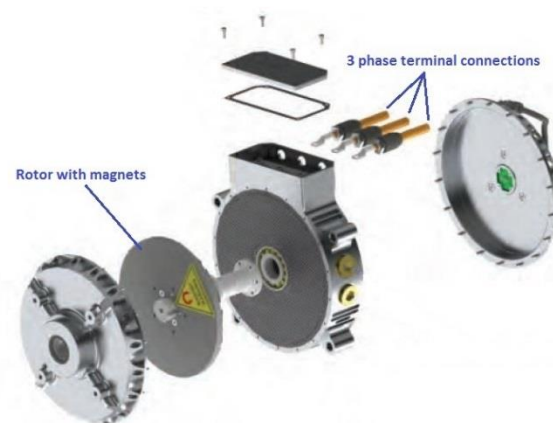


Figure 2-13 - Axial flux motor construction (Source: Ashwoods Automotive Ltd)

One of the biggest advantages of axial flux electric motors is the capability to mechanically weaken the field. Figure 2-13 shows the construction of an axial flux electric motor developed by the industrial partner. The arrangement of the stator and rotor in an axial flux motor allows its air gap to be changed easily when compared to radial flux motors. As the rotor is moved away from the stator, the magnetic flux density in the air gap is reduced and hence the motor will not achieve the same maximum torque that it did with minimum air gap. But the reduction in the flux density also reduces the back EMF of the machine, allowing the motor to reach a higher speed than what it normally can achieve. This method of field weakening can be less problematic than electrical field weakening as there is no 'negative current' applied to weaken the field. Hence there is no risk of demagnetising the rotor magnets using this method. Studies have shown that motors with varying air gap have more advantages than conventional fixed air gap motors because their operating points can be chosen based on the least losses encountered. Due to the fact that variable air gap motors have a varying torque constant value, they have lower spinning losses, but also they have higher torque losses as there is higher amount of magnetic leakage in the air gap due to the higher gap between the stator and the rotor [48].

High cost of electric motors has always been a hindrance in its acceptance among automotive manufacturers. Reduction in manufacturing and R&D costs are possible in different ways, but may reduce the performance of the machine. Adding ferrites in the magnet reduce the cost considerably, but add extra weight to the electric machine for the same power output of a permanent magnet machine. Reduction in

R&D costs is possible by automating procedures and reduction in man hours on the manufacturing/testing facility, although initial investment costs will be high. This thesis discusses automated testing of the motors as a method to help reduce cost of testing and validation of motors. Field weakening is an important parameter in permanent magnet machines, to improve high speed operation of the machine. Axial flux motors provide the option to vary the air gap between the stator and the rotor, which is analysed later in the thesis.

2.4. Driver behaviour

A driver is one of the most important parameters in an automobile. Driving style has a significant impact on the fuel consumption of the vehicle, which is evident by the ever growing attraction of driver behaviour improvement courses. Reducing exhaust emissions from vehicles has always been on the high priority list among car manufacturers and government bodies. With strict regulations, there has been significant focus by automotive manufacturers on improving Internal Combustion (IC) engine efficiency through turbocharging and extreme boosting technologies. At the same time, there has been an increase of electric and hybrid electric vehicles. A number of potential routes for the latter have been pursued by engineers, which include use of electric motors with battery packs, fuel cells, super-capacitors etc. Powertrain technologies that aim to reduce fuel consumption and exhaust emissions take longer to be adopted by all manufacturers and thus their impact will be clear only after a decade [49-51]. A more practical solution to reduce fuel consumption and hence emissions in the current scenario is to concentrate on driver behaviour

improvement. This provides a much quicker return over investment to the consumer, compared to the former [22]. An added advantage of concentrating on driver behaviour improvement is that savings in fuel consumption will be preserved even after the deployment of a new technology [52]. With price of fuel progressively increasing, improving driving style provides an optimum solution to reduce vehicle running costs with minimal monetary investment in the current economic climate.

Studies have shown that concentrating on improving driving style can offer 10-15% of fuel savings [22]. Reduced rates of acceleration and generally driving more 'gently' and skilled evasion of unwanted stops can save up to 14% in fuel consumption, without increasing much of the travel time [51]. There are a number of steps that can be taken to ensure reduction in fuel consumption while driving. Previous studies have shown the impact of different mechanisms of reducing fuel consumption, but it is unclear as to how one should control their vehicle to attain the best fuel economy. Research done on driver behaviour have shown that habits of changing into a higher gear, reducing the rate of acceleration and deceleration etc. are the most effective and easiest ways to reduce fuel consumption in any vehicle [53]. In this thesis, driver behaviour improvement refers to driving optimally to attain minimum fuel consumption by operating the vehicle under conditions for best efficiency, which is shifting through gears more quickly and avoiding unnecessary events of acceleration and braking.

Optimal driver behaviour can be assessed on a number of criteria. In this thesis, it relates to a driving style that minimises the fuel consumption of a vehicle on a particular journey. Providing feedback to the driver is an essential part of driver

behaviour improvement in terms of drivers understanding when and how to improve on their existing driving style. There are a number of ways by which feedback can be provided to drivers - the driver could be given driver behaviour improvement courses which provide information on his/her driving style, or certain systems can be used in the vehicle that detect driver behaviour that contradicts optimal driving style and provides real time feedback to the driver. But care must be taken so as to not distract or deviate the driver's concentration or attention from the most important aspect of the journey, which is driving safely. Both these methods have their pros and cons.

Driver behaviour courses are effective to a certain extent, but this method cannot guarantee that drivers stick to their 'newly learnt' driving techniques. Besides, it is difficult for experienced drivers to change their respective driving styles that they are used to. Instantaneous feedback on the other hand provides drivers the opportunity to understand when and where they can or need to improve. This has its advantages, but care needs to be taken to ensure that these devices are not intrusive to the driver nor should it distract his/her attention from the road. Studies have shown that providing instantaneous feedback to the driver provides more control of the driver's actions for improving driving style. It also helps preserve good driver behaviour for a longer term [51]. One of the reasons for this is that the driver knows exactly when and how he/she has deviated from the optimum driving style and has the opportunity to improve whilst still in the process of driving. If a device in the vehicle continues to advice on improving driving style, drivers tend not to fall back to their original driving style, instead continue to improve and drive more economically.

Even though driving calmly and shifting early may reduce fuel consumption, they will not provide a complete understanding on how to achieve optimal driving style. Hooker [53] collected extensive data from real world driving and chassis dynamometer tests of 15 different types of vehicles ranging from a four cylinder car to a V8 pick-up truck, from 5 different manufacturers. The researcher acknowledges the fact that traffic conditions like movement of other vehicles and pedestrians have an impact on fuel consumption of the vehicle, but for this study these conditions and also the timing of traffic lights were ignored; or rather it was assumed that these conditions do not affect a driver's ability to drive in the optimal fashion. It is not possible to identify an optimal driving behaviour for every possible traffic situation, but it is possible to calculate an optimal control for a few simulations which can act as an example for other driving situations.

One of the positives from Hooker's test was that the vehicle model used was based on statistical data collected from 15 vehicles, rather than an engineering model of the car's behaviour. Thus the predictions of his optimal driving style are not based on how the vehicle *should* behave in relation to its design, but how it *does* behave in accordance with chassis dynamometer and real world test data collected. The data collected from testing of the vehicles was used to determine optimal driving style for each type of vehicle and the results were compared against each other to understand whether it is possible to converge at one driving style for different type of vehicles. The driver behaviour predictions were based on a number of key vehicle parameters, like speed, acceleration, engine/vehicle load etc. The first stage of data collection involved steady state testing of each vehicle on the chassis dynamometer where over

a thousand measurements of fuel consumption were taken for different engine operation speed and load points. The load in a petrol engine vehicle was expressed as a function of the manifold vacuum, and for a diesel engine, the load was the pedal position [53]. The second stage of data collection involved taking fuel consumption measurements on the test track so as to cover nearly all operating points of engine speed and load. This was performed for different vehicle speeds and accelerations. The third stage involved data analysis to correlate the measured fuel consumption from the track test to the measured fuel usage from the chassis dynamometer tests. These were compared and analysed to create certain fuel economy maps for each vehicle. This formed the 'pre-requisite' for the dynamic programming used to determine optimum driving style. The mathematical problem consisted of four different questions –

- a. *Cruising problem* – how to achieve minimum fuel consumption on a level road when at a steady stated speed.
- b. *Acceleration to cruising speed problem* – how to accelerate from zero speed to a cruising speed most efficiently.
- c. *Driving between stop signs problem* – how to minimise fuel consumption when driving on level surfaces when covering fixed distances before stopping.
- d. *Driving over hills problem* – how to minimise fuel consumption when driving over roads with gradients that are not equal to zero.

Dynamic programming provided solutions to these mathematical problems. Most of the solutions were generic to what drivers would usually do given these circumstances, while others gave an indication of a trade-off between two solutions.

The cruising problem had the simplest solution - to achieve the least fuel consumption on a level road at a certain speed, one needs to cruise at that speed with minimal speed fluctuations or changes in engine operating points. Acceleration to a cruising speed was where a trade-off was required between the disadvantage of fast acceleration, which consumes more fuel to overcome the initial inertia, and the disadvantage of slow acceleration which involves having to cruise at a higher speed (which consumes more fuel) to overcome the time lost from the slow rate of change of speed. However, it was determined that over an average speed and time, the rate of acceleration did not make a huge impact on the fuel consumption. Regarding optimum driving style in the city to cover 'blocks' of 300m each before reaching the next set of traffic lights, it was concluded that the fuel consumption was sensitive to how quickly one covers the block, which meant rapid accelerations would again be a negative for fuel economy [53]. The same was the result of driving at different gradients. Thus according to the researcher, the optimal driving style simulation was applicable to different vehicles for the latter two problems. This research highlighted one of the main issues in economical driving- acceleration, and thus addressing it was a critical path in the thesis.

A number of driver behaviour improvement courses, or 'eco-driving' courses where the driver is directed to drive more moderately has been attempted in the past [50]. Only a few studies report the long term impact. A study on driver behaviour monitoring for commercial buses in Sweden after drivers underwent an eco-driving course showed an improvement of 2% in fuel consumption 12 months after completion of the course [54]. The Centre of Renewable Energy Sources of Greece

conducted a trial eco-driving course for buses in Athens, and observed 4.35% savings in fuel usage as early as two months after the course [55]. Beusen [56] conducted an experiment on driver behaviour with thirty drivers driving their own cars. Since tracking fuel purchase and usage from the drivers was tedious and caused volunteers to back out, he decided to collect data using a device connected to the On-board Diagnostics (OBD) port using Controller Area Network (CAN) communication. This avoids any user induced error in providing information, as the data collected will be fool-proof and accurate, and also reduces the burden on the volunteer. The device also had a GPS sensor that would detect the position of the vehicle at every instant and also calculate its speed, and also a GPRS modem that would send data stored on the memory card of the device to a server on a daily basis. Various parameters like engine speed, throttle position, mileage, gear position, engine coolant temperature and instantaneous fuel consumption were logged using the CAN communication on the vehicle.

Drivers were asked to provide information on their travel motive and the correct driver for a particular trip, to avoid discrepancies arising from multiple users of one car for different trips. Using CAN loggers are an effective way to retrieve information from vehicles, but they can be tricky, as different manufacturers use different addresses to transmit certain vehicle parameters. This meant the researchers had to use a case by case testing method to find key vehicle parameters for each vehicle. Also, not all parameters were readily available, and not all drivers provided enough information regarding multiple driver usage or motive of trips. This reduced the useful data sample for analysis from thirty cars to just ten. This sample size is too

small to understand a general impact of eco-driving courses on a broader scale, but can be used to co-relate the effect of these courses on individual drivers [56].

Drivers were allowed to view their GPS trackers online on the servers, but were not provided any feedback during the first round of the experiment so as to obtain their 'baseline' driving styles. Halfway through the experiment, all drivers were asked to participate in a four hour eco-driving course. The course consisted of a drive prior to a lecture session on basic fuel efficient driving styles, followed by a second drive in the same vehicle with advice from an instructor. The basic rules for fuel efficient driving provided to the drivers were to shift early into higher gears, use the highest gear possible at steady speeds, to maintain a steady speed by anticipating the flow of traffic and to smoothly decelerate by lifting off the pedal when the car is in gear. Certain additional rules like turning the engine off during long stops and avoiding over speeding (above 120k/hr which is the legal speed limit in Belgium) were also directed towards the drivers during the course. Over a period of 10 months, over 2000 hours and 116,000 kms worth of driving data was collected from these drivers which allowed for a good analysis of the effect of the eco-driving course.

A number of parameters were calculated to assess driver behaviour. Total distance covered, average speed, average shifting point, percentage of deceleration using engine brake, percentage of heavy acceleration, deceleration and time idling were some of the important ones. On further analysis of the data at the end of the test, it was clear that the eco-driving course had a significant impact on the fuel consumption of the sample as a whole. It was observed that there was no reduction in the average speed or weekly distance, suggesting that drivers did not change their

travel patterns. Thus the reduction in fuel consumption was predominantly due to the change in driver behaviour. The course made considerable impact on most of the driver behaviour improvement parameters, except idling time and average gear shifting points.

An overall savings of 6% among the ten drivers was seen for the experiment, with individual drivers showing improvements from 12% to -3%. Drivers that showed relatively less improvement (~1%) had showed significant improvement in time spent in lower engine speeds, but their average shift points did not improve, which provided an insight into the importance of shifting gears at the right time. There was a week by week improvement through the ten months of the trial, with a major change in driving style right after the eco-course mid-way through the experiment. The interesting fact was that four out of the ten drivers had already started improving their driving styles in the weeks prior to the course. This was evident from data collected and certain parameters analysed on their driving behaviour [56]. This also highlights a concern of the author of the thesis that drivers who participated in experiments of driving style in most of the literature discussed were aware that they were being tested to understand their driving style and its impact on fuel consumption. This may have caused the data collected to be skewed.

Based on existing literature available in 1997, Van der Voort *et.al.* [51] developed a system that provides immediate feedback to the driver when he/she deviates from a certain set rules that define good driver behaviour, based on using minimum fuel consumption for certain manoeuvres. He studied the disadvantages of similar devices used in the past and concluded that the new device would provide the driver with

clear and non-contradictory feedback taking into account the context that the vehicle is in. It would also place no extra burden on the driver which is too hard to process with the existing task of driving and also work within an urban and extra urban environment [51]. The system incorporated a data logging device which used various sensors to collect key vehicle parameters, a data processing module to instantaneously assess driving style, and a Human Machine Interface (HMI) that advised the driver on how to change his/her driving style. The system architecture consisted of a normative model in which optimum driving styles for various types of driving situations are defined, for example, acceleration, cruising events, braking etc. These different situations are called 'states' and it will be easy to determine the instantaneous state of operation of the driver. Using state machine architecture improves the efficiency of the code and reduces the actual size and programming power required for an operation. In this case, determining each state is critical as optimal driver behaviour depends heavily on how the vehicle is driven at that particular moment. The system is dependent on different on-board vehicle sensors to provide inputs to it at the right time.

Key vehicle parameters logged include engine speed, vehicle speed, pedal position, gear position, clutch (engaged or disengaged), braking force, steering angle and headway. Steering angle and headway need additional sensors to be measured accurately, but are not essential for the determination of fuel economy. However, they provide improvement in assessing the context the vehicle is in. Steering angle measurement helps isolate events that have a significant effect on the fuel consumption of the vehicle - say in the case of braking for a sharp corner, an

overtaking manoeuvre or getting onto the motorway from a slip road. Headway is the distance or time from the vehicle in front or behind the measured vehicle. It provides an indication as to whether the situation is safe to provide feedback to the driver or whether to wait until a later time to ensure the driver is not distracted from the concentration required on the road.

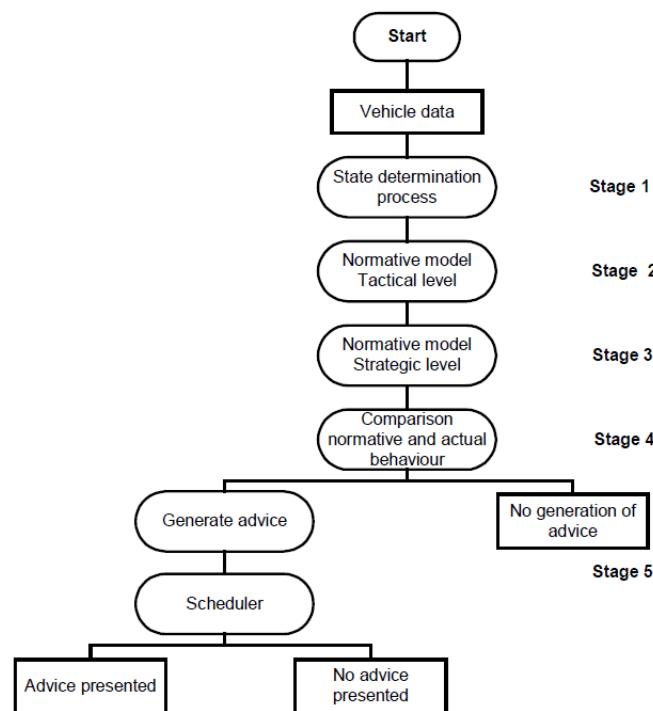


Figure 2-14 - Structure of total model used in Van der Voort's driver behaviour improvement tool ^[51]

Figure 2-14 shows the model used in the programme of the driver behaviour improvement tool. From the data collected from the sensors, the current state of the vehicle is determined. Identical states are grouped together and called a manoeuvre, which is defined as a unit for analysis. This unit is then compared with an optimal driving style. The model also consists of the engine operation map, and part of the algorithm tries to help the driver operate the vehicle in the lowest BSFC point on the

engine map. The tactical level of the normative model is concerned with the instantaneous activities and compares them to the optimal driving style. The next level is the strategic normative model, which gathers a bit more data to assess the driving behaviour over a longer period of time to ascertain a temporal context [51].

The actual driving style is then compared to the normative driving model and if the difference between measured driving parameters and optimal driving style is large, the driver's behaviour is classified as non-optimal and the decision is made to provide feedback to the driver. The scheduler ensures that feedback is only provided when it is safe to do so, based on the determination of the existing context of the vehicle. The scheduler includes a safety check, which runs every time a feedback is provided to the driver. In every case, safety takes priority over fuel consumption for good reason, and a feedback may be cancelled if it is deemed to be delivered in a dangerous situation [52]. The feedback is provided through an HMI which is a display screen next to the steering wheel.

To test the device, a group of drivers were first asked to drive in a fuel efficient manner on a driving simulator before the device was fitted on. The drivers achieved a fuel saving of 9% with just driving in a fuel efficient manner without support, while with the device providing advice to drivers, they were able to achieve a reduction in fuel consumption of 16%. The reduction in fuel consumption was mainly due to a change in driver behaviour, which involved changing into higher gears sooner during the acceleration phase. It was also observed that drivers began anticipating the flow of traffic to try and reduce unnecessary braking and acceleration events. The device was then used on the road in real traffic conditions. 36 drivers drove over a specified

route over five times with them either having support from the device or under their normal driving style. It was observed that the driver advisory tool helped save 11% in fuel consumption across the range of vehicles. Over urban sections of the route, participants were able to save up to 20% in fuel compared to their normal driving styles. The researchers concluded that the advisory tool played a significant role in the reduction of fuel consumption, mainly by driving in the appropriate gear (shifting into higher gears earlier), anticipating traffic flow and also switching off the vehicle in long idling instances. It was also observed that drivers were smoother in their driving style with the device providing them with feedback [52].

Studies have shown that driver behaviour has an impact on the fuel consumption of the vehicle. Fuel consumption again has a direct correlation to exhaust emissions, mainly carbon dioxide (CO₂) emissions from the vehicle. Experiments were conducted by De Vlieger *et. al* [57] where, a sample of seven drivers were asked to drive different cars calmly, normally and aggressively to measure the difference in exhaust emissions caused due to driver behaviour. Calm driving meant anticipating other road users and lower rates of acceleration and deceleration, while normal driving involved moderate events. Aggressive driving which involved severe acceleration and braking events had an increased fuel consumption by up to 40% when compared to normal driving style. It was observed that a bad driving behaviour resulted in CO emissions being up to three times higher, and HC and NO_x emissions being two times higher compared to normal driving.

Pedal position has an important role in the fuel consumption of the vehicle. Petrol engine vehicles usually run on a stoichiometric air fuel ratio or leaner. This provides

good fuel economy as there is no excess fuel being wasted unburned in the exhaust. Calm driving which involves steady movements of the accelerator pedal helps maintain stoichiometric ratio for longer periods of time. Tests were conducted by Alessandrini *et. al* [58] on the chassis dynamometer to baseline the 'calm' and 'aggressive' driving styles of drivers. This was then used to assess driving performance of drivers in the real world, by connecting a data logging device to the OBD port of the vehicle to collect key vehicle parameters. A GPS sensor was also fitted to the vehicle to identify its position and context of instantaneous operation. Aggressive driving style was categorised by detecting pedal position changes of 25% in less than one second, which caused a non-stoichiometric mixture being injected into the cylinders of the petrol engine. It was observed that pedal position was independent of the drive cycle and that different drivers had different pedal usage patterns in the same traffic conditions.

It was observed in Van der Voort's [51] experiment that the average speed of the journey does not get affected as a result of moderate driving when driver behaviour improvement tools are used. One of the main reasons for the decrease in fuel consumption was due to the early shifting (mainly from 2nd to 3rd gear) during the acceleration phase of driving. It was also seen that there was a decrease in the maximum deceleration of the vehicle over the entire speed range between normal driving and advisory tool aided driving. Tests conducted on the chassis dynamometer at the University of Bath on a Citroen Berlingo, managed to obtain a 3.6% in fuel savings over the New European Drive Cycle (NEDC) by changing the gear shift points. To achieve this, the vehicle was initially mapped on the dynamometer and a

backward facing computational model of the vehicle powertrain was developed in Simulink. This model is more representative of the vehicle performance than using data from steady state engine map data. Around four minutes of data was collected at each speed. Data collected at low speeds and low loads were not as usable as the ones collected at high speed and load conditions. It was also observed that the engine does not produce useful tractive force until the pedal position is greater than 25% and this force is saturated when the pedal position is 70%. On a cold engine, changing the gear shift points helped save 4.3% over the baseline test of the vehicle with the standard NEDC shift points, which accounted for a 4.5% reduction in CO₂/km [59]. This along with other technologies will help achieve the 10g/km of CO₂ reduction from additional complimentary measures for new car fleets, a regulation set by the European Union [3]. However it is not clear whether the savings achieved on chassis dynamometer testing of NEDC would result in similar savings in real world conditions, as the NEDC is not viewed as representation of real world conditions.

Based on surveys and road test experiments conducted on a number of drivers, Gonder *et. al* [60] said that adopting efficient driving styles can save up to 20% in fuel when compared to aggressive driving style, whilst a more realistic shift from moderate to efficient driving style would result in 5-10% savings in fuel consumption. The researcher acknowledges the importance of external factors beyond the drivers' control to improve, like traffic situation, lack of torque/power of the vehicle and in certain cases anxiety of getting to the destination quickly. For many drivers, the perceived value of a fractional reduction in their spend on fuel costs was insufficient compared to the idea of changing their driving behaviour [60]. The survey highlighted

that for individuals with an open-minded approach to improvement in their driving styles, clear feedback on how to improve with respect to a reference point (say current speed, acceleration, fuel consumption etc.) need to be provided in order to maximise the improvement. The author recognises that commercial fleets of vehicles have the greatest potential in reducing fuel consumption by change in driving style due to the fact that these vehicles are not driven by their owners nor do the drivers pay for the fuel, thereby eliminating the motivation to drive conservatively and save fuel. This rationale was acknowledged when the driver behaviour improvement tool described in this thesis was developed.

The study also highlighted the fact that incentivising drivers was a good way to motivate them to improve their driving style [60]. This formed the basis of a research study based in Spain, where 'gamification' was used to motivate drivers to improve their driving style. In the study, the researchers talk about using features of gaming in real driving situations to enable drivers to compete with each other and improve their driving style [61]. Gamification is increasing in popularity due to its proven track record of working in certain situations. The researchers decided to adapt this to real world fleet vehicle scenarios with 36 drivers in three different cities in Spain. For the awareness game, certain rules were set, like – the driver must not over speed, accelerate harsh or brake unnecessarily etc. The driver was scored based on his/her adherence to the rules and the fuel consumption benefits seen in driving the vehicle. There is also a leader board which ranks drivers based on their performance, but care is taken so as to compare only similar drivers against each other. Other gaming features like 'badges' incentivise even further, with drivers being able to unlock

certain features and challenges and scoring mechanisms etc. Tips and tricks on how to improve driver behaviour to reduce fuel consumption were provided to the driver in between the experiment.

It was observed that 5-25% improvement in fuel consumption can be achieved if the drivers take the right feedback and make necessary changes to their driving style. To rank the drivers effectively, a fuzzy logic system was developed that identified each of the driver's driving style and scaled it to a standard score between 0 and 10. The ranking system took into account a number of external conditions that may have affected the fuel consumption of the vehicle and corrections were applied for it, before making comparisons between drivers. Parameters like average speed (to determine what type of road the driver chose for the journey), time of the day (to understand whether the chosen time of travel is during rush hour), weather, trip duration/distance etc. were assessed before fuel consumption figures were compared between drivers.

Driver behaviour was analysed based on certain driving characteristics. The first is the percentage of sudden acceleration or deceleration events, which tend to show a general aggressiveness of the driver. Another parameter is the standard deviation of vehicle speed, which is used mainly when the vehicle is not accelerating. This gives an indication of the smoothness of the driving style of a driver. Fuel consumption is reduced when effective cruising is carried out. Percentage of high engine speed and high vehicle speed show inefficient driving styles, although this can also mean that the vehicle is on a motorway at high speeds. In this case it needs to be checked as to whether the vehicle is in its highest possible gear or not. A term called Positive Kinetic

Intensity is also used to measure the aggressivity of driving style and it depends on the intensity of positive accelerations of the vehicle [61].

$$PKI = \frac{\sum (v_i - v_{i-1})^2}{d} \quad - (3)$$

where, v is vehicle speed in m/s and d is distance in meters between v_i and v_{i-1} [61].

A low value of PKI means low aggressivity of the driver [62]. These parameters were analysed on the data collected and the results were normalised to a score between 0 and 10, using which the drivers were compared. When the concept was tested on the drivers, there was a decrease in fuel consumption of the vehicles. There was a significant increase in the motivation of drivers to drive conservatively to save on fuel. The researchers acknowledge the importance of feedback, because before it was introduced, drivers took more time in adopting an improved driving style. Feedback also ensures that drivers do not tend to fall back to their normal driving styles.

The experiment was conducted on two sets of drivers, one which only had the driving style feedback, while the other which had both feedback and participated in the social game. It was noted that there was more improvement in various driving parameters of the drivers who participated in the driving feedback experiment with the social game when compared to the former [61]. This showed that gamification can be an effective tool in improving driving style by mainly incentivising the driver and keeping up the motivation to continue improving. This results of this particular research study into gamification also corroborated well with the findings of this thesis.

According to Ericsson, although driving pattern is mostly related to the speed profile of the vehicle, other parameters and conditions like gear shifting, route of choice, travel times, stops per kilometre, running speed (excluding stops or idling), average speed, acceleration and deceleration values, running time etc. need to be included in the assessment [63]. 62 different parameters were defined that are linked directly to the driving style of a particular driver. Table 2-1 shows the 62 parameters identified in this literature. Of these, 44 were used to describe the instances, frequency and intensity of speed, acceleration and deceleration of the driving behaviour, while the remaining 18 were used to interpret engine speed and gear choices. Driving styles were analysed for nearly 19,000 kms worth of driving data representing 2,500 different journeys using five cars of different sizes and performance, each equipped with data logging hardware that collected the essential parameters necessary for detection of driving style.

After the definition of the 62 different parameters, factorial analysis by regression and ANOVA was performed on these values to examine the elemental properties of driving behaviour. This reduced the number of active parameters to 16 from 62, each characterising one aspect of driving pattern. Regression analysis on the 16 factors and their relation to emission and fuel consumption were performed and it was seen that 9 out of the 16 had significant impact [63]. The same data was later used in another study to identify other factors of driving that affect fuel consumption. This revealed a few different results, some of which were easily predictable, like the fact that average speed was lower during peak hours when compared to off peak hours, while there

were other correlations like the fact that men tend to have higher average acceleration values than women [64].

It was concluded that driving pattern is a complicated phenomenon, which is affected by a number of different variables ranging from the driver and the vehicle to the environment and traffic conditions. For a more precise understanding of driving pattern and variation in driving style, more number of parameters need to be carefully logged and assessed, making every experiment more complicated and time consuming. It was studied as to how different influencing factors like street environment, traffic conditions and the driver, affect driving pattern and fuel consumption.

It was evident that street conditions and type had the biggest impact on driving pattern, followed by the driver. Different drivers drive in different ways, but the level of the impact of the driver on fuel consumption was less than that of the street type chosen for the journey. This also highlighted the need to have a number of random drivers when experimenting for driver pattern, otherwise the results may be skewed and biased. Regarding male and female participants, it is clear that the driving styles of both genders are different, with men having higher average accelerations spending more time in higher acceleration classes, with women having lower average accelerations and spending higher time in lower acceleration classes [64]. The study thus recommended for gender be added as another driving variable in addition to traffic and the vehicle conditions.

Table 2-1 - Driving pattern parameters identified by Eva Ericsson to assess driving behaviour [62]

Driving parameters	
Average speed	
S.D. of speed	
Average acceleration	
S.D. of acceleration	
Average deceleration	
Deceleration SD.	
Number of acceleration/deceleration shifts per 100 metres where the difference between adjacent local max-speed and min-speed was	> 2 km/h
	> 10 km/h
Number of acceleration/deceleration shifts per 100 seconds where the difference between adjacent local max-speed and min-speed was	> 2 km/h
	> 10 km/h
Relative positive acceleration: $1/x \int a \, dt$, x = total distance	
Integral of the square of the acceleration : $1/n \int a^2 \, dt$, n = no time steps	
% of time when speed < 2km/h	
Average stop duration	
Number of stops per kilometre	
% of time in speed interval	0-15 km/h
	15-30 km/h
	30-50 km/h
	50-70 km/h
	70-90 km/h
% of time in speed interval	90-110 km/h
	> 110 km/h
% of time in deceleration interval	(-10)-(-2.5) m/s ²
	(-2.5)-(-1.5) m/s ²
	(-1.5)-(-1.0) m/s ²
	(-1.0)-(-0.5) m/s ²
% of time in acceleration interval	(-0.5)-(0) m/s ²
	0-0.5 m/s ²
	0.5-1.0 m/s ²
	1.0-1.5 m/s ²
	1.5-2.5 m/s ²
	2.5—10 m/s ²
Average engine speed	
Engine speed SD.	
% of time with engine speed	0-1500 rpm
	1500-2500 rpm
	2500-3500 rpm
	> 3500rpm
% of time in gear 2 with engine speed	0-1500 rpm
	1500-2500 rpm

	2500-3500 rpm
	> 3500rpm
% of time in gear 3 with engine speed	0-1500 rpm
	1500-2500 rpm
	2500-3500 rpm
	> 3500rpm
% of time in gear 4 with engine speed	0-1500 rpm
	1500-2500 rpm
	2500-3500 rpm
	> 3500rpm
% of time in gear 5 with engine speed	0-1500 rpm
	1500-2500 rpm
	2500-3500 rpm
	> 3500rpm
Positive kinetic energy, PKE: $(\Sigma(v_f^2 - v_s^2))/x$ when $dv/dt > 0$, v_f = final speed, v_s = start speed, x = distance	
% of time when (va) is	< 0 m ² /s ³
	0-3 m ² /s ³
	3-6 m ² /s ³
	6-10 m ² /s ³
	10-15 m ² /s ³
	>15 m ² /s ³
Average (va)	

Introduction to driver behaviour improvement device

Taking into account the strengths and weaknesses of driver behaviour improvement solutions described in the literature, a new driver behaviour improvement device for commercial fleet of vehicles was developed at the University of Bath. One of the biggest drawbacks in previous literature that led to the development of the feedback tool, was the fact that all the participants in the experiment knew that they were being tested to understand the link between driving style and fuel consumption, which may have made them conscious while undertaking the baseline testing of their driving style, thus skewing the results. In psychological terms, this problem where the subjects' knowledge of being part of an experiment may change their actual behaviour is known as the Hawthorne Effect [65]. To avoid this problem, once the

driver feedback system was developed, it was tested on different commercial fleets, firstly with the unit behaving as a data logging system without the driver's knowledge of its presence, recording the drivers' baseline or 'normal' driving style, and then with the device turned on providing instantaneous feedback to the driver [50].

The driver behaviour improvement device is called Lightfoot in the commercial market and it can be fitted on to any vehicle to provide audible and visual feedback to the driver on his/her driving style. The device provides feedback based on the driver's performance. Information recorded from the vehicle is processed by the device and a report is also sent to the fleet manager who can then rank the drivers based on their performance. The device consists of a display unit that is fitted into the instrument panel of the vehicle and consists of two sets of LEDs, one showing short term (or instantaneous) driver performance and the other providing long term driver performance. The display unit also consists of an upshift indicator which asks the driver to shift up a gear when required. Audible warnings are played to the driver whenever the system detects a poor driving style. If these warnings are ignored, a violation is recorded. The device records the number of warnings and violations received on a Central server maintained by the industrial partner and the information regarding drivers is sent to the fleet manager of the particular company, who can then rank/incentivise drivers based on their performance. The major advantage of this system is that drivers are constantly given feedback on their driving style, which would prevent them from falling back to their original driving style as in the case of a passive system.

The algorithm for the driver feedback tool was developed in Simulink®, which is a block diagram based environment for multi-domain simulation and development of complex systems [66]. The device measures the vehicle speed to calculate a parameter known as Inertial Power Surrogate (IPS), which defines aggressivity of a driver. This was calculated as the product of vehicle speed and acceleration [67].

$$\text{Inertial Power Surrogate} = v \times a \quad - (4)$$

where, v is the vehicle speed in m/s , and a is the acceleration in m/s^2 [67].

The value of inertial power surrogate is in its representation of the inertial load and kinetic energy of the vehicle. IPS is thus a useful measure, as it signifies the rate of application of kinetic energy, which is directly linked to the measure of aggressive driving characteristics.

The system detects aggressive acceleration from the driver and compares it to known values collected from similar vehicles and determines whether the driver is aggressive or not; he/she is given a warning if found to be aggressive. Figure 2-15 shows the IPS calculation logic used in the development of the driver advisory tool. As mentioned above, the short term inertial power surrogate values are calculated as the product of the vehicle speed and acceleration, and filtered. The long term value is calculated in a similar way, but certain correction factors are added to this calculation to determine the final IPS_{LT} value, as it is this value that controls the audible warnings and violations of the system. These correction factors ensure that drivers are not unfairly penalised for certain unavoidable aggressive driving behaviours. These features were later improved and enhanced and will be discussed in detail in Chapter 4.

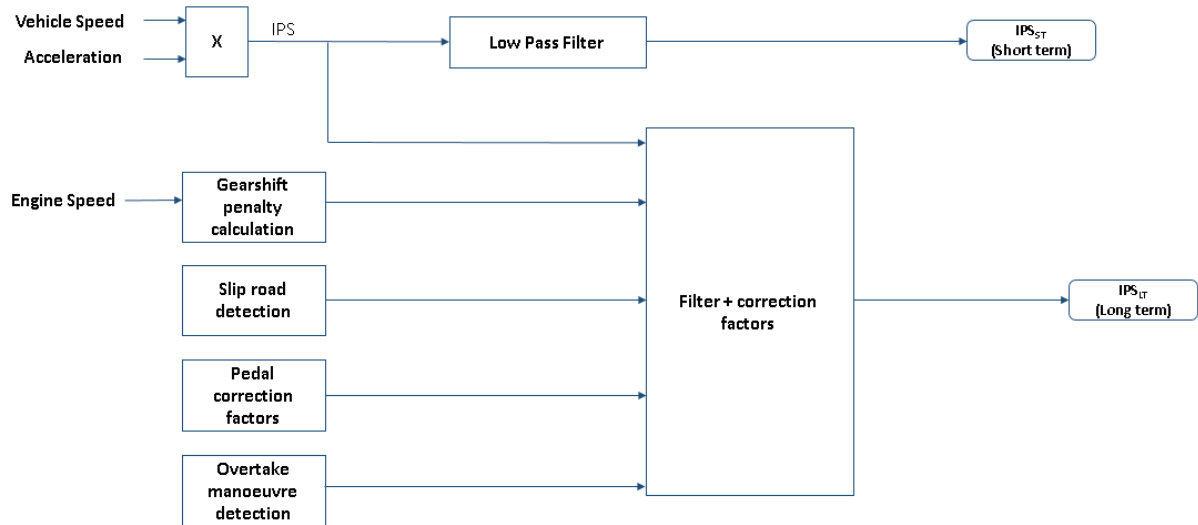


Figure 2-15 - Representation of the IPS logic used in the initial driver advisory tool algorithm

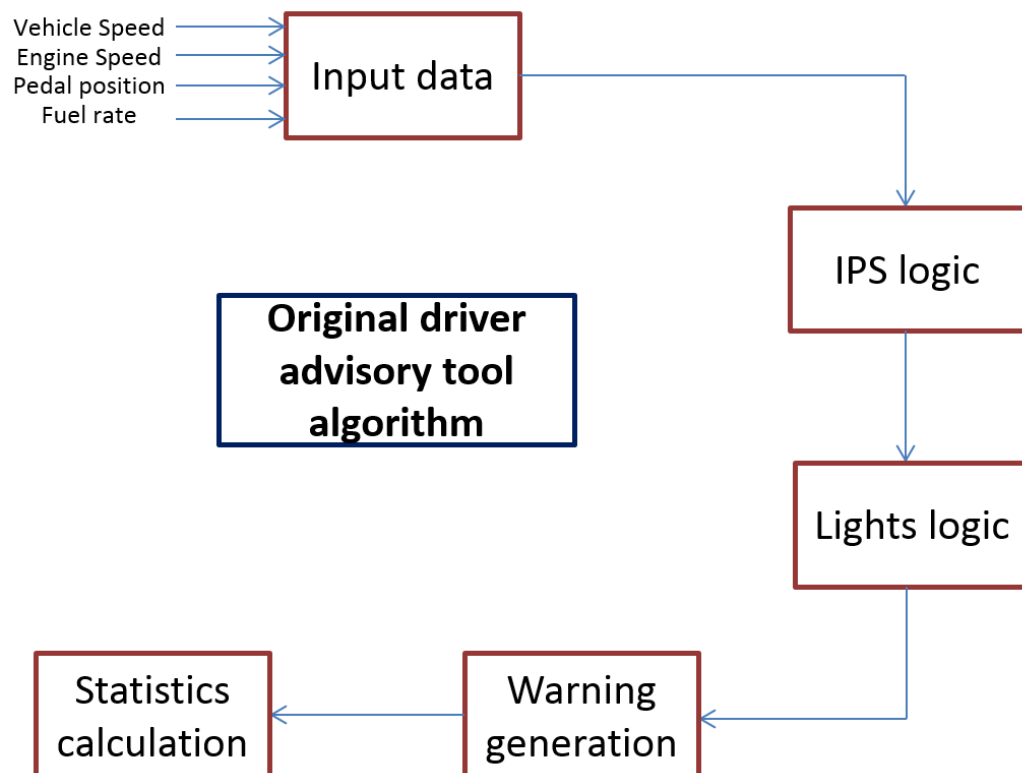


Figure 2-16 - Schematic representation of the initial driver advisory tool algorithm

Figure 2-16 shows the flow diagram of the first algorithm developed for the driver advisory tool. The system takes in vehicle speed, engine speed, throttle position and fuel injection rate from the on-board CAN system of the vehicle to determine certain key parameters of driver behaviour and provides necessary feedback on the driver's performance. A set of 9 LEDs show the instantaneous IPS, called short term IPS (IPS_{ST}). A moving average of this value gives the long term IPS (IPS_{LT}), which controls another set of 5 LEDs. The value of IPS_{LT} with respect to various thresholds set in the algorithm of the device gives audible warnings to the driver. The driver is given penalties if the audible warnings are ignored.

The fuel injection rate is used to determine the fuel consumption of the vehicle, while the engine speed is used to advise the driver on when to shift to a higher gear. Captured data is processed by the device and a report with information including distance travelled, average fuel consumption, number of warnings received etc. is sent to the fleet manager of the company that owns the van, who can then assess each driver's performance and rank them accordingly. This accountability is an essential aspect of the system if improvements are to be widespread and sustained.

At the code level, the algorithm is divided into five stages. The first is the data processing stage, where data from the CAN network of the vehicle is converted into a useful range. Input variables like vehicle speed, engine speed, pedal position and fuel injection rate have a range and an offset value specified in the CAN communication protocol by the manufacturer. These values have to be back calculated to obtain sensible input parameters. This first stage also converts certain input parameters into

known quantities for use later in the code. For example, OBD fuel rate is converted using constants provided by the manufacturer into gallons per injection.

The next stage is where the algorithm calculates the Inertial Power Surrogate (IPS) which was defined in the literature. IPS is calculated in two different ways, one is instantaneous, responding quickly to driver behaviour – called short term IPS, and the other is a moving average of this value known as long term IPS. Both these values are calculated and tuned in this stage of the code. This stage also conditions the signal and adds penalties to the IPS value for bad driving behaviour seen. If the driver does not shift even after 2200 rpm, a penalty is added for this as well.

The lights logic section is where both short and long term IPS is converted to visual feedback to the driver as lights. Nine short term lights ranging from green, amber and red show the driver his/her instantaneous performance, with green being moderate driving and red showing aggressive driving behaviour. Five long term lights, two green, two amber and one red shows the long term performance of the driver. The long term IPS lights affect the audible feedback provided to the driver in the form of warnings and violations.

The next stage is to generate warnings from the information based on the long term lights. It also makes sure that the next warning is given only after a stipulated amount of time. This is to give the driver a fair opportunity to improve his driving style. Also, from a safety point of view, the driver may have driven aggressively due to the traffic situation around him, in which case there should be no more messages played to driver in case it may distract him from his/her driving. The number of violations are stored locally on the memory card of the device, and also externally on a bespoke

server. This is then passed on to the customer of the product on a regular basis as agreed with the customer. The last stage of the system is where various driver/vehicle statistics like average vehicle speed, engine speed and fuel consumption are calculated. Validation of the algorithm of the driver behaviour improvement device, software code, field trials and data analysis of initial trials constituted the first work of the author's PhD thesis.

2.5. Summary

Hybrid and electric vehicles form an essential part of current day objectives in reducing exhaust emissions from vehicles. Reduction in energy used in the vehicle during real world driving scenarios is essential to help reduce transport CO₂ emissions. There are different elements in a vehicle that need to perform in synchronisation to achieve the net target CO₂ reduction. Thus, focussing on powertrain alone will not provide the required benefits. However, powertrain is an essential part of the vehicle, and reduction in cost of hybrids and electric powertrain is an essential route to making low exhaust emission technologies more attractive to the consumer. This chapter highlighted some of the key areas where cost of electric powertrains can be reduced and how to bring down their manufacturing costs, which fed into the work undertaken in conjunction with the industrial partner as part of this thesis.

Various powertrain technologies being developed currently with the aim of reducing fuel consumption and exhaust emissions take a lot of time to be adopted by all car manufacturers. Thus their impact can be seen only after a decade or more. A quicker

solution to reduce fuel consumption and exhaust emissions is by changing driver behaviour. Previous literature has proved the concept and also highlighted that driver behaviour improvement courses do not provide longer term improvement in fuel consumption, as drivers tend to fall back onto their original driving habits at the end of the course. Constant driver feedback is required to sustain fuel consumption reduction figures. The device provides the driver two warnings before a 'violation' is recorded. The violations are then communicated to the fleet manager of the company who can then rank the drivers based on his/her performance. This method of ensuring accountability is an essential aspect of the device, if improvements are to be widespread and sustained.

To assess the benefits of the device, it was essential for it to be tested on different fleets of vehicles in the 'real world'. Previous studies where drivers were aware of the fact that they were being tested to understand a link between their respective driving style and fuel consumption may have caused results to be slightly skewed. This was taken into consideration during the field trial experiments conducted as part of the assessment of the device. It was also important to understand the different parameters and factors that add up to the improvement in fuel consumption, and try and understand why some vehicles save more fuel when compared to others. Hence this research attempts to identify direct links between driver behaviour and energy consumption of the vehicle (for both IC engine and electric vehicle) along with adding systems to improve the utility of the driver behaviour system. This thesis also aims to improve the efficiency of electric powertrain when working in conjunction with the driver advisory tool helps to improve energy savings.

2.6. Research Aims and Objectives

The aim of this thesis is to develop a driver advisory tool that provides consistent real-time feedback to drivers on how to improve their driving style to reduce fuel consumption, and to test and validate the benefits of a similar system on a vehicle equipped with a low cost fully electric powertrain.

Understanding the potential for further research on the literature discussed, the scope of this thesis can be split into four sections:

1. Undertake a field trial experiment of the driver behaviour management tool, analyse the results to assess the effectiveness of the device in reducing fuel consumption, and also understand the parameters that caused the improvement in fuel consumption.
2. Improve the driver advisory tool to make it more generally applicable to different vehicle makes and types.
3. Measure and analyse the performance of axial flux electric motors for traction applications and identify improvements. Develop and test control strategy for a variable air gap electric motor concept.
4. Apply driver behaviour improvement device to fully electric vehicles and assess resulting improvements in the range of the vehicle.

2.7. Work division

Work done as part of this thesis was divided into different sections. Initial work of the author revolved around the software validation and coding of the algorithm for a driver behaviour improvement device to reduce fuel consumption, while the hardware was developed by the industrial partner on the project. Further work on this was done so as to be used on fully electric vehicles to improve the driving range by reducing the energy consumption from the battery pack. Figure 2-17 shows the work structure followed for the thesis.

Initial work involved undertaking field trials of the driver behaviour improvement device and analysing results from it. Understanding driving style and parameters that lead to fuel consumption was a key part of the thesis. Improvements like cruise control detection, sensitivity option, vehicle idling detection and many more were added into the system to achieve optimal functionality from the system, and was tested on different vans and cars. Feedback from these tests allowed for tweaking of various gains and offsets, after which the software was made available for commercial usage. The knowledge gained from the IC engine version of the driver advisory tool was used to develop a new version for use on fully electric vehicles. The motivation to save on fuel consumption is replaced with the need to reduce the drain on the battery and hence increase driving range of the vehicle. Hence, this version of the advisory tool takes into account both positive and negative accelerations. The positive accelerations are reduced to lower the rate of discharge on the battery, while encouraging effective decelerations ensure an increase in the energy recovered during braking, which can be stored in the battery pack.

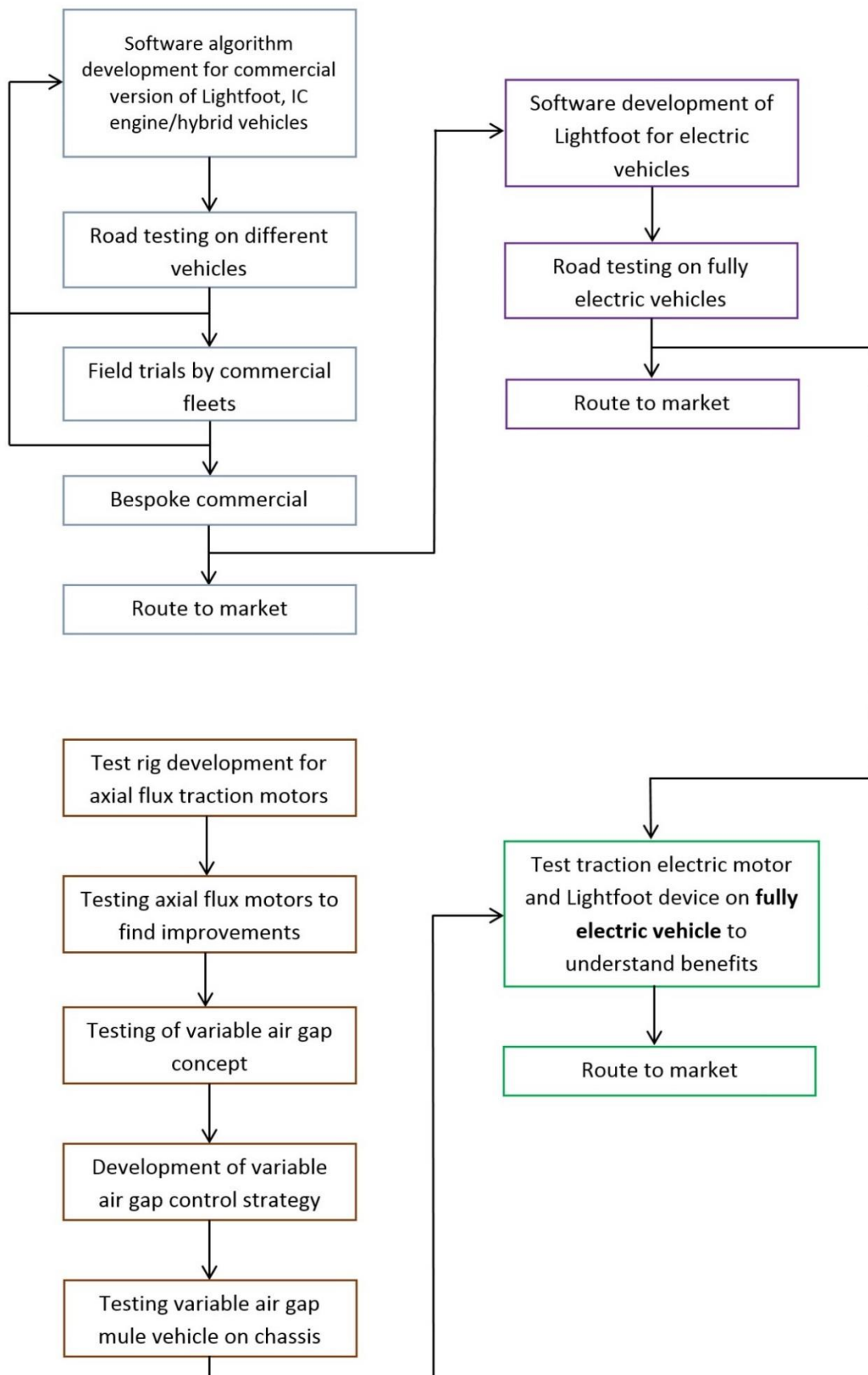


Figure 2-17 - Work division for the thesis

Drivers were also asked to brake gently where possible, so as to regenerate energy more effectively into the battery pack. High deceleration values provide high currents for a very short period of time, which may be higher than the rating of the motor inverters. In this case, the vehicle brakes have a more significant role to play in stopping the vehicle, by converting kinetic energy of the wheels into heat. The device encourages drivers to anticipate traffic and brake over a longer period so as to effectively use all of the regenerative capacity of the electric motor/generator. A gentle braking behaviour also smoothens the charging process of the battery pack by providing a steadier charge when braking, rather than high amplitude pulses.

A test rig was developed at the University of Bath to test axial flux electric motors for hybrid and electric vehicle traction applications. The aim was to test the motors with a varying air gap technology. Baseline testing of this concept was conducted on the test rig, and a prototype unit developed by the industrial partner was fitted in a mule vehicle, which was tested on the chassis dynamometer facility at the University of Bath. A control strategy for the variable air gap actuation was developed to be used on a fully electric vehicle.

A second test rig was developed for the industrial partner to undertake research testing of electric motors. The test rig was flexible to run in a manual mode with an operator using it, or in a fully automated mode to run through different tests. The test rig was used to test and improve designs of low cost electric motors, and helped reduce the research and development costs by reducing the man-hours required to run tests. This rig currently resides in the electric motor manufacturing plant of the industrial partner Ashwoods, and helps in streamlining the acceptance tests of

motors being manufactured. The rig thus currently functions as an End of Line test facility and can also be used for research testing when required.

In the process of testing motors, different traction controllers were trialled. Research into mechanical field weakening showed promising results. A control strategy for a variable air gap motor was developed and trialled on the rig. The electric motor tested and calibrated was integrated into a fully functional vehicle by the industrial partner. This vehicle was used to test the electric vehicle version of the driver advisory tool to understand the potential benefits on the range of the vehicle.

2.8. Research Contributions

The work presented in this thesis offers a significant research contribution to existing literature and knowledge in the area of research into driver behaviour and electrified powertrain development. The main contributions and novelty of the research has been mentioned below:

1. In the development of the driver behaviour improvement device, the parameter IPS (defined in previous literature) has been extended to be used as a measure of aggressivity, as this value can be physically represented as the rate of change of kinetic energy of the vehicle, which in this thesis is closely linked to aggressive driving characteristics.
2. Driver behaviour and driving characteristics have been analysed based on driving pattern parameters that were defined by Eva Ericsson in previous

literature [63]. The logged statistics of the driver advisory tool helped identify a few other parameters that helped identify aggressive driving characteristics.

3. A novel method of determining the optimal gear of vehicle operation to achieve best fuel consumption and driveability was developed and tested. A novel method of automatically adapting and learning the number of gears of the vehicle was also developed so as to be fitted in any vehicle of any type with the no calibration or set up procedures.
4. A method was created to detect excessive idling in vehicles where the device would advise the driver to switch the engine OFF. This works as a manual 'Start-Stop' micro-hybrid system.
5. A novel solution to automatically adjust sensitivity of the driver advisory tool was developed, that recognises a new driver and helps him/her into adjusting to the system before increasing the sensitivity to achieve higher fuel savings.
6. The driver advisory tool logic was extended to develop a driver behaviour improvement device for electric vehicles, which also advised the drivers on braking behaviour so as to maximise energy recovery.
7. New electric motor testing methods and test procedures for traction motor applications were created so as to quickly detect faults and also rigorously test the performance of the machine.
8. Control strategy for a motor that had a dynamically variable air gap was identified, that enabled the electric machine to operate in the most efficient region as possible.

Chapter 3 - Driver Behaviour analysis

This chapter is concerned with the analysis of the field trials conducted for the initial version of the driver advisory tool to understand where and how savings in fuel consumption are achieved. Different parameters devised by researchers mentioned in the literature are used, in order to verify the improvements in fuel consumption observed with the use of the driver advisory tool.

Work published in:

1. "Analysis of a Driver Behaviour Improvement Tool to Reduce Fuel Consumption," Presented at *IEEE International Conference for Connected Vehicles and Expo (ICCVE), Beijing, 2012*
2. "A Driver Advisory Tool to Reduce Fuel Consumption", *SAE Conference*, 2013
3. "Development and Field Trial of a Driver Assistance System to Encourage Eco-Driving in Light Commercial Vehicle Fleets," *IEEE Intelligent Transportation Systems Journal*
4. This work was used to underpin one of the research impact case studies for Research Excellence Framework (REF) 2014, for the Department of Mechanical Engineering at the University of Bath

3.1. Field trials

Any new device developed for mass market use has to undergo field trials to understand the benefits it will have in the real world. This process will also highlight any problems that the device has, which may have been overlooked during the development stage. The driver advisory tool was tested on different Ford Transit vehicles before a version was released to be trialled by different companies having commercial fleet of vans. The Ford Transit was the preferred vehicle of choice for a number of reasons, mainly due to its popularity, ruggedness, reliability and practicality. Also, the industrial partner was involved in conversions of standard Ford Transit vehicles into hybrid vehicles. This gave the opportunity for more vehicles to be tested and fitted with the driver advisory tool. It was initially intended to be sold with the hybrid pack as an add-on feature to increase on the potential savings in fuel usage. However, the product on its own gained more interest after the initial trials.

It was decided to overcome some of the limitations of existing literature, where the participants of the driver behaviour experiment were aware of the fact that they were being tested to determine the link between driving pattern and fuel consumption. Although there is no evidence to prove that their consciousness of this fact would have caused them to drive better or worse during their 'baseline' or 'normal' driving test phase, there is no proof to say it did not have an effect. This may have skewed the results of the overall savings that were discussed in different literature. To overcome this issue, it was decided that the device would be tested in two stages – first, without the driver's knowledge of him/her being tested, and the second with the driver's knowledge - at the same time providing feedback.

A total of 15 light commercial vehicles, all of them Ford Transits, owned by different commercial companies were tested for a period of four weeks. Table 3-1 shows the description of the different ranges of Ford Transit vehicle used in the field trials [68]. In general, the companies employed large fleets of vehicles to support their respective core areas of operation. The main motivation for these companies to be part of the trial was that fact that the vans were owned by the commercial companies, but they were being driven by drivers who did not own the vans. This meant the drivers were not paying for the fuel usage of the vehicle and it was not their obligation to help their parent company save on fuel consumption with the vehicles. However, since the companies were obviously interested in the potential economic benefits of using the driver advisory tool, they were interested in participating in the trials.

Table 3-1 - Specification of the different Ford Transit vans used in the field trials [67]

Vehicle Model	Ford Transit
Emission stages	Euro 4
Year built	2008, 2009, 2010, 2011
Engines	2.4L Duratorq 2.2L Duratorq
Transmissions	6 Speed Manual - MT82 6 Speed Manual transaxle - VMT6 5 speed Manual transaxle - VXT75

Since the ownership of the vehicle was with the commercial company, this experiment provided a good opportunity to further their commitment to reduce carbon dioxide emissions and the amount spent on fuel used per vehicle. This fact also outweighed the moral privileges of the drivers not knowing the presence of the device logging their driving style, as the benefits from the former significantly exceed the latter.

During first stage of testing of the driver advisory tool, drivers were unaware of the device being present in their vehicle. This was achieved by the ensuring the device with the data logger being installed in the vehicle, without the display unit, and with the audio feedback being turned off. This was undertaken during the weekends (or off-duty times) to minimise or avoid disruption to the 'normal' operation of the vehicles/companies. This also meant drivers were not aware of the fact that the device that had been fitted in the vehicle that they drove, and data was being recorded to understand their 'normal' driving style. On average, the fitting of the device took around 20 minutes per vehicle. This first stage of the data collection took two weeks, and will hereby be called – 'baseline trial' or 'blind trial'. For all the companies that were part of the field trial experiment, the vehicles were driven by the same individual for the period of the trial. The fleet manager was advised to bring to the attention of the researchers, any driver changes to any of the vehicles during the field trial experiments. This baseline trial phase provided the opportunity to understand the 'normal' driver behaviour of each driver.

Table 3-2 - Details of companies and their vehicles that were involved in the field trials ^[67]

	Company description/vehicle use	No. of vehicles
Company A	Technical call-out service	3
Company B	Retail parts delivery	3
Company C	Fresh produce delivery	2
Company D	Technical call-out service	2
Company E	Site visits	2
Company F	Technical call-out service	2
Company G	Support service	1
	Total number of vehicles	15

Table 3-2 shows the details of the companies that were part of the initial trials of the product [68]. The names of the companies have been obscured for confidentiality purposes, but the function of their respective vans that were part of the field trial experiments are detailed in the table.

At the end of the baseline testing stage, the audible and visual feedback were switched ON for the second stage of the field trial experiments. The device was no longer just logging the vehicle parameters, but also providing instructions to the driver to improve his/her driving style. This test stage lasted for another two weeks, and this phase will hereby be referred to as the ‘interface trial’ or ‘live trial’. In total, 15 Ford Transit vans were tested for four weeks, and 39,000kms of data was recorded and analysed, which represented 5,587 different trips and 1,107 hours of driving.

Vehicle data was collected from the CAN channels of the vehicle that was broadcast on through On-Board Diagnostics (OBD) port. The important parameters logged included vehicle speed, throttle position, engine speed and fuel injection rate. Information on vehicle cargo mass was unavailable and the author acknowledges the importance of total vehicle weight on fuel consumption. However, the vehicles that were involved in the field trials were generally operating on similar daily routines with similar routes and more or less the same cargo, over the baseline and interface trials. This meant an average over two weeks may not skew the results. The data was *polled* from the broadcast CAN communication at its maximum rate available, and was transferred to the embedded code of the driver advisory tool at a frequency of 10Hz. This incoming data was used by the algorithm as explained in the literature, before outputting flags for audible and visual feedback. The audible feedback was for 'Warning 1', 'Warning 2' and 'Violation', while the visual feedback were for the in the form of LED lights.



Figure 3-1 - Instrument panel display of the driver advisory tool [68]

Figure 3-1 shows the instrument panel display for driver advisory device [69]. The nine LED lights that represent instantaneous IPS_{ST} can be seen at the bottom of the panel, while the five long term IPS_{LT} LEDs that affect the warnings and violation are in the centre of the instrument panel. The aim of the driver is to predominantly drive in the green region to avoid receiving penalties. The small green triangle next to the long term lights is the gear shift indicator, which turns ON when the appropriate gear shift flag is activated based on the algorithm. Ignoring this adds a penalty, which moves the position of the lights from the green into the amber or red.

3.1.1. Results from field trials

All the data collected from the vans were processed and analysed to understand the benefit of driver behaviour with respect to savings in fuel economy. Fuel consumption was calculated as the litres of fuel used for 100 kilometres (L/100km) of distance travelled. The absolute value of fuel consumption was not compared between vans for two reasons – firstly, due to the possibility of the presence of a calibration error in the ECU fuel measurements of the vehicle (which may or may not be present in other vehicles). Secondly, different companies had different purposes for their vehicles and hence different driving patterns, drive cycles and environmental conditions, which meant their respective fuel consumptions may be very different.

Data to calculate fuel consumption was analysed on a day to day basis and the findings were shared with the companies that were involved, at the end of the trial. Table 3-3 shows preliminary results from the data collected for the entire fleet. It was observed that, there was a reduction in fuel consumption of 7.6% during the interface trial, while the reduction in engine speed from the baseline to the interface trial was

13.4%. It needs to be emphasised that this data was corrected by removing any of the idling times above 90 seconds, which corresponded to the 97th percentile of idling times for all the vans, and any data above this value had a significant contribution in distorting the results. This also helped in comparing vans against one another in terms of aggressivity reduction and percentage improvement in fuel consumption.

Table 3-3 - Calculated results from test data collected from the field trial experiment

	Baseline	Interface	% Change
Fuel Consumption (L/100km)	9.68	8.94	-7.64
Engine speed (rpm)	1748	1513	-13.44
Pedal position (%)	17.30	14.60	-15.60
Inertial Power Surrogate (m^2/s^3)	7.50	6.27	-16.40

Aggressivity was measured as the inertial power surrogate (units - m^2/s^3), which was defined as the product of vehicle speed (in m/s) and the acceleration (in m/s^2). The algorithm for the driver advisory tool detects non-optimal driving style by comparing the measured value of inertial power surrogate against previously benchmarked values. It is evident from the table that there has been a significant reduction in the aggressivity using the device. Perhaps a more significant contribution of the device is in the reduction of various parameters that contribute directly towards the fuel consumption, like engine speed and pedal position.

The results suggest that with the driver advisory tool providing appropriate feedback, drivers tend to drive in a less aggressive manner, with lower engine speeds and

earlier shifts when compared to their normal driving behaviour that was recorded during the blind phase of the trials. Table 3-4 shows the percentage savings of each of the vans over the four week trial period, for different parameters that are directly or indirectly linked to driver aggressivity and fuel consumption. Even though the average savings in fuel consumption was 7.6%, the highest savings were seen by Van 3 and Van 8, which recorded around 12% in fuel consumption savings. These vans also recorded a similar figure in the reduction of IPS of around 21.5%, suggesting that there is an indirect link between the two parameters.

A reduction in the average in IPS suggests that less tractive energy is used per unit distance travelled, for the interface trial when compared to that of the baseline trial. This was mainly due to a reduction in the rates of acceleration during the interface trial. The average speed for most of the vans in the trial were similar before and after the device was switched ON. This was another reason as to why IPS was used for determining aggressivity of the driver, as it not only takes into account the rate of acceleration of the vehicle, but also the vehicle speed. Thus if one van is much more heavily loaded than the other, they can both still rely on the same driver advisory tool algorithm, as the system is designed around IPS baseline values, and they are the same regardless of the weight of the vehicle. Average acceleration values for the interface trials were observed to have reduced, which suggests that drivers accelerated more gently to achieve the same speeds as they did during the baseline trial periods. Similarly, the reduction in inertial power surrogate is understood to be linked in the same way. Engine speed has a direct correlation to the fuel consumed by the vehicle. For the same tractive effort, a reduction in engine speed corresponds to a

reduction in fuel used by the vehicle. Hence it indicates that the engine was operating at a more efficient point in the engine map during the interface trial.

Table 3-4 - Percentage change in various parameters for each of the 15 vans involved in the field trial experiment

		Engine Speed	Average Acceleration	Average IPS	Fuel Consumption
Company A	Van 1	-5.54	-13.43	-4.41	-9.16
	Van 2	-9.66	0.10	-7.12	-0.43
	Van 3	-14.76	-13.16	-21.39	-12.03
Company B	Van 4	-18.88	-7.84	-17.07	-11.08
	Van 5	-10.04	-21.61	-19.46	-9.89
	Van 6	-14.50	-7.93	-11.25	-1.75
Company C	Van 7	-7.78	-13.79	-13.03	-8.97
	Van 8	-6.34	-18.55	-21.59	-11.82
Company D	Van 9	0.51	-14.69	12.45	-8.48
	Van 10	-9.90	-6.65	-11.43	-3.44
Company E	Van 11	-7.74	-1.93	-5.26	-1.53
	Van 12	-12.44	1.37	4.88	-2.75
Company F	Van 13	-1.21	-4.01	3.50	-5.25
	Van 14	-8.76	-5.68	-8.90	-3.82
Company G	Van 15	-8.09	-6.84	-2.66	-8.84

A reduction in different metrics such as average engine speed, acceleration and inertial power surrogate can be observed between the baseline and interface trials, all of which contribute to a reduction in fuel consumption. Statistical analysis of the standard deviation confirmed the effectiveness of the device.

One of the most important parameters in driver behaviour improvement as highlighted by previous literature is the reduction of engine speed. In general, higher the speed of the engine, the more fuel it consumes for the same engine power. This is one of the reasons why eco-driving courses advise drivers to shift up sooner into a higher gear.

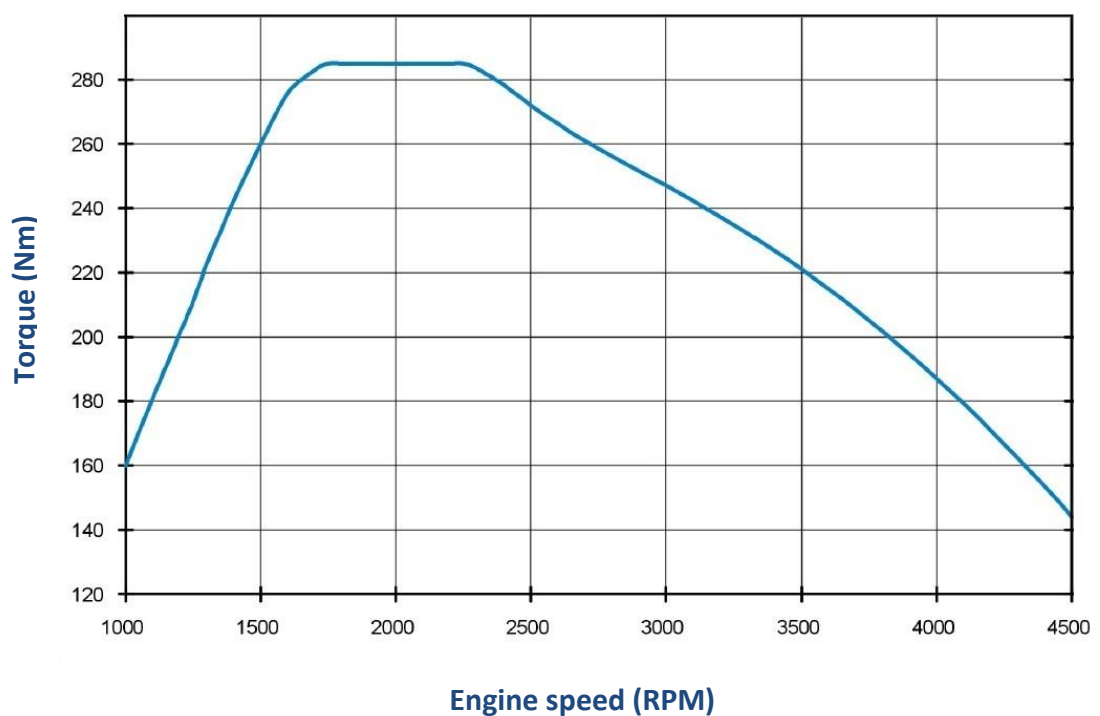


Figure 3-2 - Engine speed vs torque of a Ford Transit 2.2L Duratorq 110PS (Source: Ford Motor Company) ^[69]

Figure 3-2 shows the engine torque speed envelope of a Ford Transit 2.2L 110PS engine [70]. Diesel engines tend to be most efficient at loads near the maximum torque regions [71]. In the case of diesel engines, the maximum load corresponds to the maximum pedal position, as engine load is an indicator of the instantaneous torque requested with respect to the maximum torque available at that speed. Since most vehicle applications do not require maximum torque of the vehicle, drivers tend to operate at a much lower torque, when compared to the limiting torque at that speed. This means that the less efficient operating region is used predominantly. It also follows that a powerful method to achieve improved economy is to operate at a lower engine speed. This is achieved by running in a higher gear using the gearbox.

As the vehicle speed increases, the engine speed rises due to the direct coupling through the gearbox. Once the engine speed rises to a point where the required tractive effort cannot be applied due to the limiting torque values at high speeds, the driver changes gear to bring the engine operating point to a lower speed, but higher torque compared to the previous gear, to maintain the power required to accelerate. The load on the engine increases due to the increase in aerodynamic drag of the vehicle (which is a function of the square of the vehicle speed), and due to the increase in rolling resistance at higher speeds (because of the increased inertia causing the restitution of elastic deformation energy that causes vibration in the tread of the tyre, which is consumed by hysteresis [72]). Since the engine speed is lowered when shifting up a gear, the torque has to be increased to maintain constant power to continue accelerating the vehicle at the same rate compared to the previous gear. This increase in engine load translates to the engine providing higher

torque output, which transpires into engine operation at a higher efficiency region. Hence earlier shifts into higher gears improve the fuel economy of the vehicle by moving the engine operating point into a more efficient region with lower BSFC. This is the reason most new generation of vehicles developed for the European market have a 6th gear ratio compared to what was available 6-7 years ago.

Driving experience helps the driver in not attempting to drive close to the limiting torque values of the engine at very low engine speed. This is due to a lack of performance as well as poor engine NVH refinement in these regions. This is useful as these regions tend to be inefficient [71]. Behaviour is adapted because there will be a shortage of torque output from the engine at very low speeds to provide the required tractive effort to accelerate the vehicle.

The driver advisory tool helps in reducing the average engine operating speed by asking the driver to shift up a gear. The upshift indicator flag/light asks the driver to shift up into a higher gear, if the engine speed was higher than a default value of 2200rpm. If the vehicle had a factory gear shift indicator, that value over-rides the gear shift flag from the advisory tool algorithm, in controlling the upshift light to the user. This single speed limiter for engine speed is not a very effective solution, as different engines have different torque-speed envelopes, and different vehicles have different engine load characteristics. This will also cause an issue where the driver may receive an unfair gearshift penalty when he/she tries to overtake a vehicle, or accelerate to join the motorway from the slip road. This issue was addressed as part of the thesis and will be discussed in the next chapter.

Figure 3-3 shows the comparison of the probability distribution of engine speeds between baseline and interface trials for all the vans tested in the field trial experiment. The majority of the automotive engines idle at around 750-800rpm. During the course of driving in the urban environment, a significant proportion of the time is spent in idling, either consciously or unintentionally. This idling speed was included in the calculation for the histogram presented in figure, but the figure was truncated at 950rpm due to the high concentration of idle data below this point, compared to the other engine speeds. The baseline engine speed is visibly spread across a wider range of engine area, while the concentration of engine speeds for the interface trial has noticeably shifted to the lower end of the spectrum. This highlights the effect of the gear upshift lights, which penalise the drivers, when ignored. This again shows the impact of the operating gear on fuel consumption of the vehicle. It provides an indication of the effort of fine-tuning required by automotive manufacturers when designing/developing gearboxes, to find a trade-off between engine speed, vehicle speed and fuel consumption of the vehicle.

It can be seen in the histogram that there is the presence of a spike in the baseline and interface trial data around the 2200rpm mark. This is not an anomaly, but corresponds to the engine speed when the vehicle is cruising at 100km/hr in 6th gear. Most of the Ford Transit vans that were part of the experiment were electronically limited to 100km/hr, and hence the high concentration of data points at this mark. The results from the trials show a clear reduction in average engine speed, vehicle speed, throttle position and inertial power surrogate values, suggesting that drivers became a lot smoother in their driving behaviour by reducing harsh accelerations and

shifting earlier into higher gears. This confirmed that driver behaviour improvement can result in better fuel economy of the vehicle.

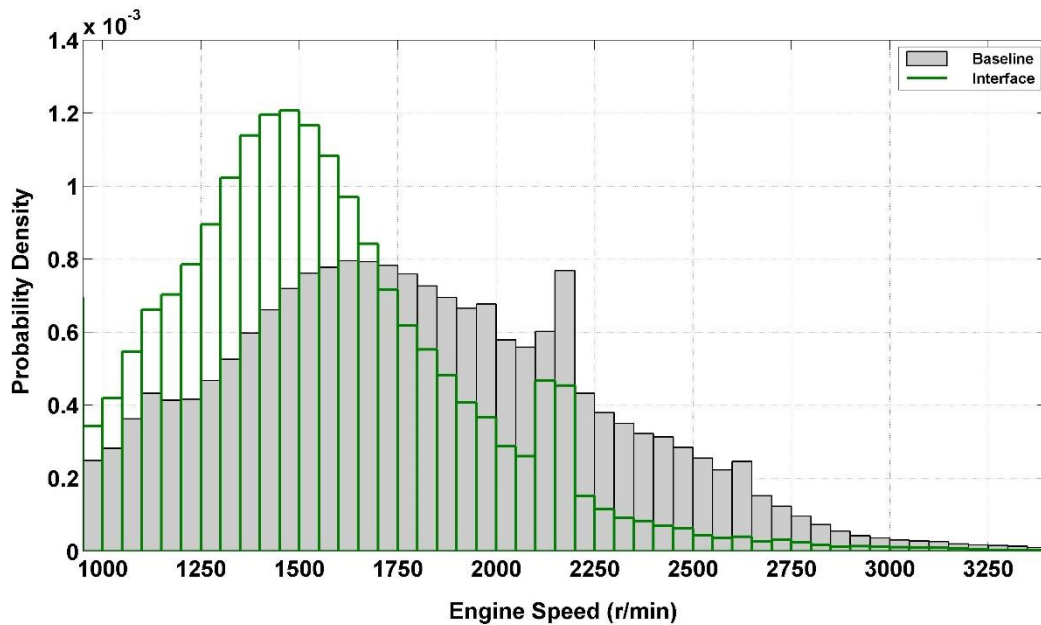


Figure 3-3 - Probability distribution of engine speed (Baseline vs Interface trials)

Analysis of the data collected from field trials was divided into two stages. The first stage involved simple driving pattern analysis and their link to improvement in fuel consumption for different drivers, whilst the second stage involved creating a simple model to predict the fuel economy savings a user can achieve by using the vehicle.

3.2. Preliminary data analysis

To understand where and how different drivers managed to save on fuel consumption, it was necessary to explore a few more parameters. The factors short-listed for the preliminary analysis included relative positive acceleration, inertial power surrogate, specific work done and pedal busyness. Relative positive acceleration is the integral of the product of speed and positive acceleration over the

total distance travelled [64, 73]. Specific work is the energy required per kilometre to propel the vehicle. This was calculated by assuming a constant frontal area and mass for every vehicle. Again the absolute value of this parameter may not be entirely correct, but it can be used for comparison between the baseline and interface trials and different drivers.

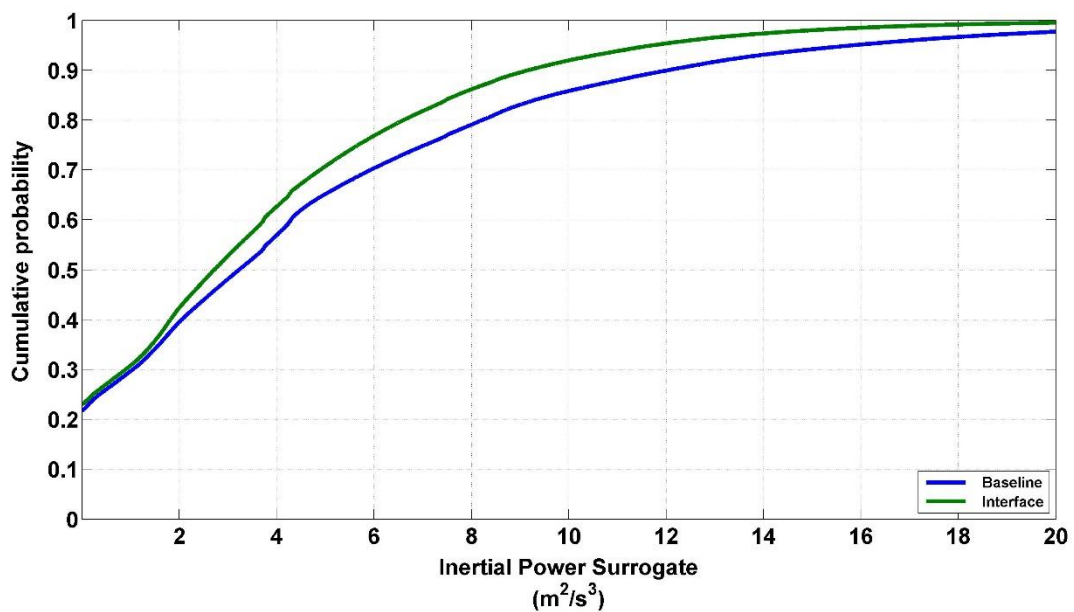


Figure 3-4 - Cumulative probability of Inertial Power Surrogate (m^2/s^3)

Figure 3-4 shows the cumulative probability distribution of the inertial power surrogate for both baseline and interface trials. To arrive at this plot, some filtering of the data had to be performed by excluding certain regions, namely all deceleration values and idling conditions. Deceleration values were ignored, as this plot was intended to highlight the shift towards lower IPS values in the propulsion phase (positive acceleration), whilst idling was ignored to avoid the cumulative distribution starting at a higher ordinate value (due to the vehicle speed being zero during idling, which would cause IPS to be zero). Hence the Y-intercept value (at $0 \text{ m}^2/\text{s}^3$ IPS)

corresponds to vehicle cruising with no noticeable change in speed (hence acceleration is zero, which results in IPS being zero).

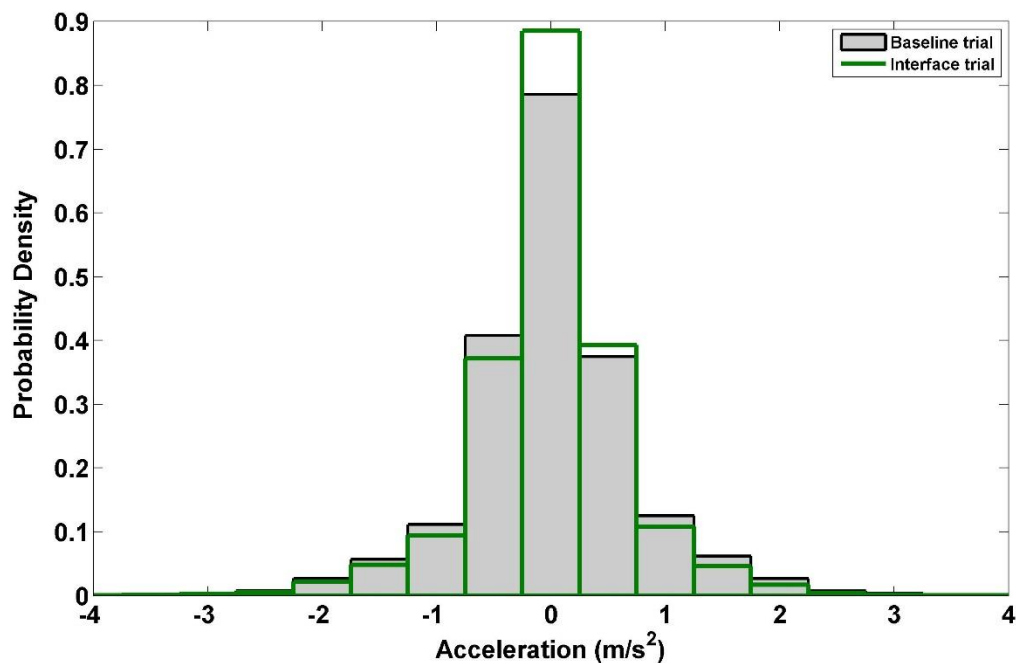


Figure 3-5 - Acceleration and deceleration histogram for vans

It can be clearly seen that there is a higher concentration of IPS values towards the left of the graph from the $2\text{m}^2/\text{s}^3$ value during the interface trial depicting the effective operation of the device. This shift suggests a clear indication in the reduction of higher values of IPS for the interface trial. This is mainly due to the reduction in harsh accelerations which result in higher values of IPS. This suggests that during the interface trial, drivers happened to be driving in a much smoother and less aggressive fashion when compared to the baseline trials. Analysis of this pattern helped explain the relation between fuel consumption and the time spent in high values of average acceleration and inertial power surrogate.

Similar patterns were observed on further analysis of the acceleration profiles. Figure 3-5 shows the acceleration and deceleration histogram for baseline and interface trials for all vehicles. A similar filtering mechanism had to be used so as to improve quality of the plot. All idling parameters were removed so that there is no big spike in the reading at zero acceleration (when the vehicle is stationary). Similar to the previous IPS case, zero acceleration value represents cruising of the vehicle with minimal change in speed. It can be observed that there is a shift from higher acceleration values to lower ones (from high values of 2 to 3m/s² to much lower values in comparison like 0.5 to 1m/s²). This reiterates the fact that there is a reduction in harsh acceleration with the device in operation. This was one of the key factors contributing to the reduction in fuel consumption of the vehicle. Reduction in harsh acceleration also encourages a change from an uncomfortable driving experience into a calmer and smoother driving style. The increase in data points for the cruising phase (zero acceleration) during the interface trials meant that drivers were smoother and did not have consecutive harsh throttle and brake usage.

The driver advisory tool monitors and provides feedback on driving style by taking into account only the positive acceleration phase of driving, as this corresponds directly to fuel consumption. However, from the histogram it is evident there is also a reduction in the deceleration values during the interface trials when compared to the baseline. This is assumed to be a result of the drivers being calmer and less harsh in their driving style, and hence having lesser deceleration values by avoiding unnecessary changes in speed. The reduced deceleration values have corresponded to an increase in cruising (zero acceleration) during the interface trial. This behaviour

was not due to an inherent function of the device, but is a result of a generally calmer and smoother driving style adopted by the drivers.

Braking gently in IC engine powered vehicles does not provide any real benefit, because when the vehicle needs to come to a complete stop, the kinetic energy has to be dissipated in some way or the other. Usually this energy is converted into heat energy in the brakes, while some of it is lost in engine braking and other friction in the drive-train. However in the case of hybrid and electric vehicles, braking gently is useful in terms of converting the kinetic energy into electrical energy using the traction motor/generator, and then storing it in the batteries. This phenomenon provides a significant contribution to the energy transfer and storage in hybrid and electric vehicles and is called regenerative braking or Kinetic Energy Recover System (KERS). This phenomenon and the potential to increase the energy savings in an electric vehicle was the motivation behind the development of the electric version of the driver advisory tool, which will be discussed in the coming chapters.

From the reduction in average pedal position, vehicle speed and engine speed, it is clear that there is a change in driving pattern using the advisory tool. To understand the effect of the device on the driver's pedal usage, histograms of pedal position are not very effective, mainly due to the fact that a person's foot on the pedals are not very steady. Nevertheless, a driver's pedal usage can be examined by the use of a parameter called Pedal busyness, defined by Brace *et. al* [74] as the cumulative sum of the rate of change of pedal position over a complete cycle. The actual value of this parameter has little significance, but gives an idea of the oscillatory use of the pedal, and can be compared against the pedal busyness value of his/her interface trial.

Figure 3-6 shows the rate of change of pedal position for baseline and interface trial for a particular Van 1. The red line shows reference line for zero rate of change of pedal, indicating a theoretical best for driving, which is almost never achievable. It can be seen that there is clear a reduction in the amplitudes of the interface trial, showing that drivers had significantly lesser oscillatory movement of the pedal when feedback on driving was given to the drivers.

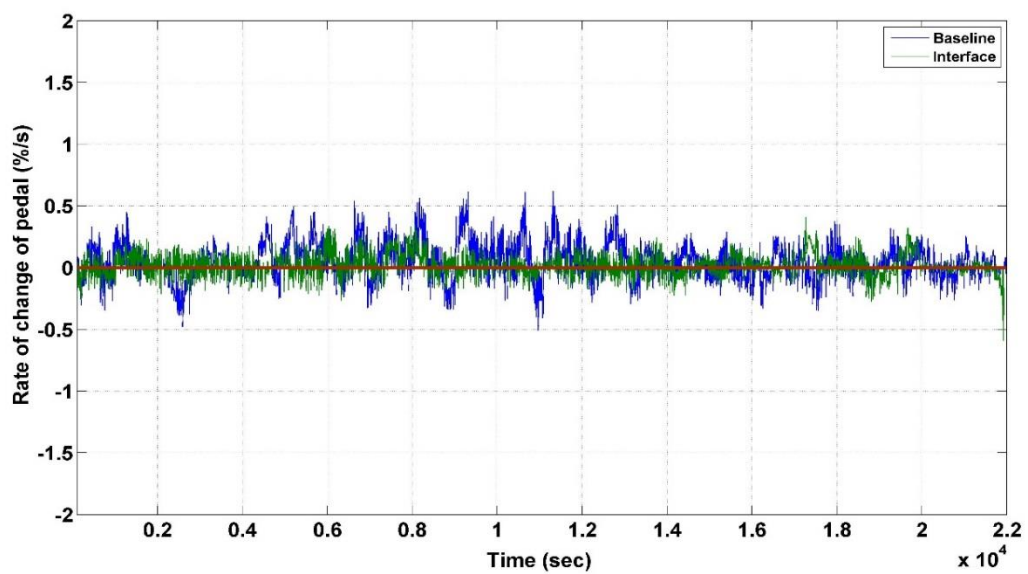


Figure 3-6 - Rate of change of pedal usage for baseline and interface trials

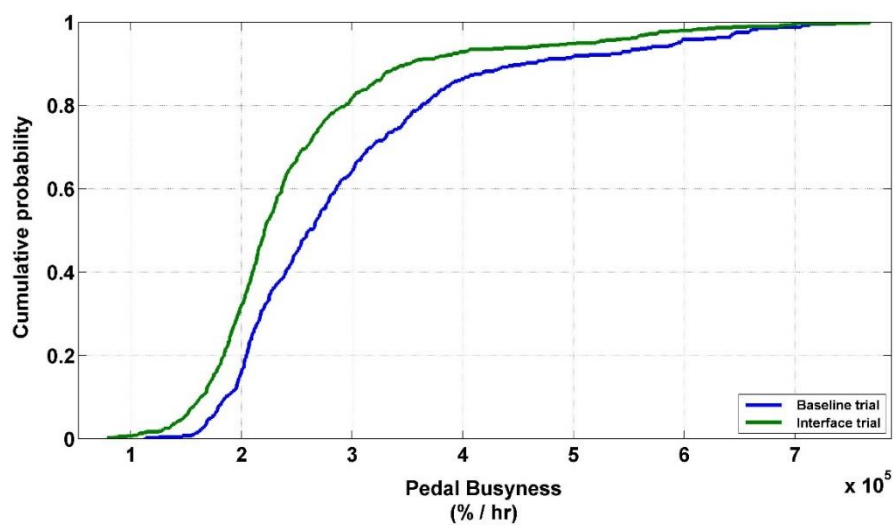


Figure 3-7 - Cumulative probability of pedal busyness

Since by definition, pedal busyness is the sum of pedal position changes during a given period of time or cycle, a cycle time had to be defined for this analysis. The data collected was initially filtered by removing all idling, as pedal busyness is a measure of the change in pedal during driving of the vehicle and not when it stationary (where pedal position and its change is zero). The remaining data was divided into sections of one hour each. Hence the pedal busyness in this case was the total number of pedal position changes over a period of one hour. This would make it easier to compare absolute values of pedal busyness between the baseline and interface trials.

Figure 3-7 shows the cumulative probability of pedal busyness for the baseline and interface trials of the vans involved in the field trial experiments. It can be seen from that there is clear evidence of reduction in pedal busyness during the interface trial when compared to the baseline testing phase. The graph starts from a non-zero point due to the idling values being deleted. It can be seen that during interface trials, the pedal usage is less when compared to baseline tests. This is evident from the higher concentration of data in the lower pedal busyness values during the interface trials, and hence a shift towards the left when compared to the baseline test data. This curve helps understand that drivers were smoother in their pedal usage during the interface trials, which resulted in a smoother and calmer driver style. This also shows that the real time audible and visual feedback provided by the driver behaviour improvement device did help drivers improve their driving style. The evidence of increased cruising periods in the acceleration histogram, the reduction of the rate of change of pedal usage, and the shift to the left of the plot of cumulative probability of pedal busyness during the interface trial, suggests that the driver advisory tool not

only had significant impact driver's acceleration and inertial power surrogate, but also their pedal usage, making them much calmer and smoother in their throttle pedal operations, which in effect resulted in a better driving style. This shows that there exists a direct link between the use of the advisory tool and driving style.

The effect of the driver advisory tool in reducing the specific work done by the vehicle was touched upon earlier. For this calculation, the inertial load of the vehicle and the aerodynamic drag had to be determined; this meant assuming a constant frontal area and mass for all the vehicles that were used in the trial. Specific work is the work done per kilometre by the vehicle. It is calculated based on the data for each vehicle and comparisons are done between the baseline and interface trials. It provides an indication of the tractive effort provided by the engine to propel the vehicle when mass and other parameters remain the same. On average, a 6.5% reduction in energy used per kilometre of journey was observed for the interface trial when compared to the baseline trials, over the entire fleet of tested vehicles. Since the tractive effort required by the vehicle to get to a certain speed is dependent on the acceleration of the vehicle, this reduction in energy used per kilometre is mainly accounted to the decrease in harsh accelerations during the interface testing of the device.

When each van was considered on its own, it was observed that there was a reduction in the energy used per kilometre, even for vans that showed only a small improvement in fuel consumption. This meant some vans did not show much improvement in fuel consumption even after a reduction in key driving pattern parameters like acceleration, IPS reduction and pedal busyness. This may be because the vans were loaded differently during the interface trials or that they operated on a

different drive cycle when compared to their respective baseline testing conditions, in which case they are to be regarded as anomalies. These conditions will be further analysed in the coming sections.

3.2.1. Prediction of driver behaviour improvement

Different driving pattern parameters were analysed and it was found that reduction in inertial power surrogate, harsh accelerations and engine speeds were good indicators to the decrease in fuel consumption of the vehicle. In other words, vans that had the greatest reduction in time spent in higher values of IPS had the best increase in fuel economy. A simple model was developed to present the benefits of using the driver advisory tool to help improve fuel consumption.

In the real world, to predict a clear benefit when using the device, it is essential for a number of other factors to remain unchanged, like vehicle loading, route chosen and drive cycle etc. when performing comparisons. For the purpose of this analysis, Vans 9, 11 and 12 had to be omitted from the data set because their operating conditions seemed to have changed between the baseline and interface trials. Their presence in the prediction study would have caused the results to skew slightly due to the presence of a different drive cycle between the two phases of study. Although Van 9 had comparatively good fuel consumption savings, it was noticed that this particular van had a higher average speed during the interface trial when compared to the baseline trial phase. This suggested that during the interface trial, the vehicle had a different operating cycle, maybe one that included more motorway driving than the baseline trial phase. This meant this data set had to be removed to avoid bias in the model creation.

When analysing the speed and acceleration profiles of vans 11 and 12 (which belonged to the same company), a reduction in higher accelerations, IPS and pedal busyness were observed. Even though the vehicle showed savings in fuel consumption during the interface trials, they were not relatively high as expected. A deeper look into the work done per kilometre of these two vans revealed that the energy used per kilometre had risen during the interface trial even though all the other driving pattern parameters had reduced. The only constants assumed in the energy used per kilometre calculations are vehicle frontal area (which is still assumed to have not changed) and vehicle mass. A change in vehicle mass (operating payload), or the vehicle operating in a much more demanding driving cycle during the interface trials, are the only plausible explanations which would have resulted in the increase in specific work done with all other parameters seen to have reduced.

Figure 3-8 shows the reduction in engine speed for all the vans (with the same three vans excluded), when using the device. The red dot data points correspond to the remaining 12 vans considered in the analysis. The X-axis denotes the average engine speed during the baseline testing phase while the Y-axis represents the average engine speed during the interface testing phase. The profile of the reduction in average engine speeds can be best characterised by a quadratic fit. This is best interpreted due to the fact that drivers who had a high number of warnings and a higher average engine speed in the beginning of the baseline phase to start with, had the highest opportunity or room to improve when compared to those who were relatively good to start with.

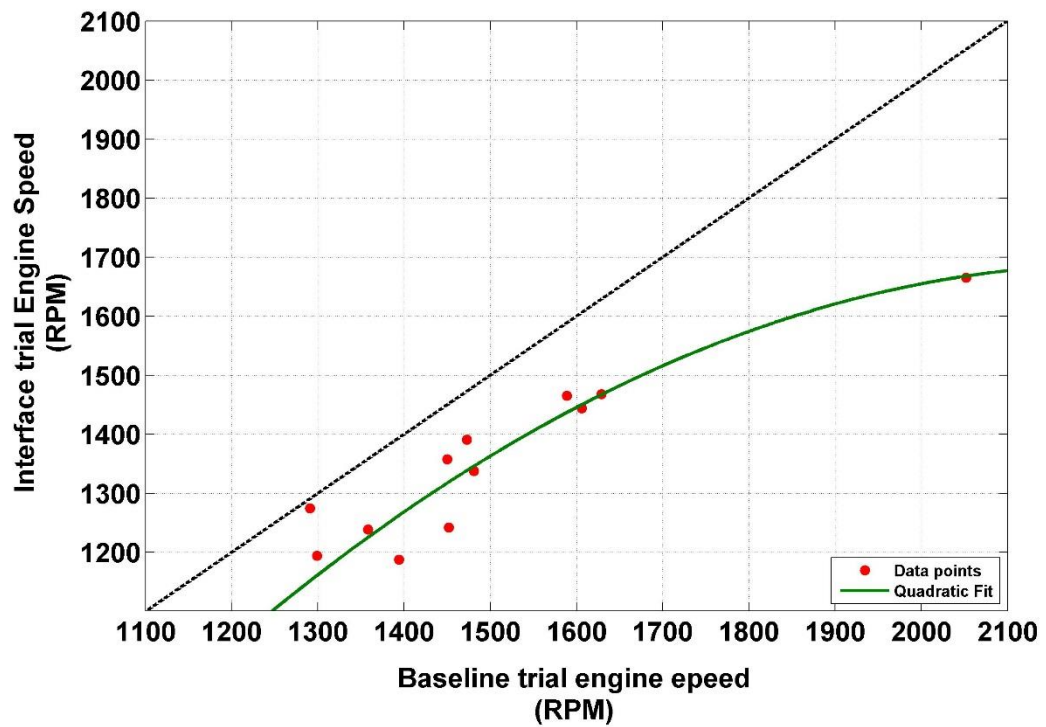


Figure 3-8 - Quadratic fit showing average values of engine speed being reduced with the use of the advisory tool

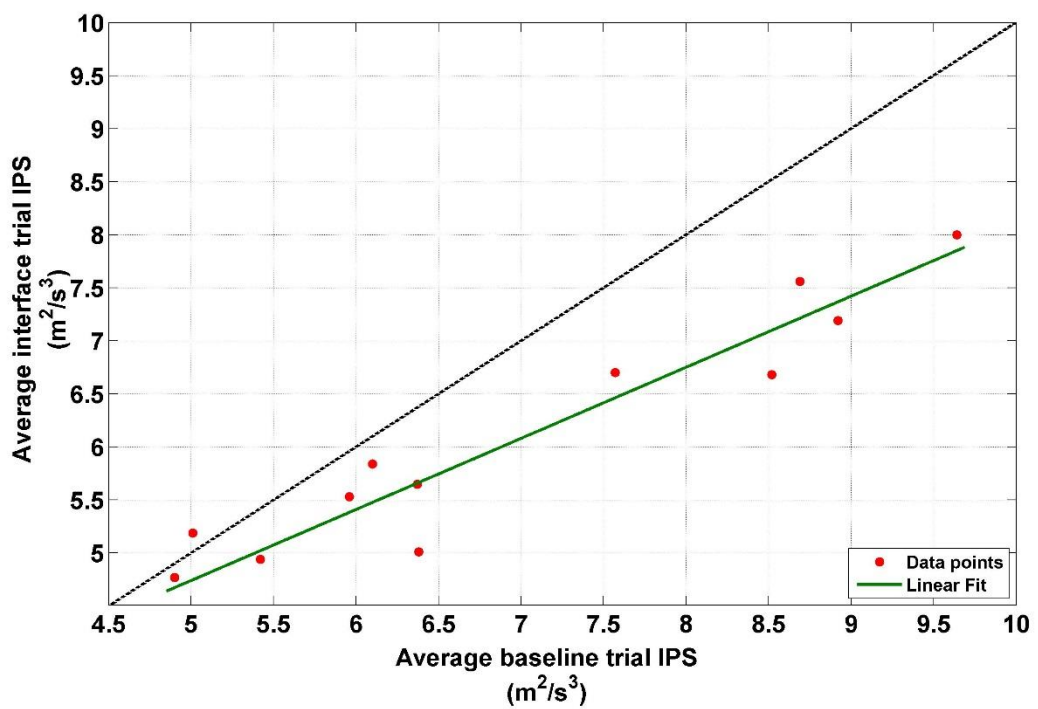


Figure 3-9 - Linear fit showing the average values of IPS being reduced with the use of the driver advisory tool

This can be seen in the lower left hand side of the graph where, drivers who had comparatively lower average engine speed to start with had lesser improvements of this parameter than those who were driving at higher values of engine speed during the baseline trials. The limiting factors of vehicle operation and driveability become more prominent towards the lower engine speed side of the plot, and hence it is not possible for drivers who already have a good driving style with low average engine speed in the baseline trials to improve by significant amounts during their respective interface trials. This is evident in the plot by observing that the curve is relatively close to the $x=y$ line at low values of engine speeds and then diverges progressively, showing that vans that operated in higher average engine speeds during the baseline trials had a more prominent reduction during the interface trials. The lower engine speed during the baseline trials might be due to the fact that some drivers may have already been intentionally early shifting into higher gears to drive economically, or that they would have been following the manufacturer fitted gear upshift lights before the driver advisory device was fitted on. Either way, the middle to the right hand section of the plot shows that drivers with high average engine speeds had more room to improve their driving style and fuel consumption. The curve will tend to plateau after a certain point beyond which it will start to come down again. This quadratic association is backed by the regression analysis performed on the data, generating a coefficient of determination R^2 value (idea of goodness of fit) of 0.9139.

Figure 3-9 shows the reduction in average IPS for each of the 12 vans included in the study for the field trial experiment. A linear fit was used to describe this reduction in IPS values. The same explanation as the previous case applies where drivers with higher average IPS values to begin with during the baseline trials had more room to improve compared to those that were already at the lower end of the spectrum. IPS is linked to two parameters – acceleration and vehicle speed. Reduction in acceleration values has a direct implication on the tractive effort required by the vehicle, while the average vehicle speed mainly depends on the chosen drive cycle of the vehicle. The linear fit was backed by the regression analysis study which provided an R^2 value of 0.9194 for the plot.

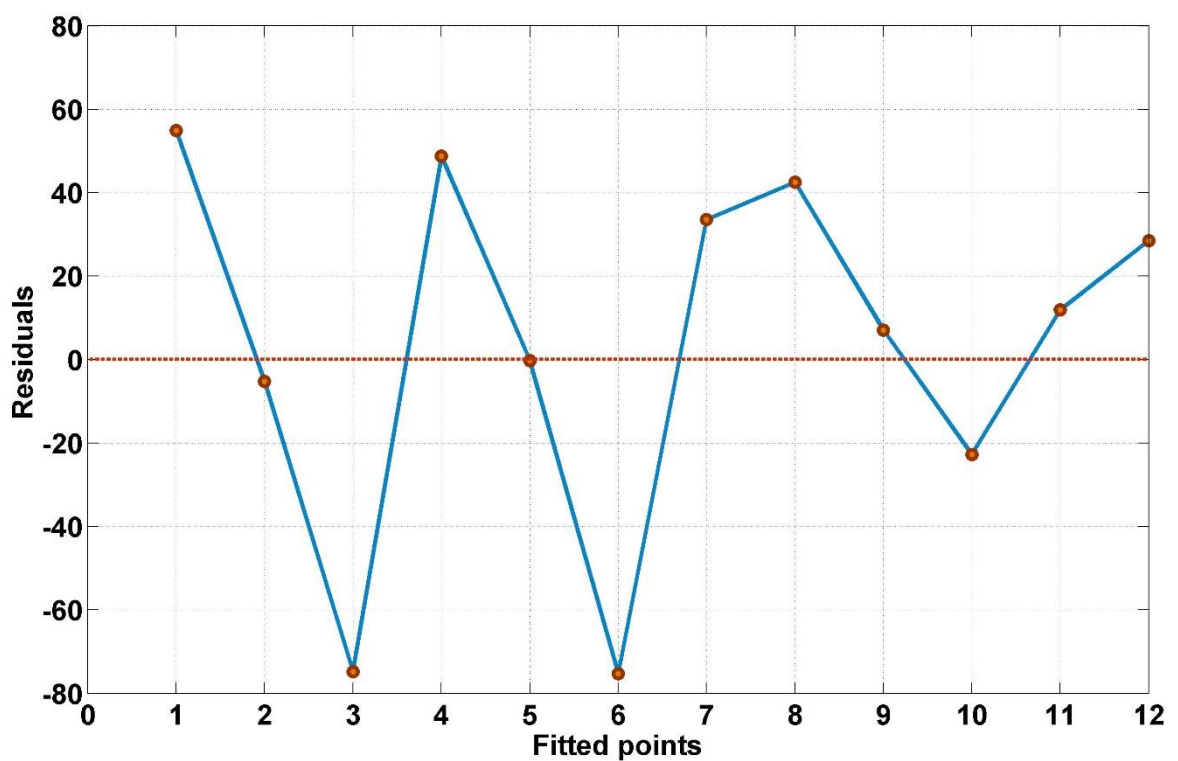


Figure 3-10 - Residual plot for the fitted model of baseline engine speed vs interface engine speed

The author recognises the limitations of R^2 values in regression plots, as they do not clearly show whether the coefficient estimates and model predictions are biased.

Since the thesis uses regression analysis and R^2 values more than once, it is worth mentioning that the residuals for each data analysis was also plotted to ensure that they are random. This is to determine whether certain patterns that the R^2 values cannot show exist or not. Figure 3-10 shows the residual plot of the fitted model baseline engine speed vs interface engine speed of the 12 vans plotted in Figure 3-8. It can be seen that the residuals are random and no clear pattern exists concluding that the fitted model shows good agreement with the actual data.

After observing the reduction in engine speed and IPS values, a simple model was created to predict the benefit of the device in saving on fuel consumption. The aim was to predict the fuel economy benefit in percentage that the advisory tool would yield if fitted onto a vehicle without having to go through time consuming baseline and interface trials. This prediction would be dependent on the availability to two key inputs to the model, namely average vehicle speed and average IPS. As mentioned earlier, the average vehicle speed provides an indication of the drive cycle the vehicle operates in, while the IPS value hints at the aggressivity of the driver.

Model Based Calibration toolbox of Matlab® was used for the creation of the model. A single stage model with two inputs – average vehicle speed and average IPS, and one output – percentage savings in fuel consumption was used for the creation of the model. Figure 3-11 shows the contour plot of the fitted model generated to present the fuel savings that a vehicle would achieve with the use of the driver advisory tool. The X-axis represents the average vehicle speed of the vehicle in km/h (baseline case), while the Y-axis denotes average IPS (baseline case). The different contour lines

show the predicted savings when using the driver behaviour improvement device for the above mentioned input parameters.

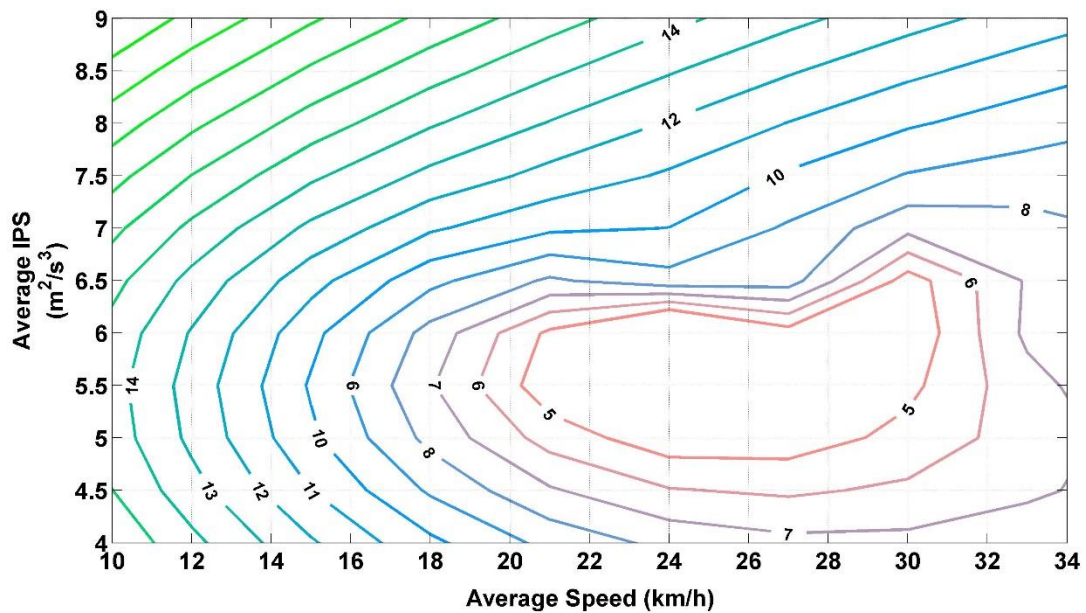


Figure 3-11 - Contour plot of the predicted fuel savings with the use of the driver advisory tool

It can be seen that fuel savings are higher when the driver has high values of IPS to begin with, with low to medium values of vehicle speed. This reinforces the developmental aims of the device, which was to improve fuel consumption by changing key driving patterns, mainly in the urban environment (where average vehicle speed is on the lower side of the spectrum). This shows that the driver advisory tool works best in city or urban driving conditions, where the driver may demand aggressive accelerations when he/she is unrestricted, although they may be unnecessary driving behaviours. The model also highlights that there is minimum improvement in fuel benefits when the vehicle operates at high average speeds and high IPS values to begin with. This is because very high values of IPS need not necessarily mean aggressive driving behaviour; they can also be high average vehicle speed, as the vehicle speed component of the absolute IPS value has more

significance, than the acceleration value which is smaller. Similarly, the contour plot also shows that if the drive cycle of the vehicle involves more of highway driving, improvements may not be as good as that seen in urban conditions. However, the device is intended to improve driving style, and if the feedback and advice are followed, there will be a resulting reduction in fuel consumption in all driving cycles, although some may be smaller than others. This is backed by the model and the contour plot, where most of the other cases show a moderate to high reduction in fuel consumption of the vehicle.

3.3. Parameterised data analysis

This section of data analysis was intended to explore further reasons as to why the driver advisory tool seemed to work very effectively on some vans, but not on others. The author acknowledges the fact that the vans are owned by different companies and their daily routes and routines may differ, making comparisons between different companies unfair. However, comparisons between vans of the same company in most cases were assumed to be fair, as they had similar drive cycles and operation routines, although the rare occasion presented different situations for the vans. Some parts of the analysis were performed using driving pattern parameters described by Ericsson [63], which were discussed in the literature. Others were analysed on a case by case basis (wherever required) for each van.

3.3.1. Detailed data analysis

The aim of this section is to explore different driving pattern parameters discussed in the literature and see their effects and contribution to the overall savings in fuel

consumption achieved by each vehicle. Of the 62 parameters mentioned by Ericsson, only 26 are being considered at this occasion. Parameters associated with deceleration values are not taken into consideration at this stage, due to the fact that the initial aim of the driver behaviour improvement device was only concerned with positive acceleration values and traction of the vehicle.

For Vans 1 and 3 from the same company, fuel savings in the range of 9.1% and 12% were seen. Reduction of certain key driving parameters was the reason behind the overall reduction in fuel consumption of the vehicle. It was earlier discussed that reduction in harsh accelerations are key to the improvement in driving style. In this scenario, harsh accelerations are any values of acceleration of the vehicle that are above 1.5m/s^2 . Earlier literature suggested the division of acceleration values into different sets and determining the percentage of time spent in each set as a good indicator of the driving style. The chosen sets were $0\text{-}0.5\text{ m/s}^2$, $1\text{-}1.5\text{ m/s}^2$, $1.5\text{-}2.5\text{ m/s}^2$ and greater than 2.5 m/s^2 .

For the purpose of demonstrating the importance of these parameters, let us consider only Van 1, which showed a 9.1% improvement in fuel savings over the interface trial. The average acceleration of the vehicle had fallen from 0.68 m/s^2 to 0.59 m/s^2 , which was already a 13% reduction. However, this value does not provide an indication as to which values of accelerations have reduced; besides a reduction in acceleration values may also result from the vehicle being driven in a different drive cycle, say a slower one. But this was not the case, as the average speed during the interface trial was around 4 km/hr greater than that of the baseline trial. It can be concluded as the drive cycles in this case are fairly similar, since the average speeds

are similar for both phases of testing. Also, the percentage of time spent under 2 km/hr, the number of stops per kilometre and the duration of each stop were similar for the baseline and interface trial, showing that both the experimental stages had similar drive cycles. Thus the difference in average acceleration is due to the reduction in harsh higher values of acceleration.

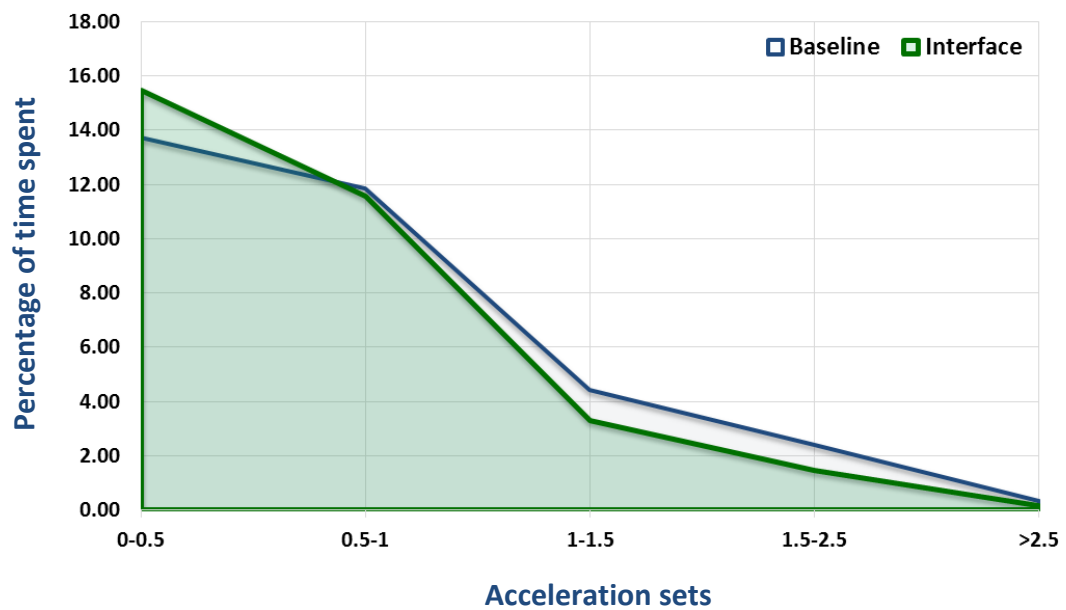


Figure 3-12 - Percentage of time Van 1 spent in different sets of acceleration during baseline and interface trials

Figure 3-12 shows the percentage of time Van 1 spent in different sets of acceleration values. It can be seen that during the interface trials, there has been a reduction in the acceleration values that fall in the bracket of high or harsh accelerations (above 1.5 m/s²). Since all the parameters relating to drive cycle remain the same for the baseline and interface trial, reduction of this high acceleration values correspond to a calmer and less aggressive driving style during the interface trial. This slower rate of acceleration meant that the tractive effort required by the vehicle was lowered (because tractive force required by the vehicle to accelerate $F_T = \text{mass} \times \text{acceleration}$, according to Newton's second law of motion). A reduction in tractive effort meant

lesser fuel required by the vehicle, and hence a reduction in fuel consumption was seen.

Another major contributor to the reduction in fuel consumption was the reduction in high values of engine speed. Figure 3-13 shows the distribution of time spent in different sets of engine speed values for Van 1. It can be seen that with the driver advisory tool in operation, there is a clear reduction in the mid to high range engine speeds during the interface trial. Reduction in engine speed is mainly associated with shifting the vehicle into a higher gear. Hence, there is an increase in the data set for the 0-1500rpm condition. This reduction corresponds to a decrease in the fuel consumption of the vehicle by moving the engine operation point to a lower speed and a higher torque value. Higher the load on the engine (closer to the limiting torque curve), better the brake specific fuel consumption of the vehicle [71].

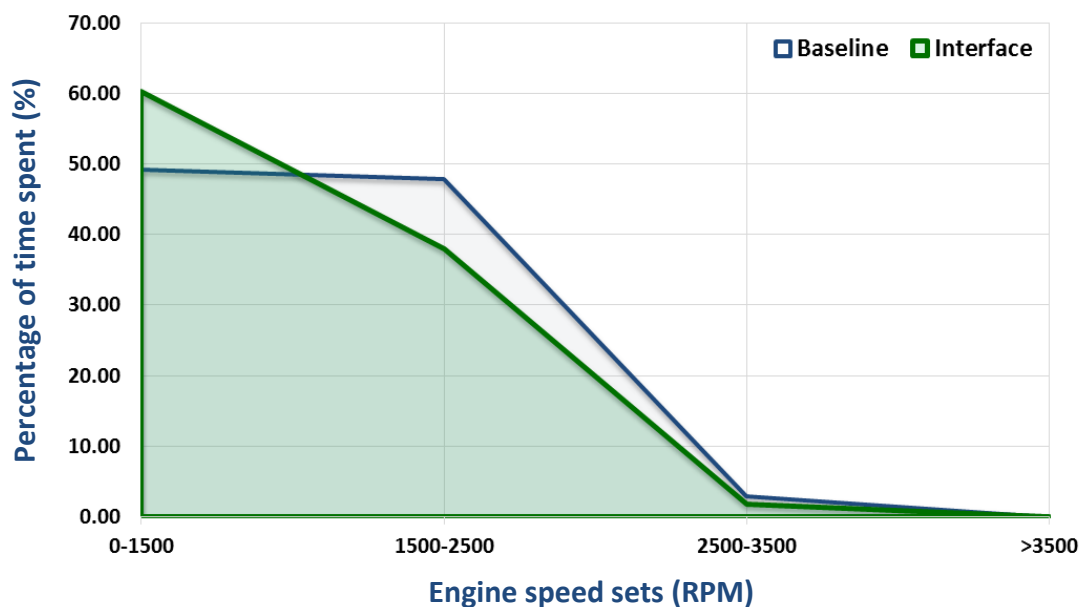


Figure 3-13 - Percentage of time Van 1 spent in different sets of engine speeds during baseline and interface trials

This overall reduction in higher values of engine speed is reflected in the average engine speed of Van 1 of 1391rpm during the interface trials, from 1473rpm for the baseline trial. The manufacturer upshift lights hence did provide some benefit in accomplishing a reduction in fuel consumption. However, this was later revealed to be non-optimal (based on driver feedback), as the manufacturer upshift lights asked drivers to shift up a gear even in certain situations where they were heavily loaded or going uphill. The solution for this problem will be discussed later in Chapter 4.

Two aspects of engine speed reduction are outside the scope of this research, but worth exploring in the future are – the effects of reduction in engine speed and its relation to increase amounts of nitrous oxide emissions [75], and the potential reduction in engine wear and tear due to lower average running speeds. The effect of the driver advisory tool on NO_x emissions is not considered in this study, as the research is aimed at modifying driver behaviour for improved fuel economy, and not focussed on engine modifications. Although NO_x emissions tend to increase with the reduction in engine speed, using less power to propel the vehicle when using the advisory tool potentially further reduces the NO_x emissions [76]. Due to the inherent trade-off between NO_x and fuel consumption for diesel vehicles, reducing the power consumed by the vehicle means less NO_x emissions, in the absence of expensive after treatment processes. The reduction in engine speed reduces the potential wear and tear in moving vehicle components, like engine, driveline, wheels and tyres etc. Unfortunately the time and resources required for either of the above mentioned studies limits it being a part of this research, but is proposed as a future work.

Another interesting parameter analysed was Relative Positive Acceleration, which seemed to have reduced by 19% from 0.21m/s^2 during the baseline phase to 0.17m/s^2 during the interface trial. Regression analysis was performed on different parameters that were thought to have an impact on the reduction in fuel consumption between the baseline and interface trials.

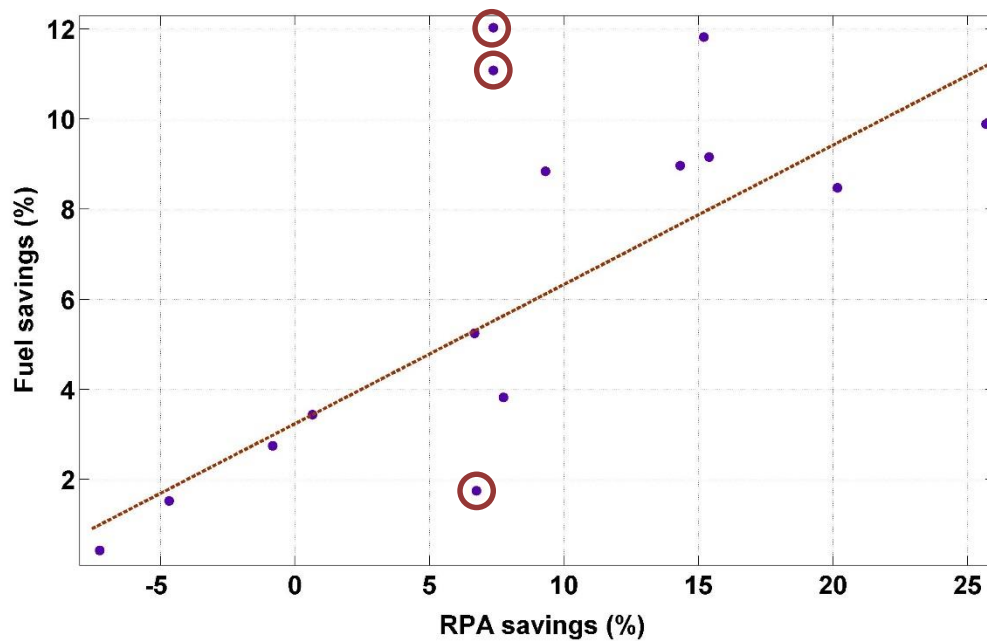


Figure 3-14 - Plot showing the relation between Relative Positive Acceleration and Fuel savings ($R^2 = 0.86$)

Figure 3-14 shows the percentage savings in relative positive acceleration for all vans, plotted against their respective savings in fuel consumption, with 3 vans excluded. These were the same three vans excluded in the analyses presented in the previous section. Linear regression analysis with percentage reduction in RPA chosen as the independent variable, and savings in fuel consumption regarded as the dependent variable was performed. Amongst all the variables considered, reduction in RPA had the closest correlation to reduction in fuel consumption (with an R^2 value of 0.8601). It needs to be mentioned that the overall reduction in fuel consumption is due to a

combination of factors, although statistically RPA had the best correlation amongst the parameters analysed in this thesis.

Reduction in IPS is also a contributor to the reduction in fuel consumption. Since this value is a combination of acceleration and speed, it is hard to understand the effect of individual contribution of speed and acceleration in reducing fuel consumption. The average IPS for Van 1 reduced by 4.4%. However, consider Van 9, which had an 8.5% reduction in fuel consumed during the interface trial, when compared to the baseline trials. The average acceleration of this vehicle reduced by 15.7% from 0.70 m/s^2 to 0.59 m/s^2 . This shows an overall reduction in aggressive driving behaviour, as there is also reduction in the time spent in higher values of acceleration, while an increase in lower to medium values of acceleration in the interface trial when compared to the baseline trial period. There is also a reduction in RPA values suggesting a decrease in aggressive driving. The improvement in fuel consumption and driving parameters were considered significant for the participating company in the trial. However, it describes a different story regarding IPS value, which increased by 12.5% from $5.43 \text{ m}^2/\text{s}^3$ to $6.11 \text{ m}^2/\text{s}^3$. The value contradicts the previous numbers in terms of understanding aggressivity, as it had always been said that reduction in IPS equals to a reduction in aggressivity. In this particular case however, the interface trial had a much higher average speed value of 40.1 km/hr , a 46.8% increase from the baseline trial value of 27.3 km/hr . This meant the Van 9 operated in a drive cycle with higher average speed (say, more of motorway driving) during the interface trial when compared to the baseline trials. This high average vehicle speed during the interface trial had a much bigger impact on the absolute value of IPS, which is a product of

vehicle speed and acceleration. This was the main reason Van 9 was excluded from the model creation and few other analyses performed on the data set. This shows the effect of average speed on the IPS value. It also brings to the attention that aggressivity can be compared using IPS value only if the vehicles operate in roughly similar drive cycle, with similar average speed.

Once Vans 9, 11 and 12 were removed from the analysis, a graph between reduction in IPS values and savings achieved in fuel consumption for all vans was plotted (see Figure 3-15). Regression analysis performed to determine correlation between these two parameters provided an R^2 value of 0.8559 which again showed there exists a relation between reduction in aggressivity and fuel consumption.

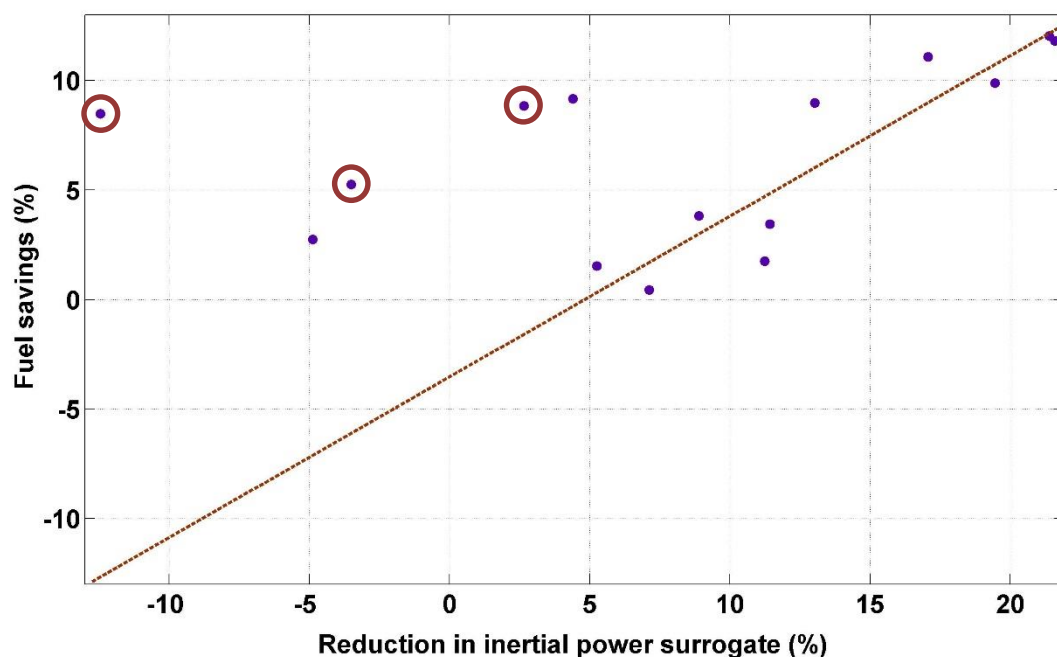


Figure 3-15 - Plot showing the relation between Inertial Power Surrogate and Fuel savings ($R^2 = 0.86$)

Analysis of Van 6 followed next. Having achieved a reduction of 1.75% in fuel consumption, this was not the lowest, but was much lower than the fuel savings achieved by Vans 4 and 5 of the same company (11.1% and 9.9% respectively).

Analyses on this van showed a reduction in all the important metrics of fuel consumption reduction, but still only managed to provide a fairly small reduction in overall fuel consumption.

Table 3-5 shows the different driving pattern parameters analysed for Van 6 to understand the lack of substantial savings when compared to the other two vans belonging to the same company. A reduction in key values like average acceleration, average IPS, RPA etc. showed a reduction in aggressivity of the driver during his interface trial, when compared to that of his baseline trials. A reduction in average engine speed during the interface trials shows that he drove more efficiently by shifting into higher gears sooner.

Other metrics like number of stops per kilometre and the average duration of the stops may provide an indication as to how well the driver anticipates traffic situations. A good indicator of driving style is how efficiently a driver navigates stop-start situations, where he/she anticipates situations of slow traffic, or traffic lights or a roundabout and plans ahead so as not to come to a complete halt (wherever applicable). These metrics provide only an indication of whether the driver might have anticipated traffic flow or not. The author acknowledges that the number of stops per kilometre and average stop duration may have been due to external factors that affect driving, like environmental or traffic conditions. Thus, improvements in these parameters may not necessarily be due to the driver advisory tool. Certain values like decrease in the time spent in high acceleration values and high inertial power surrogate values during the interface trial show a definitive decrease in aggressivity due to the presence of the driver advisory tool.

Table 3-5 - Analysis of different driving pattern parameters for Van 6

Van 6 analysis				
		Baseline	Interface	% change
Fuel consumption (L/100km)		9.74	9.57	-1.75
Average vehicle speed (km/hr)		28.23	27.75	-1.7
Average engine speed (RPM)		1452	1242	-14.5
Average acceleration (RPM)		0.79	0.72	-8.9
Relative positive acceleration (m/s ²)		0.27	0.25	-7.4
Average Inertial Power Surrogate (m ² /s ³)		6.37	5.65	-11.3
No. of stops per kilometre		1.78	1.75	-1.7
Average stop duration (sec)		13.66	12.74	-6.7
Percentage of time spent in different speed distribution sets	0-15 km/hr	20.09	20.33	1.2
	15-30 km/hr	21.13	21.02	-0.5
	30-50 km/hr	28.09	28.95	3.1
	50-70 km/hr	11.23	12.32	9.7
	70-90 km/hr	2.76	2	-27.5
	90-110 km/hr	1.45	1.13	-22.1
	> 110 km/hr	0.7	0.16	-77.1
Percentage of time spent in different acceleration distribution sets	0-0.5 m/s ²	11.66	12.86	10.3
	0.5-1 m/s ²	12.35	13.35	8.1
	1-1.5 m/s ²	5.67	5.41	-4.6
	1.5-2.5 m/s ²	3.19	2.53	-20.7
	> 2.5 m/s ²	0.59	0.4	-32.2
Percentage of time spent in different Inertial Power Surrogate distribution sets	0-3 m ² /s ³	9.9	10	1.0
	3-6 m ² /s ³	10.33	12	16.2
	6-10 m ² /s ³	7.11	7.78	9.4
	10-15 m ² /s ³	3.57	3.43	-3.9
	> 15 m ² /s ³	2.55	1.34	-47.5
Specific work done (KJ/km)		12.33	11.5	-6.7

Thus there was a clear decrease in harsh driving patterns, as average vehicle speed remained more or less the same (meaning similar drive cycles) between baseline and interface trials. The specific work done by the vehicle shows that the energy consumed per kilometre during the interface trials were lower than that of the baseline trials. This again reinforces the fact that the driver drove less aggressive during the interface trial. This is also evident by the increase in time spent in lower to medium values of acceleration and power factors. The analysis of this vehicle concluded that the driver of Van 6 was already good to start with during the baseline trial, which indicates why he only managed marginal improvements compared to the other drivers who undertook the experiment, notably Vans 4 and 5 of the same company. This was inferred by comparing different driving pattern metrics of the three vans of Company B against each other. It was instantly evident that the driver of Van 6 had a good driving style to start with. Even during the baseline phase, this driver had spent considerably less time in the higher values of IPS, when compared to other drivers of company B for their respective baseline trials.

Van 6 also had an average engine speed of 1452rpm during the baseline trial, which was already below the total average for engine speed for all vans – 1539rpm. Vans 4 and 5 from the same company had an average engine speed of 2052rpm and 1606rpm respectively. The driver advisory tool helped them improve to a much lower value of engine speed – 1665rpm and 1444rpm, while the driver of Van 6 managed to reduce his average engine speed even further to 1242rpm. This again correlates to the model described in the previous section which showed that the advisory tool has more potential in helping drivers who have more room for improvement (high engine

speeds, high IPS values etc.) than for those who are already fairly good to start with. One of the other issues this section highlighted was the excessive idling of some vans, which caused a spike in fuel consumption, thus preventing them vans from being compared with each other (unless anything above 97th percentile of idling was removed). Hence, it is beneficial to change the driver's behaviour to avoid unnecessary idling conditions, and this will be discussed in the next chapter.

3.3.2. Use of other metrics

All of the driving pattern parameters described by Ericsson [63] in the literature were useful in understanding factors that account for reduction in the overall aggressivity of the driver and fuel consumption. Reduction in important metrics like RPA, average IPS and average acceleration etc. have proven to directly correlate to the savings achieved in fuel consumption for each van. However, there may be some cases where these parameters alone cannot help understand the savings (or lack of savings for that matter) in fuel consumption, which is a limiting factor of existing driving pattern analysis. Literature explained the uses of these metrics, but it needs to be emphasised that all these parameters may not still provide a 100% satisfactory understanding of driving behaviour. This is mainly due to the impossibility of owning unlimited resources and time to collect information about every variable associated with driving pattern, which includes climatic or weather conditions, traffic situation, time of the day, route chosen, familiarity of the route, purpose of travel and many more. One such case where it was difficult to understand the reasons for lack of savings using similar methodology used in previous section is explained in this section.

In the fifteen vans that were tested by different drivers for the field trial experiments, Van 2 had the lowest savings in fuel consumption, with only 0.43% improvement in the interface trials when compared to its respective baseline trial. However, Vans 1 and 3 of the same Company A had savings of 9.16% and 12% respectively. Analysis on Vans 1 and 3 helped correlate fuel consumption savings to reduction in a number of driving pattern metrics similar to the conditions described in the previous section. Van 2 however, told a different story for the various driving pattern metrics. Most of the parameters showed a reduction, which seemed to conclude to a definitive reduction in aggressivity, which would help attain an increase in fuel savings. However, there was only a marginal reduction in fuel consumption. This meant this data collected from this van had to be analysed in more detail.

Table 3-6 shows different driving pattern parameters of Van 2 analysed and presented in a tabular format. Similar to the previous table, this shows reduction in various factors proven to have a link to aggressivity and hence fuel consumption, like average acceleration, average IPS and average engine speed value. The average speed, number of stops per kilometre and the average duration of each stop is roughly similar for the interface trials when compared to the respective baseline testing phase.

It can also be seen that there is a significant decrease in the time spent in higher values of acceleration and IPS, which shows an overall reduction in aggressivity of the driver, but does not shed light on the reason for such a small improvement in fuel consumption. This situation compelled to explore alternate explanations for the poor increase in fuel consumption.

Table 3-6 - Analysis of different driving pattern parameters for Van 2

Van 2 analysis				
		Baseline	Interface	% change
Fuel consumption (L/100km)		9.12	9.09	-0.3
Average vehicle speed (km/hr)		23.82	21.18	-11.1
Average engine speed (RPM)		1481	1338	-9.7
Average acceleration (RPM)		0.8	0.8	0.0
Relative positive acceleration (m/s ²)		0.27	0.29	7.4
Average Inertial Power Surrogate (m ² /s ³)		5.96	5.53	-7.2
No. of stops per kilometre		3.06	3.41	11.4
Average stop duration (sec)		16.16	17.13	6.0
Percentage of time spent in different speed distribution sets	0-15 km/hr	22.22	20.63	-7.2
	15-30 km/hr	19.98	23.09	15.6
	30-50 km/hr	26.75	30.35	13.5
	50-70 km/hr	5.05	4.4	-12.9
	70-90 km/hr	2.12	0.37	-82.5
	90-110 km/hr	2.67	0	-100.0
	> 110 km/hr	0.06	0	-100.0
Percentage of time spent in different acceleration distribution sets	0-0.5 m/s ²	9.99	9.91	-0.8
	0.5-1 m/s ²	11.22	11.85	5.6
	1-1.5 m/s ²	5.46	5.74	5.1
	1.5-2.5 m/s ²	3.06	3.08	0.7
	> 2.5 m/s ²	0.51	0.47	-7.8
Percentage of time spent in different Inertial Power Surrogate distribution sets	0-3 m ² /s ³	10.12	10.55	4.2
	3-6 m ² /s ³	8.37	9.56	14.2
	6-10 m ² /s ³	6.45	6.39	-0.9
	10-15 m ² /s ³	3.25	3.13	-3.7
	> 15 m ² /s ³	2.05	1.42	-30.7

The results analysed so far were comparisons between the two week baseline trial and the two week interface trial. It was decided to look into the warnings and violations the driver for Van 2 received on a daily basis. Drivers ranged from tens to hundreds of warnings and violations per day during their baseline testing, when the device was fitted; but neither audible nor visual feedback were given to the drivers, as the device was only logging data. However, the number of warnings and violations that would have been communicated to the driver had the audible and visual feedback been activated during the baseline trial, was being logged as the driver advisory tool was active when collecting data. This number reduced drastically during the interface trial when the drivers started to react to feedback provided and improved their driving style. So it was natural to see the number of warnings and violations per day, drop to a number under ten, a lot of times even zero. However for Van 2, strangely, the number of warnings and violations were different for every day. Some days had very few, while others a substantial amount, similar to those that were seen during the baseline trial of most vehicles.

Van 1 had a total of 19 warnings in 14 days, with an average of 0.014 warnings per kilometre. Van 3 had even better improvements, with only 6 warnings in 14 days, with an average of 0.008 warnings per kilometre. Van 2 however had a staggering 722 warnings in 14 days with 128 violations, thus making a total of 850 for warnings, 2 and violations during the interface trial. A total penalty number of this proportion was a familiar range during the baseline trials, where drivers were not given any feedback at all.

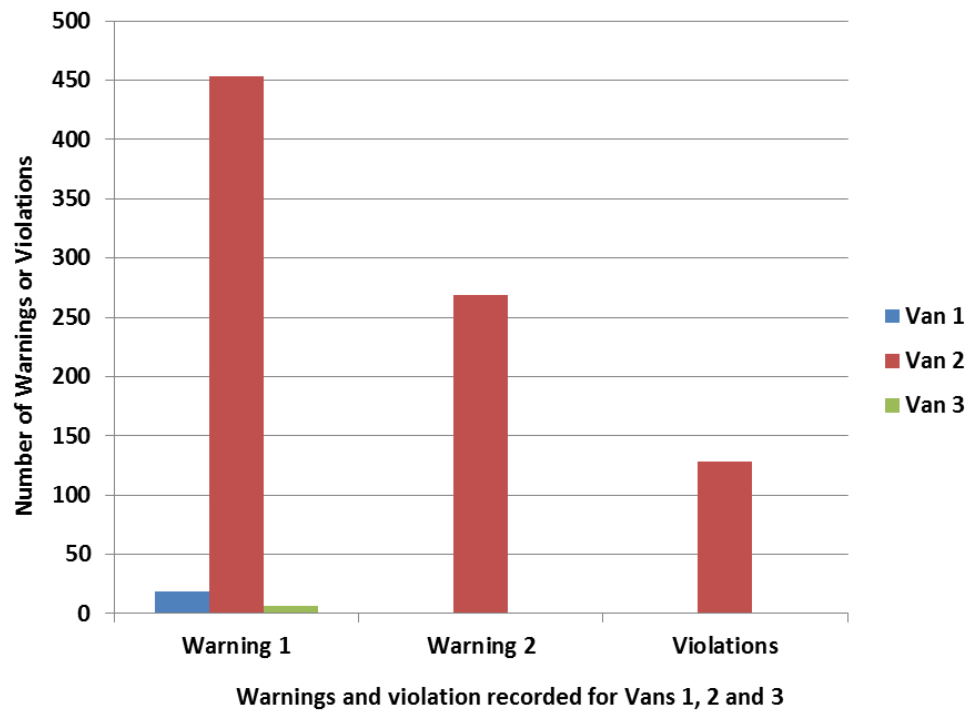


Figure 3-16 - Number of Warning 1s, Warning 2s and Violations recorded for interface trials for Vans 1, 2 and 3 of Company A

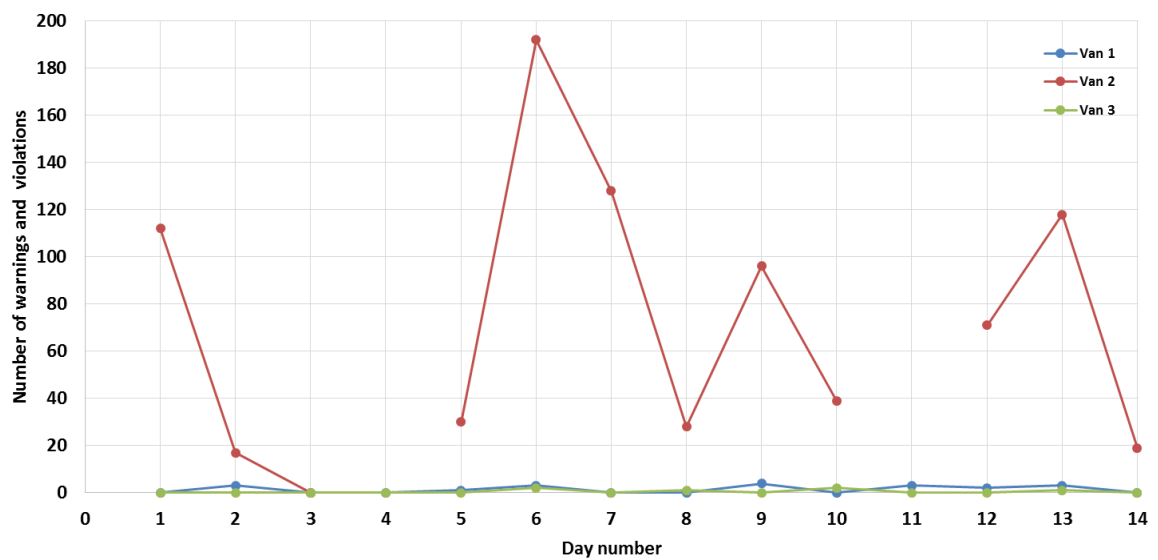


Figure 3-17 - Warnings and violations for Vans 1, 2 and 3 on a daily basis during the interface trials

Figure 3-16 shows the graphical representation of the total number of warnings and violations for the interface trial for each of the vans belonging to Company A. The high number of warnings and violations for Van 2 meant that this van needed to be analysed on a day to day basis. Figure 3-17 shows the number of warnings and violations for each of the vans of Company A on a daily basis for the interface trial. The breaks in the line for Van 2 is due to the fact that the van was not used during one of the days of the weekend, while Vans 1 and 3 had smaller trips during the weekends of the interface trials. The substantial number of warnings and violations correlated to the poor savings in fuel consumption for Van 2. It seemed to suggest that the poor driving style adopted by the driver of Van 2, by neglecting the feedback provided by the driver advisory tool was the reason for the poor fuel consumption savings.

On careful analysis, there were few days during the interface trials where the number of violations were comparatively lower than the others, like days 2, 3, 5, 8 and 14. It brought suspicions as to whether the audible feedback was available to the driver or not on all days during the interface trial. However, a mechanical malfunction was ruled out, because it would be strange to have the system not working on some days and fix itself on others. This meant the only other possibility was a change in the driver during this trial. This seemed more plausible explanation. Considering only the five days (2, 3, 5, 8 and 14) of the total twelve in the two week period of interface trial, fuel consumption was calculated to be 8.6 L/100 kilometres, compared to that of the baseline testing of 9.12 L/100km. This showed an increase of 5.7% in fuel economy of the vehicle. These findings were reported to Company A, who had

checked their records to confirm that a driver change had in fact taken place due to one of the drivers falling sick, who returned towards the end of the trial. This information was not provided to the industrial partner or the author by Company A during the trial, but was later confirmed. This improvement meant that all the vehicles in Company A had reasonable increase in fuel economy with the use of the driver advisory tool. Unfortunately, this detailed data analysis was only performed after the initial savings in fuel consumption were shared with the participants. This meant that the overall savings in fuel consumption achieved (that had been published) with the use of the driver advisory tool, was under-rated due to the slightly skewed low fuel savings of Van 2.

There was more than one driver change for Van 2 during the interface trial. The inconsistent number of warnings and violations on a daily basis (Figure 3-17) may be due to the fact that the driver(s) did not have sufficient time or opportunity to get accustomed to the driver advisory tool. The author believes that it is important for drivers to be gradually familiarised with the system, rather than be displeased with the sudden warnings and violations received from the advisory tool. This analysis gave rise to the concept of introducing a sensitivity control for the device, whereby the fleet manager could progressively increase the '*strictness*' of the device based on the drivers' improvement in driving behaviour. This update will be discussed in the next chapter.

3.4. Summary

Analysis of the data collected during the field trial experiment of the driver behaviour improvement device has been discussed in this chapter. 15 vans were tested over a period of four weeks (two weeks of baseline testing and two weeks of interface trials) with over 39,000km worth of data being collected. The device was seen to help save on average of 7.6% in fuel consumption across the entire fleet, with the highest savings being 12%. This saving is a reliable figure due to the fact that the drivers were unaware of the system collecting information on their innate driving behaviour during the baseline tests. The reduction in fuel consumption was a result of change in driver behaviour, which was evident from the reduction of various metrics of driving pattern like Inertial Power Surrogate, pedal busyness, harsh accelerations etc. It was also seen that drivers tended to brake gently as well, which was believed to be the result of their relaxed and calmer driving style.

A simple model was also created to understand the savings that the device would provide if used on a vehicle. Different driving pattern parameters were used to understand why some vehicles achieved better savings than others, and deeper research was carried out to determine where and how savings were made. Also, the driving pattern parameters that had the best correlation to reduction in fuel consumption of the vehicle were identified as RPA and IPS. It was also seen that these parameters alone cannot provide a complete assessment of driving behaviour, as a number of external factors like - like traffic and climatic conditions, vehicle type etc. affect the way a vehicle is driven.

An example of one van which showed the least improvement (0.43%) in fuel consumption was analysed in more detail to identify the reason for the poor improvement in fuel consumption, even though most of the driving pattern parameters reduced. This was due to a driver change during the field trial which was unreported to the author, which skewed the results slightly. Once the days of the driver change were removed from the analysis, Van 6 showed an improvement of 5.7%. It was also seen that from Van 6 that, the driver advisory tool is more effective on drivers who have more room for improvement than those who are already good to start with.

It was clear from data analysis that the driver advisory tool helped achieve significant reduction in fuel consumption by improving driving style. Through the analysis process and feedback from drivers, various improvements in the device with regards to drivability and functionality were identified. One of these was the need for control of sensitivity of the device, so that drivers have the opportunity to gradually become accustomed to the warnings and violations (feedback) from the tool. It was also seen from the data that certain vans had excessive idling events, which led to the decision to delete all idling above 90 seconds (97th percentile of total idling) for most of the analysis phase. This also provided the need for introducing idling warnings and penalties for excessive/unnecessary idling of the vehicle. Other updates like cruise control detection and a generic version suitable for use on any vehicle are explained in the next chapter. These were identified as essential requirements for the device to work in its optimum manner, and hence were added as new functionalities to the device.

Chapter 4 - Updated version of driver advisory tool

This chapter focusses on the update of the algorithm of the driver advisory tool, to iron out drivability and control issues relating to the previously trialled version. Additional functionalities like sensitivity control, and idling warnings and penalties have been introduced into the system for optimal performance of the driver advisory tool. This version is also capable of being fitted to any type of vehicle with minimal or no changes.

4.1. Introduction

Considerable amount of data was collected from the field trial experiment of the driver advisory tool. This served the purpose of analysing and understanding different driving parameters and contributors to the reduction in fuel consumption that was observed over the entire fleet. At the same time, the engagement with different commercial organisations and the industrial partner on the project, helped obtain substantial amount of driver and company feedback. There was also interest from different companies that were part of the trial, for the unit to be fitted on to the rest of their fleet. Since the initial product was developed for use only on Ford Transit vehicles, a new version would have to be developed for each type vehicle, which induced a range of issues from practicality through to development and production costs. Driver advisory tools from the literature had certain parameters that needed to be tweaked for every different type of vehicle the device was fitted on [51, 52, 56]. To overcome these issues present in the literature and fill the research gap, it was decided to develop, test and release a single updated version of the driver advisory tool, so as to be capable of being fitted onto any type of vehicle with no change in hardware or software. This version would also have additional functionality improvements with respect to sensitivity control, penalties for excessive idling, cruise control detection etc.

Development of the new version of the driver advisory tool showcased an array of complications which required careful simulation and testing, so as to be safe and reliable before deployment onto vehicles. Due to the increase in functionality of the device, the updated algorithm had more number of inputs and outputs, and also an

increase in the number of data processing blocks to achieve the required functional performance. Updates on the device ranged from sensitivity control, to detection of long idling periods. This chapter discusses some of the various stages involved in the algorithm development of the updated version of the driver advisory tool, and its simulation and testing.

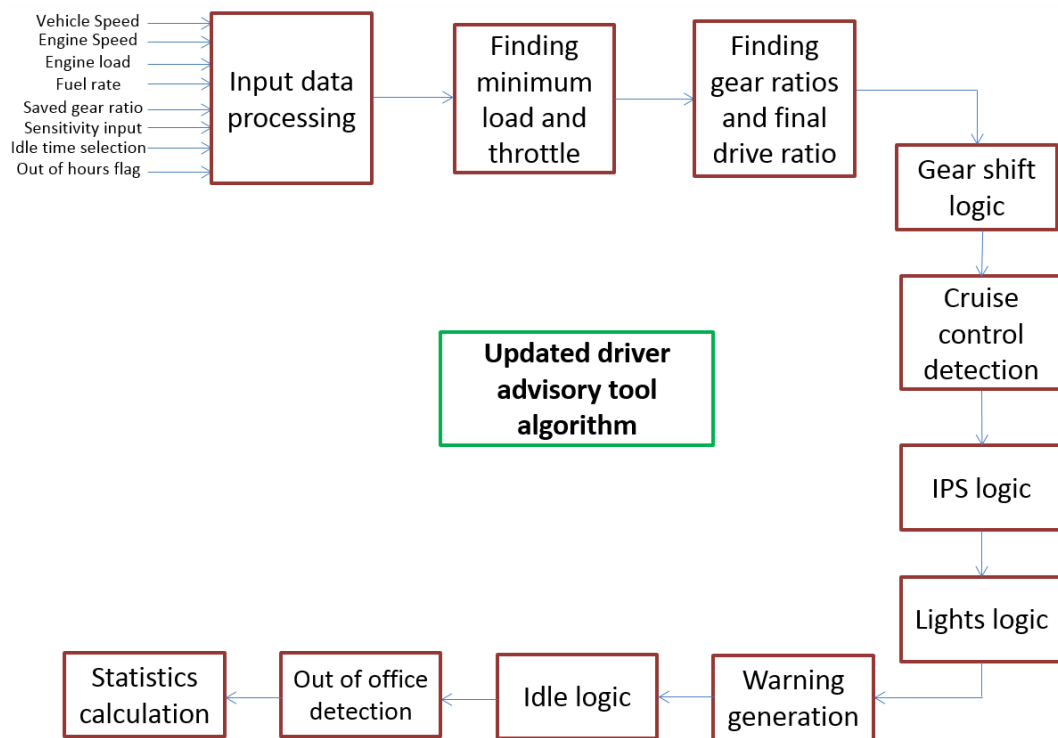


Figure 4-1 - Schematic representation of the updated version of the driver advisory tool

Figure 4-1 shows the schematic representation of the updated version of the driver advisory tool. Compared to the algorithm represented in Figure 2-16, it is evident that there is a significant increase in the number of inputs and strategy blocks. An increase in the number of input parameters is due to the increase in the requirements for drivability and functioning of the updated version of the driver advisory tool. The incoming raw data from the vehicle On-Board Diagnostics (OBD) port (CAN communication broadcast) and the memory of the device, was first processed into

useful information in the data processing block. Gains and offsets of the different vehicle parameters were applied and the incoming data was converted into known units. The driver advisory tool still relies on information from the vehicle CAN communication network obtained via plugging into the vehicle OBD II port. This provides access to several key vehicle parameters that are essential for the algorithm of unit. All new generation of on-road vehicles (under 6.5 tonnes) have to be equipped with OBD II CAN communication network, which mean that certain key vehicle parameters have to be broadcast as per government regulation [77]. This regulation was intended for vehicle servicing (or repair) and certification tests that may need to be conducted on the vehicle by technicians other than the vehicle manufacturing company. This allows for the driver behaviour improvement tool to take advantage and use the key parameters that are broadcast on the CAN, for the determination of driving style.

It needs to be mentioned that there is another major difference between the old version and the updated version of the driver advisory tool. This is the replacement of the pedal position channel with engine load data (which will be explained in detail later in the chapter). The initial version of the device was developed solely for use on Ford Transit vehicles, which broadcast its pedal position, which enabled the algorithm to use this data. It is not a regulatory requirement to have vehicle pedal position broadcast on the OBD II CAN network. Thus it was difficult to identify this parameter on the CAN network for vans from other manufacturers like Citroen, Renault, Mercedes, Vauxhall etc. This meant every time the device had to be fitted on to a vehicle, the entire CAN database may have to be searched via trial and error method

to identify this one parameter. It was hence decided to pursue an alternative avenue, by using engine load as the driving input for the main algorithm, as this parameter is readily available in the Mode 1 list of the vehicle CAN communication. This chapter details some of the additions made into the updated driver advisory tool algorithm to improve the functionality and drivability of the driver advisory tool. These changes were an essential part of the device, as all the updates need to work in conjunction for the optimal performance of the system in helping drivers achieve significant savings in fuel consumption.

4.2. Addition of sensitivity function

One of the first updates was to add a sensitivity control for the device. This would help fleet managers control the rate at which the device provides feedback to the drivers. In other words, this was intended to control the *strictness* of the advisory tool in providing feedback/advice and penalties to the driver for his/her driving style. The sensitivity of the device can be controlled between a value of 1 and 5, with 1 being the least sensitive to driver input, while 5 being the most sensitive. It is worth mentioning that adjusting the sensitivity does not change the physical values at which warnings and violations are provided to the user, but changes the rate at which it reaches these values. The long term IPS_{LT} lights trigger warnings and violations. These lights work as a moving average of the short term IPS_{ST} lights, which provide a visual representation of the instantaneous driving performance of the driver. The moving average is a mathematical low pass filter that allows signals with a frequency below a cut off frequency to pass through, and attenuates high frequency data [78].

The intention of the sensitivity control was to help drivers get used to the system gradually, rather than have a negative feeling towards the *strict* advice provided from the first day of use. Studies have also shown that adjusting the sensitivity of a driver advisory tool according to the driver's growing skill or improvement can have better results when compared to a non-adaptive system [79].

The levels of inertial power surrogate values at which warnings 1, 2 and fault are generated are - $7.7\text{m}^2/\text{s}^3$, $11.55\text{m}^2/\text{s}^3$ and $14.25\text{m}^2/\text{s}^3$ respectively. These points were chosen after a number of trials using data collected from different driving scenarios, during the initial development stage of the tool. It also relates to the high values of IPS specified in the literature by Ericsson [63]. Since these limits were enforced on the low pass filtered value of instantaneous IPS, short sudden manoeuvres during driving do not produce warnings or violations. Though these manoeuvres may trigger a change in the short term IPS lights moving into the red phase, they may not trigger a change in the long term IPS values, due to the moving average filter. This was provided so as to not to have continuous change in IPS values and lights which may distract the driver.

Figure 4-2 shows the change in long term IPS values for three different sensitivity levels for the same vehicle data of 50 seconds. This data is post processed and simulated to highlight the rate of change of IPS_{LT} when sensitivity is adjusted. Sensitivity is changed when the fleet manager changes the sensitivity control input. This triggers a change in the gains where the instantaneous IPS_{ST} is converted to long term IPS_{LT} . The gains were carefully chosen based on trials simulations on existing data. They were later tested on road and tweaked to arrive at the final values used

for the creation of the updated algorithm. These gains also change with the instantaneous vehicle speed. At high vehicle speeds, the gain is reduced so as to allow the driver to accelerate as required, because the component of vehicle speed in Inertial Power Surrogate ($v \times a$) calculation is more significant than the acceleration component. This can be seen in the figure, where at low values of IPS_{LT} , the rate of change of IPS_{LT} for sensitivity level 5 below the 3910 second mark is higher than that of sensitivity level 1 at the same time, while at higher values of IPS (beyond 3920 second mark), the rate of increase of IPS_{LT} for all the three levels of sensitivity shown are similar. In short, a two dimensional look up table was used to choose the optimum sensitivity gains based on the sensitivity input from the fleet manager and the instantaneous vehicle speed.

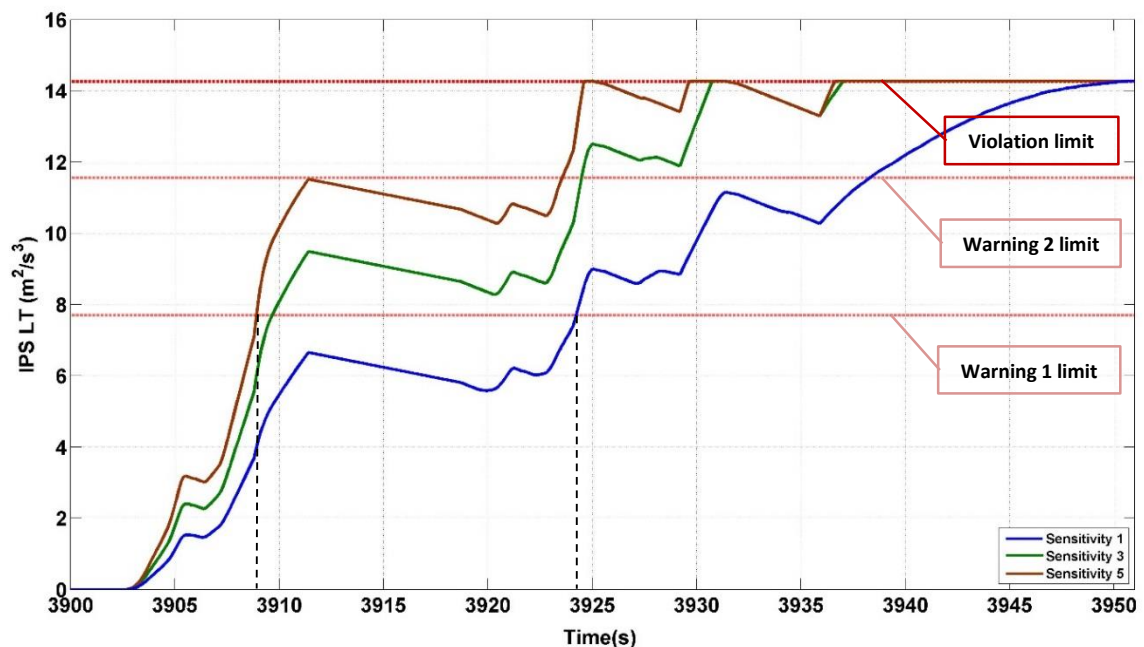


Figure 4-2 - Difference in sensitivity settings for the same vehicle data

As mentioned earlier it can be seen that the limits at which warnings and violations are reached remain unchanged for any value of sensitivity, but the rate at which the driver reaches these values changes. For Sensitivity level 1, the driver has more room for harsher accelerations when compared to higher sensitivity levels. For the highest level of sensitivity 5, it can be seen that the driver would have received the first warning at the 3908th second mark, while for sensitivity level 1, the driver would have received the first warning at the 3924th second mark, which is 16 seconds later. The same can be said for the second warning and the violation. It needs to be mentioned that once the driver receives a violation, the long term IPS is capped at the third limit of $14.25\text{m}^2/\text{s}^3$ until the driver improves his driving style to bring the IPS_{LT} below this level. In the case of the first level of sensitivity, the driver would have received a recorded violation only at the 3951st second, which is considerably later than when he/she would have received the same if sensitivity level 5 was selected – 3924th second, 26 seconds earlier. This shows that sensitivity control using the gains of the low pass filter proved effective. It needs to be mentioned that once a violation is received the driver will be allowed 10 seconds to improve his/her driving style before he/she is awarded another recorded violation. This allows ample amount of time for the driver to change his/her driving style, in case the violation was unfair, due to a quick and sudden unavoidable manoeuvre.

When the device is first installed in a vehicle, sensitivity level 1 is selected as the default option. This helps drivers get accustomed to the device, and then sensitivity is progressively increased over time. This way, drivers do not feel that fleet managers have unreasonable expectations of improvement from them from day 1 of use, when

they are given a high number of warnings; rather this sensitivity control helps them get used to the device gradually. Fleet managers can then steadily increase the sensitivity to help achieve more savings from the vehicles, depending on the driver's improvement.

4.3. Minimum pedal issue

Another issue seen at the same time for Euro 5 versions of Ford Transits was that, the pedal position had an offset fluctuating between 17 and 18%, even when there was no driver pedal usage. This was a rather strange issue, and queries sent to the manufacturer did not provide any useful answers.

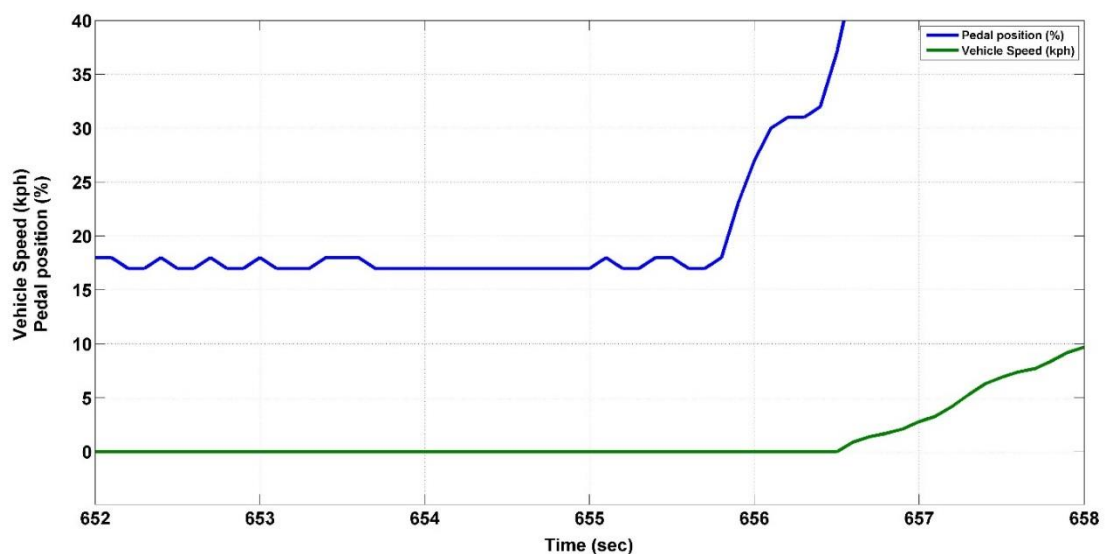


Figure 4-3 - Minimum pedal position for Euro 5 Ford Transit van

Figure 4-3 illustrates this based on a Euro 5 Ford Transit van. It can be seen that when vehicle speed is zero (vehicle idling), the pedal position oscillates between 17 and 18%, when it should actually be zero. The figure shows only 6 seconds of vehicle idling, but the same pattern was seen for different Euro 5 Ford Transit data. Pedal

position increases from 655.8th second as the driver begins his procedure to accelerate the vehicle. This is seen by the increase in vehicle speed that shortly followed.

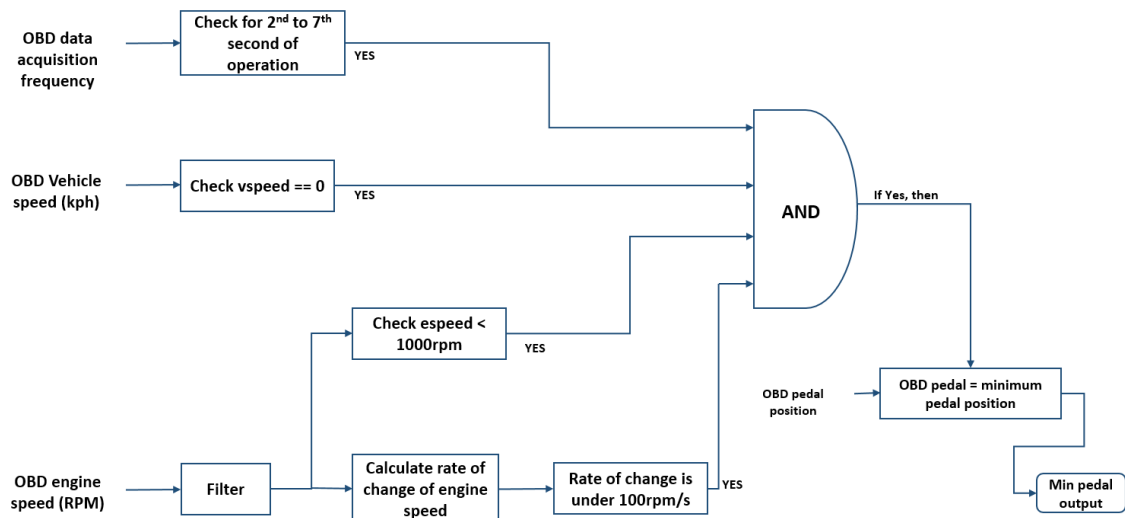


Figure 4-4 - Representation of the algorithm used to detect minimum pedal position

Rather than subtract this offset from the Euro 5 van, it was thus decided to incorporate an algorithm into the device that would detect the minimum pedal position of the vehicle. This would identify any pedal position offsets that may be present in vehicles of different makes, and correct for the same. A representation of the algorithm developed in Simulink® is shown in Figure 4-4. This procedure is done during the vehicle start up stage. A default pedal position value of 20% is used to compare and identify the minimum pedal position during the first seven seconds after the engine is switched ON - when the vehicle is stationary and idling. This default value ensures that a wrong minimum pedal value is not selected when the vehicle stalls and restarts; at this stage the driver may still be applying pedal, while the vehicle stalls momentarily and starts automatically, which may restart the device, which would engage the minimum pedal finding algorithm.

The data acquisition rate frequency is used to count the time step to measure first seven seconds of data (actual pedal position finding algorithm works only between the 2nd and the 7th second). At the same time vehicle speed is checked to see if it equals zero, whilst engine speed data is checked to see if it is below 1000rpm (second check to determine idling). Also, the derivative of engine speed is checked to see if the rate of change of engine speed is below a 100rpm, to ensure idling. If all these cases are satisfied, then minimum pedal value is the minimum of the instantaneous pedal position between the 2nd and the 7th second after the vehicle is switched ON. This value is stored through the running of the vehicle till it switches OFF. Once it switches ON again, the same procedure repeats. It was decided not to save the minimum pedal position value on memory, but rather search for it every time the vehicle starts. This is just in anticipation of any software update that may be performed on the vehicle by the manufacturer during a regular service, which may or may not change the original pedal offset. This logic was later changed and replaced with engine load, as not all vehicles had a readily available pedal position on their CAN system. A more complicated minimum load measurement will be discussed later in this chapter.

4.4. Cruise control detection

Since the driver advisory tool is concerned with reducing aggressivity of the driver, the algorithm uses pedal position, vehicle speed, engine speed and IPS values to determine the driving style of the driver. When he/she drives in a non-optimal fashion, the IPS_{LT} value climbs to a point to serve the driver with warnings and

violations. Once the driver drives in the high IPS_{LT} region and triggers the red lights on the dash board, he/she can only bring the lights back to green (lower IPS_{LT}) by driving calmly and less aggressively. Stopping at a traffic light with zero vehicle speed, or idling will not help reduce the IPS_{LT} ; as this denotes a change in traffic situations and not generally an improved driving style. Hence there are systems in place to detect vehicle speed less than 2 kph, and pedal position less than 5% to freeze the IPS_{ST} and IPS_{LT} at its old position. Thus, the logic that controls IPS_{ST} and IPS_{LT} is only active when the vehicle is moving. To bring the IPS_{LT} lights down to the green region from the red, the driver needs to drive less aggressively, with lesser pedal position changes and lower acceleration rates.

There are certain scenarios where pedal position becomes a crucial factor in the IPS_{LT} calculation of the advisory tool. This is because the system was designed keeping drivability in mind, and also not to unfairly present drivers with high IPS_{LT} lights (or warnings). Take the example of the vehicle going downhill. A small pedal input will increase the vehicle speed (which eventually will increase IPS), due to the negative gradient and inertia of the vehicle, when compared to a flat surface. Thus when going downhill, a driver requires less pedal usage to reach a particular speed than what he/she would need when on a flat surface, with all other conditions remaining the same. However, in some situations it is hard to anticipate the acceleration of the vehicle when going downhill, and the driver might apply the same pedal position that he/she is used to on a flat surface. To identify and screen out these situations from unfairly giving drivers a warning or violation, there are pedal position correction factors that come into effect at low pedal position values. These corrections are

added to the IPS_{LT} calculations before they control the lights, or warnings and violations. At very low values of pedal position, the driver is allowed to accelerate, and he/she will not be penalised for this. But as pedal position increases, the correction factor changes, and the driver will not have this perk to assist in driving in the lower lights. In simpler terms, at low pedal position values, IPS_{LT} will not increase with IPS_{ST} as it would in the case of high pedal position values.

This was added into the system as an improvement in driveability of the device, and seemed to work well among the participants of the field trial experiment. However, some fleet managers involved in the experiment discovered a problem with drivers bypassing the device by using cruise control to accelerate, so that their IPS_{LT} would drop down quickly. This is because when the driver has a high IPS_{LT} , using cruise to accelerate would trick the algorithm into believing that very low (or zero) pedal position was used to drive the vehicle. This would engage the low gains for pedal correction (originally put in place for low pedal value correction, as explained earlier), and IPS_{LT} will drop very quickly. This was a cunning method of exploiting a driveability improvement property of the device by some drivers, to elude the essential functionality of driver advisory tool. Thus, it was important that the updated version detected the use of cruise control to ensure that the lights come down to green at the same rate as it would if the driver used the pedals to accelerate. It needs to be reiterated that the device does not discourage the use of cruise control, but only treats it as a normal rate of acceleration using the pedals.

Determination of whether the vehicle accelerated due to cruise control or gradient required careful assessment. A correction for this issue had to be incorporated into

the pedal correction factor of IPS_{LT} calculation in such a way that the driver would not get the benefit of pedal correction factor if he/she had high IPS_{ST} values at zero pedal position. This could not easily be solved, as in real driving scenarios there are a number of situations where the vehicle will accelerate with zero pedal position (maybe for very short periods of time). Hence, all acceleration events with zero pedal cannot be generalised as cruise control. These events thus needed to be separated from situations of the use of cruise control to accelerate. An example of this event can be a situation where the vehicle is going downhill, or when the driver accelerates and lifts off the pedal momentarily (say to change gear), where the vehicle will still continue to accelerate for a split second due to the inertia of the vehicle.

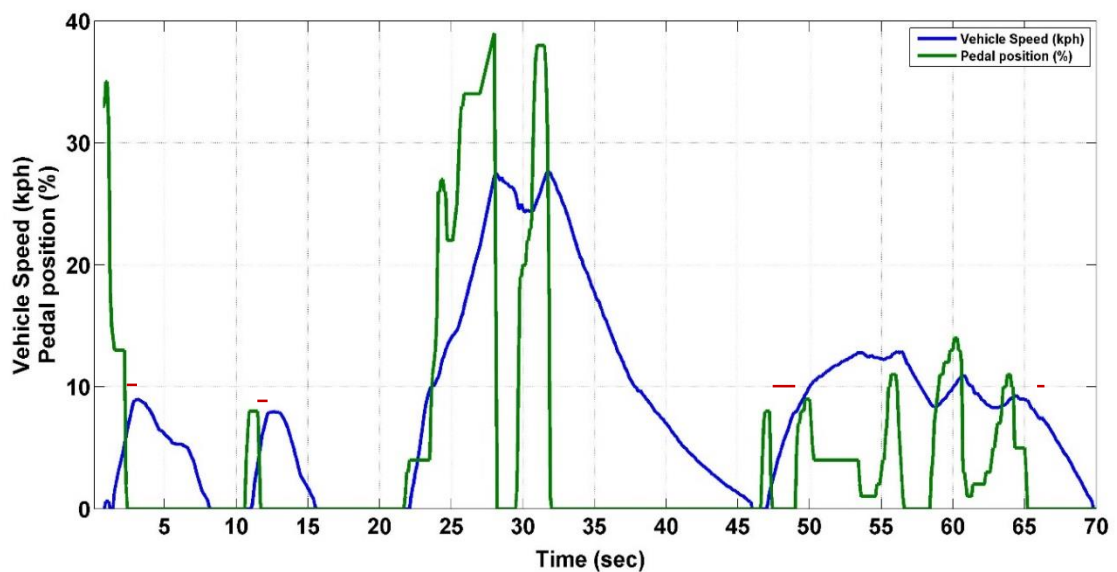


Figure 4-5 - Acceleration events with zero pedal position that are NOT due to the use of cruise control

Take the example in Figure 4-5 which shows vehicle speed and pedal position for a van for 70 seconds of running. The red lines show the duration of the events where pedal position is zero and the vehicle is accelerating. These events last from half a second to 1.5 second durations, in this 70 second journey alone. Take the case of the

first red line at the 2 second mark, which lasts up to the 3rd second. This is due to the driver accelerating and then lifting off the pedal which causes the vehicle to continue accelerating for a one second after pedal lift-off, due to the inertia of the vehicle. The same is the case for the 2nd and 4th 'red lines'. The third red line case however, is due to the effect of both inertia due to previous acceleration using pedal and also the vehicle rolling forward due to a negative gradient. This was clear from the difference in power factor, vehicle speed and duration of acceleration without pedal (1.5 seconds in this case), when compared to the previous three events. Similar events to these had to be screened out, so as not to penalise drivers unfairly.

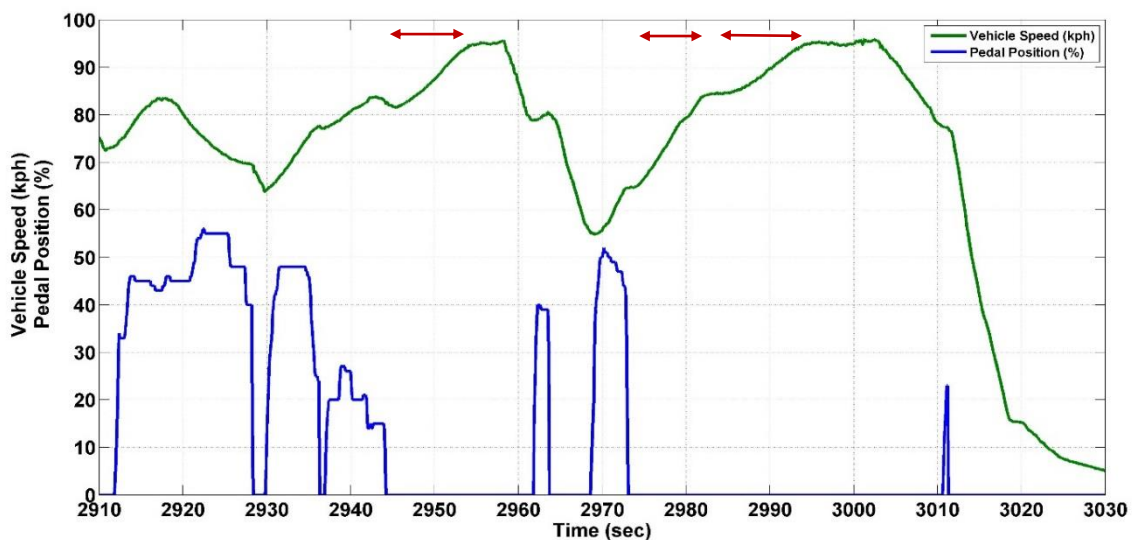


Figure 4-6 - Acceleration events with no pedal usage that are due to the use of cruise control

Figure 4-6 shows three separate cruise control acceleration events for a van for 120 seconds of vehicle running. These three events are highlighted using red lines. It can easily be observed that these events are at high speeds and the acceleration is for a longer duration of time with zero pedal usage. To confirm this, cruise control on three different vehicles were trialled on the road and on the chassis dynamometer to understand the time taken to accelerate from 64 to 80 kph (40 to 60 mph) and 80 to

96 kph (50 to 60 mph) – both seen in figure 38. Other acceleration events were also examined to identify the inertial power surrogate, acceleration and vehicle speed during different acceleration events. This helped differentiate cruise control events from that of inertia and negative gradients.

This analysis was used for the implementation of a two dimensional look up table based on IPS_{ST} (which is a function of speed and acceleration of the vehicle) and instantaneous pedal position to determine the pedal correction factor, which would be used for the calculation of IPS_{LT} . After the analysis, it was decided that any acceleration events with zero pedal that were higher than an IPS_{ST} value of $5.8 \text{ m}^2/\text{s}^3$ will start to be penalised more using a higher pedal correction coefficient (maximum pedal correction coefficient was 1, while minimum was 0.5). If the IPS_{ST} with zero pedal was higher than $9.64 \text{ m}^2/\text{s}^3$, the driver would get no benefit from pedal correction (pedal correction coefficient equal to 1). This meant drivers will not see a considerable drop in IPS_{LT} when accelerating with the help of cruise control, but will see the same rise or drop in IPS_{LT} (and lights) as they would in the case of using the pedal to accelerate. However, if the driver applies a small pedal to accelerate (say 5%), it will be evident that he/she is not using cruise control, and in that case the driver would receive a small room for pedal correction up to $11.5 \text{ m}^2/\text{s}^3$, beyond which pedal correction coefficient will be set to 1. From pedal position of 15% and upwards, the driver will have a pedal position correction factor of 1 for all values of IPS_{LT} . This was because the pedal correction was only intended to give drivers a small window of IPS_{LT} increase without warnings or violations, to enhance driveability using the system for very low pedal usage.

4.5. Gear up-shift algorithm

Gear shifting is an essential part of driving. Gear shifting at optimal points is an ever more important aspect when it comes to improving driving style. Literature discussed tests conducted at the University of Bath that showed a 3.6% increase in fuel economy when the NEDC shifts points were changed [59]. Results from the field trial experiments also helped understand savings in fuel consumptions due to reduction in engine speed when shifting gears early. Various other literature suggests to the same conclusion [80-84], with different engineers attempting different strategies. With regard to the driver advisory tool developed at the University of Bath, an up-shift light was present on the dashboard, which asked the driver is asked to shift up a gear. An audible 'bong' is played through the speakers to remind the driver to shift up a gear.

For the initial version of the driver advisory tool used for the field trial experiments, the up-shift light was the same as the van manufacturer's up-shift light. In the case of older vehicles where there was no up-shift light available, drivers were asked to shift up at 2200rpm. This meant it was required to understand whether the vehicle had 5 or 6 gears, so that the driver is not asked to shift up a gear when he/she is already in the final gear. For the 15 vans involved in the field trial experiments, this was not an issue, as there were only three possible combinations of number of gears and final drive ratios present. To accommodate for the different combinations, one parameter had to be changed in the algorithm for each device before being fitted on to the respective vehicle. This would ensure that the driver is not asked to shift up a gear when he/she is already in the final gear.

A secondary update of this system allowed the industrial partner to choose an option before fitting on to the vehicle, which would automatically select the right value from the different combinations of number of gears and final drive ratios. Based on the input selected, the algorithm selects an appropriate value of gearbox and final drive combination to determine the ratio of the highest gear for that vehicle. These numbers were pre-calculated based on existing data from different Ford Transit vans having different gearbox and final drive ratio combinations.

However, for the driver advisory tool to be capable of being fitted on to any vehicle, this arrangement of either choosing the manufacturer gear up-shift light, or selecting the appropriate combination would not work for two reasons. Firstly, not all vehicles have an in-built gear up-shift light. Secondly, different vehicle manufacturers use different gear ratios and final drive ratios, making the total number of possibilities a very large number to collate. This called for the development of a new gear up-shift strategy. This development stage will be further divided into two sections – firstly, a method of determining the highest gear ratio (including final drive ratio), and secondly, an up-shift strategy that asks the driver to shift up a gear. Both these aspects combined together enable driver advisory tool algorithm to work optimally to help achieve an increase in fuel economy.

4.5.1. Determination of highest gear ratio

It is essential to determine the highest gear ratio (including final drive ratio) for the advisory tool to know whether there is a higher gear available for the driver to shift into. After trialling different ideas, it was concluded that it was not possible for the author or the industrial partner to collate driveline information for all the vehicles. It

was decided to include a gear ratio learning algorithm in the gear shift strategy to detect the ratio of the highest gear of the vehicle. The ratio of the highest is determined by dividing the vehicle speed (in kph) by the engine speed (in rpm). Asking the driver to change up a gear is essential only if the vehicle is equipped with a manual transmission gearbox. In this case, the ratio of vehicle speed to engine speed will remain a constant as the road wheels are mechanically hard coupled to the engine via the gearbox and final drive. The only constantly changing ratio of this power transmission route is the gearbox. So a change in the ratio of vehicle speed to engine speed (from now this ratio will be called V/E) will give an indication of the gear ratio of the vehicle. The algorithm was designed to detect the highest V/E value, and then store it on the memory of the device. If there is no value being found, the system would use a default low value of 0.027 as the highest gear ratio. As the driver shifts up a gear to a value that is above this default value, the new value is saved by the highest gear ratio searching algorithm. For optimum results, it was advised that as soon as the device is fitted on to a vehicle, the device fitting engineer should drive the vehicle using all the gears, so that the advisory tool system can learn the number of gears on the vehicle and update the default highest gear value with the newly determined one.

The absolute value of the ratio of the highest gear will not be the same as the gear ratio of the vehicle, because V/E ratio includes the final drive ratio of the vehicle. There are certain scenarios where V/E will not be steady value. These needed to be carefully identified and excluded from the determination of highest gear ratio. One example of this situation is when the driver changes a gear. Figure 4-7 shows the ratio

of vehicle speed to engine speed for a 2000 second real world running of a van. In an ideal vehicle, the small spikes (low amplitude fluctuation spikes) seen in the plot would not exist. This is believed to be due to the play in the gearbox and final drive units. The spikes with considerably higher amplitude (after the relatively constant V/E line) shows when the driver shifts up or down a gear. The amplitude of these spikes depends on how quickly the driver changes a gear.

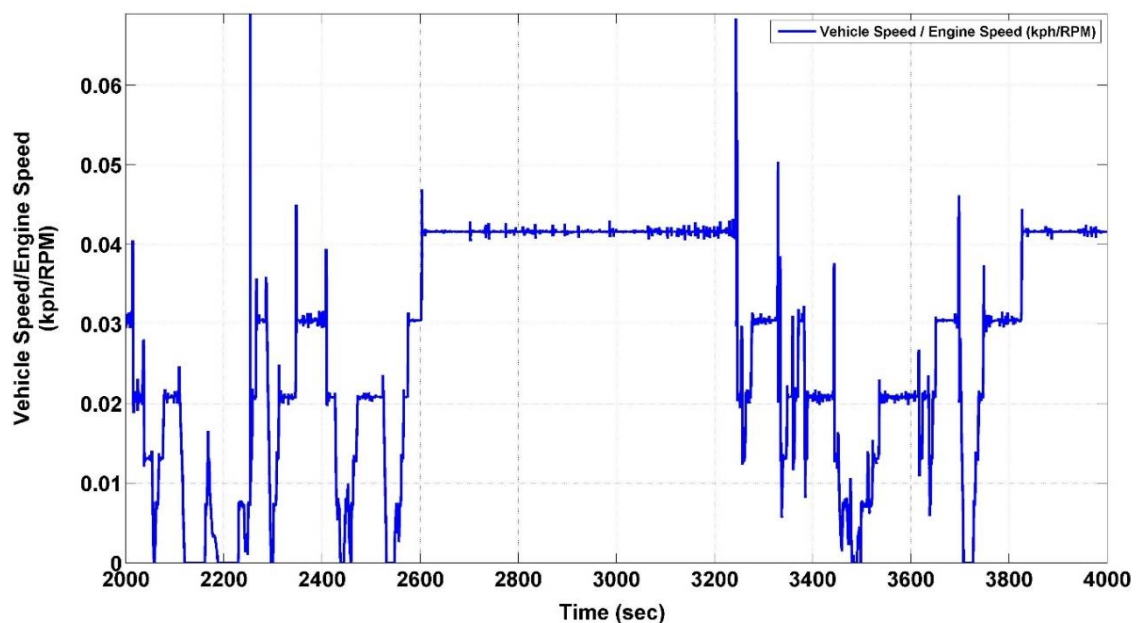


Figure 4-7 - Ratio of vehicle speed to engine speed plot for a van

When the vehicle is running in any gear, since the road wheels are mechanically connected to the engine, the vehicle V/E ratio is a constant. This is because, a change in engine speed will be translated to a change in the speed of the wheels. When the driver changes a gear, he/she presses the clutch in order to disengage the engine from the gearbox. This procedure disconnects the link between the road wheels and the engine at the gearbox. This causes the engine speed to vary disproportionately to the vehicle speed (or wheel speed). This is due to the engine friction (engine brake)

being different to vehicle deceleration, causing the engine speed to drop quickly towards 800rpm (idling engine speed) if given time. The vehicle speed on the other hand reduces much slower, as driveline friction, road resistance and aerodynamic drag have a lower effect compared to the inertia of the vehicle. In this situation, the ratio of vehicle speed to engine speed will not be constant, but will be a high value due to the denominator being a small value. The different amplitude of spikes indicate the swiftness of the shift. If the driver shifts into another gear quickly, the engine speed will not drop a considerable amount to cause a big spike. These different scenarios needed to be screened out in the highest gear ratio finding algorithm.

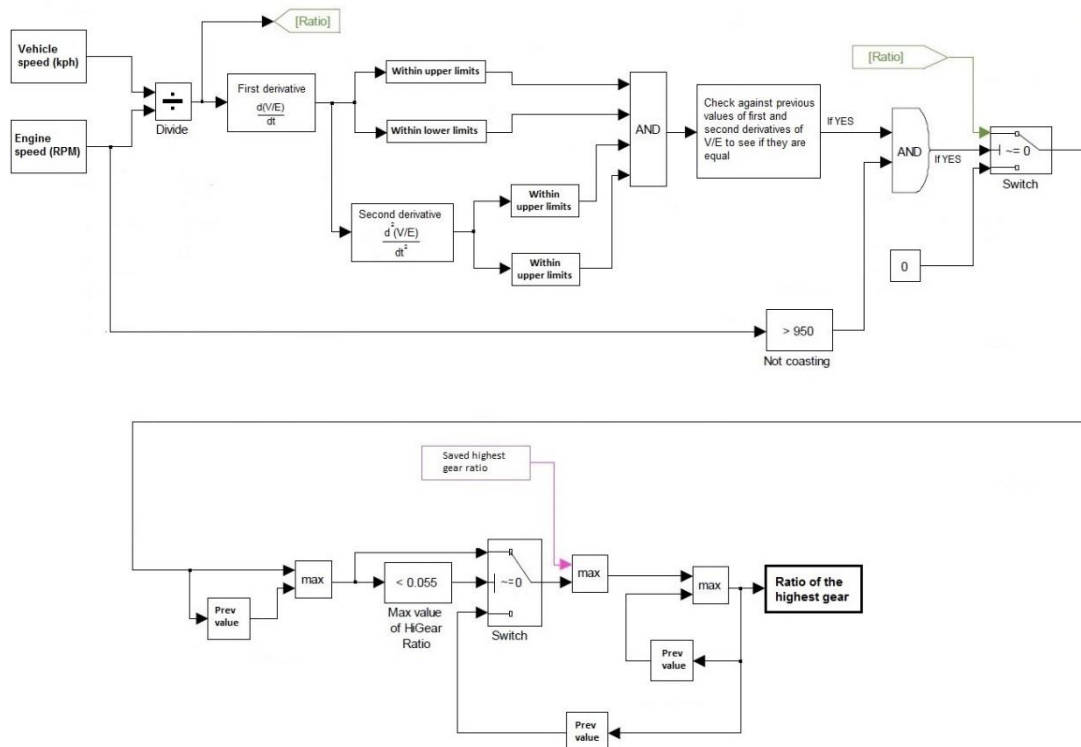


Figure 4-8 - Algorithm to detect ratio of the highest gear of the vehicle

A new algorithm was developed so as to detect ratio of the highest gear. As mentioned earlier, highest gear ratio value determined by the algorithm is stored in the memory of the device. If a new value has not been found, the system uses a default value of 0.027 as the highest gear ratio. If the driver chooses a gear that has a V/E value higher than this default value, the new value will replace the saved value.

Figure 4-8 shows the algorithm for determining the ratio of the highest gear. For this, vehicle speed was divided by engine speed (both instantaneous values obtained from the vehicle OBD). This was filtered to avoid high frequency fluctuations which may be due to the inaccuracies in measurement, or other induced noise. The concept of the algorithm depends on determining the states of operation where V/E remains a constant. For this purpose, the derivative of the filtered value of V/E and the second derivate of V/E are observed to see if both are almost equal to zero. A small amount of variation (± 0.001 for first derivative and ± 0.003 for second derivative) is allowed to take into account minor fluctuations due to noise. If both first and second derivative of V/E is close to zero for 2 seconds, and the engine speed is greater than 950 rpm (to avoid idling situations), that value is treated as the required gear ratio. If a new value is revealed, this value is compared to the previously saved value and higher of the both is selected. If any value found is higher than the saved value of the highest gear ratio, the new value is chosen as the ratio of the highest gear. This value keeps getting updated if a newer and higher value is found.

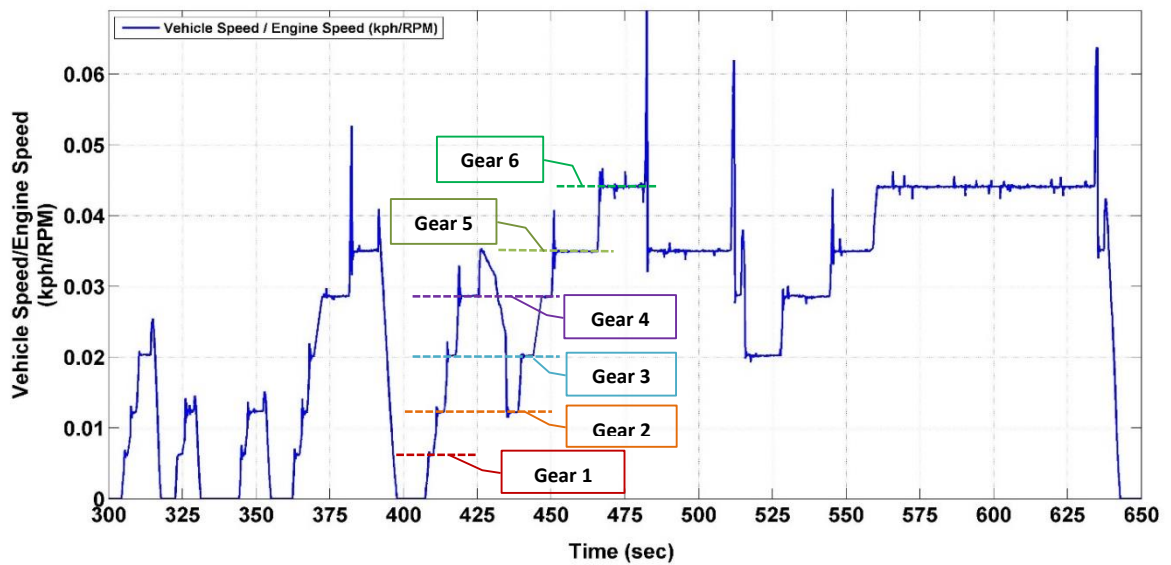


Figure 4-9 - Ratio of vehicle speed to engine speed exhibiting all 6 gears of a Ford Transit van

Figure 4-9 shows the ratio of vehicle speed to engine speed for 350 seconds of running for a 6 speed Euro 5 van. When the algorithm was applied to the data collected from the vehicle, it detected the different gears of the vehicle (highlighted in the figure). The values detected by the algorithm proved the effective working of the system. When initially tested on the road, the driver was able to drive only using the first 5 gears for (due to traffic conditions). The algorithm detected a value of 0.0349 (representing V/E for the 5th gear) as the new ratio of highest gear, and since this was higher than the default value of 0.027, the new value was saved as the ratio of the highest gear. Thus the gear shifting logic became effective, and asked the driver to shift up a gear from 4th to 5th on the next occasion. However, it had not yet detected the 6th gear as this gear had not been used, and thus the algorithm did not know about its presence. Once the driver shifted into the 6th gear, a new V/E value of 0.0442 was detected, which was higher than the previously found ratio of highest gear. Hence, the new value was used and later saved. Thereafter the driver was asked to shift up a gear from the 5th to the 6th, proving the effectiveness of the logic.

It also highlights the need for the vehicle to be driven using all the gears soon after the fitment of the driver advisory tool, so that the gear ratio finding algorithm is given the opportunity to learn the ratio of the highest gear.

4.5.2. Up-shift light algorithm

The importance of shifting up a gear has already been discussed. The driver behaviour improvement device was designed to penalise drivers not only for harsh acceleration events, but also for not shifting up a gear on time. The unit provides an indicator in the form of an up-shift light on the dashboard, and also plays an audible bong. In the case of a personal vehicle equipped with an up-shift indicator, the driver has the privilege of choosing whether or not to perform the gear shift action. However, in the case of the advisory tool, if a gear up-shift light has been shown to the driver, he/she is obligated to change up a gear. If the gear shift is not performed, the driver is penalised by adding a fixed gear shift penalty value to the instantaneous IPS_{ST} . This gives drivers a bit more time to perform the gear change before the IPS_{LT} follows the instantaneous IPS_{ST} to give the driver a warning or a violation.

A new up-shift algorithm had to be developed for the driver advisory tool due to two reasons – firstly, not all vehicles are equipped with an in-built an up-shift indicator. Secondly, feedback from some drivers who used the in-built manufacturer's up-shift indicators mentioned that it was not always possible to strictly follow them, especially when the vehicle was fully laden and going uphill. For the field trial experiments, the driver advisory tool used a one dimensional look up table with pedal position as the input to determine the appropriate up-shift engine speed. Figure 4-10 shows the representation of this logic.



Figure 4-10 - Preliminary version of the gear shift logic used in the driver advisory tool

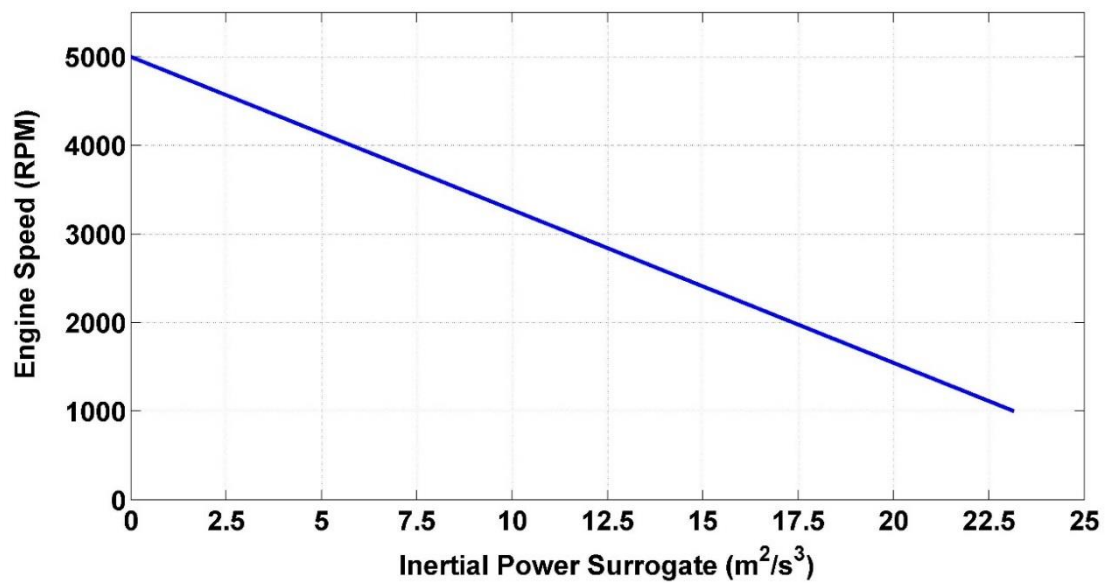


Figure 4-11 - Gear shift logic used in the updated version of the driver advisory tool

Here, a 'provisional' engine speed is chosen from the graph based on the instantaneous Inertial Power Surrogate of the vehicle. This value is multiplied by the instantaneous pedal position of the vehicle (0 to 1 representing 0 to 100%) to obtain the engine speed at which the driver will be asked to shift up a gear.

According to this logic, the driver will be asked to shift up a gear at 1900rpm if he/she uses less than 30% pedal usage. Any more than 30%, an up-shift engine speed from the graph is chosen based on instantaneous pedal position value. The up-shift engine speed is frozen at 2500rpm beyond the 70% pedal position. This means that the driver will be asked to shift up a gear irrespective of the situation at 2500rpm at the latest. Sadly, this was not beneficial from a driveability point of view and thus the system had to be redefined and improved adopting vehicle speed, acceleration and pedal position parameters to determine the optimum gear up-shift engine speed.

Figure 4-11 represents the newly developed algorithm used in the updated version of the driver advisory tool. The system chooses a 'provisional' engine speed from the plot based on the instantaneous inertial power surrogate of the vehicle, since this gives an indication to the vehicle speed and its acceleration. This value is multiplied by the instantaneous pedal position value (0 to 1 representing 0 to 100%) to get the actual engine speed at which the advisory tool will ask the driver to shift up a gear. Using this method, load (representative of pedal position), vehicle speed and acceleration have an impact on when the system asks the driver to change up a gear.

A minimum gear up-shift speed of 1800rpm and a maximum of 4000rpm have been implemented. This new algorithm meant if the driver has a low IPS value, he/she is given more room to accelerate in the same gear. This is because, if the vehicle has low IPS, the driver is driving at a very low or medium speed with minimal change in speed. In other words, he/she will be driving in a non-aggressive manner, and hence is given the opportunity to shift at a high engine speed if needed (depending on the pedal position). The advantage of this is that, if the driver is climbing uphill with a

fully laden vehicle, he/she is given the opportunity to remain in a lower gear for more time if his/her pedal position is high enough (which it might be in the case of a fully laden vehicle). If the driver applies high pedal and the vehicle accelerates, the IPS value climbs, which means a lower 'provisional' up-shift engine speed will be chosen.

For example, say the driver is driving with a low IPS value of $5 \text{ m}^2/\text{s}^3$. The 'proposed' up-shift engine speed from Figure 4-11 is 4100rpm. If the driver is in slow moving traffic and has a low pedal usage (say 30%), the driver advisory tool will ask him/her to shift up at 1800rpm (30% of 4100 = 1230rpm, which is below the minimum up-shift engine speed of 1800rpm, hence the latter is chosen). Consider another case, where the driver is climbing up a hill with a fully laden vehicle, with the same $5 \text{ m}^2/\text{s}^3$ IPS value. He/she will have a high pedal position due to the high engine torque demand, say 70%. In this case, the up-shift engine speed will be 2870rpm (70% of 4100rpm). This methodology was implemented so that drivers have the capability to drive in low gears when climbing up a hill when heavily loaded. As soon as the gradient decreases, the high pedal would cause the IPS_{ST} to change, say it increases to $12.5 \text{ m}^2/\text{s}^3$. In this case, the driver will have an up-shift speed of 1960rpm (70% of 2800rpm). This logic seemed to be effective in allowing drivers with heavily laden vehicles to apply high pedal without asking them to shift up a gear or be unfairly penalised. This update for driveability was an essential requirement for the driver advisory tool.

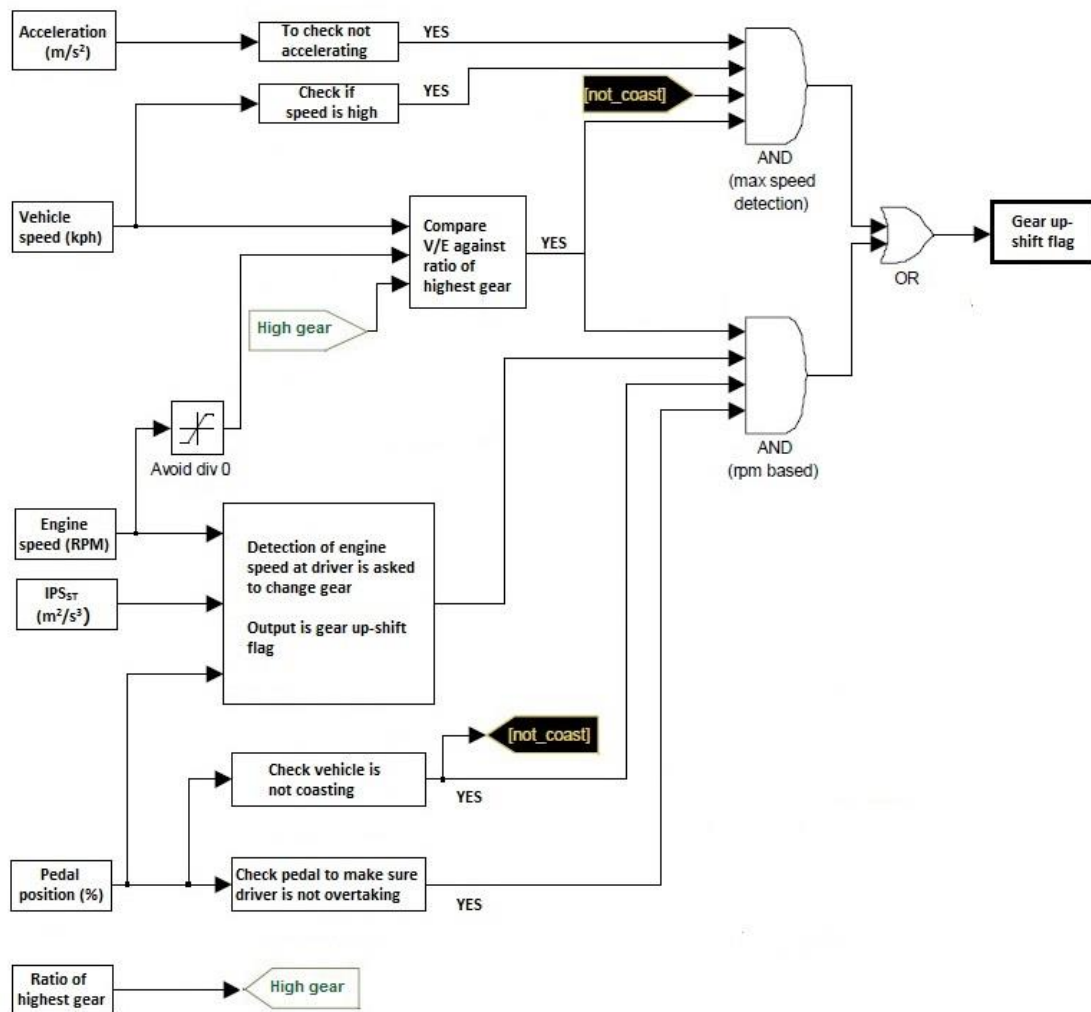


Figure 4-12 - Complete gear shift logic used in the updated version of the driver advisory tool

Figure 4-12 shows other inputs to the gear up-shift light methodology used. There are two separate methods/situations where the driver behaviour improvement device will ask the driver to shift up a gear – (a) when he/she is cruising at relatively high speed (say on an A-road/country road) when not in the highest possible gear, and (b) when the driver is driving at a speed and load condition that can be driven in a higher gear (based on logic discussed in Figure 4-11 earlier). In the first case, the acceleration of the vehicle is analysed to confirm that the driver is cruising. Vehicle speed is checked to see whether the vehicle is cruising at high speeds (say on a UK country

road, where speed limit is 60mph = 96kph). The ratio of vehicle speed to engine speed (V/E) is also calculated and compared against the ratio of the highest gear ratio determined from the logic explained in Figure 4-9. If this value is lower than the ratio of the highest gear, then the driver is asked to shift up a gear. The 'flag' for the up-shift light is raised only when all of the above mentioned conditions are met.

The second condition involves asking the driver to shift up a gear during transient driving conditions of the vehicle. This logic depends on the instantaneous inertial power surrogate values (IPS_{ST}) mentioned earlier. The inputs to the logic are engine speed, IPS_{ST} and pedal position. Engine speed at which the driver is asked to shift up a gear is calculated and compared against the current engine speed. If the current engine speed is above the value of calculated up-shift engine speed, the gear up-shift flag is raised.

However, a few other conditions have to be satisfied before this up-shift flag is transmitted to the driver. It has to be ensured that neither is the driver coasting, nor is he/she performing an overtaking manoeuvre. Pedal position is used to check both these events. If the pedal position is below a pre-determined value (say 2%), then this flag will not be raised. Also, the system allows the driver to bypass the up-shift logic to perform an aggressive overtaking manoeuvre if needed, for a short period of time. This is determined by monitoring the pedal position value and checking if it above 70%. If so, the driver will not be asked to shift up a gear. This is another driveability feature enabled in the system to ensure that the driver is not unfairly penalised. However, this does not mean he/she will not be penalised for aggressive driving as the long term and short term lights will still be working simultaneously, and the

increase in IPS_{LT} will give the driver warnings or violations. A flag latching mechanism is present in the up-shift logic where the up-shift flag is kept raised and lowered depending on the change in vehicle operating conditions (say the driver lifts off the pedal, up-shift flag is no longer enabled).

The algorithm to find the ratio of the highest gear and up-shift engine speed helped enable vehicles that are not equipped with gear up-shift lights save fuel using the driver advisory tool, by shifting sooner into a higher gear. Since this logic takes into account the current vehicle speed, acceleration and pedal position, it can be beneficial in both normal driving situations as well as heavily laden vehicle conditions.

4.6. Idling logic

Idling of the engine refers to a particular stage of driving where the vehicle is stationary with the engine is still running. This can take place at traffic lights and in heavy traffic conditions, or just in situations where the driver sits inside the vehicle with heating or cooling systems ON when the vehicle is not moving. Considerable amount of idling instances during a drive cycle can cause a significant increase in fuel consumption. During idling or low load conditions, the diesel engine tends to run richer due to less induction of air when compared to higher engine speeds. Furthermore, during idling conditions, the engine is unable to work at its peak operating temperature, and thus suffers from a drop in efficiency due to incomplete combustion of fuel. This leaves fuel residues in the exhaust, which increases fuel consumption and exhaust emissions [85]. Unwanted idling results in increased amounts of CO_2 , NO_x and particulates in the atmosphere [86]. To address these

issues, manufacturers adopt micro-hybrid solutions like Start-stop, which help in reducing exhaust emissions when idling [87]. One of the criticisms of this technology is whether the fuel consumed when restarting the engine is higher than the amount that it would otherwise save by turning it off for a few seconds. Studies have shown that the engine consumes more fuel when idling over 10 seconds than what is required to start it. Trucks in the USA have significant idling stages where it was determined that fuel consumed during 5 miles of driving is equivalent to that consumed during 10 minutes of idling [85, 88, 89].

The above mentioned are a few of the reasons pertaining to the exclusion of data relating to idling periods greater than 90 seconds when analysing data from the field trials. However, it is essential that fuel consumption needs to be reduced by avoiding unnecessary idling situations. Since excessive/unwanted idling is part of the driving style of a driver, it was decided to incorporate an idling detection and advice system for the driver advisory tool. This was introduced in the form of idling warnings and penalties, which were presented to the driver, and also reported to the fleet manager. The reduction of idling times (and hence fuel consumption) does not directly relate to the parameters of driving pattern suggested earlier in the literature. However, reducing idling times by switching the engine OFF does improve the overall driving style by motivating the driver to save fuel in every possible scenario. Any idling period greater than 90 seconds is regarded as 'high idling time period' in this study, as this value represents the 97th percentile of all idling instances for the entire data collected during the field tests.

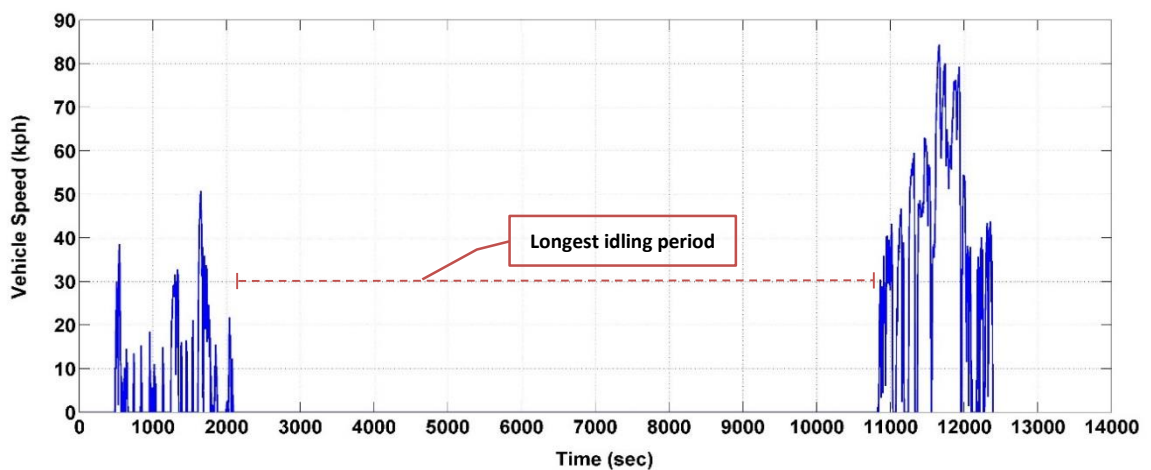


Figure 4-13 - Longest idling period for a van during field trials

During analysis of the field trial data, it was seen that certain vans had significantly high idling periods. For example, Van 3 had the single most longest idling period of 146 minutes, which is equal to 2 hours and 26 minutes (Figure 4-13). The longest idling period is evident from the graph (between 2089th second and 10832nd second – marked in red). Of the total 206 minutes (3 hours and 26 minutes) of engine running, the vehicle was idling for a total of 173 minutes (2 hours and 50 minutes), while the vehicle was moving for only 33 minutes. The total fuel consumed during the 173 minutes of idling was 1.61 litres. The total fuel consumed during the 33 minutes of vehicle moving where it travelled 18.8 kilometres was 1.28 litres of diesel. Hence for this particular instance, idling alone consumed more fuel than when the vehicle was moving. If the same driving conditions were assumed, this fuel consumed during engine idling would have been enough for another 23.6 kilometres. Other long idling periods observed for this particular van included 51 minutes, followed by six different cases of 17-19 minutes each. Similar idling patterns were observed for different vans, which proved the need for idling time reduction logic.

The idling logic consisted of issuing warnings and penalties to the driver for long durations of idling. The first idling warning was awarded at a stipulated time, after which idling penalties were given to the driver at a regular time interval of 30 seconds. When implementing the idling logic, the option of changing the idling warning time according to user/fleet requirement was added, while the penalty re-issue time was set to a constant 30 seconds. Seven different levels of idling warning times were provided as options, with lowest being the default case where the system remains disabled. This was to cater to companies that might not need the idling warning system, as certain vans use the engine to power additional equipment when the vehicle is stationary.

Table 4-1 shows the idling warning and penalty options that were part of the system. The idling warning is relayed to the driver when the vehicle has been idling for a chosen amount of time (from column 2 in Table 4-1). This is conveyed to the driver with the help of an audible message asking the driver to switch the engine OFF. As in the case of aggressive driving warnings 1 and 2, these idling warnings are not recorded nor is the driver penalised for them. However, 30 seconds after the driver has been presented with an idling warning, the driver receives a recorded idling penalty. Thereafter he/she continues to receive an idling penalty every 30 seconds till the situation changes (either the driver switches the engine OFF or he/she starts moving). When the vehicle starts to move after idling, the driver is played a message with the number of idling penalties he/she received during that particular idling instance.

Table 4-1 - Idling logic warning time selector options

Idling select option	Engine idling warning time (sec)	Engine idling penalty issue time (sec)
0	System disabled	
1	60	30
2	90	30
3	120	30
4	180	30
5	240	30
6	300	30

Figure 4-14 shows the algorithm used to convey idling warnings and penalties to the driver. Idling is detected in the previous stage by checking if vehicle speed is equal to zero and engine speed is greater than 750rpm. In this way, situations where the vehicle stalls (even though these are relatively small) will not be counted as idling. This is one of the main inputs to the idling logic – shown in Figure 4-14 as - ‘Is vehicle idling’. The ‘idling selected option’ is the chosen level of idling warning and penalty time chosen by user or the fleet manager, based on Table 4-1. The first penalty is received after the idling warning and penalty time has surpassed, with the vehicle still continuing to idle.

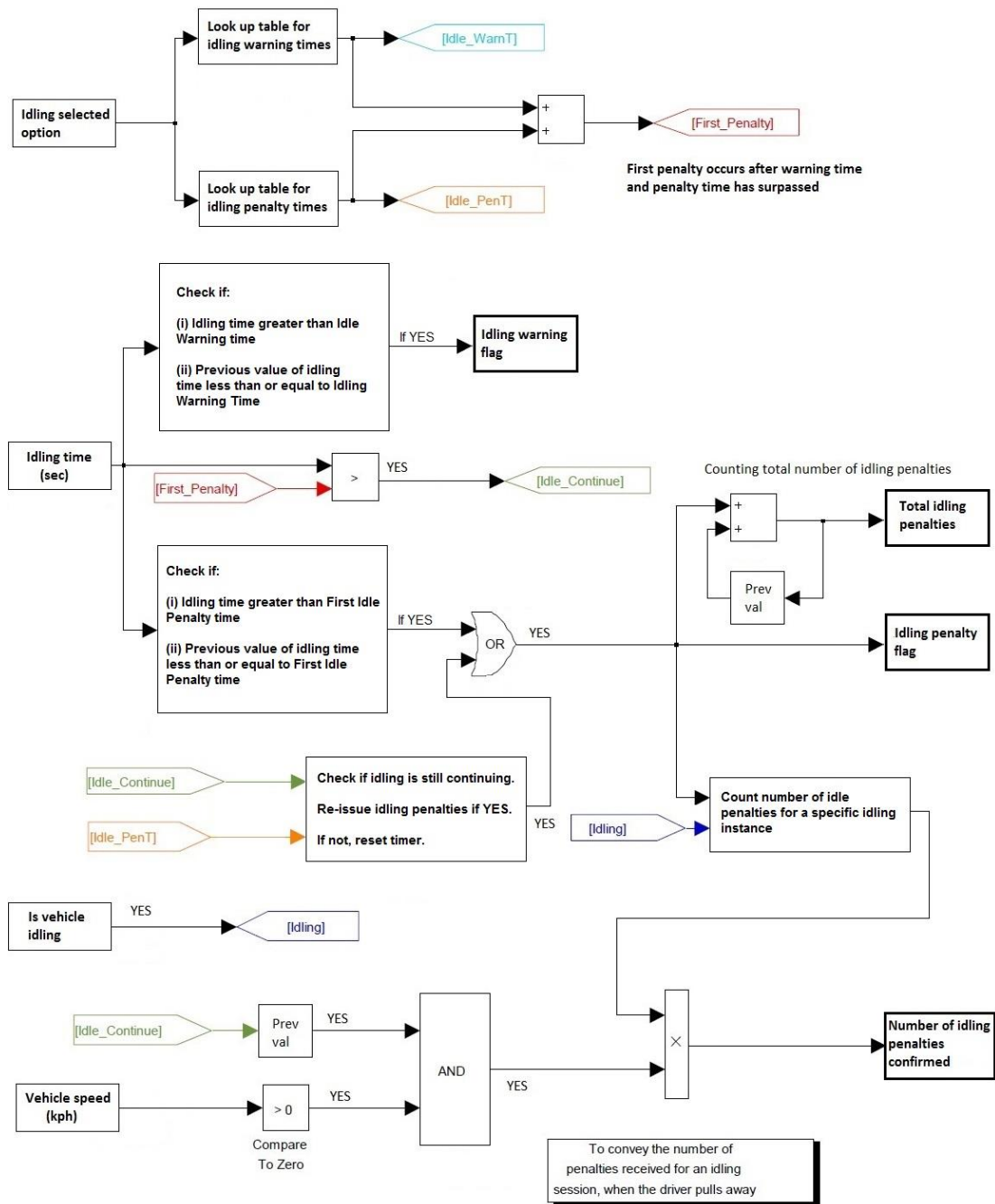


Figure 4-14 - Idling warning and penalty logic used in the driver advisory tool

A counter is present to detect the duration for which the vehicle is idling. The counter is reset every time the vehicle is not idling, and hence the idling time for that particular instance is passed into the idling logic (as 'Idling time (sec)' in figure). If the idling time is greater than the idling warning time chosen from the look up table, an idling warning flag is raised to inform the driver using an audible message to switch the engine OFF to reduce unnecessary idling. The idling flag is lowered so as not to provide additional idling warning. An idling penalty is issued (first penalty) 30 seconds after the warning has been issued. This raises the idling penalty flag which provides an audible penalty message to the driver. If the idling continues, a penalty is issued every 30 seconds (counted in the algorithm). The total number of idling penalties the driver receives is counted. Another logic counts the number of idling penalties the driver receives during one idling instance. This is conveyed to the driver via a message when he/she pulls away. This output is called 'Number of idling penalties confirmed'.

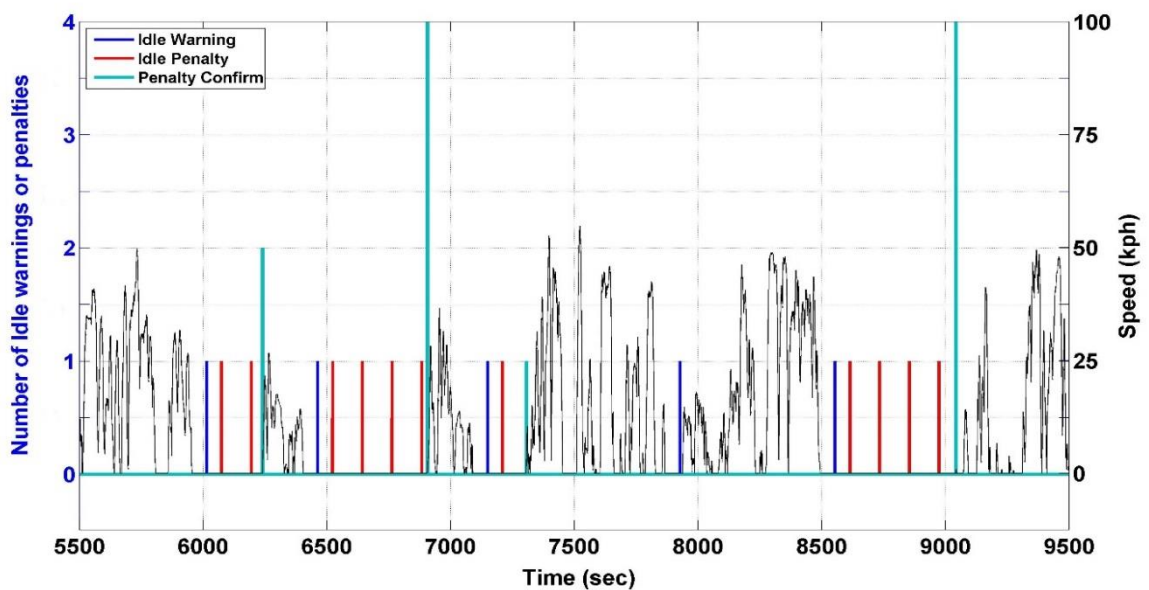


Figure 4-15 - Idling warnings and penalties conveyed to drivers

Figure 4-15 shows vehicle speed trace of a van for 4000 seconds of running. The plot shows different sections of idling where the idling logic of the driver advisory tool is in action. The blue lines indicate when an idling warning is issued to driver. The red lines show the idling penalties being issued to the driver at a regular interval of 30 seconds, after an idling warning has been conveyed to the driver. The cyan lines show the number of idling penalties conveyed to the driver just as he/she pulls away. This provides an indication as to the penalties recorded for that particular idling session. For example, for the second idling instance, the driver would have got a message saying - 'You have received 4 idling penalties'. Reducing unnecessary idling conditions in a vehicle is an essential part of improving driver behaviour. The update for detecting idling in the driver advisory tool motivates drivers to try and save fuel in every possible scenario, and not just in reducing harsh accelerations.

Based on feedback from companies that were part of the field trial experiments, an additional feature was provided to the tool to determine time used and distance covered during 'out of office hours'. The system clock on the advisory tool hardware provides time to the algorithm, which would then detect whether the vehicle is running outside the office hours. Time for office hours varies from company to company, and this information can be provided to the system, when it needs to be used. Tracking vehicle use beyond normal operating hours was useful for two purposes – firstly to know that drivers do not misuse company vehicles (as they may not be insured for personal use), and secondly to reward drivers with over-time pay/allowance for extra hours of work.

4.7. Change from pedal position to engine load

One of the reasons for the development of the updated version of the driver advisory tool was for it to be flexible enough, so as to be fitted on to any vehicle of any type, with minimal or no changes to the hardware or software. As mentioned earlier, one of the biggest issues concerning this was the availability of all necessary parameters on the OBD II CAN network for the essential functionality of the device. Vehicle parameters like engine speed, vehicle speed and fuel injection rate were available to mostly all vehicles equipped with OBD II. One of the essential parameters required for the optimisation of long term inertial power surrogate (IPS_{LT}) and gear up-shift engine speed, is pedal position. Pedal position was not easily accessible for all the different vehicles equipped with OBD II. Hence, another parameter – Engine load had to be used for the advisory tool algorithm. This meant accommodating Engine Load in all the functions where pedal position was being used.

It is a common misconception that engine load and pedal position follow a linear relation. Although in a lot of cases this is true, engine load changes at a much higher frequency and amplitude than pedal position. Engine load is dependent on the driver's input for majority of the vehicle operation condition. However, in a few other situations, the engine's operating strategy controls the engine load. For example, in the case of vehicle idling conditions, whilst the pedal position will be equal to zero, engine load will not be zero due to the fact that the engine is not switched OFF. Figure 4-16 shows the relation between pedal position and engine load for a Euro 5 it van. It can be seen that in most cases, engine load saturates at its maximum of 100% when the pedal position is over 70%.

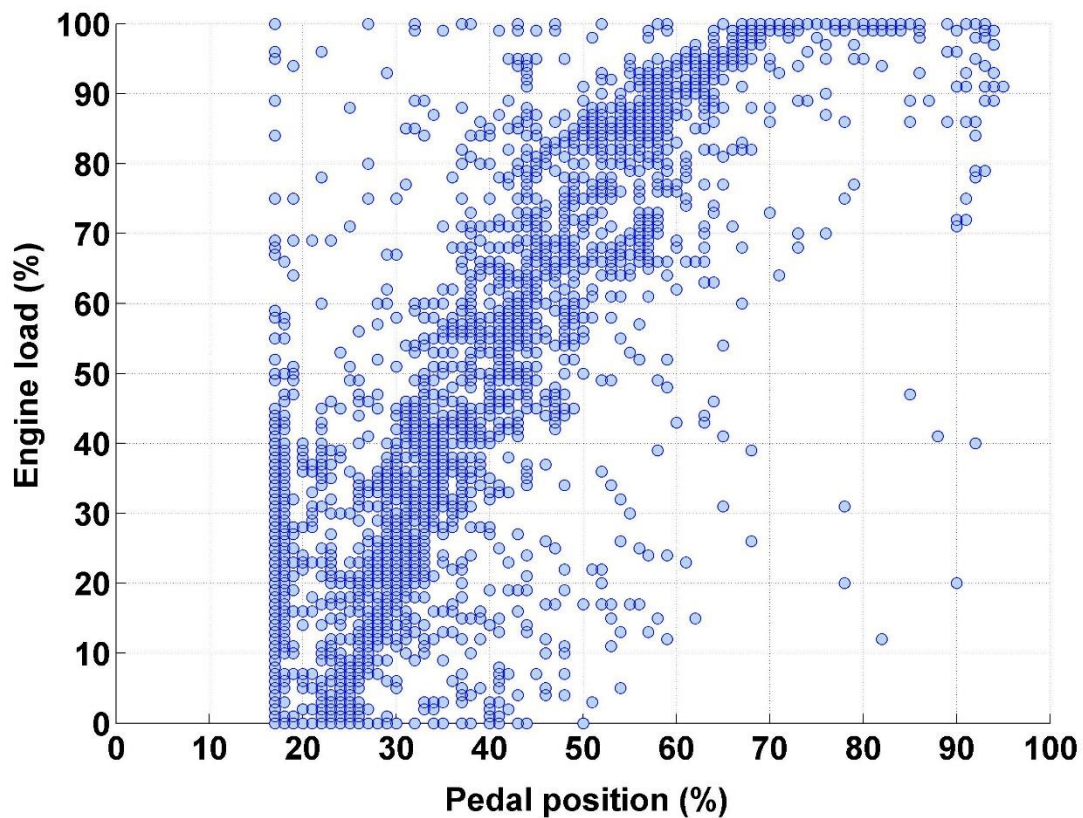


Figure 4-16 - Relation between pedal position and engine load for a Euro 5 Ford Transit van

Figure 4-17 shows the change in vehicle speed, pedal position and engine load for a Euro 5 van. The 17% offset in pedal position (when pedal is actually zero), that was mentioned earlier can also be seen in this figure. When there is no pedal input whilst in motion (say the driver has lifted off the pedal completely and the engine is braking due to friction), the engine load goes to zero. But as soon as the vehicle is switched to neutral, engine load is back up to 30% and then stabilises around 25%. It can be seen that engine load during idling conditions of the vehicle changes more often than pedal position. Pedal position in this case oscillates between 17 and 18% throughout the duration of the plot. Engine load oscillates between 20 and 27% during the first four seconds of idling, while in the second idling case it oscillates between 18 and 27%. This changes for the third case of idling, where it oscillates between 19 and 27%.

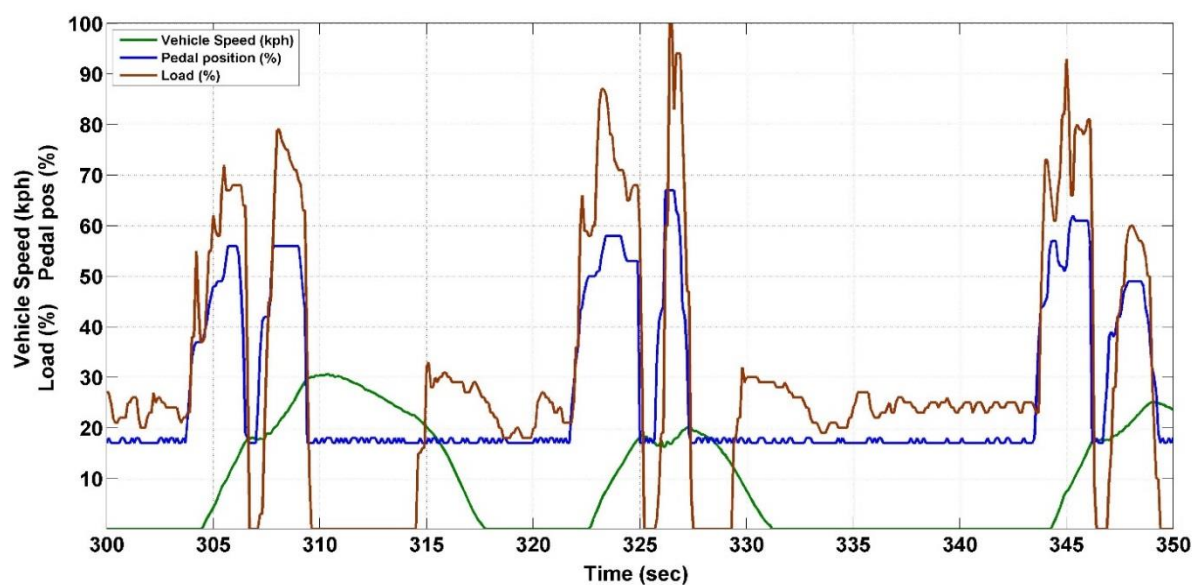


Figure 4-17 - Change in vehicle speed, pedal position and engine load of a van

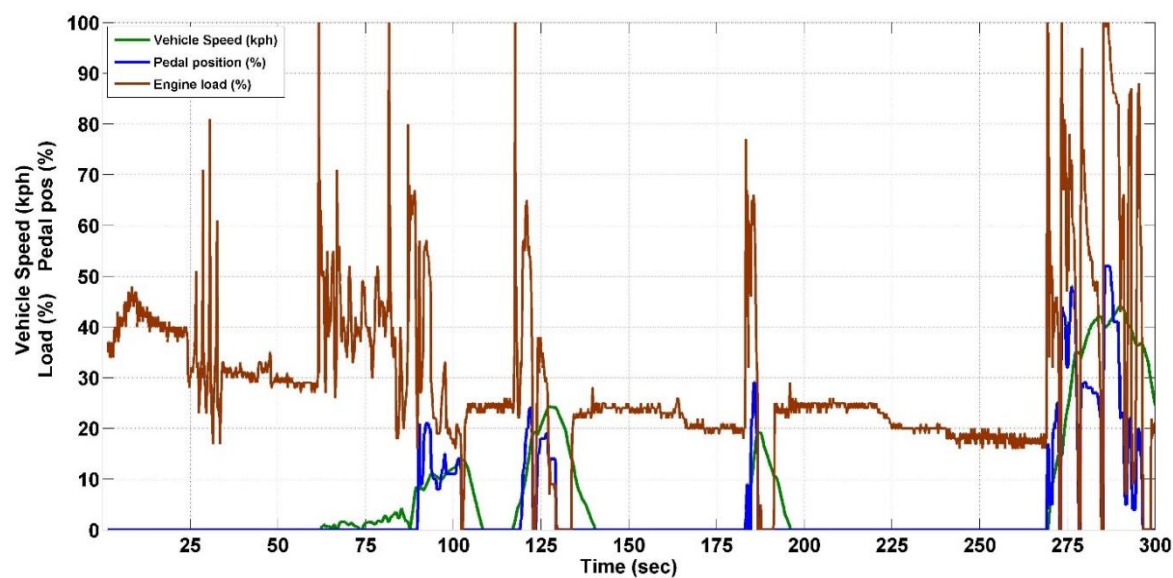


Figure 4-18 - Pedal position and engine load during cold start conditions of a van

Pedal position is zero when the driver does not use the accelerator pedal, unless in the case of Euro 5 vans, where an offset of 17% is present. However, as seen in the above Figure 4-17, engine load varies more often than pedal, and so does the minimum engine load value (during idling). This is more problematic in the case of a cold start of the engine, where the engine speed and load are slightly higher than usual for engine warm up requirements.

Figure 4-18 shows a 300 second cold start engine condition for Van 3. In contrast to the previous van, this one is a Euro 4 van, and hence the pedal position does not have an offset. It can be observed that as soon as the engine starts, the engine load reaches 47% before going down to 40%. This high engine load is due to the power required to crank the flywheel up to the rated speed of the starter motor. At the 25th second mark, there is change in load with no change in pedal position or vehicle speed. This may be due to the driver reversing the vehicle (negative vehicle speed not recorded in this case), by depressing the clutch of the vehicle and not using the accelerator pedal. At the end of this manoeuvre the minimum load value continues to decrease to 28% at the 1 minute mark. After this there is another change in engine load with very low speed of under 5 kph and no pedal. This again is due to the driver slowly releasing the clutch pedal of the vehicle to create motion in the vehicle, by resting on the idling governor. After a certain point, the driver will have to use the accelerator pedal to increase the speed of the vehicle. During the idling condition after the 100 second mark, the minimum engine load has dropped to the 25% mark, while at the 175th second mark, the minimum load is 19%. As the engine gets warmer, the minimum engine load drops further to 17% at the 250 second mark.

This constant change in engine load with zero pedal meant that a new minimum load finding algorithm needed to be developed to replace the minimum pedal position algorithm described in Figure 4-4. Figure 4-19 shows the algorithm used to determine the minimum load in an engine for a vehicle. Unlike the case of pedal position in a Euro 5 van, the minimum load keeps changing throughout the running condition of the vehicle, and also depends on different engine conditions. Hence, this algorithm is works throughout the course of the engine running, searching for the 'new' minimum load of the engine. This minimum load is used as the zero pedal position equivalent in the gear shift algorithm.

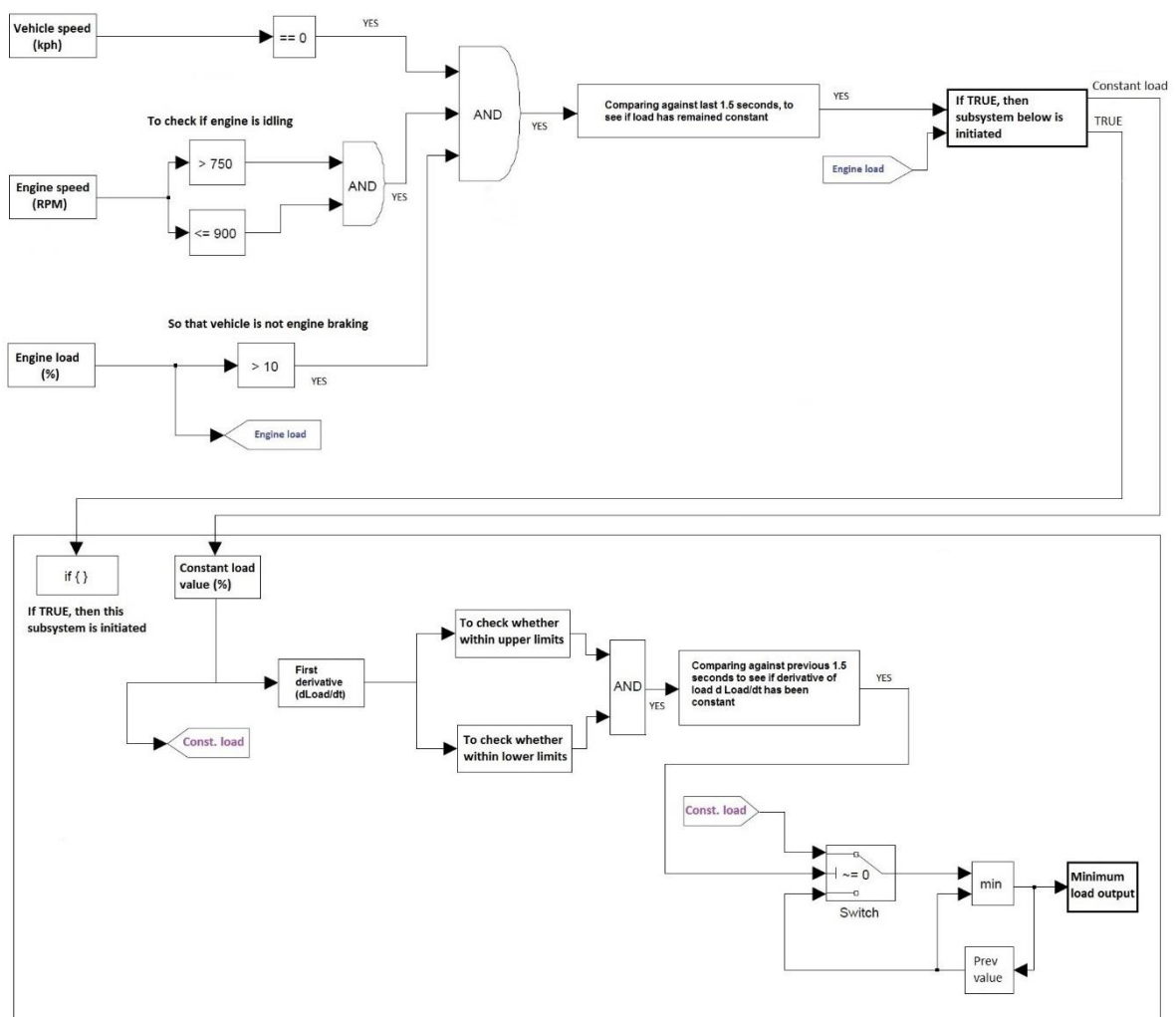


Figure 4-19 - Algorithm for determining the minimum load of an engine

Since engine load value changes often, the minimum load is calculated whenever the vehicle is stationary and idling. This is because minimum load in other cases is zero, when the driver lifts of the accelerator pedal when in motion to enable engine friction braking. Minimum load in this section refers to the minimum engine load value that represents idling condition of the vehicle (when pedal position is equal to zero). Thus, an engine speed check and an engine load check, along with vehicle speed equal to zero check, is performed to determine whether or not the vehicle is stationary and idling. If the vehicle is idling, the logic waits until the load has become constant for 1.5 seconds. If this is the case, then the derivative of the constant load value is checked to determine variability. If this value is a constant close to zero, it is compared against the previously stored/determined minimum load value. The minimum of the two is chosen as the minimum load output for that iteration. This procedure of determining the minimum operating load of the engine was crucial because pedal position was not available for all types of vehicles.

Effect of the driver advisory tool

Figure 4-20 shows the effect of the driver advisory tool in operation in modifying driver behaviour. The aggressive driving characteristics is evident from the use of high pedal and high engine speed values compared to the calm driving style with the device providing feedback on how to improve. The higher concentration of points at lower pedal usage indicate a reduction in aggressivity and a lower demand of engine power, while a reduction in engine speed shows a reduction in fuel consumption for the same engine power. A reduction in engine speed is achieved by shifting up early into higher gears by making use of the shift lights that were discussed earlier in the chapter.

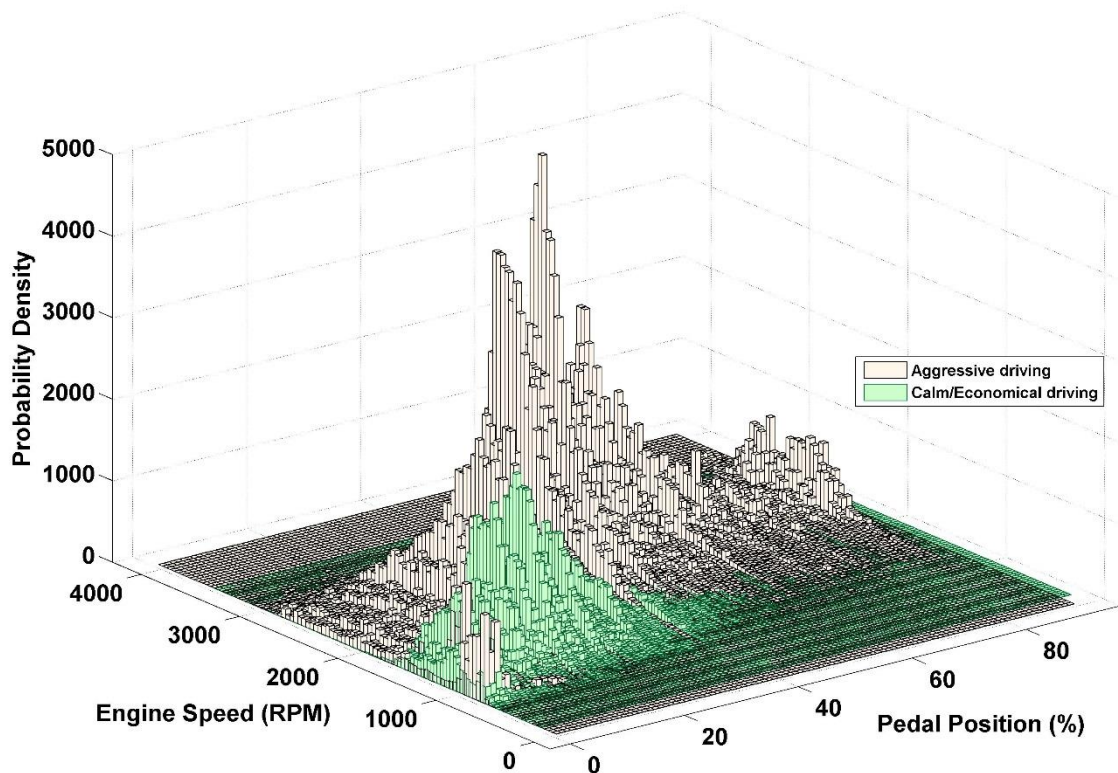


Figure 4-20 - Probability density of the pedal and engine speed of the best and worst driving characteristics (from baseline and interface trial data)

This methodology was used to generate Figure 4-21 which shows the probability density of engine speed with respect to pedal position of all the vans that were part of the field trial experiment, representing 39000kms worth of data. It can be seen from the figure that majority of the vehicle operation is below 35% pedal usage. This plot is beneficial in understanding the region of operation preferred by drivers of a diesel engine vehicle in the real world. Optimising the performance and efficiency of the vehicle in the region under 25% pedal position and 1500rpm engine speed will yield the best fuel economy benefits in the real world. The test conditions of vehicles may be different to real world traffic conditions, and this plot helps understand the preferred area of operation for the drivers of the 15 vans that were part of the trial.

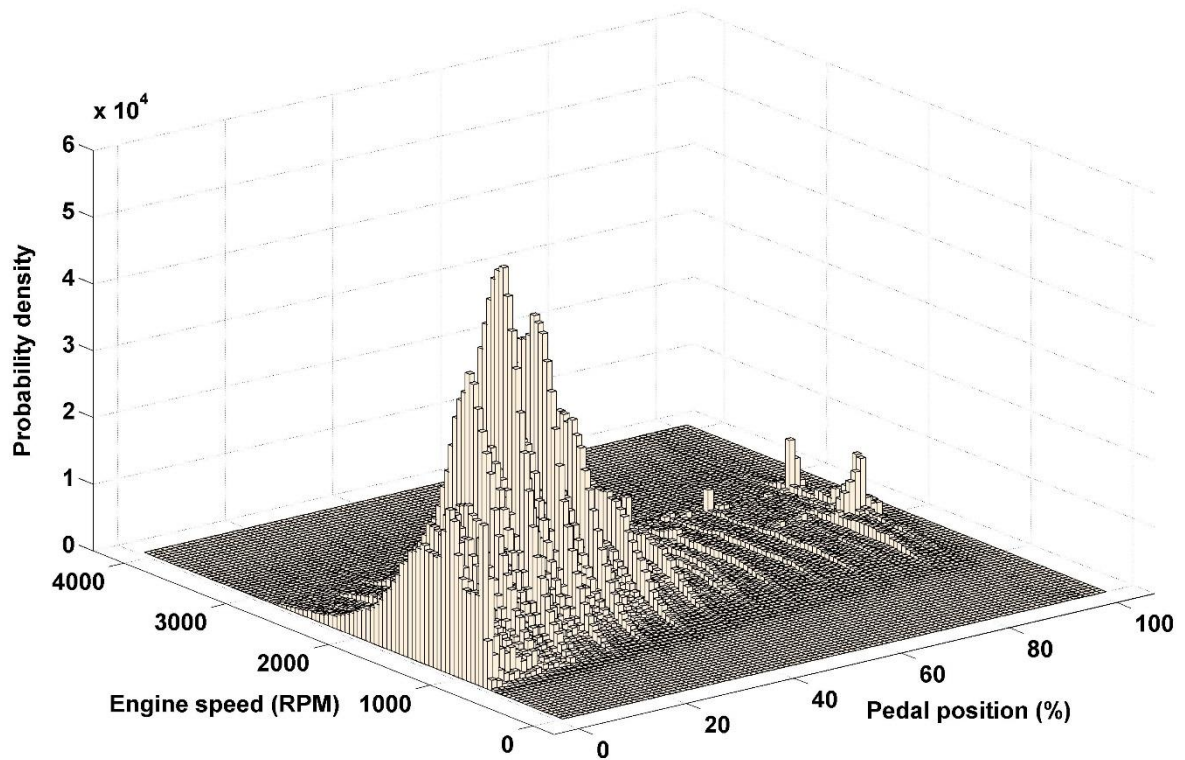


Figure 4-21 - Probability density of Pedal position and Engine Speed for all the vans that were part of the field trial experiments

4.8. Summary

This chapter highlights some of the key updates performed on the driver advisory tool to improve driveability and functionality of the device. One of the initial updates involved the sensitivity control which was essential for the device, so that drivers are provided the opportunity of gradually getting used to the device to avoid being overwhelmed by it constantly advising them on their driving style. This update was issued along with a cruise control detection logic to prevent drivers from bypassing the essential functionality of the system, by accelerating with zero pedal usage.

One of the most important aspects of driver behaviour improvement is shifting into higher gears early, thereby reducing fuel consumption. This was an essential part of the development stage of the driver advisory tool, as not all vehicle had a gear up-shift light. This problem was resolved in two stages. The first was concerned with identification of the ratio of the highest gear of the vehicle, so that the driver is not asked to shift up a gear when he/she is already in the highest gear. Secondly, an algorithm that takes into account current vehicle speed, acceleration, engine speed and pedal position was used to determine the engine speed at which the driver is asked to change the gear. This up-shift engine speed varies constantly depending on the instantaneous context of the vehicle. Driveability was a key aspect when developing the logic, to ensure that the system performs effectively in all situations, especially to avoid warnings given to the driver in situations like heavily laden conditions, or going up a hill. The gear shift logic of the tool was an essential component required for the effective functioning of the advisory tool.

Data collected from field trial experiments showed many cases of excessive idling instances (more than 90 sec). An idling warning and penalty algorithm was added to the advisory tool system to remind the driver to switch the engine OFF to save fuel. Similar savings to 'Start-stop' technology will be seen using this device, although in this case, starting and stopping of the engine will have to be done manually by the driver. The author understands that this adds extra work to the duties of the drivers, but the benefits of avoiding excessive idling provides a good reason in switching the engine OFF to conserve fuel. Idling penalties do help to change driving behaviour by motivating the driver to try and improve on fuel consumption whenever possible.

Determination of the minimum engine load was discussed for vehicles that did not have pedal position data. These updates were an essential requirement to improve the functionality of the device and further improve the driveability. Time and cost constraints prevented the author from undertaking further organised trials with the updated version of the device. However, the device was tested on different vehicles by the author and the industrial partner, and is currently being sold in the market.

The driver advisory tool had proven to save an average of 7.6% in fuel consumption when used on IC engine powered vehicles. Further research in this area was undertaken to understand the benefit of using the device on a fully electric vehicle. For this purpose, the author was involved in the development and testing of low cost electric machines for traction applications. The next chapter discusses the work carried out in testing, calibration and benchmarking of electric machines for traction applications. A new concept of mechanical field weakening is also discussed. Alternate methods to reduce research and development costs (and in effect the final cost of the electric motor) using a fully automated test rig is also discussed. This activity forms an important part of the thesis because it describes the development stage of the powertrain used in the electric vehicle that was used to test the electric version of the driver advisory tool.

Chapter 5 - Electric motor testing and development

This chapter is concerned with the development and testing of a low cost scalable electric motor for electric and hybrid vehicle traction applications. The author's role in developing the test procedure, test rig and control strategy for variable air gap axial flux motor is discussed here. A fully automated software developed by the author to test electric motors is also described in this section. The electric motor developed and tested was later used in the fully electric vehicle tested, which is discussed in the next chapter of the thesis.

Work published in:

1. "Development and Testing of a Low Cost High Performance Hybrid Vehicle Electric Motor", Presented at *SAE World Congress, 2013*
2. "Test and Simulation of Variable Air Gap Concept on Axial Flux Electric Motor," *IEEE Vehicle Power and Propulsion Conference (VPPC), 2013*

5.1. Axial flux electric motor testing

The author was significantly involved in the developmental testing and calibration of the axial flux electric motor developed by the industrial partner on the project. This work forms an integral part of the thesis because this motor was later used in the fully electric vehicle used for the trials of the electric version of the driver advisory tool. The literature review provided a brief introduction to the axial flux motor developed by the industrial partner, predominantly used as traction motors for hybrid electric vehicles. This section will cover the test procedures used to collect data from the motor and the development of test rig software and hardware used to test the machines. Two types of Ashwoods electric motors were tested to understand the optimum performance envelope for different power requirements. The first motor tested is a standard 72V motor that has now gone into production. The second motor is a high voltage machine that can be used for different applications, mainly the Variable Air Gap (VAG) technology application that will be later discussed.

The standard 72V motor consists of 8 windings on each stator pole. There are 12 stator poles and 10 magnetic rotor poles which are 7mm thick. The motor was designed and developed to be modular in terms of construction, with most of the components being made available 'off the shelf' to buy and replace [36]. The motor casing is 26cm in diameter and 10.3cm deep, with the motor weighing just under 20kg. It has the capability to work in air cooled or liquid cooled conditions. The stator poles of the machine are made of powder iron, thus reducing the cost of the machine and also reducing the potential for eddy currents to be generated within the motor, compared to conventional electric motors that use laminated steel [36, 90]. The

distance between the stator and rotor (defined as the air gap) can be varied by adding shims onto the shafts. The standard 72V motor was tested using Sevcon controllers. Table 5-1 shows the specification of the motor obtained from testing conducted at the University of Bath electric motor test facility.

Table 5-1 - Motor specifications obtained from testing the standard 72V Ashwoods electric motor

Operating DC voltage	72 V
Maximum AC current	550 A _{RMS}
Peak power	14.9 kW
Peak Torque	70.8 Nm
Continuous power	4.05 kW @ 2500 rpm
Continuous Torque	15.5 Nm @ 2500 rpm
Duty cycle power (2 mins)	12 kW@ 4000 rpm
Duty cycle torque (2 mins)	28.6 Nm @ 4000 rpm
Duty cycle power (10 mins)	6.25 kW @ 3500 rpm
Duty cycle torque (10 mins)	17.1 Nm @ 3500 rpm
Peak Efficiency	94%

5.1.1. Test rig setup at University of Bath

Test rig setup at the University of Bath comprises of a 75 kW Vascot asynchronous dynamometer that can be coupled to the electric motor to be tested. Both these units are bolted down onto a frame with one end free to slide motors on and off. An HBM torque transducer is used in between the machines to measure torque and

speed. The dynamometer and the motor were both powered and run using two separate KEB industrial inverter controller drives. The test motor can be controlled with a bespoke inverter/controller if the need arises, with the power being fed from a DC power supply (or battery emulator). In the case of the testing described in this chapter, the first motor was tested using a Sevcon inverter, while the second motor used KEB hardware to be tested. The KEB system is fed from a 415V_{ac} supply from a transformer that is rectified and filtered to maintain a fixed DC voltage. When both controllers are running, AC power is fed into the electric motor which applies a torque against the dynamometer holding a constant speed. The dynamometer generates electric power which is circulated back into the motor controller thus reducing the load on the incoming supply from the transformer. In this way, the input supply only tops up the losses in the system and circulation of energy ensures minimum wastage during the test procedure.

The test cell host PC is a Sierra CP Engineering Cadet system that allows complex control of both the drive and the test motor and also helps in data logging. Three voltage and current clamps (one per phase) measure AC voltage and current for each phase and is connected to the Dewetron high frequency data acquisition system that calculates various AC motor parameters like RMS voltage, RMS current, power factor, AC power into the motor etc. These calculated parameters are read into to CP Cadet System via serial communication, where they are logged with other test cell time stamped data. Figure 5-2 shows electric motor test facility with an axial flux electric vehicle motor coupled to dynamometer. Oil cooling setup can also be seen with the blue hoses.

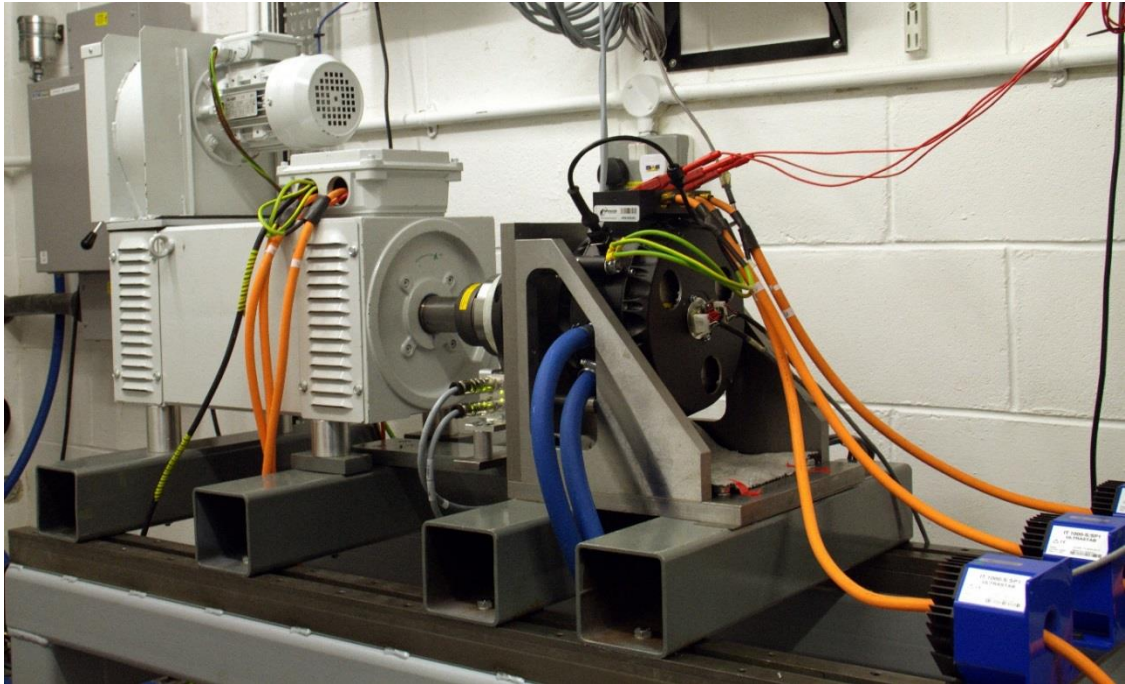


Figure 5-1 - The electric motor test facility setup at the University of Bath

5.1.2. Test procedure

Motor testing is an essential part of the development stage of the electrical machine. Important motor specifications like rated power and torque etc. were tested based on the IEC standard for rotating electric machines [91, 92]. New testing methods were defined and developed for in depth testing of the motor, to understand its performance in different working conditions. A test form was created for the compilation of results from various tests performed on a particular motor. Each test sheet was also accompanied by a set of instructions that explained to the test engineer the procedure to conduct the respective test. The different tests involved in the assessment and characterisation of each motor is detailed in this section.

Table 5-2 - Electric motor test plan

Electric motor test plan			
Sl No.	Test	Expected Results	Duration
1	Ke Test	To determine the Ke of the electric machine Helps understand if the motor is damaged. Also provides an indication to the maximum and torque and speed limit	1/2 hour
2	No load test No load no rotor test	To determine the total losses in the machine when not powered. To determine the mechanical frictional losses in the machine.	1 day
3	Torque Speed envelope test	To determine the maximum torque and speed of the electric machine	1 day
4	Efficiency map test	To determine the efficiency of operation of the electric motor at different speed and torque values	1 week
5	Duty cycle and continuous power test	Continuous power test is to determine the maximum power and torque that the motor can sustain indefinitely Duty cycle test is to determine the maximum torque and power that the motor can provide for different intervals of time.	3 weeks

Table 5-2 shows a high level test plan used for the investigation of electric motors at the University of Bath. Since the tests mentioned in the IEC standard for electric motors are generic electric motor tests, the tests did not provide the level of detail required for research and analysis into electric motor performance. This pertains to detailed tests to understand of how small changes in motor or inverter control parameters translate to performance changes and how best to test these before calibrating the electrical machine. They also did not provide an understanding into whether the motors were damaged or what particular component of the motor was damaged. The new proposed tests also help predict the performance range the motor before all the tests are done, which helps create suitable design of experiments.

The K_e test helps compare motors of different internal structure, to provide a rough indication as to the maximum speed and torque profile of the machine. It also helps determine if the motor has been damaged or if the magnets have lost their strength. The encoder of the machine is aligned at the same time by tuning it to a point where maximum torque is achieved from the machine for a given speed. The no load and no load no rotor tests are useful to determine the mechanical and electrical losses of the machine. Torque speed envelope is an essential test to determine the maximum performance of the machine. Efficiency map test defines the efficiency of the motor at different speed and load points. This is particularly useful when developing control strategies for different applications, to try and operate at the most efficient region when possible. Duty cycle testing helps define short term duty performance of the electrical machine. This is useful as the continuous power of the machine tends to be generally around $1/3^{\text{rd}}$ of the peak power. However, there may be situations where

the machine has to work on a slightly higher power for short durations, which is defined by the duty cycle test results. These tests are explained in detail below.

- **Ke test**

Ke is the back EMF constant of the motor, which is the open circuit voltage generated by the motor with respect to the speed. Ke is generally expressed in V/rad/s or V/1000rpm. Ke gives an indication to the maximum speed of the motor. For permanent magnet machines, the Ke value should be equal to the motor torque constant value (Kt, expressed in Nm/A). Thus it is possible to gain an understanding into both the torque and speed of a motor from its Ke value. It becomes even more useful to predict the performance of the motor when small changes are made to its structure.

Higher the Ke value, the more torque the motor produces for the same current. But a higher Ke value also indicates a higher back EMF would be produced by the motor for the same speed, hence the base speed (and the maximum speed) of the motor is reduced. Lower the Ke of the motor, lower is the maximum torque value. However, this also indicates that the back EMF produced by the motor is lower, which indicates the machine can achieve a higher speed than in the case of a standard machine.

The Ke test also gives an indication as to whether the motor has been damaged. If the motor is damaged during transit, or the magnets have been de-magnetised, the Ke values would reflect this. Hence it is the first test carried out during the test process. It also has the advantage that the test is carried out in open circuit conditions. Hence the motor is physically disconnected from the controller, thus isolating the high voltage battery systems.

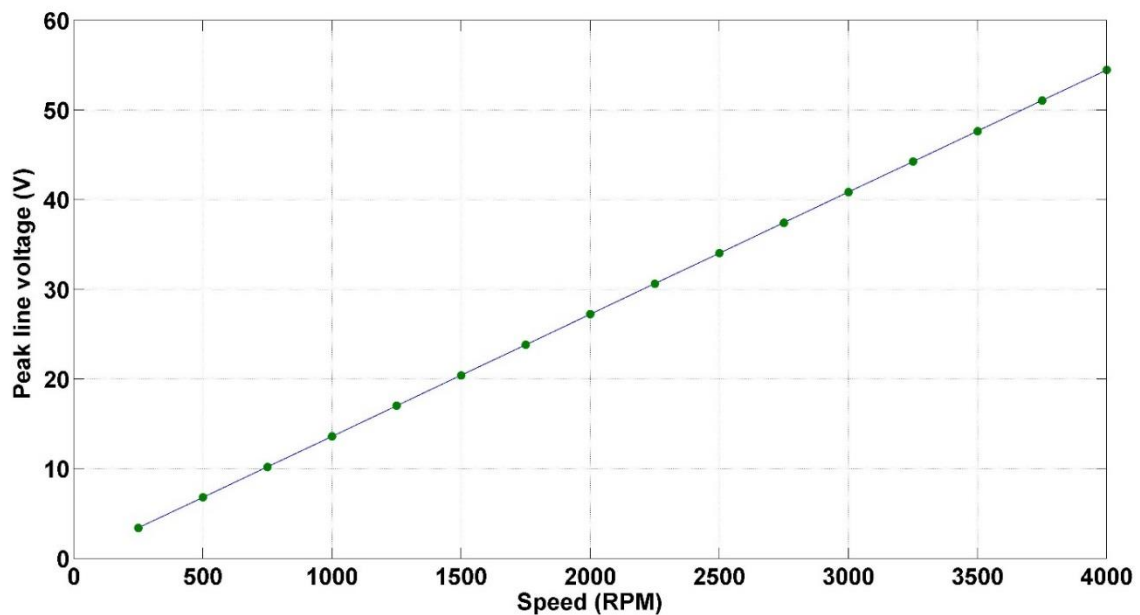


Figure 5-2 - Voltage vs Speed plot for the 72V standard motor

After the motor phase cables have been disconnected from the controller, the motor is securely tightened to the bed frame and coupled to the dynamometer. The dynamometer is spun to different speeds 250rpm apart, while terminal line voltage (between each phase) is measured. The K_e value is the ratio of peak line voltage to speed expressed in radians per second. K_e value is a constant and the test is carried out at different speeds to ensure repeatability and reliability of the measured value. Figure 5-2 shows the speed against voltage graph for the 72V standard motor. For the determination of K_e value, the peak line voltage is measured and divided by the speed of the motor in radians per second.

Consider a speed of 1000rpm, which equals 104.72 rad/s. The peak line voltage at this speed is 13.61V, which gives a K_e value of 0.13 V/rad/sec. The K_e value is calculated for different speeds and averaged to obtain the mean value.

- No load test

Once the K_e values are satisfactorily repeatable, the motor is spun using the dynamometer to assess the losses in the machine. For this test, the motor cables are connected to the controller, but the controller is switched OFF. There is only a small current flowing due to the voltage drop across the cables. This test gives an indication of the overall losses generated in the system at various speeds. This test is carried out at different speeds with 250rpm step intervals. The torque measured at the torque transducer in between the test motor and the dynamometer gives an idea of the electrical and frictional losses in the machine. These losses increase with speed as frictional losses of bearings and back EMF of the machine increases with speed.

The No load thermal test follows next. For this test, the motor cables remain connected with the controller switched OFF. The motor is spun up to 4900rpm using the dynamometer and held at that speed to measure temperature rise in different sections of the motor. 4900rpm represented maximum restricted motor speed on Ford Transit hybrid vans developed by the industrial partner. This test represented a vehicle cruising on a motorway at 60mph with the electric machine only spinning and not applying load. The stator windings which are in the path of the rotating magnetic field when the vehicle moves, has current flowing through them (according to Faraday's Laws of electromagnetic induction) [93]. This causes temperature in the stator coils to rise. This test determines the time taken for the temperature of the motor to rise due to electromagnetic activity in the machine. Also the bearings heat up quickly due to the high speed of rotation.

Figure 5-3 shows this temperature rise for different components in the machine when the motor is run at 4900rpm. It can be seen that the bearing housing of the motor heats up the quickest and reaches 95°C in just over 16 minutes. This is due to the heat produced by friction losses in the bearings along with the electrical losses in the windings. The no load test is later repeated with the rotor removed so as to isolate the electrical losses and calculate the mechanical losses in the machine.

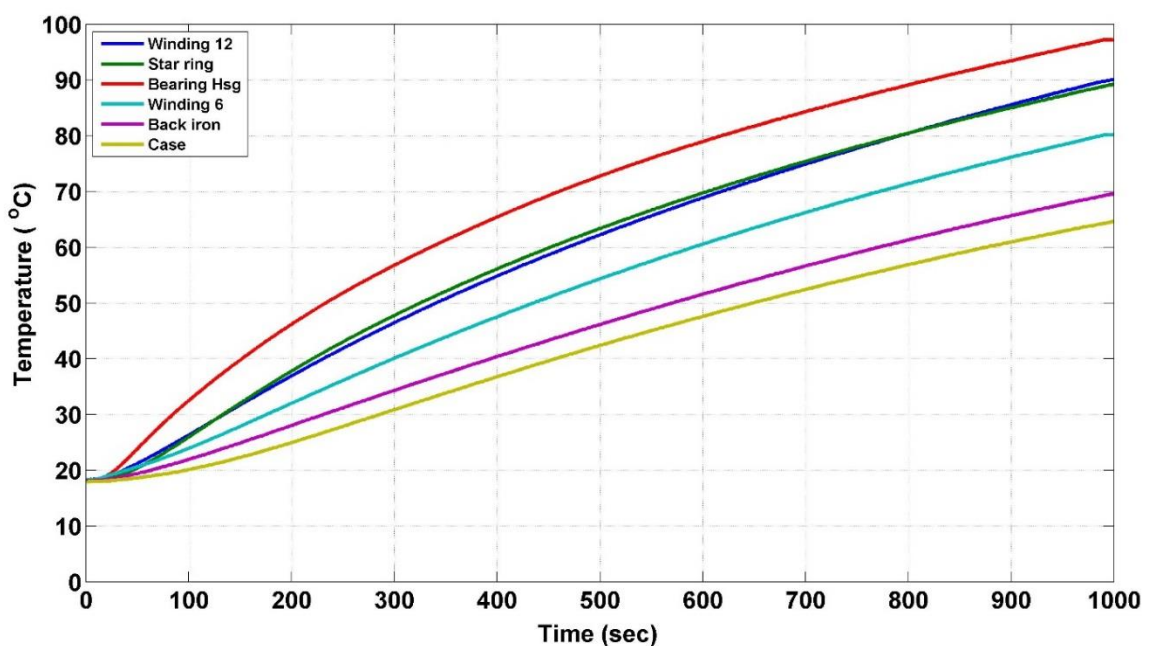


Figure 5-3 - No load temperature rise for 72V standard motor

- Torque speed envelope

One of the most important aspects of defining the performance of a machine is through the maximum torque and power graphs. This is an essential part of testing the electric machine. Torque speed envelopes provide an indication to the performance boundaries of the motor. Unlike the case of an engine, electric motors are not highly efficient at maximum torque values due to the core losses and winding losses being at their peak.

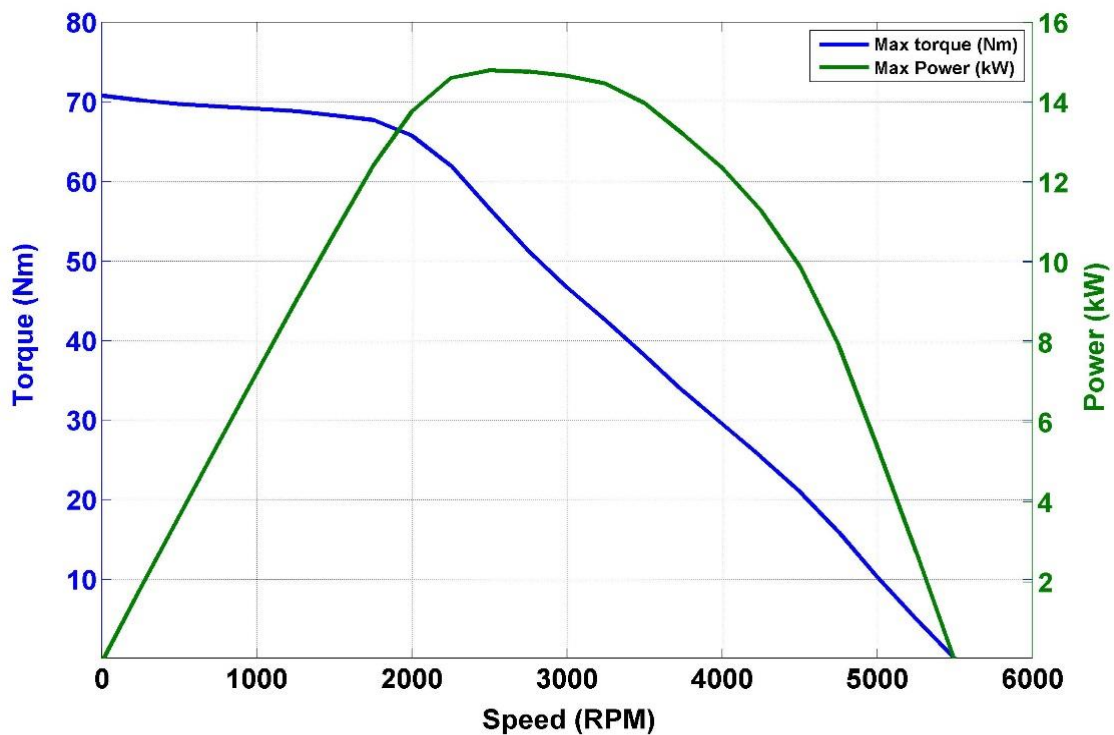


Figure 5-4 - Torque speed envelope for a 72V standard motor

Figure 5-4 shows the torque speed envelope for the electric motor. The torque speed envelope test is obtained by connecting the phase cables onto the motor and powering up the controller connected to the battery pack or power supply. Once the motor is ready to run, the dynamometer is used to set a speed. As in the previous cases, the speed is set to 250rpm and full 'throttle' is applied on the test motor. This provides the maximum torque achieved by the motor at the set maximum AC current input. In this case, the motor was limited to 550A_{AC} RMS. The motor generated a maximum of 70.8 Nm at 545A_{AC}. This provides a motor torque constant K_t of 0.13Nm/A. This is the same value of K_e determined in the previous test, proving that the values of K_e and K_t are the same.

- Efficiency map testing

The efficiency map is a contour representation of the operating efficiency of the motor along the different speed and torque conditions. The efficiency map provides an understanding into the high and low efficiency regions of the machine. To create this map, the motor has to be tested in a number of speed and torque points. For this purpose, the dynamometer is set to a specific speed, while the torque of the motor is varied in steps of 5 Nm. This provides a good degree of detail to the map. Various motor parameters like current, voltage, torque, speed, electrical power etc. are logged at each point. Motor efficiency is calculated and Matlab® Model Based Calibration toolbox is used to develop the efficiency map of the machine. Figure 5-5 shows the efficiency map of the 72V standard motor. The map is truncated using the torque speed envelope as this defines the operating region of the motor.

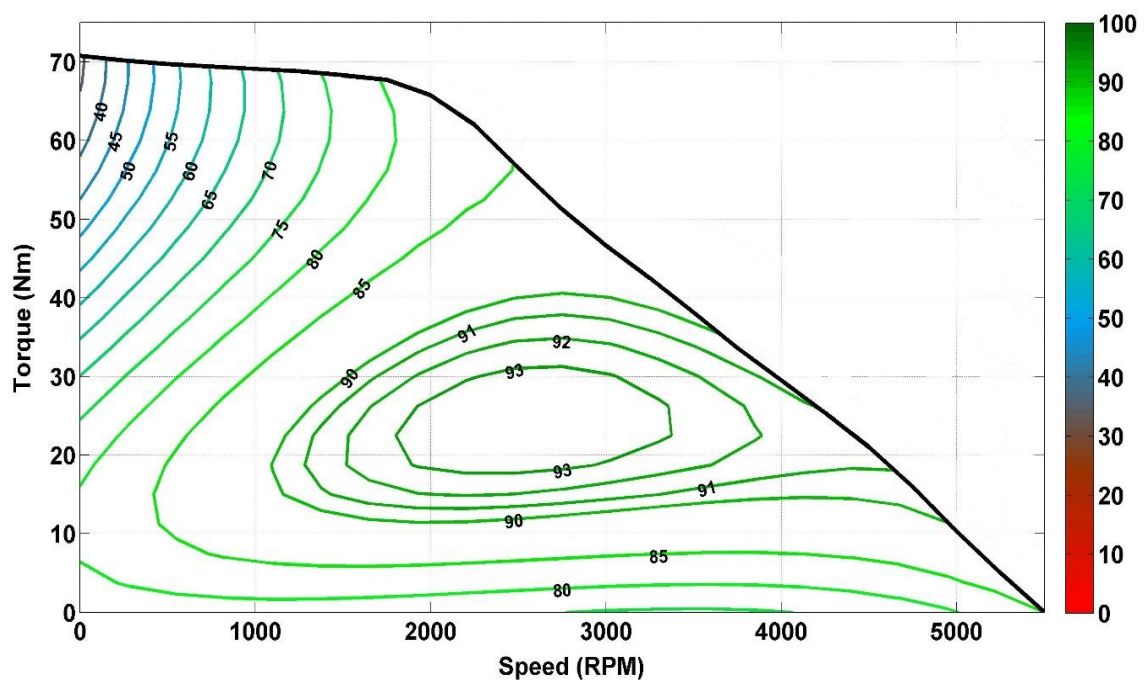


Figure 5-5 - Efficiency map of the 72V standard motor

- Duty cycle and continuous power

Duty cycle tests involve running the dynamometer at different speeds to understand the duration for which the motor can sustain a certain power/torque value. This testing involves setting the dynamometer at a speed and applying a constant torque to measure the duration for which the motor can successfully hold the torque without overheating. It provides an indication as to how long the motor can perform at different speeds at different operating torques. This test helps to develop control strategies to protect the motor and ensure reliability of the machine.

Table 5-3 - Duty cycle operation for the 72V standard motor

	5 sec		15 Sec		30 Sec		1 min		2 min		5min	
Speed (RPM)	Tq Nm	Pow kW	Tq Nm	Pow kW	Tq Nm	Pow kW	Tq Nm	Pow kW	Tq Nm	Pow kW	Tq Nm	Pow kW
1000	69.1	7.2	61.8	6.5	46.8	4.9	37.6	3.9	30.0	3.1	24.0	2.5
1500	66.9	10.5	62.4	9.8	47.5	7.5	37.3	5.9	29.5	4.6	23.0	3.6
2000	63.5	13.3	59.8	12.5	46.0	9.6	36.3	7.6	28.0	5.9	21.5	4.5
2500	57.1	15.0	57.1	15.0	45.4	11.9	36.0	9.4	27.0	7.1	20.5	5.4
3000	46.0	14.5	46.0	14.5	45.6	14.3	35.8	11.2	26.0	8.2	19.0	6.0
3500	37.1	13.6	37.1	13.6	37.1	13.6	34.9	12.8	26.0	9.5	16.0	5.9

Table 5-3 shows the duty cycle data for the standard 72V motor. The efficiency map and the duty cycle data help indicate the range of continuous operation of the machine. Different points of operation are considered when testing for the continuous power rating. Continuous power testing is carried out to identify the

maximum torque and speed that the motor can sustain indefinitely (or in other words, steady state conditions). For the standard 72V machine, continuous power of 4.05kW was achieved at 2500rpm, maintaining a constant torque of 15.5 Nm.

5.2. Variable air gap concept

Different controller parameters were attempted at improving motor torque at high speeds. Electrical field weakening settings in the Sevcon controller proved to be difficult to tune effectively to achieve a higher speed from the machine. It can be seen from Figure 5-4 that the motor has practically zero torque at 5500rpm. Magnetic field weakening using electrical strategies are often used to achieve a higher speed than the maximum speed of the machine. However, electrical field weakening has its drawbacks in terms of poor efficiency as a negative field is applied to counter the field of the magnets. Also, the negative field has the potential to damage the permanent magnets. Hence, the capability to electrically weaken the field is restricted.

It was decided to attempt to mechanically weaken the field in the machine by increasing the air gap between the stator and the rotor. For an ideal motor, the air gap should be minimum so that there is little or no flux leakage into the air gap; rather the flux is fully linked between the stator and the rotor. On increasing the distance between the stator and the rotor, more of the magnetic flux linking the stator coils with the rotor is lost in the air gap. This reduces the flux density, which in turn reduces the back EMF of the machine. This helps the motor achieve a higher speed than what it could initially achieve with standard minimum air gap. This process also reduces the peak torque values of the motor. Depending on the

requirement of the machine to perform in high torque conditions or high speed conditions, the optimum air gap can be chosen.

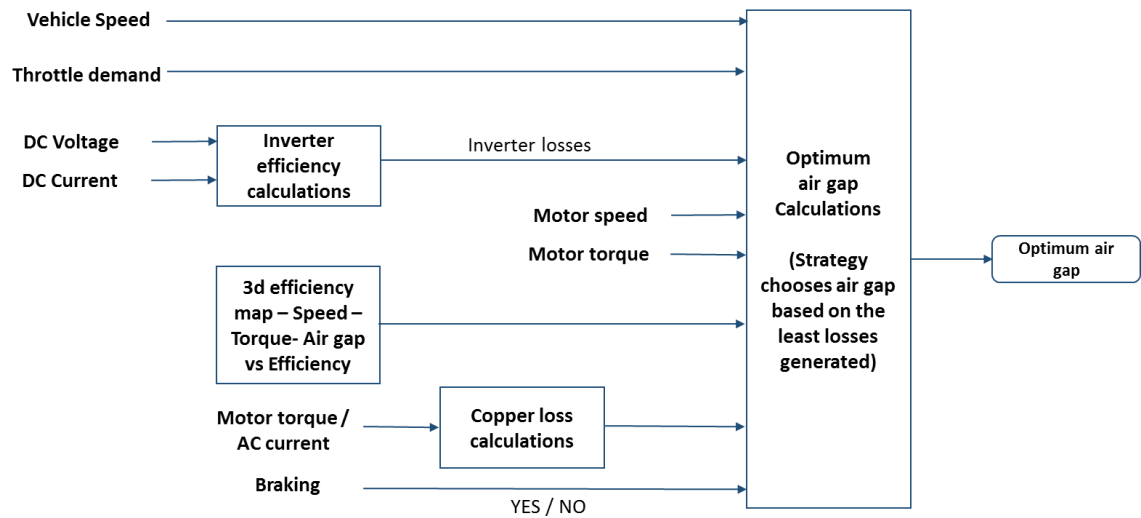


Figure 5-6 - Determination of the optimum air gap for the variable air gap control strategy

The concept was first trialled on the standard axial flux 72V single rotor machine to understand the increase in performance that can be achieved. Based on the results from this testing, a Variable Air Gap (VAG) technology was incorporated into the new 72 winding, dual rotor axial flux machine to perform at high torque and high speed conditions. This would help avoid the need for a gearbox as the motor can achieve high speeds by actuation of the air gap. A control strategy for the VAG technology motor was developed using the minimum losses approach, to determine the optimum air gap for a particular speed and torque output [94]. Figure 5-6 schematically represents the strategy used for determination of the optimum air gap of the machine. The system calculates the different losses of the machine and also has a three dimensional efficiency map data for every speed and torque for different air gaps. The optimum air gap was selected by taking into account the different losses and choosing the one that yields the least total losses for the required power output.

The testing was carried out in two stages – firstly, using the new electric motor test facility at the University of Bath to understand the performance benefit of each air gap. Secondly, use the chassis dynamometer to test a mule vehicle equipped with the VAG motor. This would help understand the benefits of the machine before implementing it in a road legal electric vehicle.

5.2.1. Variable air gap rig tests

Prior to the testing phase, it needs to be mentioned that there were considerable challenges in selecting the optimal motor controller for the application. Various controller manufacturers like Curtis, Infineon, Semikron, ZyteK and Sevcon were considered during the evaluation phase. Initial hardware, setup costs and flexibility were studied carefully before choosing Sevcon as the controller for the Toro mule vehicle. After carefully studying different industrial inverter suppliers, KEB was chosen due its ability to control both the dyno and the test motors.

To test the performance of the machine at different air gaps, the gap between the stator and the rotor was increase by adding shims. The air gap was measured for each and every test so as to understand the performance and efficiency of each point in every air gap. This was fed into the control strategy so that the motor operates in the most efficient region when possible. The advantage of mechanical field weakening can be seen in Figure 5-7. Compared to the standard machine which runs out of torque at 5500rpm, using shims to increase the air gap manually provided torques up to speeds in excess of 8000rpm, a 45% increase in speed. The K_e of the machine reduces every time the air gap is increased, showing the reduction in back EMF due to the weaker flux linkage in the machine.

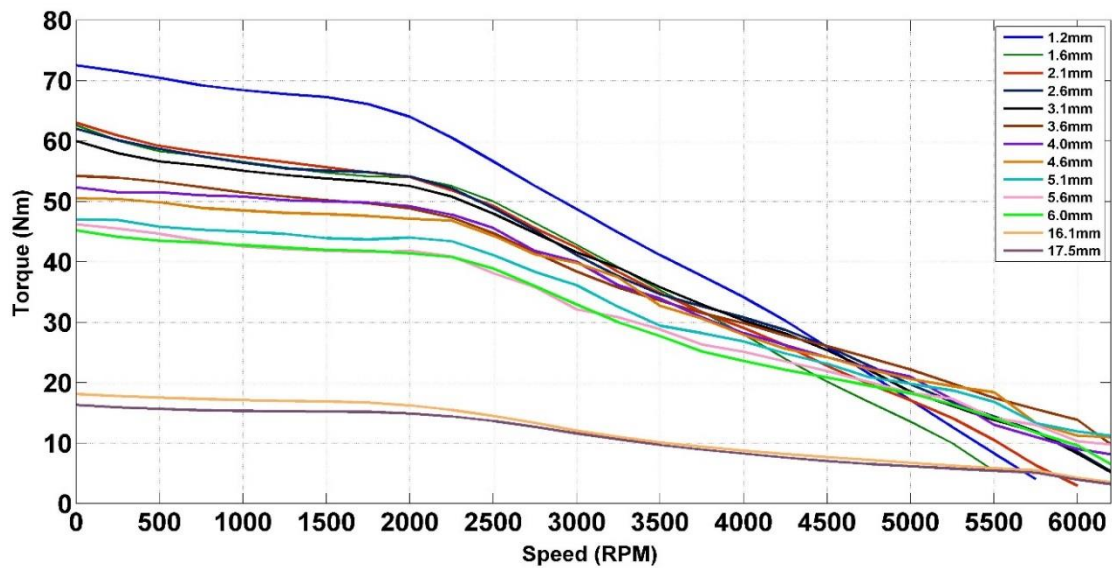


Figure 5-7 - Torque speed envelope for 72V electric motor with different air gaps

Knowledge gained from the development and testing of the first prototype motor enabled the industrial partner to develop a 72 windings higher power machine. The motor case had the same diameter of 26.3cm as the 8 windings machine, but was deeper to accommodate the second rotor. The dual rotor machine meant the stator was of a yokeless design. The copper coil used in the machine had a cross-section of 10mm^2 . Two ten pole magnetic rotors were housed on either side of the stator assembly with one rotor being allowed to be actuated to change the gap between it and the stator coils.

The first tests were carried out at 200A_{ac} current capacity on the electric motor test rig at the University, using the KEB hardware which was restricted to a minimum of 600V_{dc} capability. This meant the data collected had to then undergo post processing to exclude any data over the 72V_{ac} . Figure 5-8 shows these results obtained. The efficiency maps of each air gap were used for the development of the control

strategy. It is evident from the figure that there is a reduction in the maximum values of torque, but the increase in torque benefit at higher speeds is limited. Also, there is a lack of increase in base speed, which is due to the controller not being capable to detect a change in the motor parameters, to adjust its internal motor torque predictions accordingly. However, the biggest disadvantage was the lack of increase in torque at higher speed. Unlike the 72V standard motor where the maximum speed of the machine increased from 5500rpm to over 8000rpm, for the higher windings machine the maximum speed increased from 3200rpm to 4000rpm. It can also be seen that there is little or no benefit in increasing the air gap beyond 16mm.

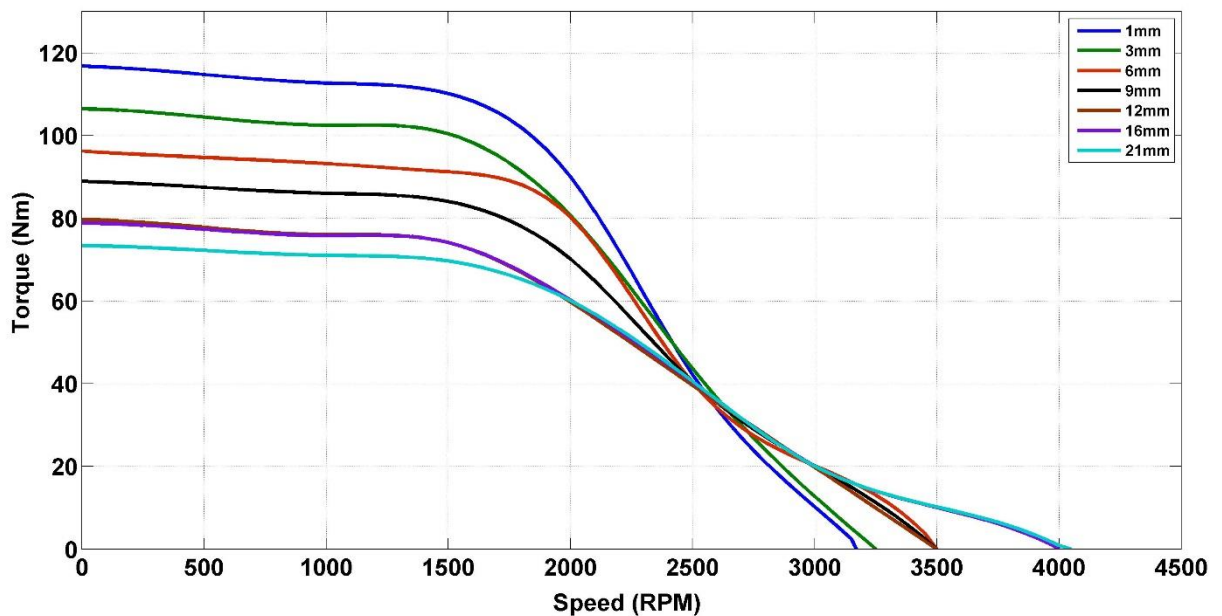


Figure 5-8 - Torque speed envelope for new 72 windings electric motor (simulated to 72V_{DC})

5.2.2. Chassis dynamometer testing of mule vehicle

To further test the performance of the VAG motor, a mule vehicle was developed to be tested on the chassis dynamometer facility at the University of Bath. This vehicle was tested to understand the benefits of the technology on a four wheeled vehicle

prior to testing on the roads. A Toro Workman buggy was used for this purpose with its IC engine replaced with the 72 windings VAG motor unit equipped with a 72V battery pack. The system had its own cooling system with a radiator to ensure



Figure 5-9 - Toro buggy used as mule vehicle for chassis dynamometer testing of the new electric motor at the University of Bath

optimal cooling of the motor and controller.

Figure 5-9 shows the power unit of the Toro vehicle. Air gap was changed using the VAG actuation system developed by the industrial partner, but the actuator position was manually changed using a control knob at the front of the vehicle. This enabled testing the vehicle at different air gaps and analysing the benefit at each point, rather than relying on the control strategy to choose the air gap. The controller used for this purposes was a 72V_{dc} Sevcon controller limited to 200A_{ac} maximum current capacity.

Using the standard VAG motor, the vehicle was initially capable of 6.5kph under standard road load simulation. The standard road load simulation was defined based on the regulation data for vehicles weighing less than 480kg. The 6.5kph vehicle speed represented 1100rpm in electric motor speed, using the vehicle's original 16.99:1 reduction gearbox and half shafts. The vehicle's 6.5kph speed restriction was due to the lack of available torque beyond 1100rpm motor speed at minimum air gap. It was noted that on increasing the air gap at high speed operation, instead of moving the operation point into the field weakening region and providing higher torque at high speeds, the Sevcon inverter tended to reduce the vehicle speed to maintain a torque that it can sustain. This was understood to be the problem in using a standard off-the-shelf controller for VAG application tests, which requires constant change in electric motor control parameters. The inverter unfortunately did not have the intelligence to detect the change in air gap, and hence restricted its performance to the torque profile that it initially calculated using the values provided to it based on the minimum air gap setting.

To understand further tractive effort capabilities of the vehicle, it was decided to change the vehicle simulation settings to a 2.3 tonne vehicle, so that a higher tractive force will be required by the motor to increase the speed of the vehicle. This would provide an indication to the maximum tractive capability of the vehicle and in turn the maximum torque available from the motor at different air gaps. Test procedure consisted of selecting an air gap for the motor and applying full throttle so as to obtain the maximum torque of the motor when it reaches a particular speed. The gradient input on the gradient simulation function of the chassis dynamometer was

increased in steps of 2%, to increase the tractive effort required by the vehicle to achieve maximum speed. The maximum wheel torque observed in this case was 4600N, which translated to 96Nm of motor torque at 1.7kph, which was 350rpm in motor speed.

With the standard settings of the controller, the motor was capable of achieving high values of torque at low speeds, but would not allow for an increase in vehicle speed (or maximum motor speed). Due to the controller attempting to maintain same torque when increasing the air gap by reducing motor speed, it was not possible to achieve a higher speed. It was therefore decided to induce extra electrical field weakening into the machine by adjusting the field weakening parameters from -10A to -50A in Sevcon. This allowed for the vehicle to achieve over 19kph (motor speed of 3300rpm). This was a significant improvement in torque at higher speed from the initial maximum value of 6.5kph (1150rpm). This induced electrical field weakening obviously reduced the maximum torque available at lower speed, but helped achieve an increase in torque at higher speed. The maximum motor speed increased by almost three fold after this change.

However, to determine the maximum torque available from the motor, it was required to change the dynamometer from road load simulation to speed control, to test the maximum torque available at each speed (similar procedure to electric motor testing, where the dynamometer is in speed control). This proved to be problematic as the chassis dynamometer had a minimum holding speed of 3kph, which translated to 550rpm motor speed. This made it difficult to test the motor at lower speeds, but it was possible to measure tractive effort (and hence motor torque) at speeds higher

than 3 kph. This method was useful to determine the increase in torque output at higher speeds, when increasing the air gap by inducing mechanical field weakening.

Table 5-4 - Toro mule vehicle chassis dynamometer testing points

Vehicle Speed (kph)	Motor Speed (rpm)	Air gaps tested (mm)
5	907	1, 5, 10, 12.5, 15, 17.5
9	1600	1, 5, 10, 12.5, 15, 17.5
12	2130	1, 5, 10, 12.5, 15, 17.5
15	2670	1, 5, 10, 12.5, 15, 17.5
17.5	3110	1, 5, 10, 12.5, 15, 17.5
20	3550	1, 5, 10, 12.5, 15, 17.5
22	3900	1, 5, 10, 12.5, 15, 17.5

Table 5-4 shows the different speeds and air gaps tested for the mule vehicle on the chassis dynamometer. For this testing purposes, the dynamometer was set to a specific vehicle speed and full throttle was applied on the vehicle. Tractive effort was measured and motor torque was calculated later. The air gap was changed to the values specified in the table, and the torque at each air gap was measured. Torque was held at each point to achieve a steady reading. Oil cooling of the motor was present to prevent it from reaching high operating temperatures. For this testing, the field weakening setting in the Sevcon controller was reverted back to -10A (default electrical field weakening setting). This allowed to analyse the effect of the mechanical field weakening.

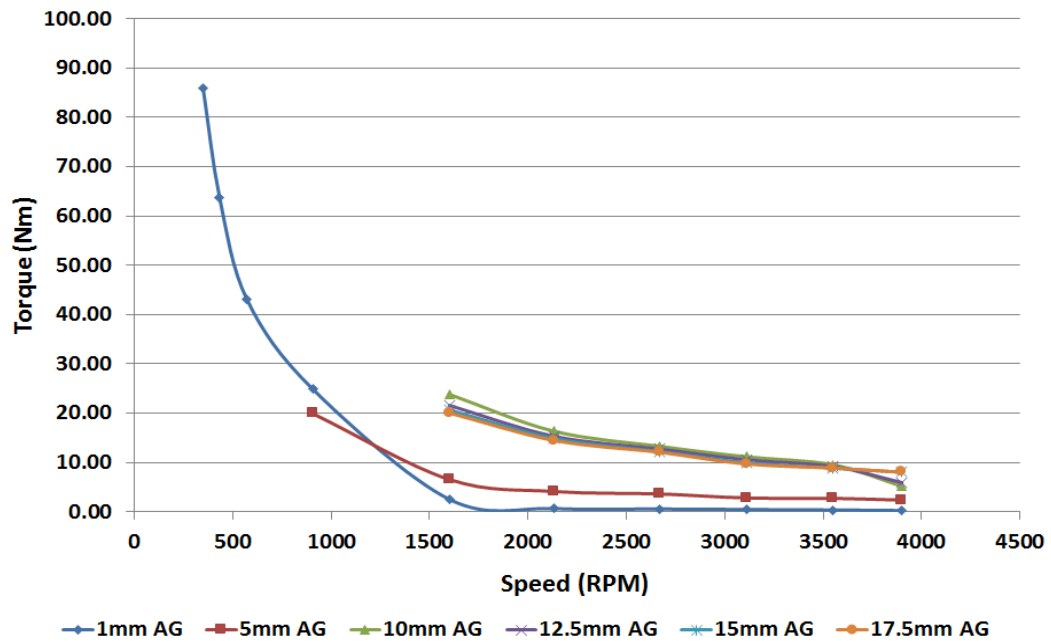


Figure 5-10 - Motor torque vs speed for different air gaps as measured on Toro mule vehicle on the chassis dynamometer

Figure 5-10 shows the effect of changing air gap and mechanical field weakening on the torque capability of the motor. It can be seen from the figure that maximum motor torque is achieved at 1mm air gap, which is the minimum gap between the stator and the rotor. However, performance at this air gap setting tails off and maximum speed achieved is around 1700rpm. With all other conditions remaining the same, the air gap was actuated to 5mm. This showed a reduction in the maximum torque values at low speeds, but the increase in air gap allowed for an increase in the torque beyond the 1250rpm mark when compared to the 1mm air gap condition. This increase in torque is because of the reduction field strength between the stator and rotor due to the increased distance between them. The reduction in field strength reduces the back EMF generated at higher speed, which allows more current to flow through the stator coils for production of torque. It can be seen that on increasing the air gap, the motor produces even higher torque at speeds above 1500rpm, which was

initially zero for minimum air gap. It was interesting to see that there was little or no benefit from actuating the air gap beyond 15mm air gap setting.

5.2.3. Discussion

Although the VAG concept on the new 72 windings higher power machine provided an increased speed compared to the minimum air gap condition, the improvement seen was much lower than expected, especially when compared to the improvement seen in the case of the 8 windings smaller machine. The lack of torque at higher speed on the 72 windings new machine is due to the fact that there is no considerable decrease in back EMF when compared to the 8 windings machine, as one would expect when the air gap is increased.

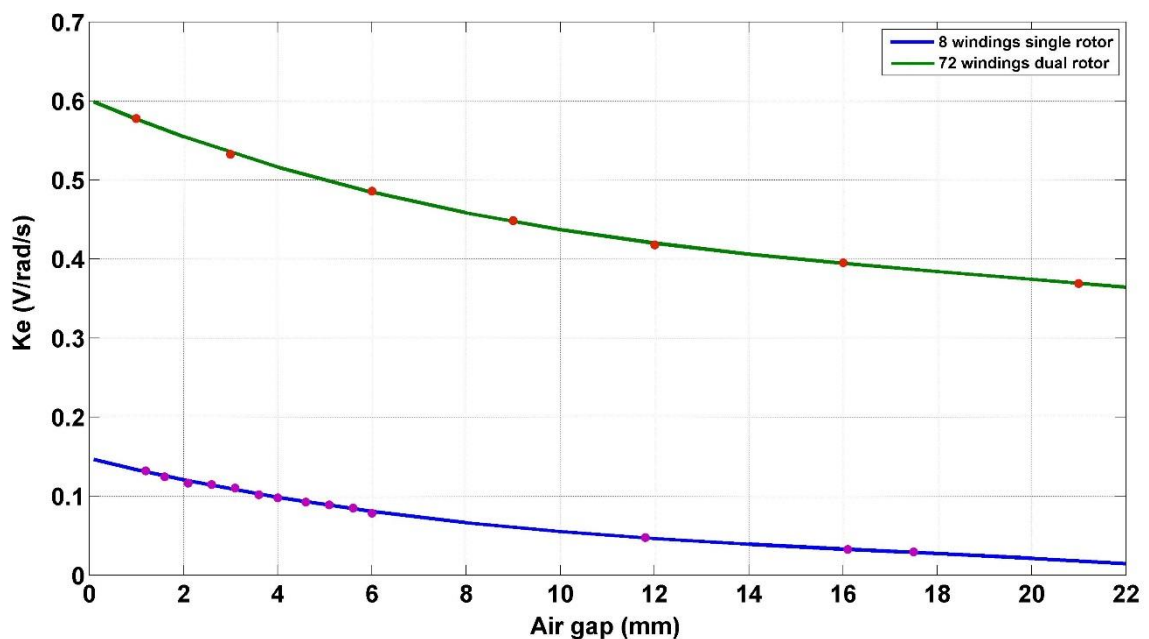


Figure 5-11 - Ke vs air gap for both 8 windings and 72 windings machine

This is evident from Figure 5-11 where comparison of Ke values for both machines against air gap is shown. Increase in air gap beyond the 25mm mark for the standard 72V motor would have resulted in back EMF reaching close to zero (meaning no more

torque available from the motor, where all the flux is being lost in the air gap), while for the 72 windings motor, it can be seen that the back EMF value seems to plateau at around 0.37 V/rad/s.

The absolute values of K_e of both motors are different due to the 72 windings motor having more turns per stator pole compared to the 8 windings machine. This machine thus has more capacity to produce torque. Aside from the increase in number of turns for the bigger machine, it also has two rotors compared to the smaller machine having only one rotor. When air gap was varied for the 8 windings machine, the rotor was moved away from the stator, hence weakening the field. When air gap was varied for the 72 windings machine, only one rotor was actuated as per the industrial partner's variable air gap design. This was found to be the major issue in not achieving effective field weakening.

Figure 5-12 shows the direction of flux lines for a single rotor axial flux motor (representation of the standard 8 windings machine) [95]. It needs to be mentioned that this figure does not show the magnetic flux lines in an axial flux machine, but only displays the direction of flux lines from the North pole magnet to the South pole magnet. When the air gap is increased by moving the rotor away from the stator, the flux linkage between the stator and rotor decreases due to the flux being lost in the air gap. This causes the back EMF to reduce, and hence a reduction in maximum torque and an increase in maximum speed of the machine. However, increasing the air gap beyond a certain point leaves no active flux linkage between the stator and the rotor; thus the motor cannot produce any more torque. This is seen in Figure 5-11 where the K_e of the 8 windings machine tends to move to zero as air gap increases.

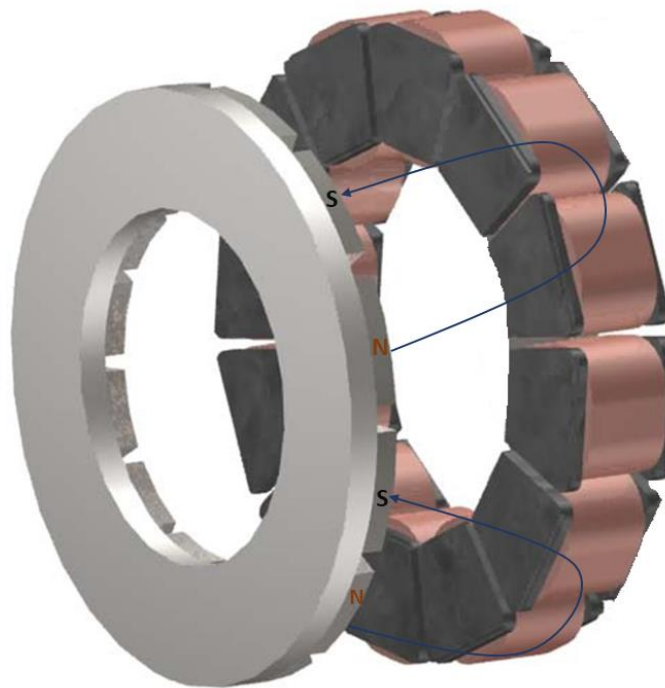


Figure 5-12 - Direction of magnetic flux lines for a single rotor motor (or equivalent of a fully actuated double rotor machine) ^[81]

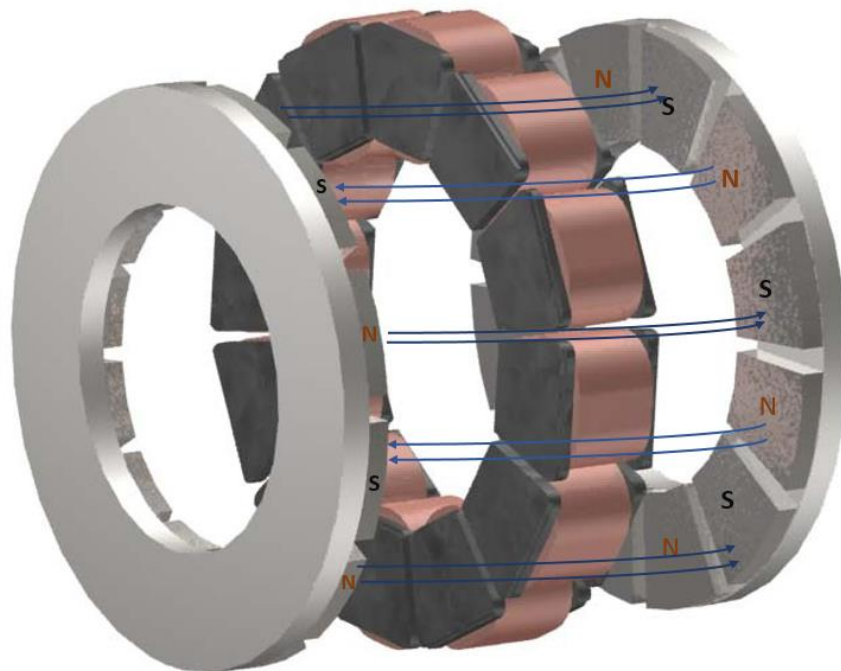


Figure 5-13 - Direction of magnetic flux lines (from North to South pole) for a dual rotor axial flux motor ^[81]

Figure 5-13 shows the direction of flux lines for a dual rotor axial flux motor (representation of a 72 windings machine) [95]. Again, this figure only displays the direction of flux lines from the North pole on one rotor to the South pole of the other rotor on the dual rotor machine. This is the designed flux path, which is the path of least reluctance. According to the industrial partner's design, only one rotor was actuated. On actuation of this one rotor, the flux linkage between the rotor and the stator is reduced. However, on actuation beyond a certain point, there is no more weakening of flux because the motor then behaves as a single rotor machine, and the direction of flux changes from what is shown in Figure 5-13 to the direction shown in Figure 5-12.

In other words, when one of the rotors is actuated too far away from the stator, the magnetic lines of force from the North pole of one rotor will follow the path of least reluctance to the South Pole of the same rotor, behaving like a single rotor standard axial flux motor. In this case, the motor will not reach a low enough K_e value as in the case of the 8 windings machine, but will plateau at a K_e value of an equivalent single rotor 72 windings machine. This is again evident in Figure 5-11, where for the 72 windings dual rotor machine, K_e is still away from zero, whilst for the 8 windings single rotor machine K_e tends to zero at high air gaps. This is the reason for observing little or no benefit from air gap actuation beyond 10mm on the Toro mule vehicle.

Due to the problems faced in inverter controller setup and single rotor actuation of the 72 windings machine, it was decided to proceed with the electric vehicle development without the Variable Air Gap technology. The minimum air gap of 1mm was chosen for this application and the motor was re-tested at 240A_{ac} capability to understand the potential of the motor (Figure 5-14 shows maximum torque power curve). It was seen that the motor produced a maximum of 51kW beyond which it is restricted by thermal restrictions of the magnets.

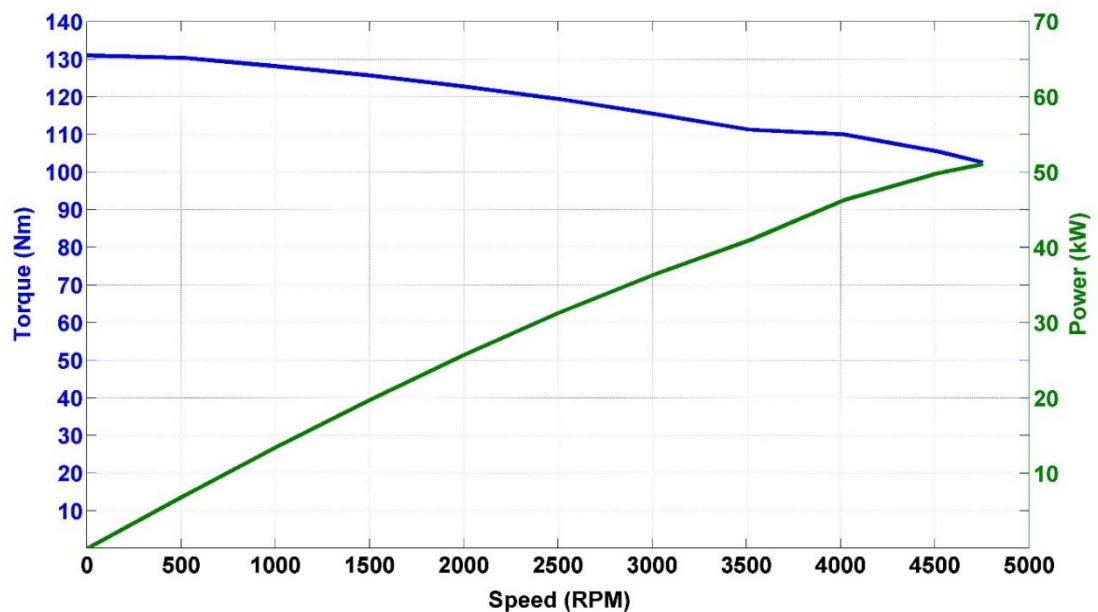


Figure 5-14 - Torque and power for the 72 windings dual rotor motor that was used in the development of the electric vehicle

Since the motor produced 51kW, and operated at a relatively high speed for its high voltage architecture (600V_{DC}), it was decided to use this 72 windings machine on the electric vehicle, without the variable air gap actuation system. This will be discussed in the next chapter.

5.3. Validation test rig development

A number of methods can be used to reduce the cost of development and manufacturing of electric motors. To further reduce the developmental cost, it was decided to build a completely automated test rig for the industrial partner to help achieve the low cost motor configuration. The test rig was aimed to be used for testing new machines as well as existing machines. This rig currently resides in the motor manufacturing plant in Weston-Super Mare. When the rig is not being used for developmental testing, it performs as an end of line test facility, ensuring that quality is maintained for the motors being manufactured. This test rig also ensures traceability, accountability and controllability of the motor manufacturing plant, people and processes.

Automating test rigs is an important aspect of the manufacturing process. Automation helps reduce the time an operator spends on performing a particular activity. It also has the advantage of reducing human error in the process. A planned and thoughtful approach is required in developing good automated hardware and software so that the scope of the tool is increased and it is user friendly [96].

It needs to be mentioned that the frame for the motors and batteries were supplied by the industrial partner, while the author was in charge of the development and specification of the software, measurement hardware and the integration of the system. Figure 5-15 shows the validation rig frame with two motors coupled together. The motor on the left acts as the dynamometer, while the motor on the bigger frame is the test motor. A quick release mechanism was also present on the frame so that motors can be mounted on and off the rig with minimum effort and time wastage.

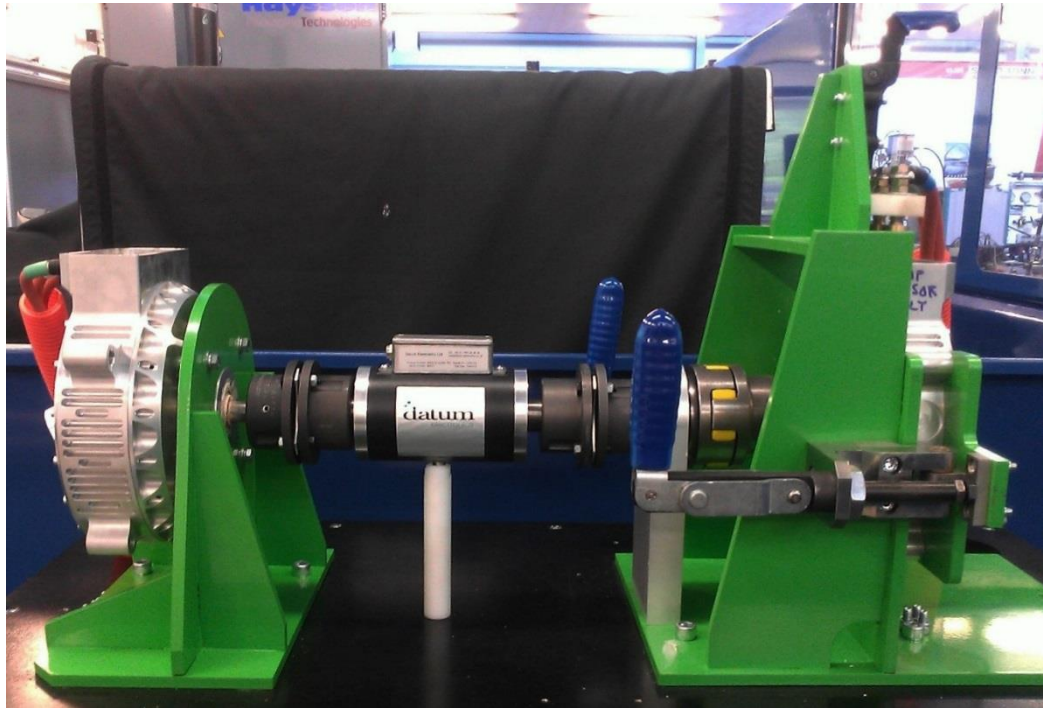


Figure 5-15 – Motor validation test rig frame with motors connected

This section of the chapter provides an insight into the development of measurement and communication hardware to be integrated into the rig, software to manually run and log data (similar to the arrangement at University of Bath), and the software to automate the entire test procedure. The three sections are explained separately.

5.3.1. Rig hardware

Hardware in this case refers to the control and measurements hardware used for the effective running of the validation rig. The dynamometer and test motor are coupled together with a Datum torque transducer in between them, which can measure torque and speed up to a range of 250Nm and 7000rpm respectively. Underneath the bed plate of the motor frames are Lithium phosphate battery packs adding up to 72V, connected to a battery management system and a battery charger. When both the motors are running, the dynamometer is in generating mode, whilst the test motor is in motoring mode. Energy circulation is ensured through the batteries while the

battery charger tops up for the losses encountered in the system. For safety purposes, the spinning motors are enclosed in a cage with poly methyl methacrylate protection (PMMA or plexiglass). The front and side doors can be slid open for access to the machines. Two safety locks on each door ensure that the motor can be powered ON only if the doors are closed and secured. Hardware and software emergency switches are also present in the case of an emergency. Figure 5-16 shows the schematic representation of the motor validation test rig.

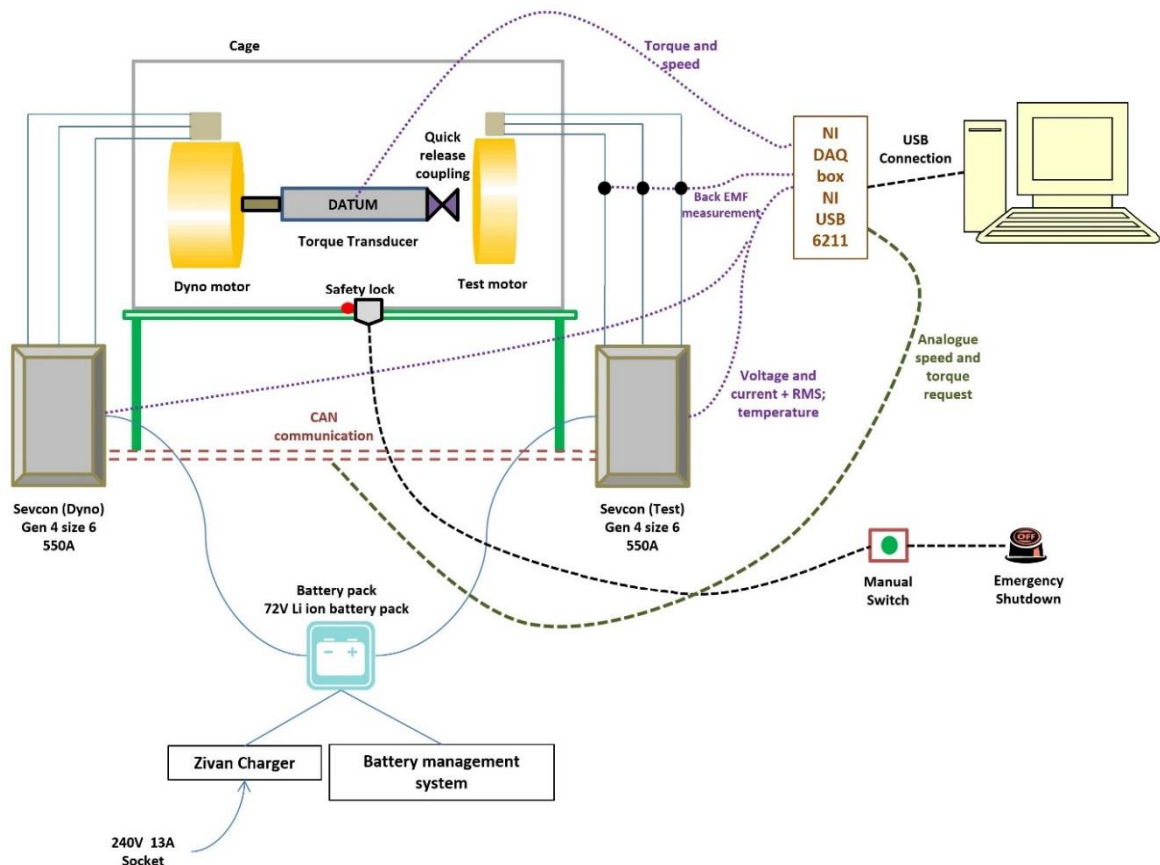


Figure 5-16 - Schematic representation of the motor validation test rig

The heart of the data acquisition (DAQ) capability of the validation rig is the National Instruments™ (NI) DAQ device. The NI 6211 DAQ box has on board analogue as well as digital input and output capabilities. This device was used to measure analogue inputs like speed, torque, back EMF, DC voltage, DC current and temperature for both dynamometer and test motors. Since some of these measurements were on high voltage systems, the incoming data was filtered and stepped down to protect the data acquisition device. Analogue outputs from the DAQ device included dynamometer and test motor throttle demands, while the digital signals were dynamometer and test motor controller 'Enable' switches and direction control. The NI DAQ was connected to a standalone PC that was equipped with NI Measurement and Communication tool to debug the device if and when the need arised. The circuit also provides necessary spike protection from any random high voltage/current signals that may damage the system.

5.3.2. Rig software

A software to control the rig was developed by the author using NI LabVIEW, which stands for Laboratory Virtual Instrument Engineering Workbench. It is a graphical programming language, developed by National Instruments™ to produce visual environments or test setups. The software was developed to provide similar functionalities to the rig that was present at the University of Bath. LabVIEW allows users to create Virtual Environments (VIs), each of which has three components - a block diagram, a front panel and a connector panel. The block diagram is the graphical source code, while the front panel is the graphical user interface.

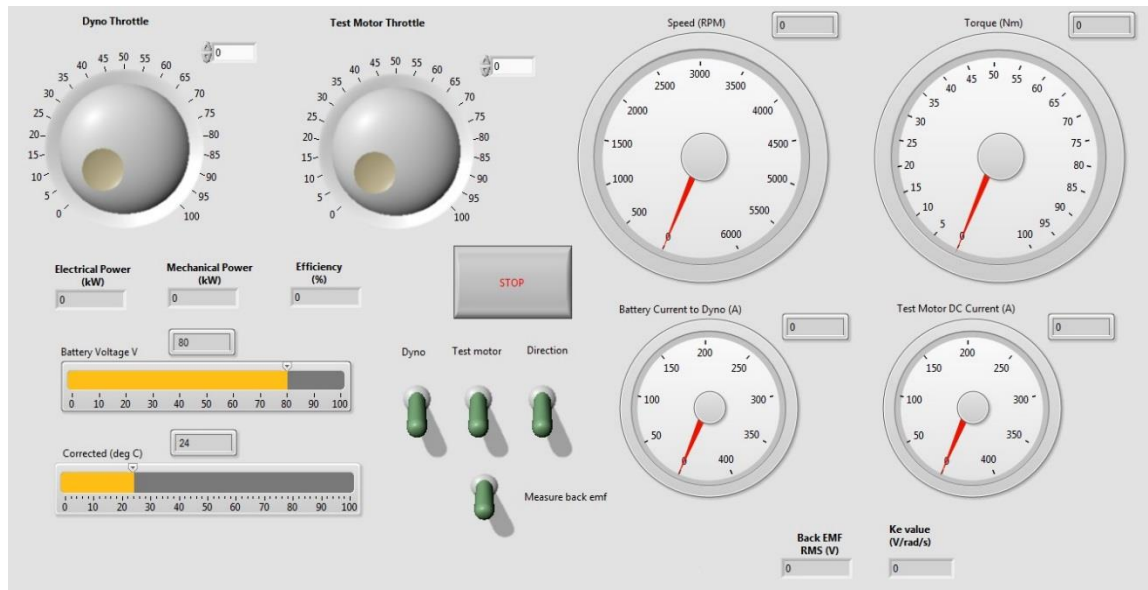


Figure 5-17 - Graphical User Interface for the test rig software

Figure 5-17 shows the graphical user interface developed for the control, test and measurement of the electric motors on the rig. The user has the capability to switch the dynamometer and test motor controllers ON and OFF using the switches in the centre of the screen. The third switch enables selection of forward or backward direction of the motor. The fourth switch is used to measure back EMF of the machine. This switch is provided to isolate and protect this high precision measurement system from high voltages/currents during normal running. Hence, this switch is to be ON only when the back EMF measurements are being taken (during open circuit conditions). Analogue outputs to the controller for dynamometer and test motor demand have a 0-100% scale on them, which represents a 0-10V DC output into the controller. Various analogue feedback provided to the user from the test rig include speed, torque, battery current to the dynamometer, battery current to the test motor, battery voltage and motor temperature. Other calculated parameters include K_e , electrical power, mechanical power and system efficiency.

5.3.3. Automated test procedure

The test rig developed was required to be flexible to perform manual tests to determine performance parameters of the motor, as well as execute automated routines to inspect quality and effectiveness of each new production motor. For this purpose, a completely automated testing algorithm was developed in LabVIEW. Finite state machine programming was used for this particular software development. Finite state machines is one of the oldest forms of modelling system behaviour and it is extensively used in software development [97]. The software is developed based on the different states the test rig is assumed to be in. States in this context refer to the different tests that need to be performed on the machine. At one point of time, the software can only be in one state. The state of operation changes from one to another when a finite number of conditions have been satisfied, or if the algorithm is triggered internally or externally to move to another state.

Figure 5-18 shows the different states involved in the state machine architecture used for the development of the automated validation test rig software. Each of the states is similar to the test procedure developed that was discussed earlier in the chapter, but here they are all completely automated. The software runs through the different tests defined, and determines whether or not the motor has passed the quality check based on data provided to it for comparison from other motors. At the end of the test, the software generates and prints a spreadsheet detailing the type of motor and the test conducted, and also highlights whether the motor has passed or failed.

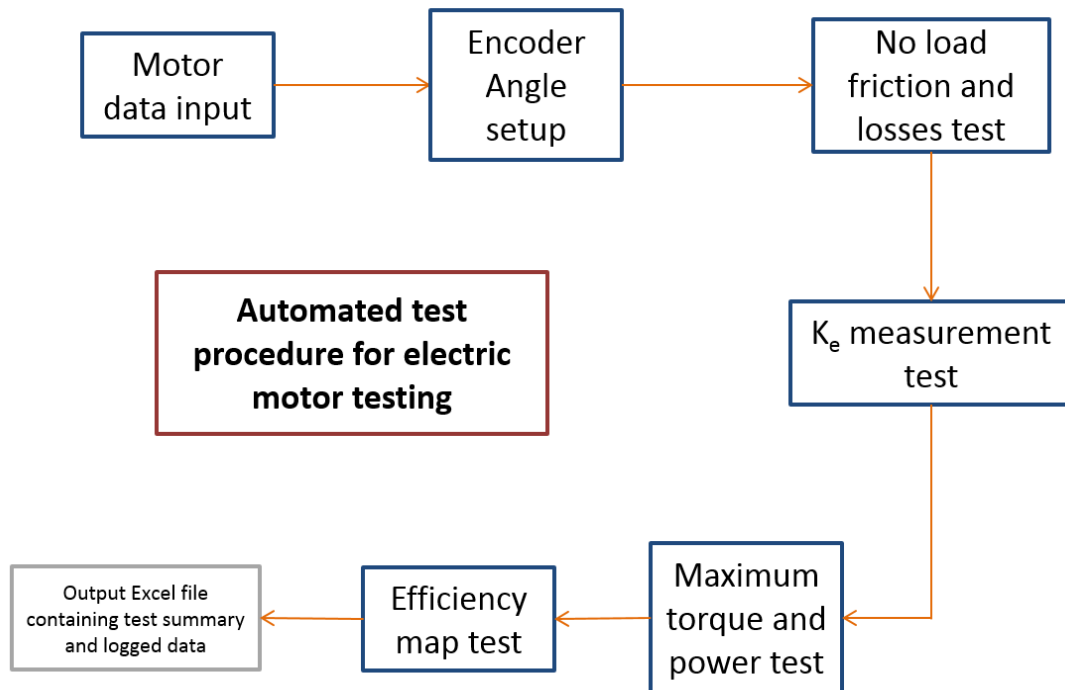


Figure 5-18 - Flow diagram of the different states involved in the automated test procedure for the motor validation rig

- Home screen

Figure 5-19 shows the start screen of the automated motor validation rig software. Tab structure is used to switch between different tests if needed. Switching between tabs is automatically controlled when the algorithm changes state, although manual control by the operator over-rides this if he/she needs to check data on the previous screen. The default run screen is the home screen, where the test technician is asked to enter details about the motor being tested. Various parameters like serial number, motor type, air gap etc. are saved to the final test report form generated by the software. The data generated for each motor tested is also saved based on the serial number of the motor, thus making the filename unique. Motor type is used to choose the type of motor being tested – say single 8 windings or double 72 windings etc. Depending on the motor type chosen, the software automatically selects the

appropriate motor data that this particular test motor needs to be compared against, to determine pass or fail criteria.

When in the home screen, the algorithm is in the 'Wait State', where it waits for the user to complete the data input process. Since the LabVIEW code of the algorithm is too large, a small section of the code can be viewed in Appendix A of this thesis. The operator has the opportunity to check if the motor and rig are secure and there are no faults on the safety circuits. Once the operator has entered all the relevant information about the motor, and the hardware is secure, he/she presses the 'Start test sequence'. On selecting this button, the algorithm moves to the next state, which is the 'Encoder angle state'. On the main screen that is visible to the user, the tab changes from the 'Test details' tab to the 'No load test' tab.

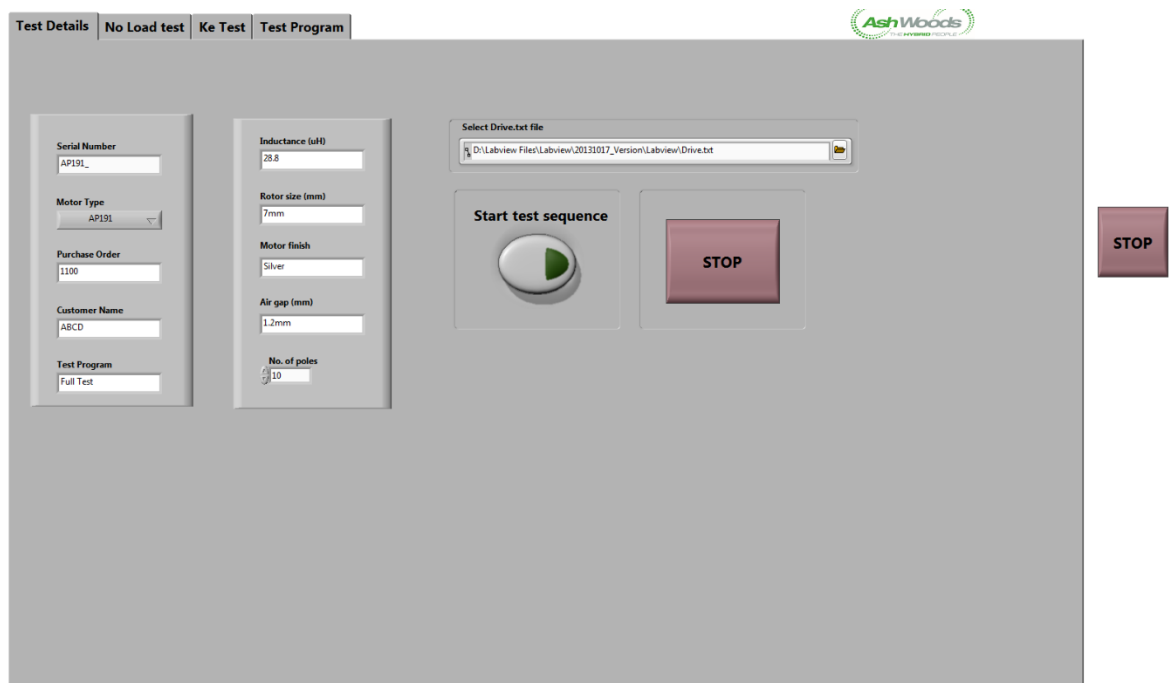


Figure 5-19 - Start screen of the validation test rig automated software

- Encoder angle test

The next stage is the encoder angle setup, which is the last step of operation for the test technician. The GUI tab moves to the 'No load test' tab, where two separate tests share the same screen. Here the encoder angle on the test motor is adjusted so as to obtain maximum speed of the motor for a particular 'throttle' demand. The encoder angle is the position of the encoder with respect to the 'Top dead centre' of the rotor, defined by the manufacturer. This provides an indication to the position of the magnetic rotor with respect to the stator.

In this state, the test motor controller is switched ON and the direction is set to forward. The technician is allowed to select a test motor throttle position of his/her choice to tune the encoder optimally. Once the encoder has been satisfactorily tuned, the engineer presses the 'Encoder angle set complete' button which spins the motor down automatically and switches the controllers OFF. The algorithm then moves to the next stage, which is the 'No load test' stage. Red lights on the GUI indicate the current state of operation.

- No load test

This state is where the electrical and frictional losses in the motor are measured. In other words, the torque required to spin the motor at different speeds is observed in this test. Here the dynamometer controller is automatically switched ON and spun through a set of pre-defined speeds. The pre-defined speeds can be changed on the main screen if needed (dynamometer throttle is made available on screen). At each speed set point, the torque value is averaged and saved. Figure 5-20 shows the no load test run GUI.

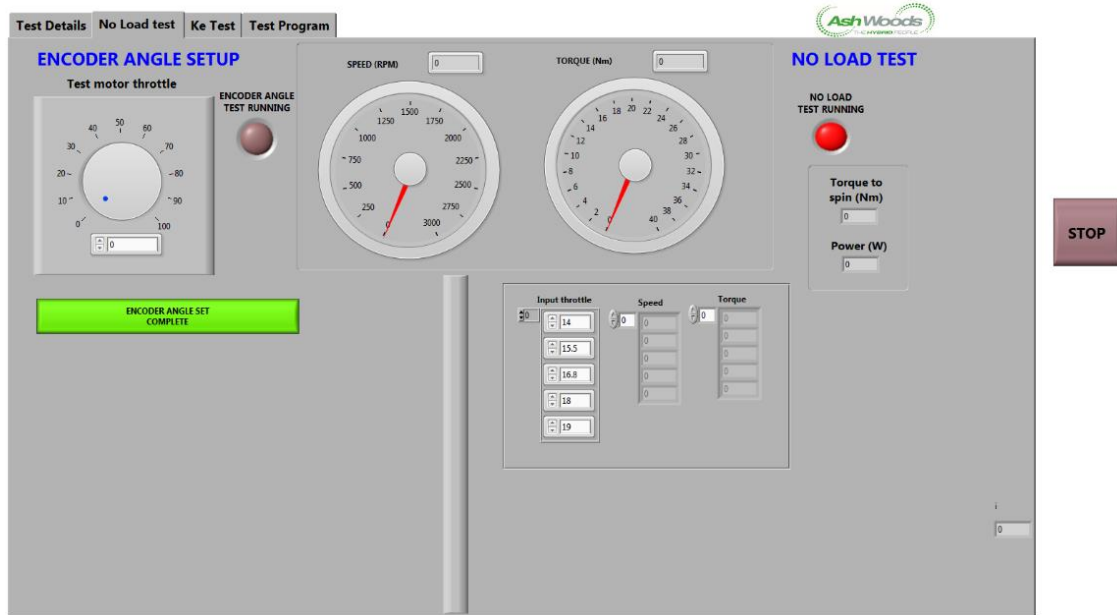


Figure 5-20 - No load test run screen on the validation test rig software

- Ke test

On completion of the no load test, the tab control moves to the next tab which reads 'Ke test'. This screen is again shared between two tests – Ke test and the peak torque test. The state machine logic now moves ahead to the Ke test logic where the motor back EMF is measured and the back EMF constant is calculated. Here, the dynamometer controller is turned ON and run through a set of pre-defined speeds. The back EMF measurement switch is also enabled so as to read the open circuit voltage of the motor when spun at different speeds. Since the Ke value is a very small number, highly precise measurements need to be taken. Hence the Ke value measurement is repeated three times over the same speed range and the measurements are averaged to calculate the final Ke value. At the end of this test, the state machine moves to the 'peak torque test' stage.

- Peak torque test

For this test, both the dynamometer and test motor controllers are switched ON automatically. The dynamometer is set to pre-defined speed steps, while the test motor throttle is set to 100% (both values can be changed on screen if required). When speed and torque at each point has steadied, torque is measured and averaged over 5 seconds and saved. Then the same procedure repeats itself for the next speed.

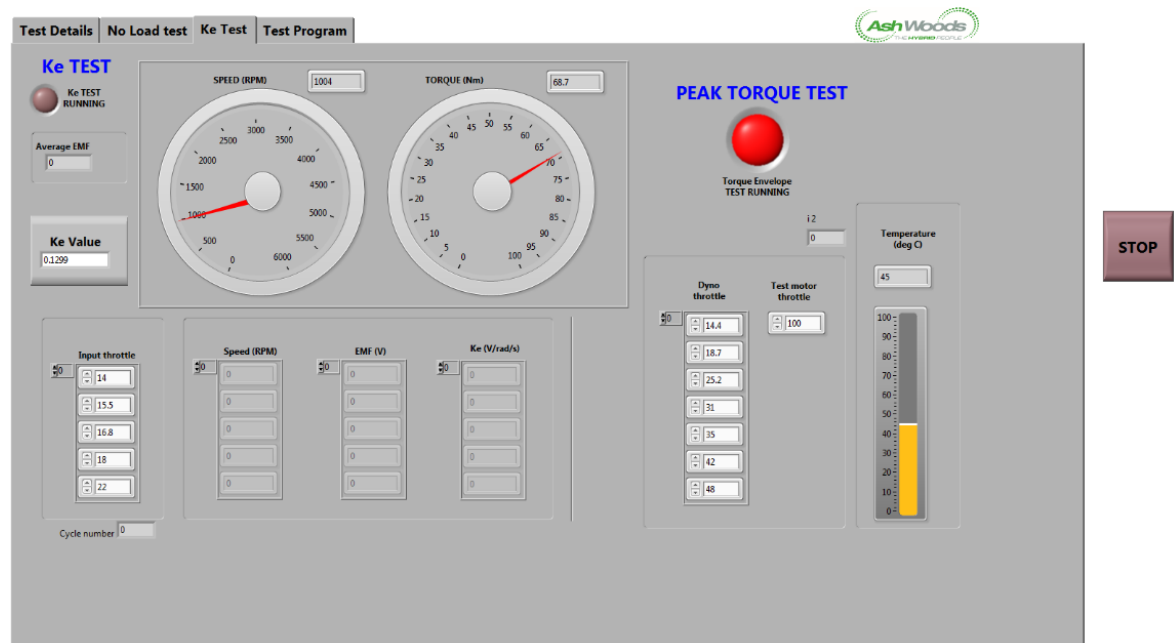


Figure 5-21 - Peak torque test run screen for the validation rig

Figure 5-21 shows the peak torque test GUI in operation. Motor temperature is monitored during this test as a high current of $550A_{ac}$ is applied through the stator coils. If the motor overheats, both motors are brought down to zero speed and the test is paused till the motor cools down, after which the test is resumed. At the end of the test, both controllers are switched OFF and the algorithm moves to the 'Main test program'.

- Main test program

The main test program is the one of the most important stages in the test procedure. The tab moves to the final screen called the 'Test program'. It is here that the motor is tested for its performance and efficiency at different speed and load points. Compared to the previous screens, it can be seen in Figure 5-22 that there is no control for either of the motors on this page. This is because the motor runs through pre-defined speed and load points read from a comparison data file. The torque and efficiency points to be compared against (and their respective tolerances) are also present in this file. Each of the comparison files has to be populated every time a new type of motor has to be tested.

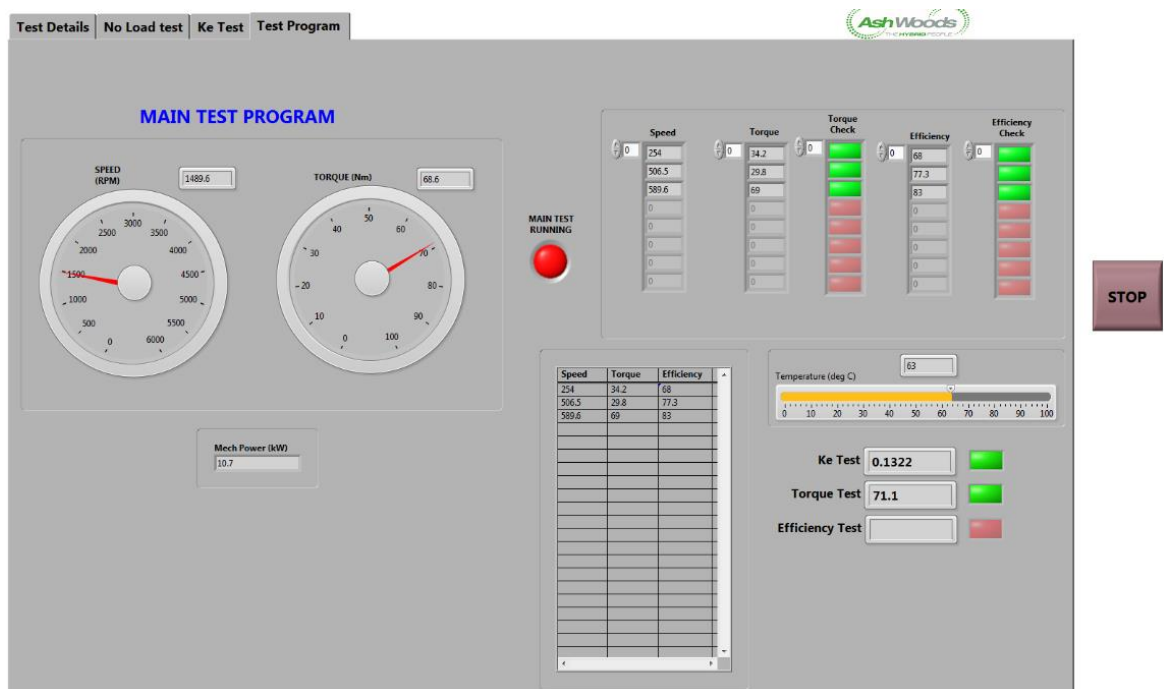


Figure 5-22 - Main test program run screen on the validation rig software

Both the motor controllers are switched ON and the first speed and load point are selected from the comparison file. The algorithm waits at each point till the speed and torque values have steadied before averaging the values for a period of 5

seconds. This data is stored and compared against values seen in the comparison files. This procedure runs through all the set points specified in the comparison file. The comparison file also specifies the tolerance limit for each parameter. It is here that the measured K_e and maximum torque values are compared to those specified in the comparison file.

Some values in Figure 5-22 are greyed out or 'greyed' red because the algorithm is in the middle of a test run when the screenshot was captured; these values had not yet been populated. Once the test is complete, both motors are spun down to a halt and the controllers are switched OFF. An excel spreadsheet with motor details, test results and plots in different tabs is saved in the name of the serial number of the test motor. The first sheet is printed and highlights the details of the motor and the tests performed on it. Details on whether or not it has passed the three important tests is also mentioned in the summary sheet. The screen then moves back to the main 'Test details' tab. The operator can now remove the motor and test the next motor in line. If the test rig has to be used for research and development testing, the software can be closed and the manual run software explained in the previous section can be used.

5.3.4. Benefits of test automation

The validation test rig helps to automate research and development testing that would otherwise require an operator to perform the tests. Reduction in operator costs helps in reducing labour costs of the development of the motor. Nevertheless, the most significant use of the validation rig was in ensuring quality and reliability of the motors being manufactured at the motor manufacturing plant.

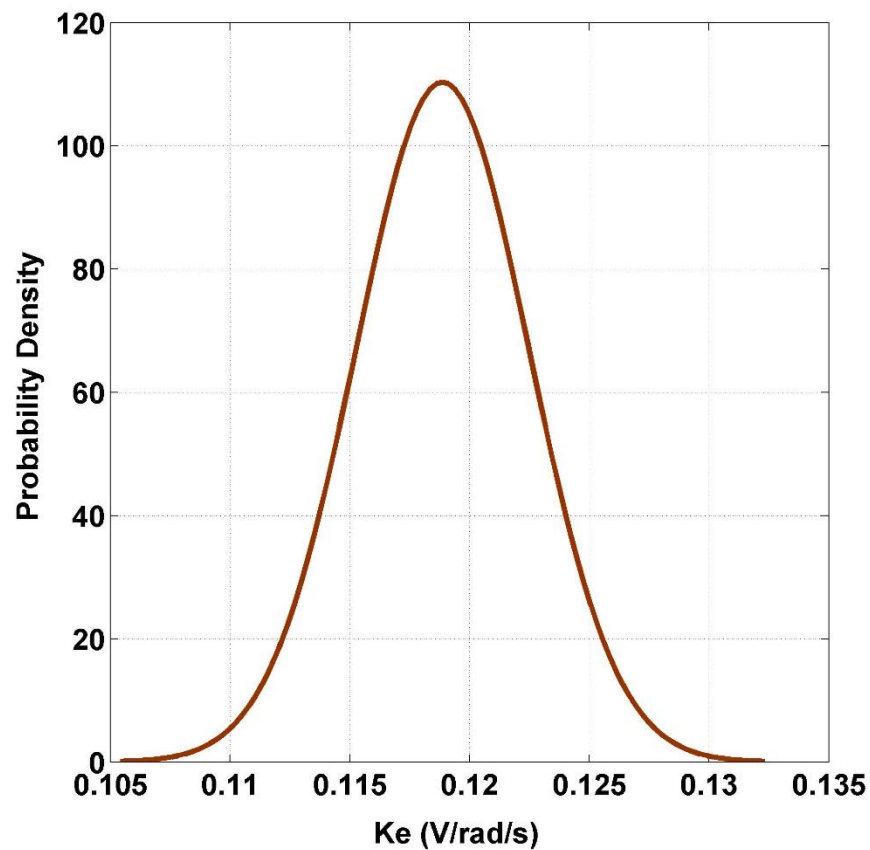


Figure 5-23 - Probability density of K_e for motors tested using the validation rig

The automated test procedure gave an indication to the repeatability and quality control of the motor produced. At the motor manufacturing plant, once a new motor is assembled, it is fitted onto the validation rig, where it runs through a series of automated tests. The repeatability of each test and the data collected is an important aspect of quality control. The K_e value being one of the most crucial parameters in motor production is the most important value that needs to be repeatable when tested. The mean of the K_e value of 40 tests at the motor manufacturing plant was 0.118V/rad/s. Figure 5-23 shows the probability density of K_e for the motors tested. This also shows that the validation rig provided an opportunity to ensure traceability, controllability, quality and repeatability of manufacturing and testing within the manufacturer's tolerance, which is an essential part of any product development.

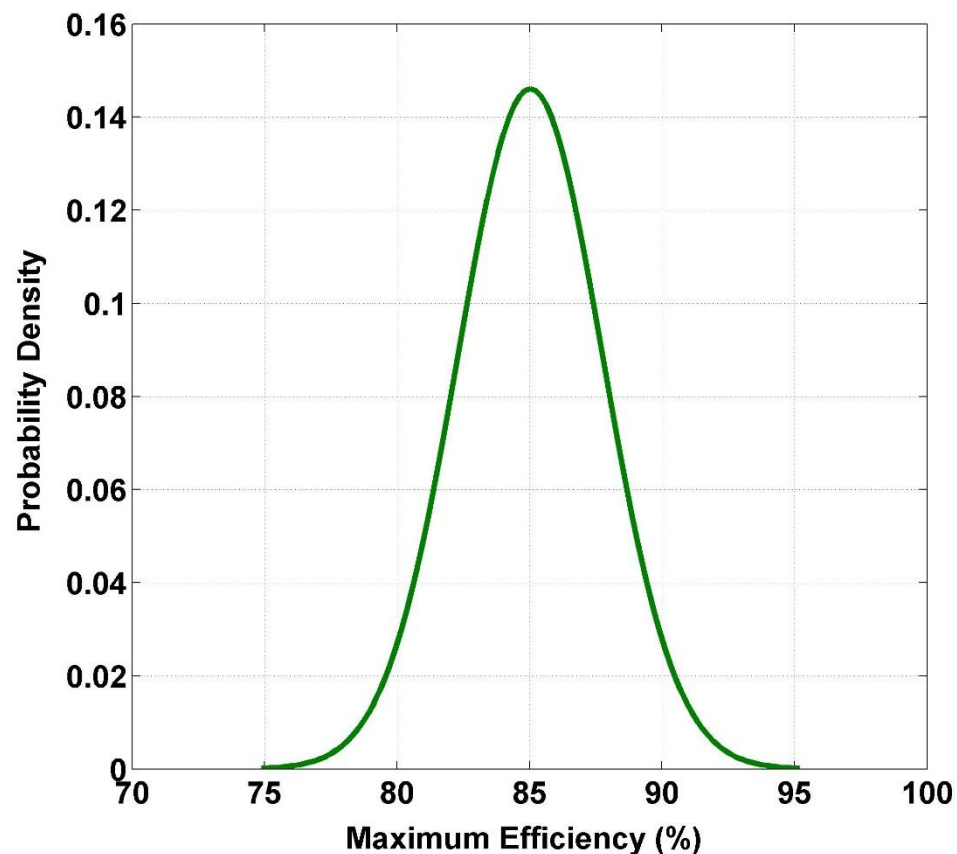


Figure 5-24 - Probability density of maximum efficiency of different motors tested on the validation rig

Figure 5-24 shows the probability density of the maximum efficiency of the system for different motors tested on the validation test rig. The mean of all the efficiencies was 85.02%. This efficiency value is lower than the actual efficiency of the motor measured at the University of Bath test facility, because on the validation rig, the efficiency measurement includes the motor and the controller. Efficiency is calculated by dividing the output mechanical power by the input DC electrical power into the controller. A 10% acceptance tolerance from the mean of the maximum efficiency was set by the industrial partner. The validation rig thus proved useful for research and developmental testing, as well as provided a means of ensuring acceptance levels on the newly built motors at the manufacturing plant.

5.4. Summary

This section discusses the work that the author was involved with regards to testing and development of electric motors. Automotive applications require electric machines that are low in cost and weight, but need fairly high performance envelopes. For this purpose it was required to effectively test electric motors and achieve the highest possible performance from the machines. Since the automotive industry is fairly new in using axial flux electric motors, new test procedures needed to be developed for this application, keeping in mind the manufacturer's requirement as well.

Based on the testing, development and calibration of a 15kW machine currently in use on several hybrid vans, the test procedures were applied to a higher winding 51kW electric motor. To further reduce the cost of the electric vehicle application the motor was intended for, a new Variable Air Gap (VAG) technology was attempted to try and abstain from the use of a gearbox. Increasing the air gap between the stator and rotor decreases the flux linkage between the stator and the rotor, thereby decreasing the back EMF of the machine, which would allow it to achieve a higher speed. The initial trials of the concept indicated a 45% increase in the maximum speed of the machine. However, the final design incorporated a mechanism that allowed only one rotor to be actuated, which did not provide the expected level of field weakening. This is due to the dual rotor machine acting as a single rotor machine on increasing the air gap beyond a critical limit of 15mm. On the basis of the results observed, it was decided to use the 51kW motor without variable air gap technology for the development of the electric vehicle.

This chapter also discussed the development of a fully flexible test rig for the research and development testing of electric motors. The test rig had similar capabilities of operation compared to the facility at the University of Bath. Flexibility to run the rig in manual control mode, as well as in a fully automated condition was one of the most significant features of the rig. The rig is beneficial for research testing as well as validation testing to detect performance drifts of newly built machines. The rig now resides in the motor manufacturing plant to ensure traceability, controllability, and accountability of the manufacturing process and also reliability of the motors. The test rig also helps save an estimated £44,000 a year in labour costs for motor production with its automated testing capabilities (at a rate of production of 2300 motors a year).

The main reason for the electric motor testing and calibration to be part of this thesis was to assist the industrial partner in the development of a fully electric vehicle. This vehicle was intended to be used for the testing of the electric version of the driver advisory tool. The 51kW axial flux electric motor that was tested and calibrated was aimed to be fitted onto a fully electric vehicle, which would help identify the benefit of changing driver behaviour to increase the range of the vehicle. Existing literature on improving driver behaviour has not been extended to electric vehicles, and this is further explained in the next chapter.

Chapter 6 - Electric vehicle testing

This chapter discusses the development of the electric version of the driver behaviour improvement device and its effect on battery state of charge and vehicle range. The electric motor discussed in the previous chapter was used in conjunction with the modified version of the driver advisory tool for electric vehicles, to understand benefits of the system in helping increase the range of the vehicle.

6.1. Electric version of the driver advisory tool

The impact of driver behaviour improvement on improving fuel consumption in vehicles was evident from the fleet trials experiments conducted on the different fleets of vehicles. It was decided to develop an electric version of the device based on the same platform, with the intention of helping drivers consume less amount of energy when driving. The lower the energy consumption of the vehicle from the battery pack, the greater the range of the vehicle. Range anxiety is a common cause of concern that inhibits people from choosing electric vehicle over conventional IC engine powered vehicles [6]. The aim of the electric version of the driver advisory tool is to help achieve more range on the electric vehicle by reducing the electrical draw on the battery.

The electric version of the driver behaviour improvement device is similar to the IC engine type, apart from the fact that it also takes into account deceleration of the vehicle, to help the driver in improving his/her braking style. The system relies on fewer parameters compared to the previous version. Here, only vehicle speed is used to determine aggressivity; as most electric vehicles are automatic, they do not require manual shifting of gears by the driver. Pedal position is used to avoid penalising drivers for performing certain manoeuvres like overtaking, acceleration from a slip road onto a motorway etc. Other important parameters like DC voltage, DC current and battery State of Charge (SOC) are logged for statistics calculation. Similar to the IC engine version of the tool, the driver will receive two warnings and a violation if aggressivity is observed for positive acceleration. For high values of negative acceleration, the driver is asked to improve his/her braking style. No warnings or

violations are recorded for deceleration events, as braking action has a direct impact on the safety of the vehicle and the driver. Thus, it was only conveyed to the driver to try and improve braking by anticipating traffic conditions, and not by enforcing the required rate of braking (for energy regeneration) at every deceleration event.

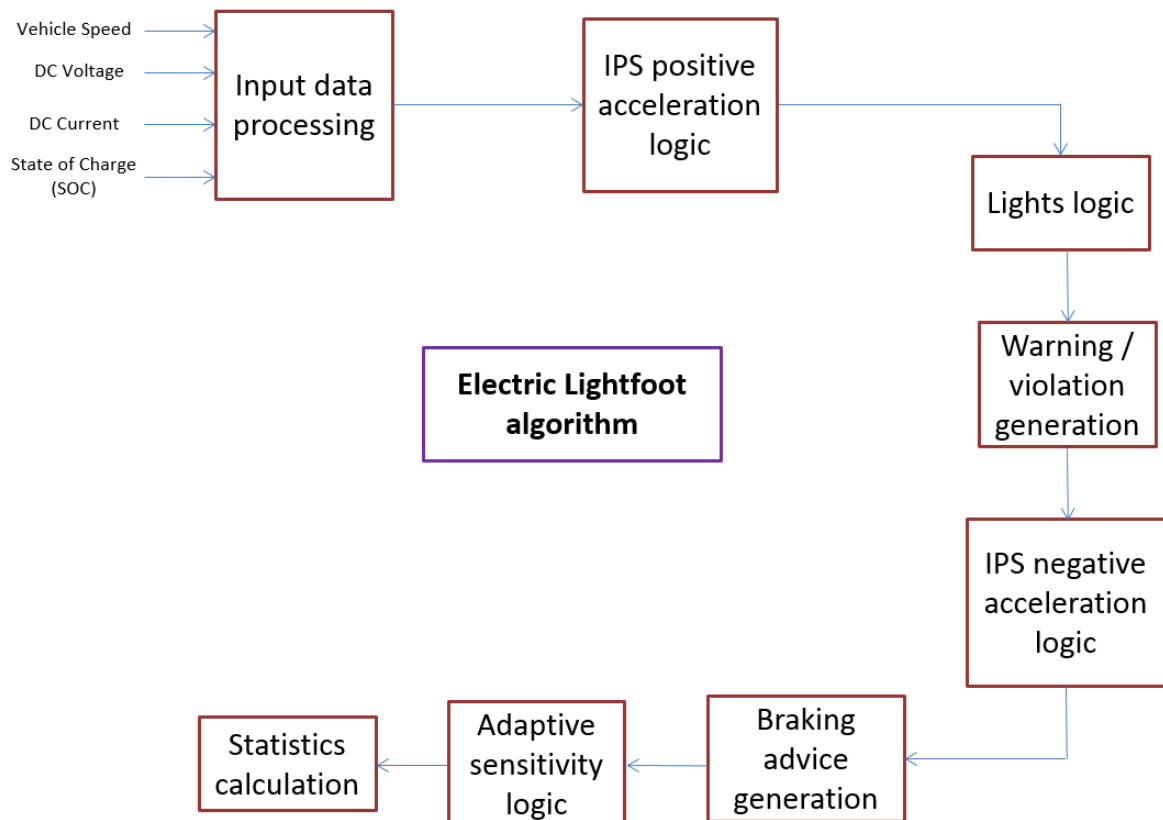


Figure 6-1 - Schematic representation of the algorithm of the driver advisory tool for electric vehicles

Figure 6-1 shows the schematic representation of algorithm of the electric version of the driver advisory tool. The biggest difference between this system and the previously explained versions is in the input parameters. DC voltage, DC current and battery SOC are used to determine the instantaneous draw on the battery of the vehicle. As explained earlier, the driver is provided warnings for harsh acceleration events, while he/she is only provided advice for braking events. The other significant difference from the IC engine version of the advisory tool is the presence of an

adaptive sensitivity control of the system. On this version of the device, neither the fleet manager nor the customer needs to worry about the sensitivity control of the system. When the device is first fitted onto the vehicle, it is set to the lowest level of sensitivity by default. The system records the number of warnings and violations the driver receives during the driving of the vehicle, and calculates the number of stops per kilometre of running. When this value is lower than a pre-determined value, the sensitivity control is increased to the next level. If the system sees a driver change (sudden change in the number of stops per kilometre), the sensitivity is adjusted accordingly so that the driver is given the opportunity to get familiarised with the device.

6.2. Electric vehicle and driver advisory tool testing

Due to the lack of large fleets of electric vehicles available for trialling the device, the electric version of the advisory tool was tested on the fully electric vehicle developed by the industrial partner on the project. The vehicle was based on the Citroen Nemo model, with its engine and existing drivetrain replaced with the axial flux electric motor explained in Chapter 5. Power is transmitted to the front wheels using a reduction speed gearbox and a differential unit on the front axle of the vehicle.

Table 6-1 shows the specification of the electric vehicle shown in Figure 6-3, developed for the testing of the electric version of the advisory tool. The vehicle weighs just over 1.2 tonnes, which is higher than the kerb weight of the original vehicle – 1090kg [98]. Even though the electric motor weighs only a fraction of the engine, the batteries add significant weight to the vehicle.

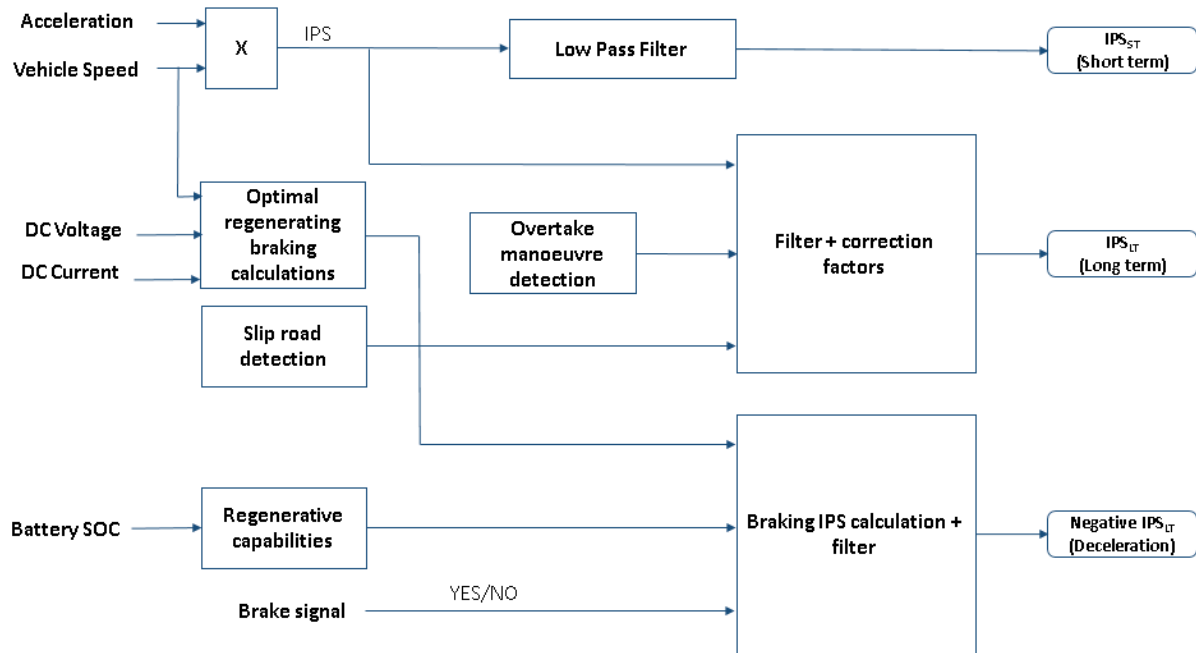


Figure 6-2 - Representation of the IPS logic used in the driver advisory tool algorithm for electric vehicles

Figure 6-2 shows the schematic representation of the IPS logic used in the electric vehicle version of the driver advisory tool. It can be seen that the fundamental aggressivity calculation logic of the system is similar to the IC engine version of the device. However, an additional novelty of the system was the inclusion of negative (deceleration) IPS, to encourage drivers to brake more gently and effectively to regenerate energy. The deceleration IPS calculations had filters and correction factors to determine the optimum braking profile based on the speed of the vehicle and the percentage of brake pedal usage. Also, if the battery state of charge was low, the driver would be encouraged to brake more effectively to regenerate more than what he/she would be told when the battery state of charge was at its maximum. This device is an extension of the research into driver behaviour improvement to reduce energy usage. It has added to existing knowledge in the field in terms of its novelty. Currently there is no research or literature focussing on improving driving style to increase the range of the vehicle.

Table 6-1 - Specification of the electric vehicle tested

Vehicle Model	Citroen Nemo modified Electric
Fuel type	Fully electric
Engine	Axial flux dual rotor 72 windings motor (Liquid cooled)
Maximum power	45 kW
Battery pack	Lithium iron phosphate 96V, 180Ah



Figure 6-3 - The Nemo vehicle converted to a fully electric vehicle used for testing of the driver advisory tool

Unlike the field trial experiments conducted on the fleets of vans, time and cost restrictions meant that the electric version of the advisory tool could only be tested on the Nemo electric vehicle. The vehicle was tested over a period of two months, where over 500km worth of data was collected. The advisory tool was switched ON for the last three weeks of the test period. It was seen that the drivers were able to achieve up to 32% increase in distance travelled per unit consumption of DC energy.

The increase in distance travelled during the interface trial of the advisory tool was a result of two separate events. One is due to the reduction in the harsh accelerations, which reduces the rate of current draw on the battery, while the other is due to the increase in regenerative braking of the vehicle, where the energy during braking events is converted and stored in the batteries as useful energy, rather than being wasted as heat. The former is slightly more complicated to understand, as normally the power consumed to achieve a certain speed on a vehicle is the same irrespective of whether it is done in a short or long period of time. However, the remaining available capacity of the battery reduces at a higher rate when the rate of energy discharge (current draw) from the battery is increased. This relation is represented by Peukert's law, which expresses the remaining capacity of the battery as a function of the rate of current draw from it [99].

$$C = I^k * t \quad - (5)$$

where, C is the capacity of the battery when discharged at a rate of 1 Amp (expressed in Ah), I is the current drawn from the battery, k is the Peukert's constant (1.3 for Lithium ion batteries), and t is the amount of time for which the battery will operate before being completely discharged [100].

According to this law, the higher the rate of current draw on the battery, the lesser is the remaining capacity of the battery. However, it needs to be mentioned that although Peukert's number provides an indication of the remaining capacity of the battery, it does not provide an accurate estimation of the actual remaining capacity. Other factors like ambient temperature, cycle life, rate of current draw etc. also have an implication on the remaining capacity of the battery [99].

Regenerative braking on the other hand is a very useful mechanism in electric vehicles to recover energy that would otherwise be wasted as heat in normal vehicles. The amount of energy recovered is dependent on the deceleration rate and the duration of the deceleration event. The regenerative braking strategy is dependent on the drivers brake input, which is converted to a brake input to the motor controller. If the driver demands a braking force higher than that can be provided by the electric motor, the friction brakes on the wheels compliment the regenerative braking system to provide the required deceleration.

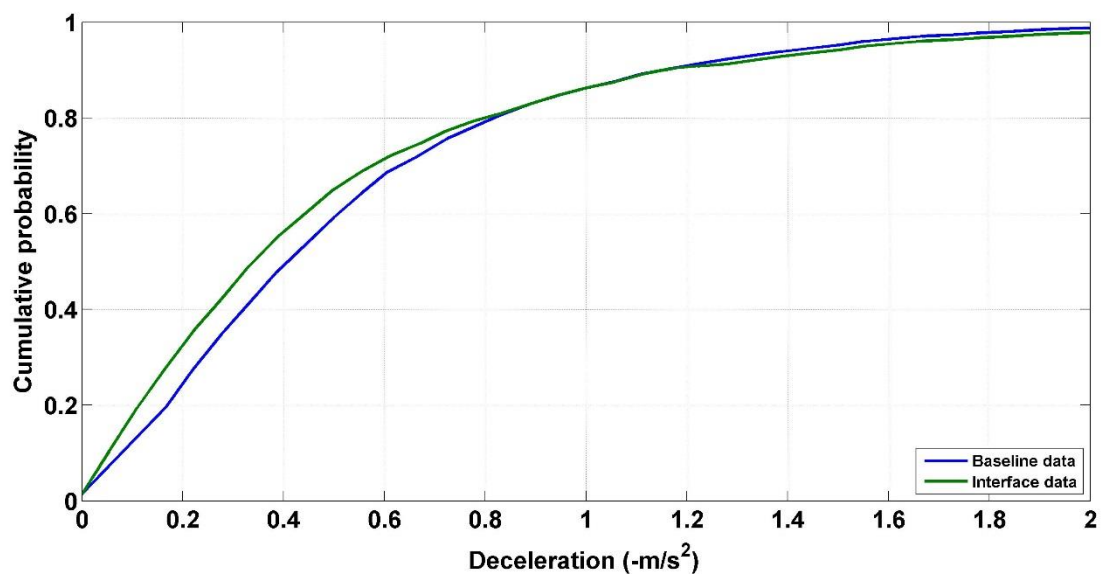


Figure 6-4 - Cumulative probability of the deceleration values for the baseline and interface trials of the driver advisory tool

During the baseline testing of the Nemo electric vehicle, drivers effectively regenerated 43.6% of the total energy used for traction purposes, while for the interface trial they managed to recover 52.8% of the total tractive energy. This additional energy recovered is one of the reasons for the increased range of the vehicle during the interface trial. This increased braking is a direct effect of the

braking advice given to the drivers. Figure 6-4 shows the cumulative probability of the deceleration events for the baseline and interface trials of the driver advisory tool. A shift towards the left of the cumulative distribution during low values of deceleration shows drivers decelerating at a lower rate during the interface trial when compared to the baseline trial. This is due to drivers braking gently (with lower rates of deceleration) when compared to their baseline driving style. It needs to be mentioned that using the driver advisory tool on conventional engine vehicles, drivers were seen to have already improved their braking style as a result of adopting a much calmer driving style. The electric version of the device only attempts to maximise this improvement, when and wherever possible.

Unlike the case of the IC engine version, where the advisory tool was critical in moving the operating point of the engine to an efficient region, for the electric version, an increase in range was possible due to a combination of reduced inertial power surrogate and the capability to recover energy that would otherwise be wasted. The vehicle achieved an average electrical power consumption of 14.24 km/kWh during the interface trial, when compared to 10.87 km/kWh during the baseline trial phase. As in the case of the IC engine version of the device, the electric version also has more potential to save electrical energy in urban driving conditions, where there is more opportunity to reduce harsh acceleration and deceleration, and also the potential to maximise energy recovered during braking, using the kinetic energy recovery system.

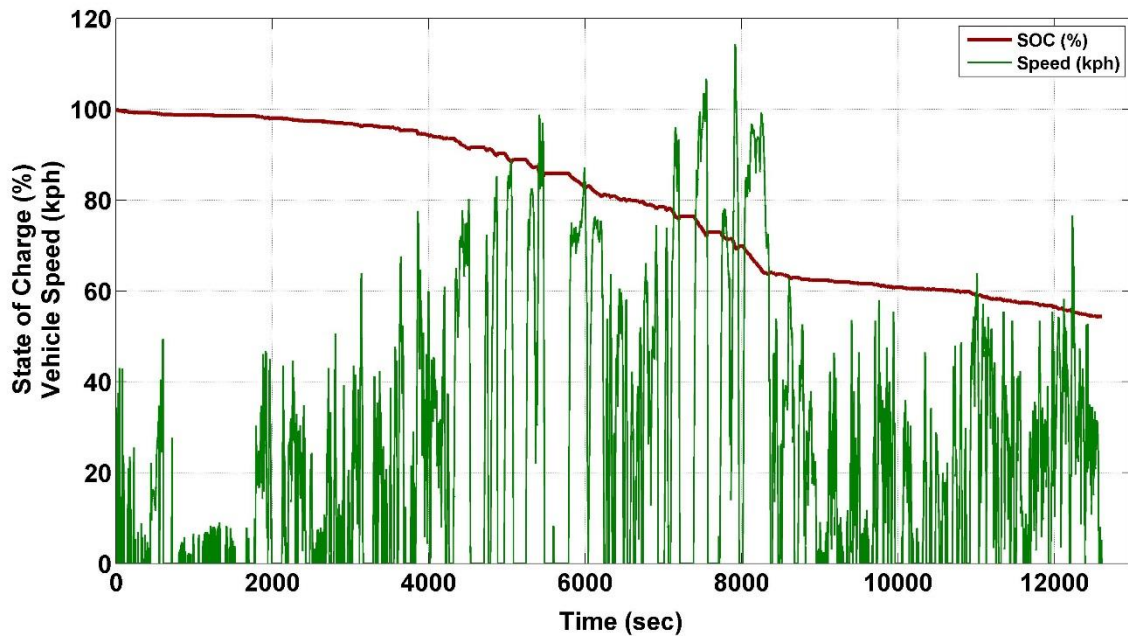


Figure 6-5 - Battery SOC and vehicle speed for one full charge run of the Nemo electric vehicle

Figure 6-5 shows the battery SOC and vehicle speed for a 3.5 hour long drive profile for the electric vehicle. This journey did not take place in one go. There are 'idling' gaps in the vehicle where the motor is not spinning, but there is always a small amount of energy being used to power ancillary components in the vehicle. It can also be seen that urban driving (under 60 kph) has lesser impact on the SOC reduction, when compared to high speed driving, where higher power is required to keep the vehicle moving. Here, the current draw on the battery is higher, which would further reduce the remaining capacity of the battery.

Since the electric version of the device was only trialled by two drivers on one vehicle (due to time and money constraints), it was decided to create a simple electric vehicle model and use the initial field trial data collected for IC engine version of the tool, to simulate potential benefits in extending the range of the electric vehicle.

6.3. Simulation of electric vehicle

It was important to understand the benefits of using the driver advisory tool on inputs from different driver characteristics. Due to time and money constraints, it was decided to develop a simple model of the Nemo electric vehicle to use vehicle speed profiles collected from different vans during the initial field trial experiments. The model was developed in the Simulink® environment with the SimPowerSystems™ library. SimPowerSystems™ provides component libraries and tools for modelling, analysing and simulating electrical systems, which can then be used to test system level performance [101]. This meant only the key driving characteristics like vehicle speed and pedal position were required as inputs to the model, while a battery model from the library was used to simulate the battery of the vehicle to determine the voltage, current and SOC.

Figure 6-6 shows the Simulink® model used for the simulation of the electric vehicle. A parameter file containing vehicle information like kerb weight, frontal area, rolling resistance etc. was used to run the simulation. Vehicle speed and pedal position from the data collected was fed into the model which was converted to useful values in the input processing block. Acceleration over a period of 0.5 seconds was also calculated, which would later be used for the determination of tractive effort. Tractive force of the vehicle is calculated in the vehicle dynamics section of the model, where two components of tractive force – vehicle inertia and aerodynamic load are calculated separately. Force required to overcome inertia is a function of vehicle acceleration and the mass of the vehicle, while the aerodynamic drag is a function of the rolling resistance of the tyres, mass, square of the speed and frontal area of the vehicle.

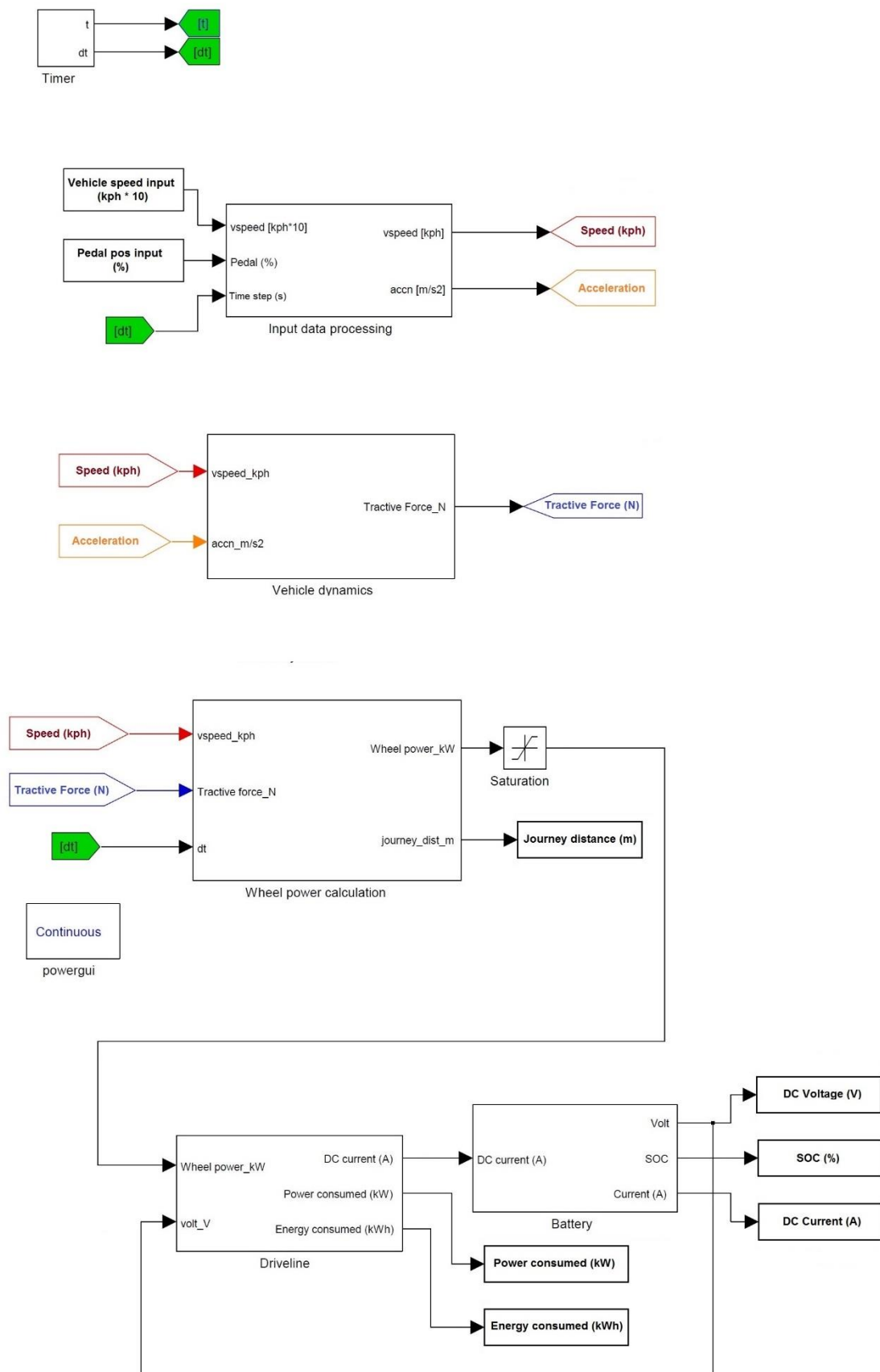


Figure 6-6 - Electric vehicle system model used for simulation

After the tractive force required to move the vehicle is calculated, the tractive power at the wheels is calculated to determine the required torque at the wheels. The driveline block is used to calculate the motor torque required, by assuming a driveline efficiency. The motor efficiency map is used to determine the motor efficiency at a particular speed and torque, while the Sevcon controller efficiency map is used to determine the inverter efficiency at each speed and load point. Application of these two efficiency points provides the DC power required from the battery, which when divided by the battery voltage, provides the current demand from the battery. An electrical battery source rated to 96V nominal and 180Ah capacity from the SimPowerSystems™ library was used in conjunction with a Controlled Current Source to simulate the battery pack of the vehicle. The chosen outputs for the system were battery voltage, current and state of charge. Data from baseline and interface trials of the IC engine version of the tool was used to simulate the electric vehicle model.

6.3.1. Results and discussion

Speed profiles from seven of the initial fifteen vehicles representing over 3500km worth of driving data was simulated using the electric vehicle model. The data was split assuming that each trip now consists of a discharge of 80% of the battery's available power. In other words, it was assumed that each trip consisted of a discharge of battery from 100% SOC to 20% SOC. This means that the battery is never completely depleted of charge, as this process is considered unhealthy for the battery. The pedal position data was only used in the advisory tool algorithm to determine when the driver would receive warnings and violations. This is similar to the IC engine case and hence is not discussed here again.

Table 6-2 - Simulation results of the benefits of electric version of the driver advisory tool

	Baseline trial simulation				Interface trial simulation				
Driver no.	Distance travelled on a single full charge (km)	Tractive energy (kWh)	Regenerated energy (kWh)	Net energy used (kWh)	Distance travelled on a single full charge (km)	Tractive energy (kWh)	Regenerated energy (kWh)	Net energy used (kWh)	Increase in range of the vehicle (%)
1	124.3	18.6	4.2	14.4	139.7	18.9	4.4	14.5	12.45
2	177.7	28.7	14.6	14.1	191.7	28.2	14	14.2	7.88
3	82.8	16	1.5	14.5	130.6	20.2	5.9	14.3	57.12
4	149.9	18.1	3.4	14.7	156.9	19.4	4.8	14.6	4.61
5	196.1	27.1	12.9	14.2	195.5	27.3	13	14.3	-0.28
6	190.8	29.9	16	13.9	194.1	28.1	13.9	14.2	1.73
7	155.9	26.3	12.3	14	181.2	27.8	13.7	14.1	16.23

Table 6-2 shows results of 14 different trips from 7 different drivers that were simulated on the electric vehicle model. Each trip consists of a discharge of the battery pack from 100% to 20% state of charge. Using the data from the field trial experiment has one drawback, which is that drivers were not asked to brake efficiently. The increased energy recovery during the interface trial is a by-product of calm and smoother driving style. It can also be seen that most vehicles consume around 14kWh which is around the 80% capacity for a 96V, 180Ah battery ($96V \times 180Ah = 17.280 \text{ kWh}$ total capacity). However, as mentioned earlier, the actual capacity depends on a number of parameters, while for the model it is assumed that only the current draw on the battery affects the state of charge (as temperature is not an input into the system). It is also assumed that each journey starts at a 100% SOC condition.

It can be seen that the average distance covered by the driver during baseline runs was simulated to be around 153 kilometres per 80% discharge of the battery, while less aggressive driving and increased regenerative braking would provide 170 kilometres on average. Drivers 5 and 6 showed the least improvement, mainly because they were the best to start with, as they managed around 190 kilometres for both the baseline and interface trial data simulation. This is analogous with the inference from the IC engine field trial experiments that drivers who are already good to start with, have the least improvements in economy when using the driver advisory system. On the other end of the spectrum, Driver 3 had the greatest improvement in simulation, from 82.8 kilometres on the baseline simulation to 130 kilometres on the interface simulation. A major contributor of this saving is the

increase in energy recovery from braking for the interface trial simulation of this particular driver, which is considerably higher than that of the baseline trial data. The simulation showed that drivers achieved 12.4% increase in kilometres travelled per unit charge (kWh) across vans. The increase in range is combination of two factors – decrease in aggressive driving style, and increase in the energy recovered through regenerative braking.

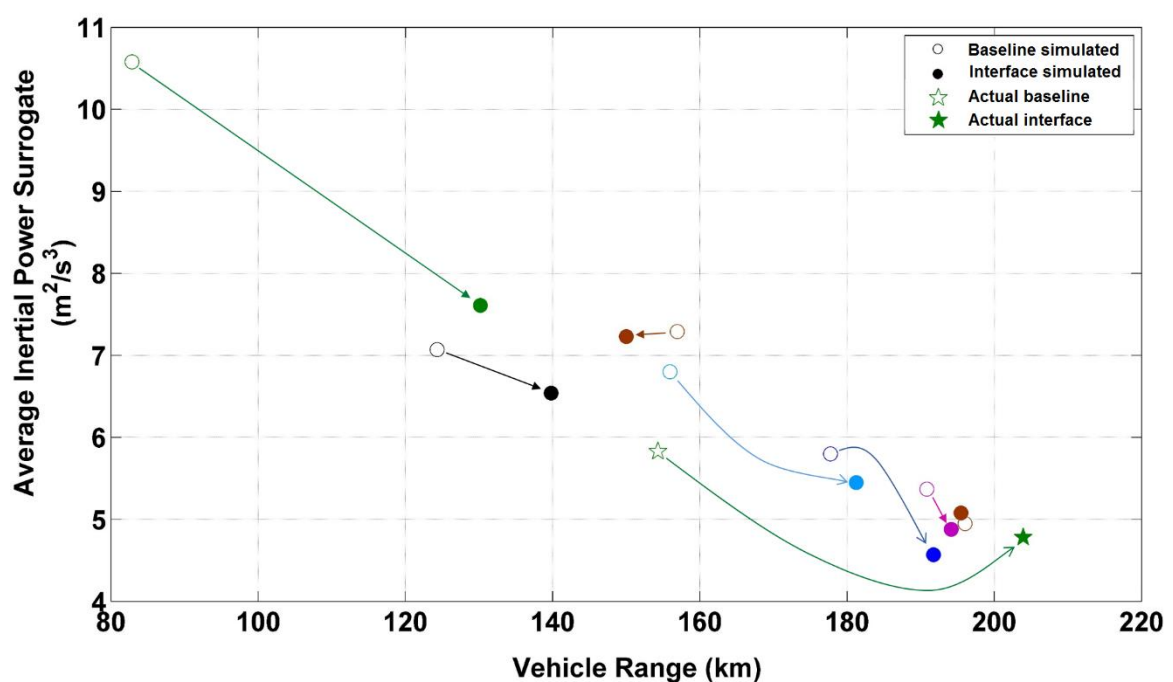


Figure 6-7 - Vehicle range and its relation to average inertial power surrogate of the simulated vans

Reduction in aggressive driving style is evident from the reduction in inertial power surrogate values. A lower acceleration means lesser current draw on the battery, which translates to an improvement in the remaining available capacity of the battery by Peukert's law. Reduction in inertial power surrogate can also indicate a reduction in vehicle speed, which again translates to less energy consumed by the vehicle, and hence an improvement in the remaining capacity of the battery. Figure 6-7 shows the effect of the reduction in average inertial power surrogate values to the range of the

electric vehicle simulated, for the baseline and interface data. For 6 out of the 8 vans shown in the figure, an increase in vehicle range was seen with the reduction of the average inertial power surrogate. However, regression analysis of the reduction in acceleration values and inertial power surrogate, against the increase in electric vehicle range did not provide a conclusive relationship between these parameters. Further testing and analysis of data is required to identify more parameters that contribute to the increase in vehicle range.

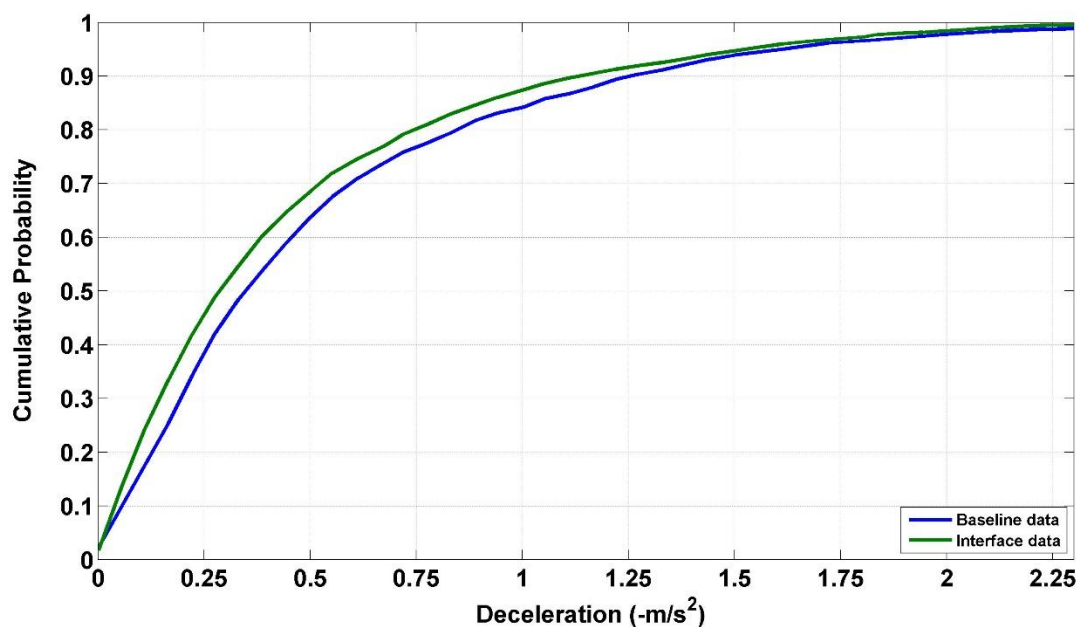


Figure 6-8 - Cumulative probability of the deceleration values of the simulated data for the electric vehicle

Figure 6-8 shows the cumulative probability of deceleration values of the data used for simulation. No modification to the driver data has been made by the vehicle model or simulation. The baseline to interface improvement is from drivers being much calmer during the interface trial due the advisory tool feedback being provided to them. A shift towards the left of the graph shows a reduction in high values of deceleration, which maximises the potential for regeneration of braking energy by the motor-generator.

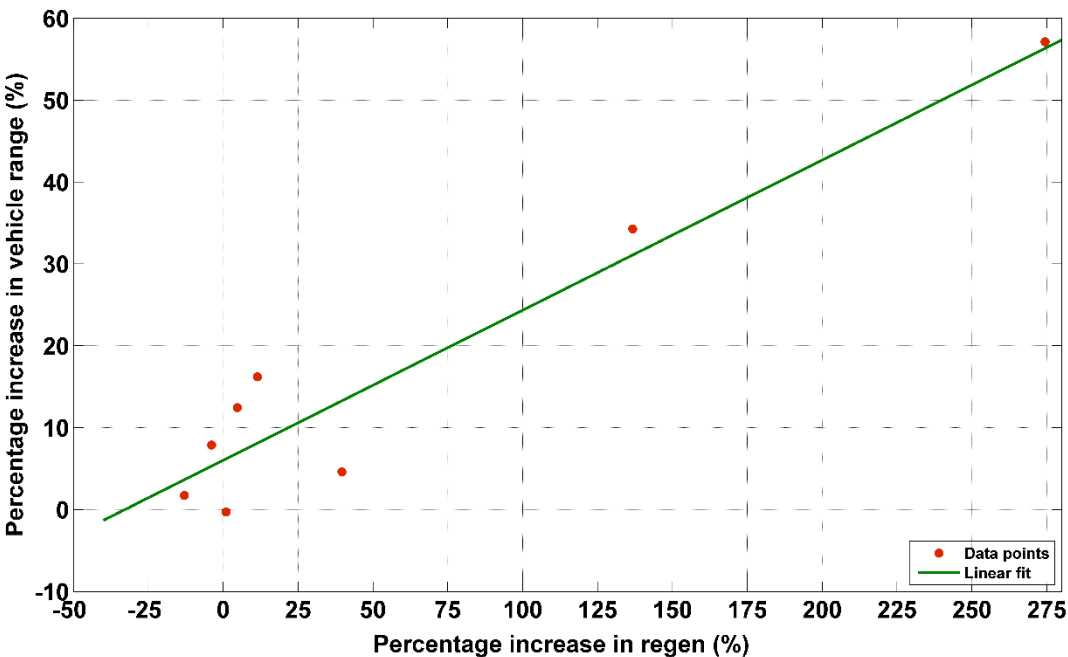


Figure 6-9 - Percentage increase in regenerative braking against the percentage increase in simulated electric vehicle range

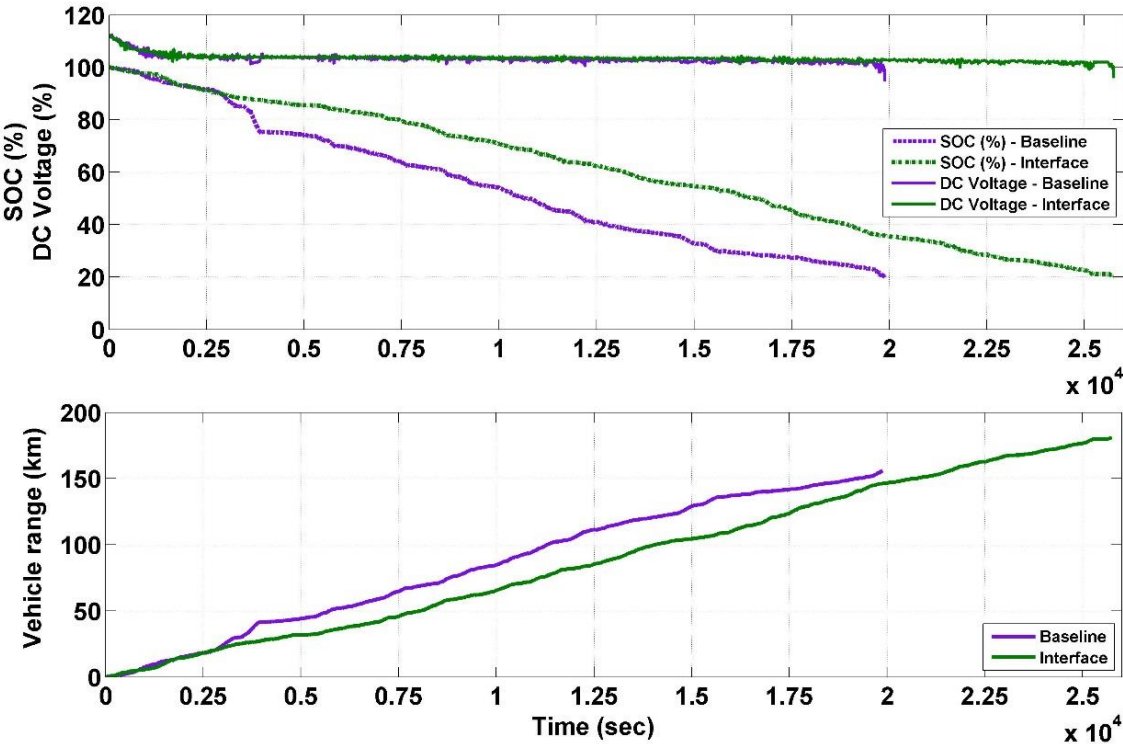


Figure 6-10 - DC voltage, SOC and vehicle range simulated using baseline and interface trial data for Driver 7

Regenerative braking has a direct correlation to the increase in range of the vehicle. This was seen by performing regression analysis on the improvement in energy regenerated against the improvement in vehicle range. Figure 6-9 shows the plot between these two parameters, for which an R^2 of 0.91 was achieved, showing good correlation between the range of the vehicle and the energy recovered from the deceleration of the vehicle.

Figure 6-10 shows the simulated DC voltage, SOC and range of the vehicle for the baseline and interface trial data of Driver 7 for one full charge depletion journey. It is evident that the battery SOC falls at a much slower rate for the interface trial data simulation, enabling the driver to cover an extra 25 kilometres. This increase is due a combination of the reduction in higher values of acceleration and IPS values, along with the fact that the driver would recover an additional 11.4% energy if braking behaviour is improved. It is evident from the vehicle data and simulation results that improving driving behaviour does have an impact on the range of the electric vehicle.

6.4. Summary

This chapter discusses the development and testing of a driver behaviour improvement device to help increase the range of electric vehicles. The existing version of the device for IC engine vehicles was modified to work on electric vehicles. Negative acceleration was added into the logic of the algorithm to provide feedback to the driver regarding effective braking for kinetic energy regeneration. The driver would still receive warnings and penalties for positive acceleration.

The electric version of the advisory tool was tested on a fully electric vehicle, based on the Citroen Nemo. The vehicle was powered using the 72 windings dual rotor axial flux electric motor described in Chapter 5, using a 96V Lithium ion battery pack. The vehicle was tested over a period of two months and over 500km worth of data was collected during this period. The drivers managed to achieve a 32% increase in distance travelled using the driver advisory tool, than without it. This increase in distance travelled was due to two separate contributions. Firstly, through the reduction in harsh accelerations (any greater than 1.5m/s^2), which meant there was lesser current draw on the battery, and hence there was a lower rate of reduction of the remaining capacity of the battery based on Peukert's law. Secondly, drivers were asked to brake more effectively for the interface trial when the advisory tool was switched ON. The effective braking during the second stage of testing helped the drivers regenerate up to 40% more than what they achieved during the baseline phase, which clearly indicates that effective braking advice has a direct correlation to improving range in an electric vehicle.

Due to project money and time constraints, further tests on the Nemo were not possible. Since only two drivers and 500kms worth of test data was collected, it was decided to develop a simple electric vehicle model in Simulink® using SimPowerSystems™ toolbox for the Lithium ion battery model. The model was then simulated using baseline and interface trial data collected during the field trial experiments of the IC engine version driver advisory tool.

Around 3500kms worth of data was simulated using the model, by splitting each journey into one full charge depletion cycle. On average, the interface trial showed that drivers would achieve a 12% increase in the distance travelled per kWh of energy. This was again due to a combination of reduction in harsh acceleration and aggressive driving characteristics, and also from effective regenerative braking. Simulation showed that there was an 11.4% increase in the braking energy regenerated during the interface trial. Regression analysis performed on the increase in braking energy regenerated to the increase in range of the vehicle showed an R^2 correlation of 0.91, indicating a clear relationship exists between these two parameters. Also, real world data on the Nemo showed that up to 40% extra energy can be regenerated effectively if the right advice on braking is given to the driver, which provided a 31% increase in the distance travelled per unit kWh of energy. From the road trials and simulations of the driver advisory tool, it is evident that a clear relation exists between driver behaviour improvement and the energy consumption of a vehicle, be it fuel usage or battery electrical energy.

Chapter 7 - Conclusion

This chapter summarises the main findings of the thesis, namely the contribution of driver behaviour improvement in reducing the fuel consumption for IC engine powered vehicles, and also in increasing the range of a fully electric vehicle. Opportunity for future work are discussed separately.

7.1. Driver behaviour and fuel consumption

Previous literature had suggested the links between driver behaviour and fuel consumption of the vehicle. This thesis discusses the development and testing of a driver behaviour improvement device that provides instantaneous feedback to the driver on how to improve his/her driving style. One of the key drawbacks identified in the previous literature was that for all the studies attempting to determine fuel savings on improving driver behaviour, the drivers were aware of the fact that they were being tested to understand the importance of improving their driving style. This would have caused them to be more conscious during their baseline testing phase, hence skewing the results. Thus, for the testing of the driver advisory tool, it was decided to fit the device in the fleet of vehicles of companies that were part of the study, and record the respective drivers' actual driving style for two weeks before switching the device ON and providing feedback to them.

It was seen that drivers achieved on average 7.6% reduction in fuel consumption over a period of two weeks, with the best savings being just over 12%. Analysis of the data collected during the field trial experiments showed that savings were achieved mainly through the reduction of aggressive and harsh driving characteristics like high values of acceleration (above 1.5m/s^2) and inertial power surrogate (above $9\text{m}^2/\text{s}^3$). Another major contributor was the reduction in engine speed, by shifting early into a higher gear. The reduction in time spent by the drivers in engine speed above 1500rpm during the interface trial helped contribute to the reduction in fuel consumption. An increase in the amount of 'zero acceleration' or cruising by the drivers was observed for the interface trial, when compared to the baseline trial. This was complemented

by the evidence of reduction in pedal busyness during the interface trials, which showed that drivers were a lot calmer and smoother in their driving style in the interface trial when compared to the baseline testing phase. This also resulted in 15.60% reduction of pedal usage when driving feedback was provided to the drivers. Use of other metrics like warnings and violations per unit kilometre or per day, help in understanding how drivers improve on a daily or weekly basis.

Testing and analysis of data showed that the driver has a significant role to play in the fuel consumption of the vehicle. Though it is impossible to drive in the most optimal fashion in the real world due to external factors such as traffic, weather, route, time of travel etc., it is possible to try and improve the existing habits of driving that cause significant increase in fuel consumption, like – harsh accelerations and decelerations, use of high engine speed, and unnecessary pedal oscillations. Simple changes to driving style like smooth and lower acceleration rates (less than 1.5 m/s^2), early shifting to a higher gear (before 1500rpm) and anticipating traffic and stops can have considerable impact on the fuel consumption of the vehicle. The novelty of the system in extending the driving pattern parameters defined by Eva Ericsson to real world driving conditions and its contribution to reduction in fuel consumption has added to the knowledge in this field. The inclusion of other systems like idle detection and the ability of the system to be fitted onto any vehicle with little or no calibration effort is novel as well. The use of the driver advisory tool helps the driver improve his/her driving style by providing constant audible and visual feedback. This constant feedback was essential, as previous literature highlighted that drivers tended to go back to their original driving style a few weeks after attending 'eco-driving' courses.

The driver advisory helps reduce exhaust gas emissions by improving driving behaviour. This low cost approach has a quicker return over investment compared to modification of the powertrain. Also, the flexibility of the system that enables it to be used on vehicles of different makes and sizes has proved to be useful, with the commercial version (known as Lightfoot) having sold over 5000 units around Europe.

7.2. Low cost electric powertrain

Reduction in the cost of electric powertrain is an essential requirement for the adoption of these technologies by manufacturers and consumers. Reduction in research and development costs will help reduce the overall reduction in price of the electric machine. This thesis discusses the testing and calibration of an axial flux electric machine that was later used on a fully electric vehicle to test the electric version of the driver advisory tool. Use of a variable air gap system which helped achieve a 45% increase in the maximum speed of the motor was demonstrated. This concept has the potential to be used in applications so as to avoid the use of a gearbox. A new approach to formulating the control strategy for the variable air gap machine was used, where different losses in the system were considered to determine the optimum air gap of the machine so that it produces the least amount of losses.

A fully automated validation test rig was developed to undertake R&D testing of electric motors to try and reduce test technician costs of running a test rig. New testing procedures were developed to determine faults early into the development stage and also to determine different performance and efficiencies of electric motors

for automotive tractive applications. This was an extension of the knowledge of IEC testing standards and procedures to incorporate different tests to ensure the effectiveness and performance of the machine in different applications. The low cost test rig developed was capable of running in a manual operator operation mode or a fully automatic testing mode. The rig now resides in the motor manufacturing plant as an automated end of line test facility, which rigorously tests electric machines after they are manufactured. The system detects variation from standard motor parameters like K_e , maximum torque and efficiency if any, and ensures quality and reliability of the motors being manufactured at the facility. The acceptance tolerance of the motors being tested can be changed according to the requirement of the company using the rig. The automated capabilities of the rig help save up to £44,000 a year in manufacturing labour costs to the industrial partner.

The dual rotor axial flux motor (72 windings) tested at the electric motor test facility, was calibrated to produce 51kW peak. The motor was then fitted onto an electric vehicle based on the Citroen Nemo, developed by the industrial partner on the project. This vehicle was used to trial the electric version of the driver advisory tool.

7.3. Driver behaviour and the range of an electric vehicle

The significance of improving driver behaviour to increase the range of an electric vehicle has been studied in this report. The device developed is similar to the IC engine version of the driver advisory tool, but in addition provides feedback to the driver on braking more effectively. The device was proposed and developed as an extension to the IC engine version of the device. The novelty of this device has to be

emphasised as it adds knowledge to the field of driver behaviour and its link to energy consumption in electric vehicle. It also is novel in its method of modifying braking behaviour to maximise the regenerative energy recovery of the vehicle. The device was trialled on the electric version of the Nemo, which helped achieve a 32% increase in the distance travelled per unit of energy (km/kWh) during the interface trial, when the device was switched ON. This increase was due to two contributors, firstly due to the reduction in harsh accelerations and aggressive driving characteristics; secondly, due to a 40% increase in energy recovered during the braking of the vehicle. The former has an impact on the remaining capacity of the battery pack, as the relation between current draw on the battery and its remaining capacity is non-linear. The latter has the potential of recovering energy that would otherwise be wasted in the form of heat during braking, and storing it in the battery pack. This further helps increase the range of the vehicle.

Since only 500 kilometres worth of electric vehicle data was available, a model of the electric vehicle was created in Simulink®. Baseline and interface data from the field trial experiments for the IC engine version of the vehicle were simulated to understand the benefit of driver behaviour improvement on battery state of charge for different drivers. Simulation results showed that if effective driving feedback is provided to the drivers, they would achieve an increase of 12.4% in the distance travelled per unit of energy. It needs to be mentioned that the simulation does not take into account the braking feedback provided to the driver, as in the case of the Nemo electric vehicle testing. Thus, this increase in distance travelled per unit of energy observed in simulation is predominantly due to the reduction in aggressivity,

which is a reduction in high values of power factor (above $9\text{m}^2/\text{s}^3$) and harsh acceleration (above 1.5 m/s^2). However, simulation showed that there was just over 11% increase in the energy recovered for the interface trial simulation data when compared to the baseline trial data. This was a secondary benefit of the calm and improved driving style where drivers anticipated traffic and braked more effectively.

In both the IC engine version and the electric version of the driver advisory tool, it was observed that the system works best for drivers who have more room for improvement. If the driving style of the driver is already good to start with, the advisory tool will provide only marginal benefits in terms of fuel savings or increase in electric vehicle range. In either case, it can be seen that driver behaviour has a significant role to play in saving energy and reducing exhaust emissions from the vehicle.

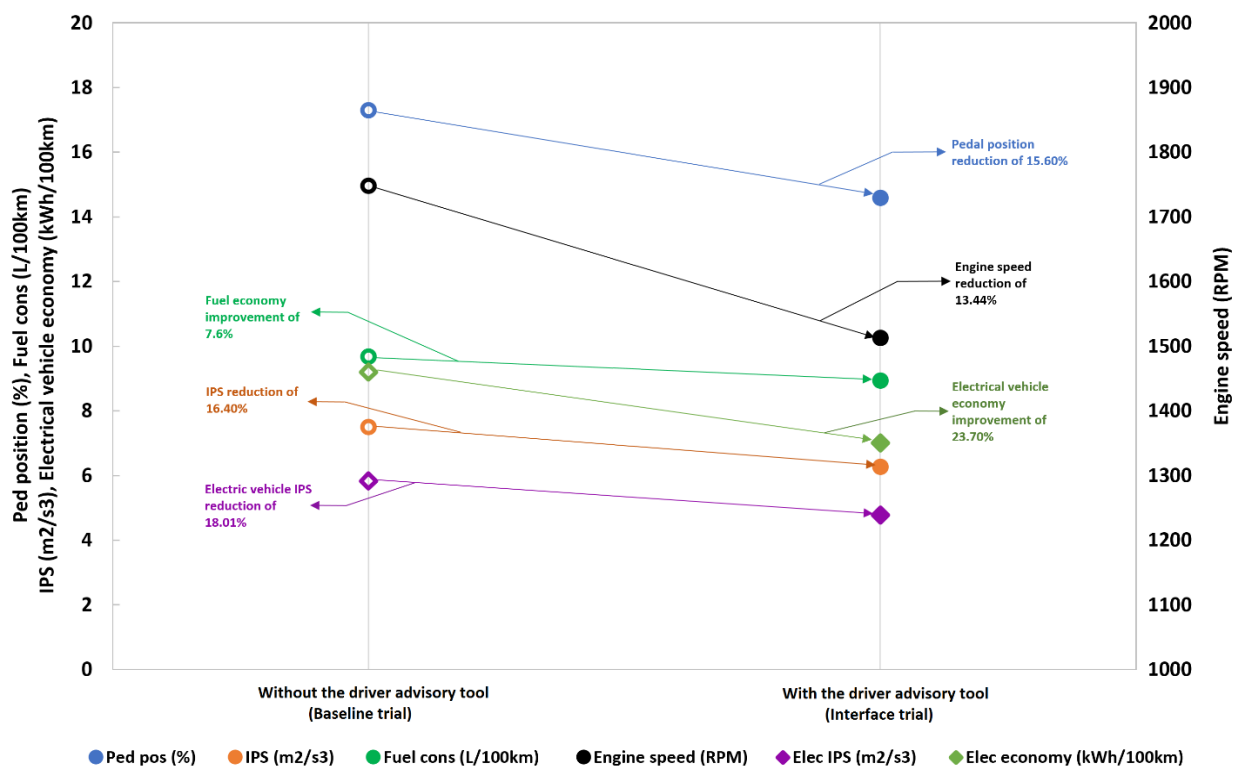


Figure 7-1 - Improvements in different driving characteristics using the driver advisory tool for conventional and electric vehicles

Figure 7-1 shows the improvements in various driving characteristics after the use of the driver advisory tool. For the IC engine version of the device, a 15.60% reduction in pedal position, 13.44% reduction in engine speed and 16.40% reduction in average IPS values translated into an overall fuel saving of 7.6% over the entire fleet. For the electric vehicle version of the device, a 23.70% reduction in the net energy used per 100 kilometres of distance represented the effectiveness of the device. In both cases, aggressivity of the driver was shown to reduce, as the average IPS in both cases reduced, along with an increase in fuel/energy economy. In the case of the electric vehicle version of the device, regenerative energy braking also contributed to the net savings. This plot summarises the findings of the thesis and also helps prove that driver behaviour management helps to reduce aggressivity of the driver and hence improve energy usage in conventional and electric vehicles.

7.4. Future work

Time and money constraints of this research work restricted the testing of the electric version of the driver advisory tool to just one vehicle. Although real test data and simulated data showed 32% and 12.4% increase respectively in the distance travelled per unit of energy, a more thorough test procedure similar to the case of the IC engine version of the device would be beneficial in understanding the energy savings in more detail. This would also help in finer tuning of the braking feedback provided to the driver, to try and achieve further savings from the system.

The effect of the driver advisory tool and its relationship to NO_x emissions was briefly discussed in Chapter 3. Due to the reduction in engine speed when shifting early into

a higher gear, there may be an increase in the NO_x emissions [75]. However, since reducing aggressivity reduces the power required to propel the vehicle, NO_x emissions are reduced. To understand the relationship and impact of the driver advisory tool on NO_x and particulates, further testing and analysis is proposed.

Although the driver advisory tool provides instantaneous feedback to the driver, it is always clearly mentioned to the driver that safety manoeuvres always take priority over warnings and penalties from the system. Although the device only provides feedback to the driver to improve his/her driving style, the driver has to pay attention to the road, and at the same time process the audible and visual feedback from the tool. It is not clear as to how much extra cognitive load has to be endured by the driver to respond to the feedback provided by the driver advisory tool. Since this study would require more testing and close monitoring of the driver's cognitive loading, it is suggested as potential future research.

REFERENCES

- 1 IMechE Low Carbon Vehicle Report. *Low Carbon Vehicles: Driving the UK's transport revolution*, 16.
- 2 2012 UK Greenhouse Gas Emissions, Final Figures. *Department of Energy & Climate Change*, 2014, 45.
- 3 Regulation (EC). European Commission regulation for new passenger cars. *Office Journal of the European Union*, 2009, L 140/141.
- 4 **Taylor, A.M.K.P.** Science review of internal combustion engines. *Energy Policy*, 2008, 36(12), 4657-4667.
- 5 Plug-in car and van grants. In Vehicles, O.f.L.E., ed. *Plug-in car grant* Gov.uk, 2012).
- 6 Public Attitudes to Electric Vehicles. *Department of Transport, UK*, 2014, 8.
- 7 **Chu, S.** Critical Materials Strategy. *US Department of Energy*, 2011, 196.
- 8 **Marlino, L.** Electric Motors and Critical Materials Breakout. *US Department of Energy*, 2012, **Energy Efficiency and Renewable Energy**, 11.
- 9 **Cluzel, C. and Douglas, C.** Cost and performance of EV batteries. *The Committee on Climate Change*, 2012, **Final Report**, 100.
- 10 **Yi, J., Wooldridge, S., Coulson, G., Hilditch, J., Iyer, C.O., Moilanen, P., Papaioannou, G., Reiche, D., Shelby, M., VanDerWege, B., Weaver, C., Xu, Z., Davis, G., Hinds, B. and Schamel, A.** Development and Optimization of the Ford 3.5L V6 EcoBoost Combustion System. *SAE Int. J. Engines*, 2009, 2(1), 1388-1407.
- 11 **Turner, J.W.G., Popplewell, A., Patel, R., Johnson, T.R., Darnton, N.J., Richardson, S., Bredda, S.W., Tudor, R.J., Bithell, C.I., Jackson, R., Remmert, S.M., Cracknell, R.F., Fernandes, J.X., Lewis, A.G.J., Akehurst, S., Brace, C.J., Copeland, C., Martinez-Botas, R., Romagnoli, A. and Burluka, A.A.** Ultra Boost for Economy: Extending the Limits of Extreme Engine Downsizing. *SAE Int. J. Engines*, 2014, 7(1), 387-417.
- 12 **Patterson, J., Hassan, M.G., Clarke, A., Shama, G., Hellgardt, K. and Chen, R.** Experimental Study of DI Diesel Engine Performance Using Three Different Biodiesel Fuels. (SAE International, 2006).
- 13 **Stobart, R.K.** Process or cycle? Putting fuel cells into their thermodynamic context. *Proceedings of the 3rd IMechE Automobile Division Southern Centre Conference on: Total Vehicle Technology; Finding the Radical, Implementing the Practical, April 26, 2004 - April 27, 2004*, pp. 167-176 (Professional Engineering Publishing, Brighton, United kingdom, 2004).
- 14 **Lakshminarasimhan, V. and Athani, G.** An Intelligent Alternator Control Mechanism for Energy Recuperation and Fuel Efficiency Improvement. *SAE Int. J. Alt. Power.*, 2013, 2(1), 217-225.
- 15 **Montalto, I., Tavella Ing, D., Casavola PhD, A. and De Cristofaro, F.** Intelligent Alternator Employment To Reduce Co2 Emission and to Improve Engine Performance. *SAE Int. J. Alt. Power.*, 2012, 1(1), 1-11.
- 16 **BMW.** BMW Efficient Dynamics.
- 17 **Ford.** Ford ECONetic Technology. 2009).
- 18 **Sayahan, A. and Asaei, B.** An intelligent alternator control approach for fuel consumption reduction. *Environment and Electrical Engineering (EEEIC), 2013 13th International Conference on*, pp. 296-300(2013).
- 19 **Stobart, R., Hounsham, S. and Weerasinghe, R.** The Controllability of Vapour Based Thermal Recovery Systems in Vehicles. (SAE International, 2007).
- 20 **Smith, K. and Thornton, M.** Feasibility of Thermoelectrics for Waste Heat Recovery in Conventional Vehicles. *Technical Report* (National Renewable Energy Laboratory, 2009).
- 21 **Renken, F.** Fuel consumption reduction by the use of Hybrid Drive systems. *Proceedings of the 8th International Scientific and Practical Conference*, 2011, 2, 6.

- 22 **Waters, M. and Laker, I.B.** Research on Fuel Conservation for Cars. *TRRL LR921*, p. 34 (Transport and Road Research Laboratory, Crowthorne, 1981).
- 23 **Uhrig, R.E.** Using Plug-in Hybrid Vehicles to Drastically Reduce Petroleum-Based Fuel Consumption and Emissions. *The BENT of Tau Beta Pi*, 2005, **XCLI**(No. 2).
- 24 **Toyota.** Technology File - Hybrid Systems.
- 25 **Ribau, J., Silva, C., Brito, F.P. and Martins, J.** Analysis of four-stroke, Wankel, and microturbine based range extenders for electric vehicles. *Energy Conversion and Management*, 2012, **58**(0), 120-133.
- 26 **Varnhagen, S., Same, A., Remillard, J. and Park, J.W.** A numerical investigation on the efficiency of range extending systems using Advanced Vehicle Simulator. *Journal of Power Sources*, 2011, **196**(6), 3360-3370.
- 27 **Govindswamy, K., Tomazic, D., Genender, P. and Schuermann, G.** The NVH Behavior of Internal Combustion Engines used in Range Extended Electric Vehicles. (SAE International, 2013).
- 28 **Aharon, I. and Kuperman, A.** Topological Overview of Powertrains for Battery-Powered Vehicles With Range Extenders. *Power Electronics, IEEE Transactions on*, 2011, **26**(3), 868-876.
- 29 **Fraidl, G.K., Beste, F., Kapus, P.E., Korman, M., Sifferlinger, B. and Benda, V.** Challenges and Solutions for Range Extenders - From Concept Considerations to Practical Experiences. (SAE International, 2011).
- 30 **Pischinger, M., Tomazic, D., Wittek, K., Esch, H.-J., Köhler, E. and Baehr, M.** A Low NVH Range-Extender Application with a Small V-2 Engine - Based on a New Vibration Compensation System. (SAE International, 2012).
- 31 **Bassett, M., Hall, J., Kennedy, G., Cains, T., Powell, J. and Warth, M.** The Development of a Range Extender Electric Vehicle Demonstrator. (SAE International, 2013).
- 32 **Henneberger, G.** Brushless motors for electric and hybrid vehicles. *Machines and Drives for Electric and Hybrid Vehicles (Digest No: 1996/152), IEE Colloquium on*, pp. 2/1-2/4(1996).
- 33 **Kverneland, H.** Permanent magnet motors lead way to better power efficiency, safety on cranes, winches. *Drilling Contractor - Lifting & Mechanical Handling*, pp. 98-101(2008).
- 34 **Aydin, M., Huang, S. and Lipo, T.A.** Axial Flux Permanent Magnet Disc Machines: A Review. *Wisconsin Electric Machines & Power Electronics Consortium*, 2004, 12.
- 35 **Slemon, G.R.** High-efficiency drives using permanent-magnet motors. *Industrial Electronics, Control, and Instrumentation*, 1993. *Proceedings of the IECON '93., International Conference on*, pp. 725-730 vol.722(1993).
- 36 **Hari, D., Brace, C., Vagg, C., Akehurst, S., Ash, L. and Strong, R.** Development and Testing of a Low Cost High Performance Hybrid Vehicle Electric Motor. (SAE International, 2013).
- 37 **Collocott, S.J., Dunlop, J.B., Gwan, P.B., Kalan, B.A., Lovatt, H.C., Wu, W. and Watterson, P.A.** Applications of rare-earth permanent magnets in electrical machines: from motors for niche applications to hybrid electric vehicles. p. 172(2007).
- 38 **Cuenca, R.M., Gaines, L.L. and Vyas, A.D.** Evaluation of Electric Vehicle Production and Operating Costs. *Center for Transportation Research, Energy Systems Division*, 1999, 102.
- 39 **Matsushashi, D., Matsuo, K., Okitsu, T., Ashikaga, T. and Mizuno, T.** Comparison study of various motors for EVs and the potentiality of a ferrite magnet motor. *Power Electronics Conference (IPEC-Hiroshima 2014 - ECCE-ASIA), 2014 International*, pp. 1886-1891(2014).
- 40 **Sung-II, K., Jinwoo, C., Sunghyuk, P., Taesang, P. and Seongtaek, L.** Characteristics comparison of a conventional and modified spoke-type ferrite magnet motor for traction

drives of low-speed electric vehicles. *Energy Conversion Congress and Exposition (ECCE), 2012 IEEE*, pp. 3048-3054(2012).

41 Jajtic, Z., Ulmar, E., Volmert, C., Fretzscner, S., Pommer, H. and Dorfner, M.

Segmented electric machine - modular motor and system topology for direct drives. *Electric Drives Production Conference (EDPC), 2011 1st International*, pp. 36-39(2011).

42 Seok-Myeong, J., Hyun-Jun, P., Ji-Hwan, C., Cheol, H. and Man-Soo, C. Analysis on the Magnetic Force Characteristics of Segmented Magnet Used in Large Permanent-Magnet Wind Power Generator. *Magnetics, IEEE Transactions on*, 2013, **49**(7), 3981-3984.

43 Profumo, F., Zheng, Z. and Tenconi, A. Axial flux machines drives: a new viable solution for electric cars. *Industrial Electronics, IEEE Transactions on*, 1997, **44**(1), 39-45.

44 Cavagnino, A., Lazzari, M., Profumo, F. and Tenconi, A. A comparison between the axial flux and the radial flux structures for PM synchronous motors. *Industry Applications, IEEE Transactions on*, 2002, **38**(6), 1517-1524.

45 Theraja, A.K. *ABC of Electrical Engineering: Cover Basic Electrical Engineering and Electrical Machines For 1st Year Students of B. E (all Branches), B. Tech and A.I.M. E.* (S Chand, 2012).

46 Fita, D. Field weakening control of PMSM. *Department of Electrical and Computer Engineering*, p. 217 (Addis Ababa University, 2005).

47 Woolmer, T.J. and McCulloch, M.D. Analysis of the Yokeless And Segmented Armature Machine. *Electric Machines & Drives Conference, 2007. IEMDC '07. IEEE International*, pp. 704-708(2007).

48 Jermakian, J., Mohd, M.-S. and Motevalli, V. Testing and Modeling of Variable Airgap Axial Flux Brushless DC Motor. (SAE International, 2001).

49 Alson, J., Ellies, B. and Ganss, D. Interim Report: New Powertrain Technologies and Their Projected Costs. (U.S. Environmental Protection Agency, 2005).

50 Hari, D., Brace, C.J., Vagg, C., Poxon, J. and Ash, L. Analysis of a Driver Behaviour Improvement Tool to Reduce Fuel Consumption. *Connected Vehicles and Expo (ICCVE), 2012 International Conference on*, pp. 208-213(2012).

51 van der Voort, M., Dougherty, M.S. and van Maarseveen, M. A prototype fuel-efficiency support tool. *Transportation Research Part C: Emerging Technologies*, 2001, **9**(4), 279-296.

52 Van der Voort, M.C. Fest - A new driver support tool that reduces fuel consumption and emissions. *International Conference on Advanced Driver Assistance Systems, September 17, 2001 - September 18, 2001*, pp. 90-93 (Institution of Engineering and Technology, Birmingham, United kingdom, 2001).

53 Hooker, J.N. Optimal driving for single-vehicle fuel economy. *Transportation Research Part A: General*, 1988, **22**(3), 183-201.

54 af Wählberg, A.E. Long-term effects of training in economical driving: Fuel consumption, accidents, driver acceleration behavior and technical feedback. *International Journal of Industrial Ergonomics*, 2007, **37**(4), 333-343.

55 Zarkadoula, M., Zoidis, G. and Tritopoulou, E. Training urban bus drivers to promote smart driving: A note on a Greek eco-driving pilot program. *Transportation Research Part D: Transport and Environment*, 2007, **12**(6), 449-451.

56 Beusen, B., Broekx, S., Denys, T., Beckx, C., Degraeuwe, B., Gijsbers, M., Scheepers, K., Govaerts, L., Torfs, R. and Panis, L.I. Using on-board logging devices to study the longer-term impact of an eco-driving course. *Transportation Research Part D: Transport and Environment*, 2009, **14**(7), 514-520.

57 De Vlieger, I. On-board emission and fuel consumption measurement campaign on petrol-driven passenger cars. *Atmospheric Environment*, 1997, **31**(22), 3753-3761.

58 Alessandrini, A., Filippi, F., Orecchini, F. and Ortenzi, F. A new method for collecting vehicle behaviour in daily use for energy and environmental analysis. *Proceedings of the*

Institution of Mechanical Engineers, Part D: Journal of Automobile Engineering, 2006, **220**(11), 1527-1537.

59 Vagg, C., Brace, C.J., Wijetunge, R., Akehurst, S. and Ash, L. Development of a new method to assess fuel saving using gear shift indicators. *Proceedings of the Institution of Mechanical Engineers, Part D: Journal of Automobile Engineering*, 2012.

60 Gonder, J., Earleywine, M. and Sparks, W. Analyzing Vehicle Fuel Saving Opportunities through Intelligent Driver Feedback. *SAE Int. J. Passeng. Cars - Electron. Electr. Syst.*, 2012, **5**(2), 450-461.

61 Corcoba-Magana, V. and Munoz-Organero, M. GAFU: Using a gamification tool to save fuel. *IEEE Intelligent Transportation Systems (Approved for Publication)*, 2014(Magazine ICCVE Special Issue), 14.

62 Frith, W. and Cenek, P. AA Research: Standard Metrics for Transport and Driver Safety and Fuel Economy. *Opus International*, 2012, 51.

63 Ericsson, E. Independent driving pattern factors and their influence on fuel-use and exhaust emission factors. *Transportation Research Part D: Transport and Environment*, 2001, **6**(5), 325-345.

64 Ericsson, E. Variability in urban driving patterns. *Transportation Research Part D: Transport and Environment*, 2000, **5**(5), 337-354.

65 Adair, J.G. The Hawthorne effect: A reconsideration of the methodological artifact. *Journal of Applied Psychology*, 1984, **69**(2), 334-345.

66 Mathworks. Simulink - Simulation and Model-Based Design.

67 Fomunung, I., Washington, S. and Guensler, R. A statistical model for estimating oxides of nitrogen emissions from light duty motor vehicles. *Transportation Research Part D: Transport and Environment*, 1999, **4**(5), 333-352.

68 Vagg, C., Brace, C.J., Hari, D., Akehurst, S., Poxon, J. and Ash, L. Development and Field Trial of a Driver Assistance System to Encourage Eco-Driving in Light Commercial Vehicle Fleets. *Intelligent Transportation Systems, IEEE Transactions on*, 2013, **14**(2), 796-805.

69 Automotive, A. Ashwoods EcoDrive+. 2011).

70 Body and Equipment Mounting Manual Ford Transit 2006. In Company, F.M., ed, p. 306 (Ford Motors Company, 2011).

71 Stone, R. *Introduction to Internal Combustion Engines*. (Society of Automotive Engineers, 1999).

72 Rolling resistance force. *European Tyre School*Tampere University of Technology, Finland.

73 Weijer, C.J.T. Heavy-duty emission factors, development of representative driving cycles and prediction of emissions in real life. *Mechanical Engineering* (Graz University of Technology, Graz, Austria, 1997).

74 Brace, C.J., Burke, R. and Moffa, J. Increasing accuracy and repeatability of fuel consumption measurement in chassis dynamometer testing. *Proceedings of the Institution of Mechanical Engineers, Part D: Journal of Automobile Engineering*, 2009, **223**(9), 1163-1177.

75 Agudelo, J., Benjumea, P. and Villegas, A.P. Evaluation of nitrogen oxide emissions and smoke opacity in a HSDI diesel engine fuelled with palm oil biodiesel. *Department of Engineering, University of Antioquia*, 2010, 10.

76 Brace, C.J. Transient Modelling of a DI TCi Diesel Engine. *Mechanical Engineering* (University of Bath, Bath, 1996).

77 On-Board Diagnostics. *Regulations* (Environment Protection Agency (EPA).

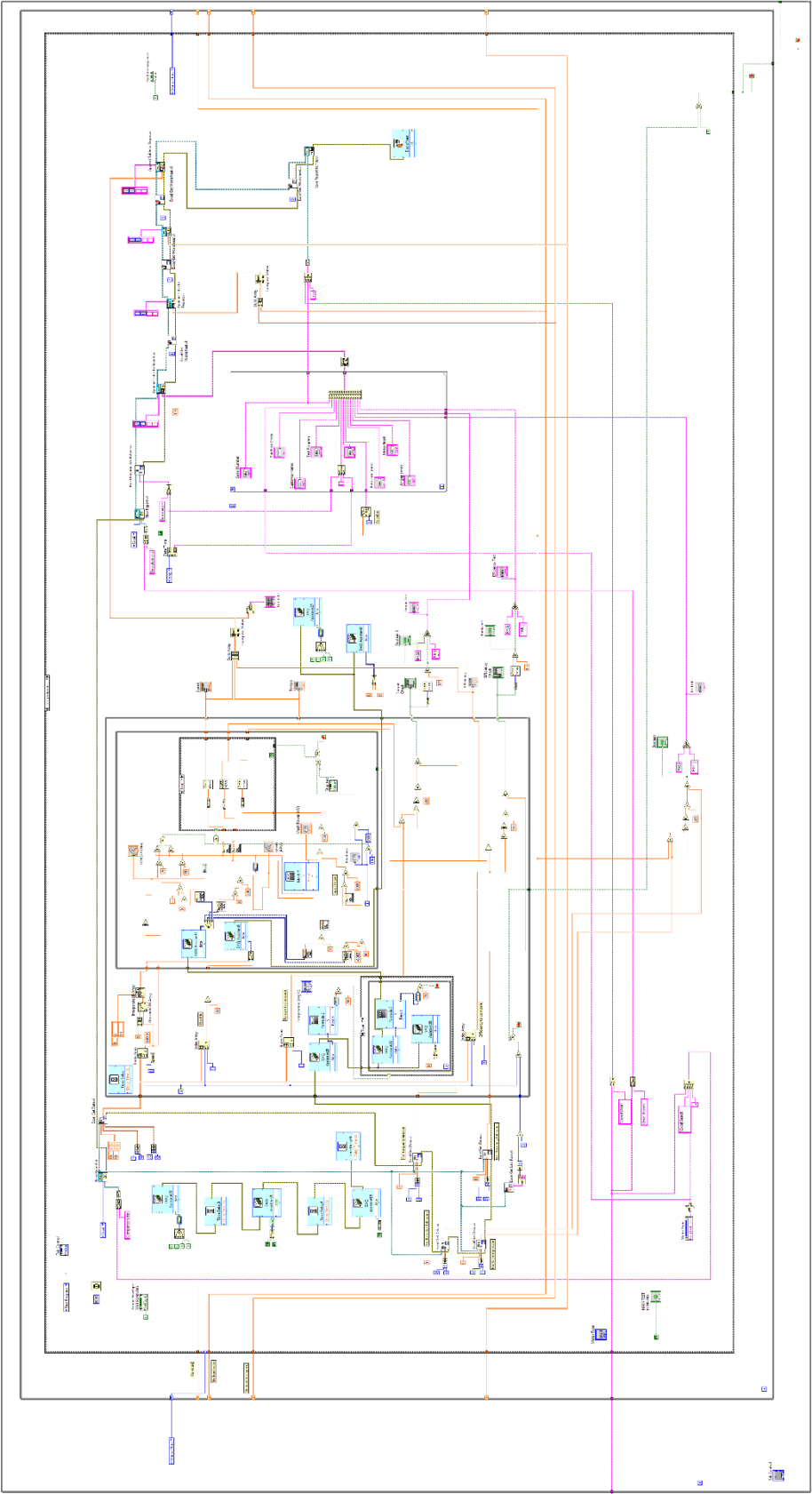
78 Jan-Dong, T. and Cheng-Yuan, C. A novel coupled-line low pass filter design. *Electromagnetic Compatibility (APEMC), 2010 Asia-Pacific Symposium on*, pp. 732-735(2010).

79 Wada, T., Yoshimura, K., Doi, S.I., Youhata, H. and Tomiyama, K. Proposal of an eco-driving assist system adaptive to driver's skill. *Intelligent Transportation Systems (ITSC), 2011 14th International IEEE Conference on*, pp. 1880-1885(2011).

- 80 Casavola, A., Prodi, G. and Rocca, G.** Efficient gear shifting strategies for green driving policies. *2010 American Control Conference, ACC 2010, June 30, 2010 - July 2, 2010*, pp. 4331-4336 (IEEE Computer Society, Baltimore, MD, United states, 2010).
- 81 Eckert, J.J., Santiciolli, F.M., Costa, E.d.S., Corrêa, F.C., Dionísio, H.J. and Dedini, F.G.** Vehicle gear shifting co-simulation to optimise performance and fuel consumption in the Brazilian Standard Urban Driving Cycle. *Blucher Engineering Proceedings*, 2014, **1**(XXII Simpósio Internacional de Engenharia Automotiva), 645-631.
- 82 Ivarsson, M., Åslund, J. and Nielsen, L.** Impacts of AMT Gear-Shifting on Fuel Optimal Look Ahead Control. (SAE International, 2010).
- 83 Mashadi, B., Amiri-rad, Y., Afkar, A. and Mahmoodi-kaleybar, M.** Simulation of automobile fuel consumption and emissions for various driver's manual shifting habits. *Journal of Central South University*, 2014, **21**(3), 1058-1066.
- 84 Reghunath, S.K., Sharma, D. and Athreya, A.S.** Optimal Gearshift Strategy using Predictive Algorithm for Fuel Economy Improvement. (SAE International, 2014).
- 85 Rahman, S.M.A., Masjuki, H.H., Kalam, M.A., Abedin, M.J., Sanjid, A. and Sajjad, H.** Impact of idling on fuel consumption and exhaust emissions and available idle-reduction technologies for diesel vehicles – A review. *Energy Conversion and Management*, 2013, **74**(0), 171-182.
- 86 Khatri, D.S., Ramesh, A. and Babu, M.K.G.** Comparative Studies on the Idling Performance of a Three Cylinder Passenger Car Engine Fitted with a Carburettor and a Single Point Electronic Gasoline Fuel Injection System. (SAE International, 1997).
- 87 Matsuura, M., Korematsu, K. and Tanaka, J.** Fuel Consumption Improvement of Vehicles by Idling Stop. (SAE International, 2004).
- 88 Brodrick, C.-J., Dwyer, H.A., Farshchi, M., Harris, D.B. and King, F.G.** Effects of Engine Speed and Accessory Load on Idling Emissions from Heavy-Duty Diesel Truck Engines. *Journal of the Air & Waste Management Association*, 2002, **52**(9), 1026-1031.
- 89 Van den Berg, A.J.** Truckstop electrification: Reducing CO₂ emissions from mobile sources while they are stationary. *Energy Conversion and Management*, 1996, **37**(6–8), 879-884.
- 90 Jack, A.G., Mecrow, B.C., Dickinson, P.G., Stephenson, D., Burdess, J.S., Fawcett, J.N. and Evans, T.** Permanent magnet machines with powdered iron cores and pre-pressed windings. *Industry Applications Conference, 1999. Thirty-Fourth IAS Annual Meeting. Conference Record of the 1999 IEEE*, pp. 97-103 vol.1011999).
- 91 (IEC), I.E.C.** Rotating electrical machines - Rating and performance. *IEC 60034-12004*.
- 92 (IEC), I.E.C.** Rotating electrical machines - Specific methods for determining separate losses of large machines from tests. *IEC 60034-2-2*, p. 302010).
- 93 Electrical4u.** Faraday's Law of Electromagnetic Induction.
- 94 Dian, L., Hari, D., Vagg, C., Ash, L., Akehurst, S. and Brace, C.** Test and Simulation of Variable Air Gap Concept on Axial Flux Electric Motor. *Vehicle Power and Propulsion Conference (VPPC), 2013 IEEE*, pp. 1-62013).
- 95 Richard, M.G.** New Electric Motor is 50% Smaller but has 2x More Torque. (Tree Hugger, 2009).
- 96 V, P., Anand, S. and R, B.** Software test automation - the ground realities realized. *Journal of Theoretical and Applied Information Technology*, 2012, **43**(2), 7.
- 97 Wright, D.R.** Finite State Machines. (North Carolina State University, 2005).
- 98 Citroen.** Citroen Nemo vehicle. 2009).
- 99 Omar, N., Bossche, P.V.d., Coosemans, T. and Mierlo, J.V.** Peukert Revisited—Critical Appraisal and Need for Modification for Lithium-Ion Batteries. pp. 5625-5641 (*Energies* 2013, 2013).
- 100 Oswal, M., Paul, J. and Zhao, R.** A comparative study of Lithium ion batteries. (University of Southern California, 2010).

101 Mathworks. SimPowerSystems - Model and simulate electrical power systems.
Simulink.

Appendix A – Labview code for automated validation rig



Appendix B – Validation rig manual

The following manual was provided to the operators of the validation test described in Chapter 5, which currently resides in the motor manufacturing plant at Weston-Super Mare. The manual provides a brief explanation of the test rig setup and step by step instructions on how to use the rig.

END OF LINE RIG MANUAL

TEST RIG SETUP

The motor monitor consists of a NI USB DAQ (NI 6211) device and also processes various signals being recorded. The monitor has input channels - Battery EMF, Motor EMFs, dynamometer and test motor DC currents, motor temperature, motor speed and torque. It also has two analogue output channels for dynamometer and test motor throttle demands and also three digital output channels. The analogue and digital outputs should be connected to the control box using BNC connectors. Both switches on the control box need to be switched ON to enable software control of Sevcons. The motor monitor has to be switched ON only after the USB cable has been plugged in and NI DAQ has been detected on PC.

SOFTWARE

Software setup

After the software is installed, the Drive.txt in the main folder has to be updated with the current location of the main program. In the main program folder, a sub-folder named 'Excel Based' contains a text file – Motor Types.txt. This has to be updated every time a new motor type is available. The contents of this text file will be available as a drop down menu in the main program.

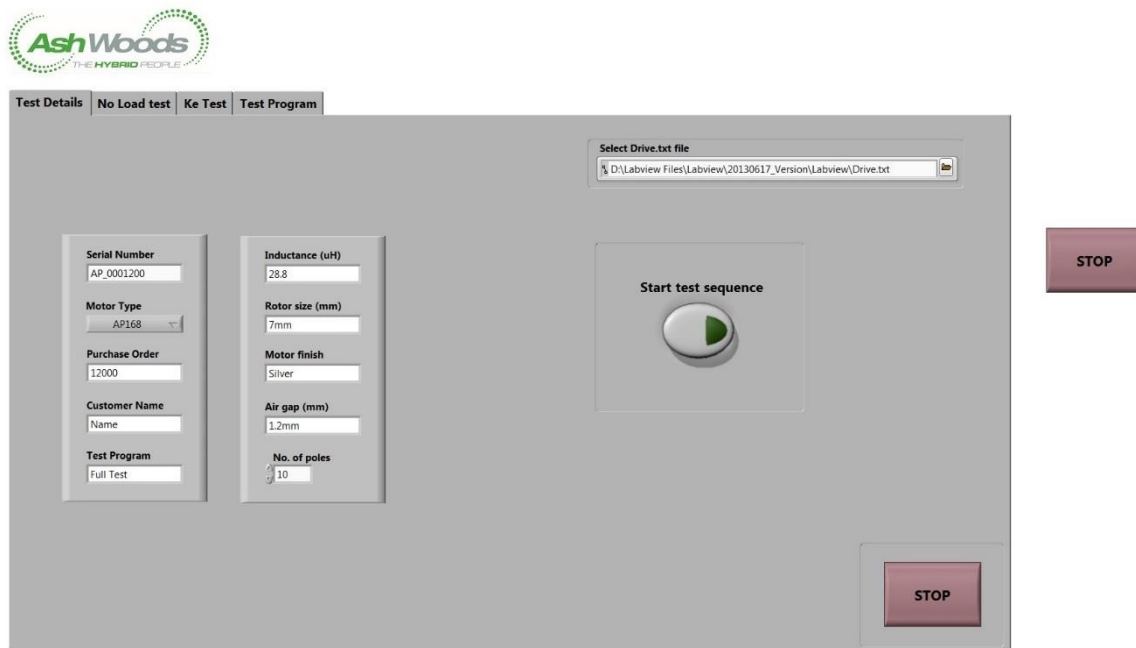


Figure 1 – The test details tab

The data for comparison is also to be saved in this folder. For each motor type, a comparison file has to be created in the format – ‘Motor type_Comparison.xlsx’. It should be noted that the same name/type of motor specified in Motor Types.txt should be used as the ‘Motor type’ for comparison. Speed and throttle values to run through in the main test procedure, torque and efficiency values to be compared against and their respective tolerances have to be specified in the comparison file. All saved excel files corresponding to each motor serial number will be saved in the folder ‘Saved Data’.

Running the rig

Load the test motor onto the test bench and lock it into position. Lower the power connectors and close the front door of the protective cover. Both switches on the control box and the motor monitor should be switched ON.

Run the EoL Program.

1. In the ‘Test Details’ tab, enter test details such as Serial number, purchase order number etc. and select the appropriate motor type to be tested. Also confirm the location of the ‘Drive.txt’ file. Once the operator is ready to run the test, press ‘Start test sequence’ button on the screen. See figure 1.
2. Once the ‘Start test sequence’ button is pressed, the program moves to the ‘No Load test’ tab to perform next two tests - encoder angle adjustment and no load test. For encoder angle adjustment, test motor Sevcon will automatically turn ON, allowing the operator to set a throttle value. The recommended throttle value is 10.9%. This can either be set using the control knob or simply by typing in the value. See figure 2. Once throttle position is set, change the encoder position on the motor through the side access on the protective cover. Set this to the most optimum position by viewing motor speed on the screen. Press ‘Encoder Angle set complete’ button when finished.

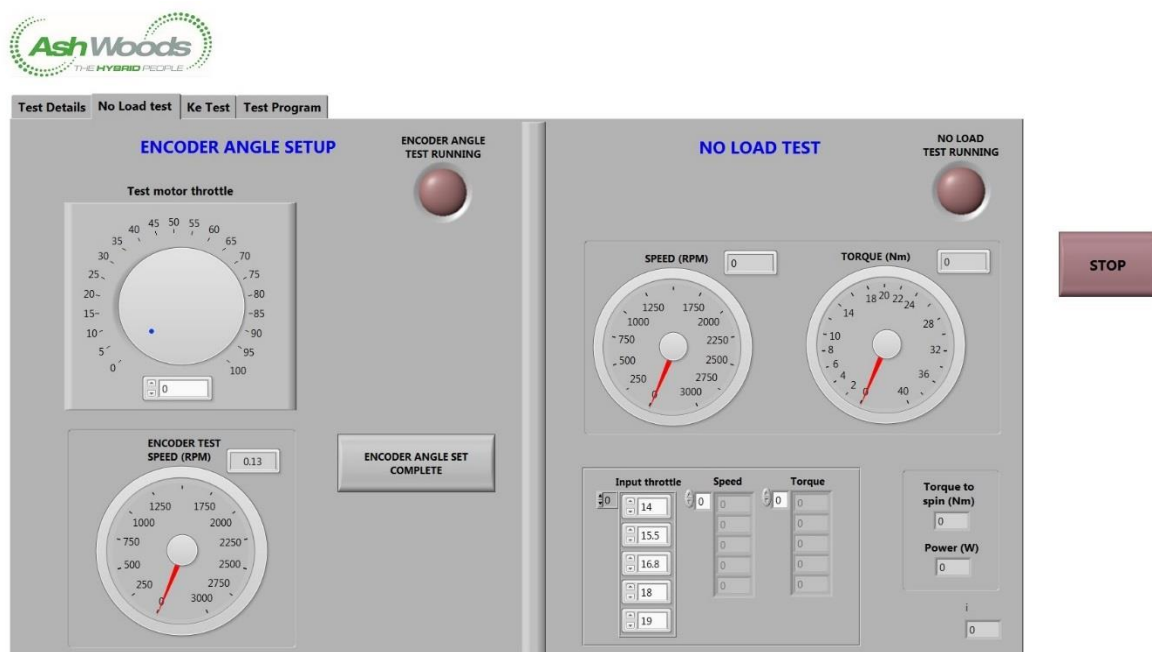


Figure 2 – No load test tab

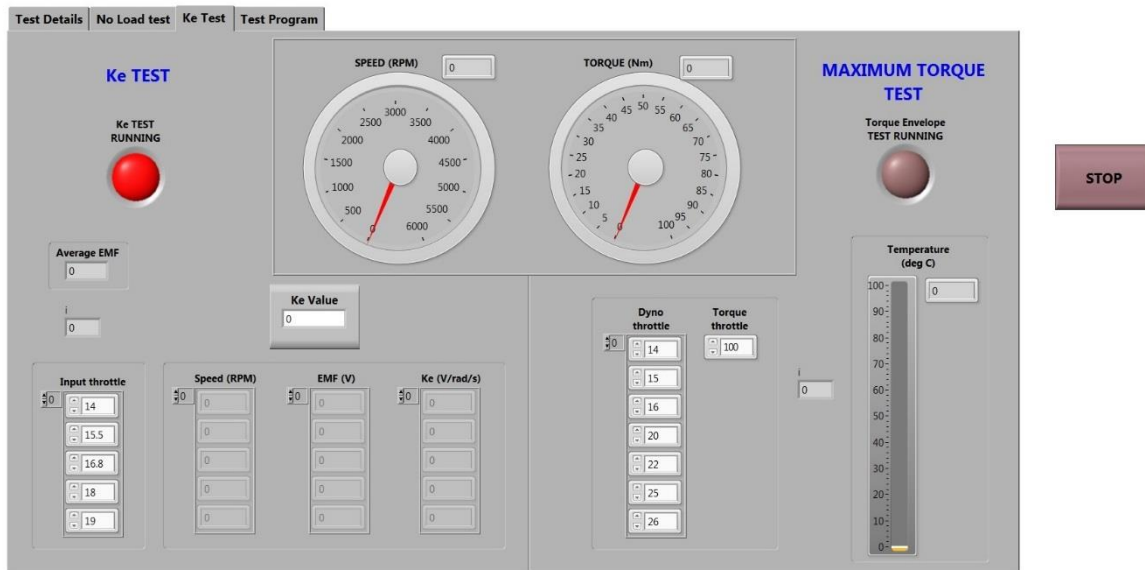


Figure 3 – Ke test tab

3. The test moves to the next procedure, which is the No Load torque/power test. For this test, Sevcon 2 switches OFF and Sevcon 1 is switched ON. The dynamometer spins the test motor to different set speeds, and torque and power required to spin the motor at these speeds are recorded.

4. The test then moves on to the 'Ke test' tab, where the dynamometer spins the motor to different set speeds, measuring the voltage across three terminals of the motor. Ke is automatically calculated from the voltage and speed. When the test is running, the LED on the screen lights up. See figure 3.

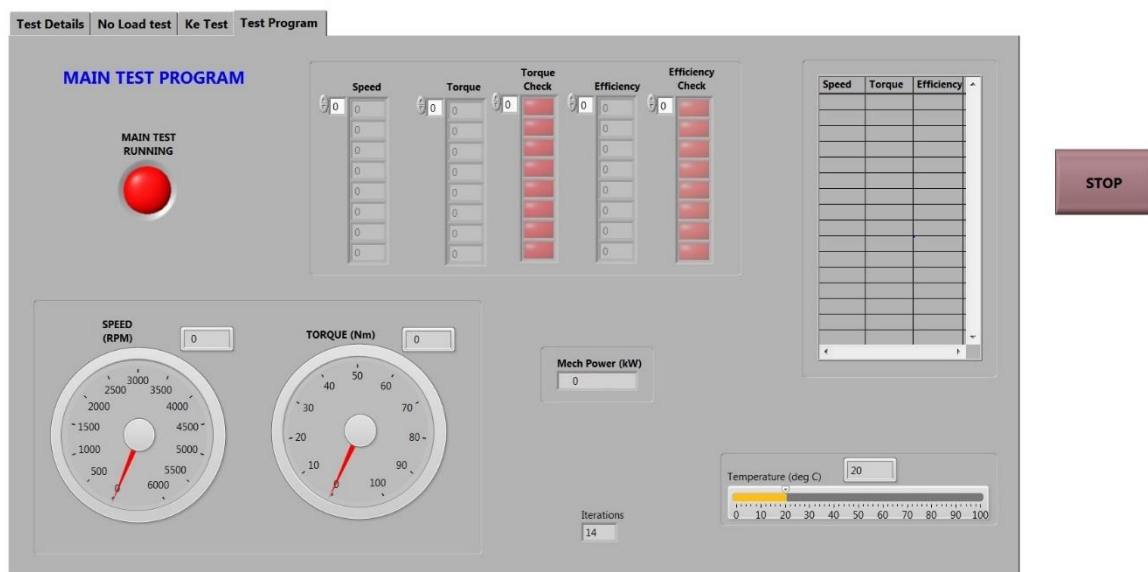


Figure 4 – Ke test tab

5. The test programs now moves onto the 'Maximum torque test', where the dynamometer sets different speeds and the 100% throttle is applied on the test motor. This provides the torque speed envelope for the motor. DC current is also recorded during the test.

6. After this, the tab is changes to 'Test program', where the main test program begins. Both dynamometer and test motor Sevcons are switched ON automatically. The program runs through the set speed and throttle range provided in Comparison file for that particular motor type. Upon completion of the test sequence, an excel file containing the test summary and data is saved in the folder 'Saved Data' bearing the serial number as filename for each test. The program then waits for an operator input to go to the main screen and start a new test.

When in the front screen, it is important to close the excel files that are open before repeating steps 1-6 to run the next test.

Software developed by:

Deepak Hari
Research Engineer
Powertrain and Vehicle Research Centre
Dept. of Mechanical Engineering
University of Bath
Bath BA2 7AY, UK

